sid.inpe.br/mtc-m21b/2014/09.24.16.28-TDI

THE ROLE OF COMPUTATIONAL STEERING IN SPACE ENGINEERING ACTIVITIES ASSISTED BY MODELLING AND SIMULATION

Leandro Toss Hoffmann

Doctorate Thesis of the Graduate Course in Space Engineering and Technology/Space Systems of Management and Engineering, guided by Dr. Leonel Fernando Perondi, approved in november 27, 2014.

URL of the original document:
<http://urlib.net/8JMKD3MGP5W34M/3H56LQH>

INPE
São José dos Campos
2014

PUBLISHED BY:

Instituto Nacional de Pesquisas Espaciais - INPE
Gabinete do Diretor (GB)
Serviço de Informação e Documentação (SID)
Caixa Postal 515 - CEP 12.245-970
São José dos Campos - SP - Brasil
Tel.:(012) 3208-6923/6921
Fax: (012) 3208-6919
E-mail: pubtc@sid.inpe.br

sid.inpe.br/mtc-m21b/2014/09.24.16.28-TDI

THE ROLE OF COMPUTATIONAL STEERING IN SPACE ENGINEERING ACTIVITIES ASSISTED BY MODELLING AND SIMULATION

Leandro Toss Hoffmann

Doctorate Thesis of the Graduate Course in Space Engineering and Technology/Space Systems of Management and Engineering, guided by Dr. Leonel Fernando Perondi, approved in november 27, 2014.

URL of the original document:
<http://urlib.net/8JMKD3MGP5W34M/3H56LQH>

INPE
São José dos Campos
2014

Cataloging in Publication Data

Hoffmann, Leandro Toss.

H675r The role of computational steering in space engineering activities assisted by modelling and simulation / Leandro Toss Hoffmann. – São José dos Campos : INPE, 2014.

xxx + 239 p. ; (sid.inpe.br/mtc-m21b/2014/09.24.16.28-TDI)

Thesis (Doctorate in Space Engineering and Technology/Space Systems of Management and Engineering) – Instituto Nacional de Pesquisas Espaciais, São José dos Campos, 2014.

Guiding : Dr. Leonel Fernando Perondi.

1. Computerized simulation 2. Space systems engineering 3. Steering 4. Human-computer interface. 5. Software reuse. I.Title.

CDU 629.78:004

Aprovado (a) pela Banca Examinadora em cumprimento ao requisito exigido para obtenção do Título de ***Doutor(a)*** em

Engenharia e Tecnologia Espaciais/Gerenciamento de Sistemas Espaciais

Dra.	Ana Maria Ambrosio	[illegible]
		Presidente / INPE / São José dos Campos - SP
Dr.	Leonel Fernando Perondi	[illegible]
		Orientador(a) / INPE / São José dos Campos - SP
Dr.	Fabiano Luis de Sousa	[illegible]
		Membro da Banca / INPE / SJCampos - SP
Dr.	Valdemir Carrara	[illegible]
		Membro da Banca / INPE / SJCampos - SP
Dr.	Fausto de Oliveira Ramos	[illegible]
		Convidado(a) / IAE / São José dos Campos - SP
Dra.	Emilia Villani	[illegible]
		Convidado(a) / Ita / São José dos Campos - SP

Este trabalho foi aprovado por:

( ) maioria simples

(X) unanimidade

[illegible]

Aluno (a): ***Leandro Toss Hoffmann***

São José dos Campos, 27 de Novembro de 2014

“ ‘en avant’ . . . ce doit être la devise de l’humanite!”

“ ‘avante’... este deve ser o lema da humanidade!”

JULES VERNE, 1881

AGRADECIMENTOS

Ao longo dos últimos anos, diversas pessoas e instituições contribuíram de maneira fundamental para que os resultados desta pesquisa fossem alcançados.

Inicialmente, gostaria de agradecer profundamente ao professor Leonel Fernando Perondi, Ph.D., por aceitar a orientação deste trabalho e guiar sua evolução com sabedoria e incansáveis aulas, não somente em temas da área espacial, mas também sobre o nosso papel no desenvolvimento de uma sociedade mais igualitária.

Agradeço também aos membros da banca pela disponibilidade e dedicação em participar da defesa, contribuindo com valiosas contribuições para o aperfeiçoamento desta pesquisa.

Aos diversos docentes do curso de pós-graduação em Engenharia e Tecnologia Espaciais ofereço minha gratidão e respeito pelos conhecimentos transmitidos. Em especial à professora Dra. Ana Maria Ambrosio da qual recebi os primeiros conceitos de simuladores de satélites.

Muito tenho em agradecer aos diversos colegas do Instituto Nacional de Pesquisas Espaciais, pela troca de experiências e por contribuições que, mesmo de maneira informal, foram decisivas no direcionamento do trabalho. Em particular, cito o meu amigo e colega Mario Celso Padovan de Almeida que me ensinou diversos princípios fundamentais de engenharia espacial.

Aos colegas da Divisão de Desenvolvimento de Sistemas de Solo, na pessoa de Rubens Gatto, pela disponibilidade e apoio no progresso deste trabalho. Em especial à futura doutora Denise Rotondi de Azevedo com a qual realizei diversos estudos aprofundados no tema de simulação de satélites. Também ao amigo Joaquim Pedro Barreto que realizou a organização do código fonte das interfaces do padrão SMP2.

À equipe de desenvolvimento do sistema de controle e atitude da Plataforma Multi-Missão Brasileira, de maneira muito especial aos professores Dr. Roberto Vieira da Fonseca Lopes e Dr. Ijar Milagre da Fonseca, com os quais tive o privilégio de trabalhar e absorver uma pequena parcela de suas experiências.

Aos bolsistas do projeto de capacitação em software de controle de atitude de satélites para a eletrônica de suporte de solo, apoiado pelo Conselho Nacional de Desenvolvimento Científico e Tecnológico (CNPq), pela contribuição na modelagem e verificação de componentes de simulação utilizados neste trabalho.

Ao grupo de subsistema térmico do INPE, na pessoa do Dr. Douglas Silva e ao professor Dr. Fabiano Luis de Sousa pelo suporte no uso da ferramenta Sinda/Fluint e na modelagem dos cenários de térmica.

À equipe do projeto de Sistemas Inerciais para Aplicações Aeroespacial (SIA), na pessoa do Prof. Dr. Waldemar de Castro Leite Filho por apoiar o desenvolvimento do protótipo utilizado neste trabalho e ao Prof. Dr. Valdemir Carrara pelos conhecimentos transmitidos.

Aproveito esta oportunidade para expressar minha gratidão e sincero apreço aos colegas do Centro Europeu de Investigação e Tecnologia Espaciais (European Space Research and Technology Centre – ESTEC), da Agência Espacial Europeia, por propiciar o aprofundamento dos conhecimentos práticos em técnicas de infraestruturas de simulação e validação de computadores de bordo. Em particular ao Eng. Joachim Fuchs por viabilizar os estágios e aos líderes Eng. Kjeld Hjortnaes e Eng. Robert Blommestijn, juntamente com os demais colegas de departamento, por me receberem em suas instalações,. Em especial ao Eng. Quirien Wijnands que conduziu minhas atividades com grande mestria e garantiu que minhas metas de aprendizado fossem atingidas [1].

Ao meu irmão Eng. Cleber Toss Hoffmann pelo imenso companheirismo e pelo apoio técnico no desenvolvimento do estudo de caso com hardware na malha.

Finalmente, mas não menos importante, à minha esposa Laura, filha Gisele e mãe Goret que me acompanharam nesta trajetória, provendo o suporte emocional e incentivo para a conclusão deste projeto.

[1]ACKNOWLEDGEMENTS: I take this opportunity to express my gratitude and sincere appreciation to the colleagues from the European Space Research and Technology Centre (ESTEC) of the European Space Agency, for making possible the development of my practical skills in simulation infrastructures and on-board computer validation techniques. Particularly to Mr. Joachim Fuchs for enabling the internships and to Mr. Kjeld Hjortnaes and Mr. Robert Blommestijn, together with other department colleagues, to welcome me into their facilities. Special thanks to Mr. Quirien Wijnands for guiding my activities with great mastery and for ensuring that my learning goals could be achieved.

ABSTRACT

Nowadays, computational simulation has a fundamental role on supporting engineering activities across the life cycle of a space mission. As a consequence, the pursuit for leaner processes and flexible tools has been the focus of numerous investigations in the system engineering and simulation fields. In this direction, the current work presents a novel approach for designing and conducting scenario of spacecraft simulation, envisaging the improvement of space engineering practices by employing computational steering methods. In the context of a scientific application, steering is a technique to enhance the level of user interaction in a computational system in order to allow a specialist to actively guide the course a simulation, by on-line changing model parameters and visually monitoring the effects on the scenario. In order to achieve such level of interactivity, in this work, an advanced simulation facility is proposed to combine state of art concepts on satellite simulation and the most relevant features of computational steering. The benefits of applying these concepts in the development of space systems are demonstrated in case studies inspired in real life problems, such as the verification and validation of a piece of flight software, commonly adopted to determine the direction of Sun on-board the spacecraft. The results have shown that the improvement of user interactivity in the spacecraft simulation is a promising approach to deal with geometrically complex scenarios and problems with high number of parameters, thereby contributing to streamline manifold space engineering processes.

O PAPEL DO *ESTERÇAMENTO COMPUTACIONAL* NAS ATIVIDADES DE ENGENHARIA ESPACIAL ASSISTIDAS POR MODELAGEM E SIMULAÇÃO DE SISTEMAS

RESUMO

Hoje em dia, a simulação computacional tem um papel fundamental no apoio às atividades de engenharia ao longo de todo o ciclo de vida de uma missão espacial. Como consequência, a busca por processos mais enxutos e ferramentas flexíveis tem sido o foco de inúmeras investigações nas áreas de engenharia de sistemas e simulação. Neste sentido, o presente trabalho apresenta uma nova abordagem para a concepção e condução de cenários de simulação de plataformas orbitais, visando à melhoria das práticas de engenharia espaciais por meio do emprego de métodos de *esterçamento computacional*. No contexto de aplicações científicas, *esterçamento* é uma técnica para melhorar o nível de interação do usuário em um sistema computacional de modo a permitir que um especialista possa guiar ativamente o curso de uma simulação, alterando parâmetros de modelos em tempo de execução e monitorando visualmente os efeitos no cenário. De maneira a atingir tal nível de interatividade, neste trabalho um ambiente avançado de simulação é proposto para combinar conceitos do estado da arte em simulação de satélite e as características mais relevantes de *esterçamento* computacional. Os benefícios da aplicação desses conceitos no desenvolvimento de sistemas espaciais são demonstrados em estudo de casos inpirados em problemas reais, tais como a verificação e validação de um artefato de software de voo, comumente empregado na determinação da direção do Sol a bordo da espaçonave. Os resultados mostraram que a melhoria da interatividade do usuário na simulação de satélites é uma abordagem promissora para se lidar com cenários geometricamente complexos e problemas com elevado número de parâmetros, contribuindo assim para tornar mais ágeis diversos processos de engenharia espacial.

LIST OF FIGURES

Page

LIST OF TABLES

LIST OF ACRONYMS

3D	–	Three-dimensional
AFAP	–	As Fast As Possible
AIT	–	Assembly, Integration and Test
AIV	–	Assembly, Integration and Verification
AOCS	–	Attitude and Orbit Control Subsystem
API	–	Application Programming Interface
AR	–	Augmented Reality
ARM	–	Advanced RISC Machine
AU	–	Astronomical Unit
CAD	–	Computer Aided Design
CASE	–	Computer-Aided Software Engineering
CAVE	–	(Computer Audio Visual Experience) Automatic Virtual Environment
CDR	–	Critical Design Review
CFD	–	Computational Fluid Dynamics
CRR	–	Commissioning Result Review
CSE	–	Computational Steering Environment
CSS	–	Coarse Solar Sensor
CUMULVS	–	Collaborative User Migration, User Library for Visualization and Steering
DEM	–	Discrete Element Method
DMIPS	–	Dhrystone Million Instructions Per Second
ECI	–	Earth Centred Inertial system
ECSS	–	European Cooperation for Space Standardization
EEPROM	–	Electrically Erasable Programmable Read-Only Memory
EGSE	–	Electrical Ground Support Equipment
ELR	–	End-of-Life Review
ESA	–	European Space Agency
ESOC	–	European Space Operations Centre
ESTEC	–	European Research and Technology Centre
FDIR	–	Fault Detection, Isolation and Recovery
FEM	–	Finite Elements Method
FOV	–	Field of View
FPU	–	Floating-Point Unit
FRR	–	Flight Readiness Review
GPS	–	Global Positioning System
GPU	–	Graphical Processing Units
GTK	–	Gimp Toolkit
GUI	–	Graphical User Interface
GYR	–	Gyroscope
HCI	–	Human-Computer Interaction
HITL	–	Hardware-in-the-loop

HLA	–	High Level Architecture
HW	–	Hardware
IDE	–	Integrated Design Environment
IEEE	–	Institute of Electrical and Electronics Engineers
INCOSE	–	International Council on Systems Engineering
INPE	–	Instituto Nacional de Pesquisas Espaciais
INTEGRAL	–	INTErnational Gamma-Ray Astrophysics Laboratory
IP	–	Internet Protocol
J2000	–	Julian epoch year 2000
LEO	–	Low Earth Orbit
LRR	–	Launch Readiness Review
MBSE	–	Model-Based System Engineering
M&C	–	Monitoring and Control
MCR	–	Mission Close-out Review
MCS	–	Mission Control System
MD5	–	Message-Digest algorithm 5
MDK	–	Model Development Kit
MDR	–	Mission Definition Review
MDVE	–	Model-Based Development and Verification Environment
MFC	–	Microsoft Fundation Classes
MGM	–	Magnetometer
MGT	–	Magnetometer
MOSAIC	–	Model-Oriented Software Architecture Interface Converter
MR	–	Mixed Reality
NASA	–	National Aeronautics and Space Administration
NLR	–	Nationaal Lucht-em Ruimtevaartlaboratorium
OBC	–	On-Board Computer
OBCFE	–	On-Board Computer Front-End
OBSW	–	On-Board Software
ORR	–	Operational Readiness Review
OS	–	Operating System
PC	–	Personal Computer
PDA	–	Personal Digital Assistant
PDR	–	Preliminary Design Review
PIM	–	Platform Independent Model
PMBOK	–	Project Management Body of Knowledge
PROBA	–	Project for On-Board Autonomy
PROGRESS	–	Program and Resource Steering System
PROSIM	–	Programme and Real time Operations SIMulation
PRR	–	Preliminary Requirements Review
PSE	–	Problem Solving Environment
PSM	–	Platform Specific Model

PTB	–	Project Test Bed
QR	–	Qualification Review
RAM	–	Random-Access Memory
RGB	–	Red-Green-Blue
RISC	–	Reduced Instruction Set Computing
RT	–	Real Time
RTB	–	Real-time Test Bench
SAG	–	Solar Array Generator
S/C	–	Spacecraft
SCOE	–	Special Check-Out Equipment
SCOS	–	Satellite Control and Operation System
SimDK	–	Simulation Development Kit
SIMSAT	–	Software Infrastructure for Modelling Satellites
SIMVIS	–	Simulation and Visualization tool
SMP	–	Simulation Modelling Platform
SOAP	–	Simple Object Access Protocol
SRAM	–	Static Random-Access Memory
SRR	–	System Requirements Review
STL	–	Standard Template Library
STK	–	Satellite Took Kit
STR	–	Star Tracker Sensor
SUT	–	System Under Test
SVF	–	Software Verification Facility
SW	–	Software
TCP	–	Transmission Control Protocol
TVE	–	Test and Verification Equipment
UI	–	User Interface
UML	–	Unified Modeling Language
USB	–	Universal Serial Bus
VASE	–	Visualization and Application Steering Environment
VIPER	–	VIsualization of massively Parallel simulation algorithms for Extended Research
VR	–	Virtual Reality
WAN	–	Wide Area Network
WBS	–	Work Breakdown Structure
WIMP	–	Windows, Icons, Menus and Pointing devices
w.r.t.	–	with respect to
XMI	–	XML Metadata Interchange
XML	–	eXtensible Markup Language
XMM	–	X-ray Multi-Mirror

CONTENTS

Page

1 INTRODUCTION

The work of this thesis is based on the spacecraft simulation and computational steering fields and how their techniques can support the space system engineering activities.

In the history of space exploration, simulation has been performing an important role in the spacecraft development to study complex phenomena and foresee the behaviour of systems. Combined with model driven system engineering methods, computational simulators became strategic to anticipate the verification and validation phases and thus, minimizing risks in the design and construction of satellites. Another driver is cost reduction, in the sense that these tools can lead to leaner processes, since software artefacts are more flexible to build and maintain, when compared to hardware models (HENDRICKS; EICKHOFF, 2005).

As computer power has grown over years, many improvements have been incorporated to the simulation systems: high fidelity models increase the precision and reliability of results; complex scenarios now run faster; better graphical resources ease the results interpretation; and new interfaces enhances the usability of the virtual system. As a result, computer simulators have been used in multiple applications in space system engineering, such as mission architecture optimization, feasibility studies, trade-off analysis, operability demonstrations, critical systems verification, training, among others (ECSS, 2010a).

Along with the development of more comprehensive and sophisticated tools, many efforts have been made to enhance the human-machine interface and improve their usability by incorporating innovations brought from correlated areas, such as computer graphics and virtual reality (STODDEN; GALASSO, 1995; KIMURA, 1998; MUSETH et al., 2001). As a result, nowadays most of the spacecraft simulators can take advantage of 3D graphics generator systems to explicitly display geometrical data (e.g. orbit, trajectories, and body's attitude), thus enhancing the insight into the model behaviour. In addition to that, pioneering systems in computer games are fuelling revolutionary human-in-the-loop environments, thereby new training (FREUND et al., 2003; STONE et al., 2011b; RIZE et al., 2014) and tele-operation (SAGARDIA et al., 2013; NORRIS; DAVIDOFF, 2014) applications have been proposed . In spite of important contributions to incorporate 3D visualisation and to improve the immersion experience, the online interaction in spacecraft simulation environments are essentially limited to control the visualisation system (i.e. controlling the 3D camera, selecting perspective, adjusting the zoom, etc.) or to stimulate the model from the operator's perspective.

In this context, additional improvements have been presented by recent works in applications in which the engineers can directly interact with the parameters of a 3D digital satellite mock-up. Duro et al. (2008) describe a simulation for performing virtual assembly of spacecraft hardware, which could be employed to support assembly, integration & test (AIT) activities (CADETE et al., 2010). Similarly, Fischer et al. (2012) show a collaborative simulation tool to visually assist the mechanical configuration design of a satellite in concurrent engineering sessions. Although these works point out some of the advantages in interactive simulations, their results focus on the mechanical models and geometric variables, restricting the user's interventions to a very small set of parameters that could benefit from online manipulation.

In comparison to these approaches, other scientific domains have enhanced the level of user interactivity by expanding their controlling capacity to all aspects of the computational model in a simulation application. When this control is done online by the user, while the results are continuously visualised, this simulation technique is known as computational steering (MARSHALL et al., 1990). Since its early developments, in the beginning of 90's, this method has brought flexibility to investigate the behaviour of phenomena, increasing the insight and transforming the way many scientific problems are addressed. In contrast to script mechanisms, for instance, in which test cases are controlled by a predefined set of statements and rules, computational steering let the user to freely interfere in the evolution of the simulation, bringing it to regions of interest in the state space, which would not be achieved, or at least easily performed, by means of a preordained configuration.

In this direction, envisaging the enhancement of user flexibility on conducting simulations, the **goal of this thesis** is to demonstrate the application of computational steering techniques in the context of activities typically performed in the space engineering domain. These activities support the whole life cycle of a mission, covering the conception, design, construction, integration, verification and validation, operation, and decommissioning of a spacecraft. The benefits from improving the level of interactivity in the simulation environment are evidenced by a set of case studies described in this work, wherein the engineer plays a central role on controlling the evolution of the scenario as the model behaviours are analysed.

The elaboration of illustrative scenarios is supported by a software infrastructure especially constructed to combine the most relevant computational steering features

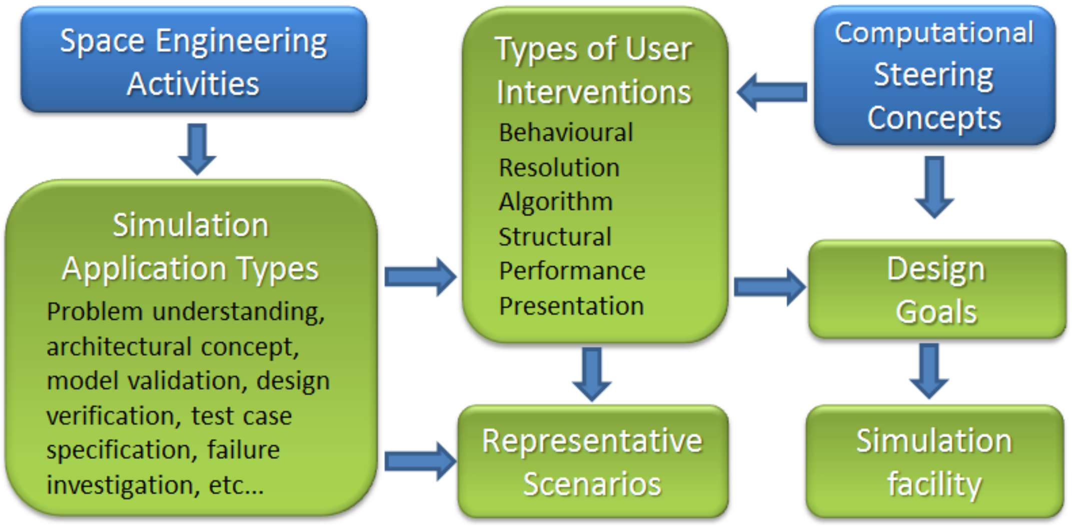
Space Engineering Activities
Simulation Application Types
Problem understanding, architectural concept, model validation, design verification, test case specification, failure investigation, etc...
Types of User Interventions
Behavioural
Resolution
Algorithm
Structural
Performance
Presentation
Computational Steering Concepts
Design Goals
Representative Scenarios
Simulation facility

Figure 1.1 - Logical workflow representing the strategy for developing this thesis.

with the state-of-the-art mechanisms in satellite simulation. Its development is guided by a set of functionalities elicited after an extensive review in the literature to examine the activities commonly present in space projects that are supported by systems modelling and simulation and to investigate the computational steering concepts and its applications. Based on the theoretical background, several types of simulation applications are identified, each of them requiring a different set of user intervention types during a simulation session. These characteristics of usage and usability drive the specification of representative scenarios that will cover a broad range of space engineering use cases and, consequently, that must be supported by the simulation infrastructure. The logical workflow representing the strategy for developing this thesis is illustrated in the Figure 1.1.

Furthermore, in order to become a cost-effective facility, the proposed software architecture must be generic to promote the reuse and to ease the reconfiguration of the environment to different use cases. For many years, the complexity on codifying such flexible software has been addressed by the adoption of generic programming methodologies, like templates, design patterns, meta-modelling, and frameworks (GIBBONS, 2007). In the spacecraft simulation context, these techniques have supported the development of Simulation Modelling Platform 2 (SMP2) standard, which defines the basis for reusing simulation artefacts among platforms and projects (ECSS, 2011a). By implementing main mechanisms of SMP2, the infrastructure designed in this work can be readily configured to a wide range of simulation applications. On the top of that, specialised steering components provide the user with a suitable interface to deal with manifold facets associated to the parameterization of a computational model (e.g. variables of the numerical method, modelling resolution, computational resources usage, and properties of the algorithm).

As a consequence, it is expected that the enhancement of interactivity level in spacecraft simulators brings more agility to the space engineering activities along the mission life cycle. Multiple use cases can benefit from the flexibility on steering the scenarios, especially when the search in the state space is huge or understanding the emergent properties of the system is complex, like those frequently found in satellite applications. In space mission concept phases, for instance, the effects on the power generation efficiency could be immediately observed while the orbital geometry is changed or the orientation of solar array generator is updated, easing the power balance analysis. Similarly, for critical on-board software verification, failures could be injected to check the implementation robustness or the environmental conditions altered to assess the performance of autonomous behaviour. This highly flexible environment is also particularly desirable in training applications for the mission control centre, whereby the tutor can increase the dynamics of the scenarios by changing its evolution accordingly to the operator responses.

Considering the context of space missions at *Instituto Nacional de Pesquisas Espaciais* (INPE), the introduction of flexible simulation infrastructures in the satellite projects may impact on the way the system engineering activities are conducted nowadays. For instance, the development of Concurrent Design Facilities, strongly based on simulation, can accelerate and bring more precision to the studies of new missions. At the same time, the reliability of critical systems, such as attitude and orbit control avionics, shall rapidly increase with the availability of high fidelity test environments.

1.1 Background and Motivation

More than fifty years have passed since *Sputnik* – the first artificial satellite in mankind history – and the space exploration still poses challenges for constructing reliable spacecraft and rockets. Particularly due to their specialized applications and harmful operational environment, hard to reproduce and to test on the ground, the manufacturing of space systems is complex and it demands well-established and controlled engineering processes.

Through the years, system engineering has developed different methodologies to reduce risks and to cope with the management of complex projects. Currently, the development life cycle of satellites does not differ much from other projects that organise the activities in initialisation, execution and closing phases, accordingly to the processes described in the best practices guides from the Project Management Body of Knowledge (PMBOK) (PMI, 2004) or the International Council on Systems Engineering (INCOSE) (ESTEFAN, 2008).

Typically, the concept, design, production and operational activities in space programmes are structured in the following phases (ECSS, 2009c) [1]:

- Phase 0 – mission analysis/needs identification;
- Phase A – feasibility;
- Phase B – preliminary definition;
- Phase C – detailed definition;
- Phase D – qualification and production;
- Phase E – utilisation; and
- Phase F – disposal.

As illustrated in Figure 1.2, special milestones, in the form of review boards, mark the transition from one phase to the next and characterise specific development stages of activities (i.e. Mission Definition Review (MDR), Preliminary Requirements Review (PRR), System Requirements Review (SRR), Preliminary Design Review (PDR), Critical Design Review (CDR), Qualification Review (QR), Acceptance Review (AR), Operational Readiness Review (ORR), Flight Readiness Review (FRR), Launch Readiness Review (LRR), Commissioning Result Review (CRR), End-of-Life Review (ELR), and Mission Close-out Review (MCR)) (ECSS, 2009c). In the beginning of the life cycle, the level of abstraction in the project is high and all the effort is focused on defining the mission concept and specifying the system. As the time evolves, the architecture is detailed, beginning from level 0 in the Work Breakdown Structure (WBS), until the engineering data is complete enough to start the production.

[1]Depending on the project or the industry, the name and number of the phases, the milestones and timing of the activities can vary, but the general scheme and approach is basically the same.

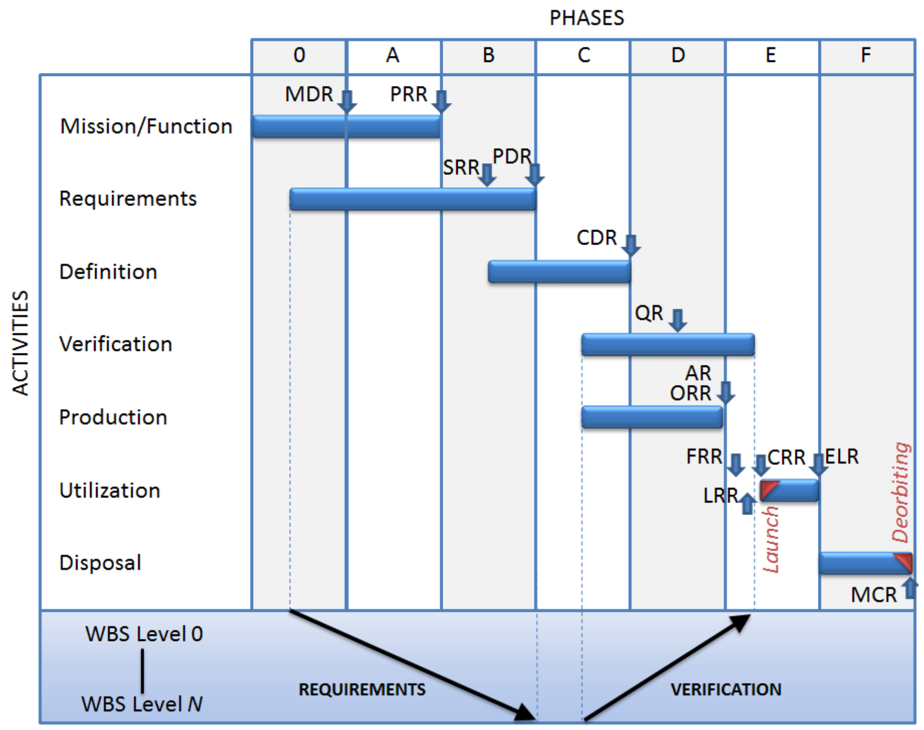

Figure 1.2 - Typical life cycle adopted in space engineering projects.
Source: Adapted from ECSS (1996) and ECSS (2009c)

In contrast to the specification phases, the production usually follows a bottom-up approach, i.e. first the low level components of the system are built and then gradually integrated and tested, until the whole system is constructed. The top-down and then bottom-up are frequently seen as the V-Model, since the graphical representation of the development life cycle resembles the shape of "Vee" character (ECSS, 2009c). Traditionally, the left side of the character represents the process chain for the definition activities, such as requirements specification, architectural and detailed design. Next, on the bottom of the "V", the implementation is performed and the then the integration, test, verification and validation steps come in sequence on the right. Lastly, the commissioning and operation of the spacecraft is represented by the phase E, which varies in lifetime depending on the mission, until its decommissioning in phase F.

The verification and validation (V&V) of the products are done against the technical specification and design, regarding their level of detail in the construction and integration step. The purpose of this phase is to ensure that the components were built without errors and the integrated system covers the final user needs (BALCI, 1995). The later a compliance issue is detected, the worst, in the sense of cost and time, it becomes to fix, due to the number of requirements affected, the potential impact on other components, and the rework (MARTIN; CARVALHO, 2005; COURTER, 2009). Hence, one way to avoid the presence of nonconformities, late on the final system, was to introduce the construction and test of intermediate products, in development process. Until today, this is the prevailing approach adopted, where the set of prototypes, including the final product, is built and known as the *model philosophy* of the mission. Each model has a clear goal to demonstrate the correctness of project design and construction process from the perspective of a certain engineering area (i.e. thermal, mechanical, electrical, etc. . .) and from a different integration level of equipment, subsystem or system (ECSS, 2009a; ECSS, 2010b).

In the traditional V&V strategy adopted in space projects, most of the engineering models are pieces of hardware and their own construction demand substantial amount of time and resources. For many missions, delaying the delivery of these models may imply major impacts in the whole schedule, particularly for those with a large number of flight computers components, whose on-board software (OBSW) depends on the hardware to be tested. In addition to that, the unavailability of hardware models in the initial phases of a project makes the early verification and validation of intermediate steps of design process a complex task.

A new improvement in the life cycle is then achieved with the introduction of Model-Based System Engineering (MBSE) concepts, wherewith the models now are formal representations that can be used to specify, verify and validate the system (ESTEFAN, 2008). As the project progresses, all the engineering information is stored in a structured form, thereby enabling an easy data exchange between team and tools. Based on the models, simulators can be used to predict the behaviour of the system, before it is actually built, and thus anticipate the execution of V&V processes, which can be done iteratively as the models are detailed.

The MBSE methods can be applied as incremental cycles of specification, design, eventually implementation, and then V&V to create nested "V" processes inside the V-Model. This paradigm, illustrated in Figure 1.3, is particularly attractive to accelerate the on-board software development process, in which computational simulators can be built from high fidelity engineering models and replace hardware prototypes. In this component, the uppermost "V" represents the design of algorithms (e.g. containing the laws for attitude control) originated from the mission definition activities and verified in a representative simulation of platform and space

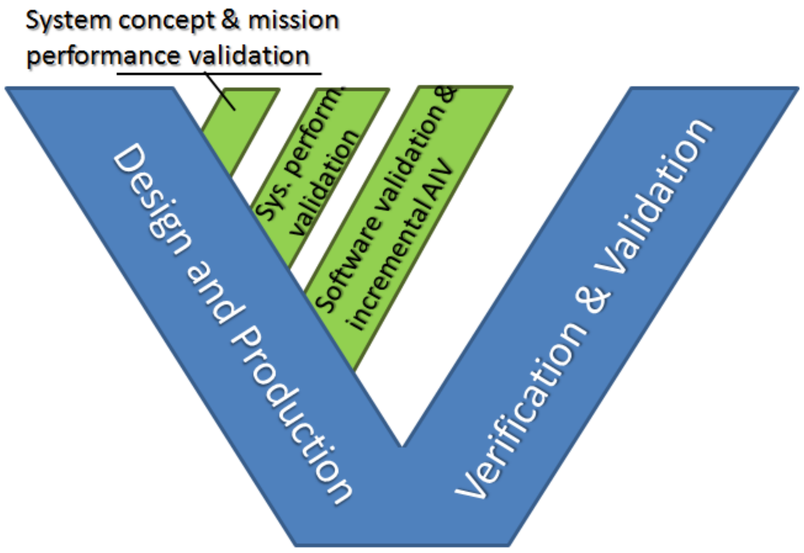
System concept & mission performance validation
Sys. perform. validation
Software validation & incremental AIV
Design and Production
Verification & Validation

Figure 1.3 - The adoption of V-Model supported by Modelling and Simulation.
Source: Adapted from ECSS (2010a)

environment. Subsequently, the OBSW model is detailed and implemented using the on-board programming language (e.g. C or Ada) and then tested with an emulator that mimics the real hardware platform. Finally, when an engineering prototype of the on-board computer becomes available, the software can be embedded and its interfaces with the real hardware can be tested.

The same approach of using simulators to anticipate the design verification of OBSW can be applied to other fields of space engineering, like thermal design, mechanical, power generation & distribution, telecommunication, and also to the ground processes such as assembly & integration and operations.

Nevertheless, the development of high fidelity and well-specialised simulation tools can be itself a complex, risky and time consuming task, which could represent no economic gain when compared to the construction of hardware models. To avoid this scenario, advanced software engineering methods have been applied to rationalize the construction of simulation infrastructures, thereby maximizing the reuse of software components, models, test procedures and development tools.

In this direction, the European space community, led by the European Space Agency (ESA), has been identifying communalities of spacecraft simulators and strategies for their efficient development. In the frame of European Cooperation for Space Standardization (ECSS) initiative, several technical memorandums have been published to promote the reuse of simulation resources along the spacecraft project and across multiple missions.

For instance, in the *System Modelling and Simulation* (ECSS-E-TM-10-21A), eight types of facilities are identified to support space engineering activities. Their configuration can evolve and new modules can be added during the progress of the project, but the infrastructure and models components can remain the same. Complementary, the *Simulation Modelling Platform* collection (ECSS-E-TM-40-07 A) defines a set of guidelines and directives to build infrastructures that allow model portability and increase the compatibility among modelling and configuration tools.

In the set of facility requirements defined by the ECSS-E-TM-10-21A it is also recognised the importance of the 3D visualization system, particularly for the early activities in the mission concept phase, as already discussed by several works in the literature (STODDEN; GALASSO, 1995; KIMURA, 1998). Nowadays, the basic 3D animation of orbit, trajectory, and attitude configuration is usually provided by well-stablished commercial and open-source products like Satellite Tool Kit (STK) of Analytical Graphics Inc. (ANALYTICAL GRAPHICS, INC, 2007), Celestia (LAUREL, 2006), OpenIGS (SKLUZACEK; PLAS, 2010), TechViz [2], and Astos [3], to which independent dynamics simulators can be attached (GENTINA, 2010; REBELO et al., 2010; WITT et al., 2010; BAI; WU, 2011; HAO et al., 2011). Alternatively, customised applications have been built directly on the basis of computer graphics libraries, such as OpenGL (HASSMANN, 2008; WU et al., 2012), Open-Scene Graph (OGS) (TANG; GUO, 2011), and Object-oriented Graphics Rendering Engine (OGRE) (GAO et al., 2011).

Furthermore, the relevance of 3D animations in the operational phase has been discussed by Chatel et al. (2006) as fundamental tools to support the analysis of spacecraft behaviour in orbit. Moreover, in this phase, 3D interfaces have been used to display the status of simulation or spacecraft parameters (DONATI et al., 2004; CERQUEIRA, 2014) and even to easy the mission documentation browsing (BETTS et al., 2002; PAPASIN et al., 2003).

Although these tools have brought productivity to simulation and reliability on assessing the models and the system behaviour, the user interactivity in the presented works are basically limited to the visualisation of scenarios and little access to the model parameters is provided.

[2]http://www.techviz.net

[3]https://www.astos.de

1.2 Contributions

The main contribution of this work is the demonstration of the role of computational steering techniques in the space engineering domain, aiming at increasing user's interactivity in simulation environments and promoting user's flexibility on controlling simulation scenarios. In conjunction with an advanced simulation facility, this approach can improve multiple engineering processes, by fostering engineering insight and reducing the effort to perform software simulations in activities like mission concept definition, budget analysis, performance evaluation, software testing, procedures verification, failure investigations and training.

This thesis is a multidisciplinary work, which is based on the latest advances on, at least, the following fields of study: space engineering, computer simulation, software engineering, and human-computer interaction (HCI). Combined, these areas have brought significant improvement for the development of complex systems and the dissemination of computer applications in many engineering domains. Looking at their contributions from the perspective of a Venn diagram, as illustrated in Figure 1.4, one could attribute the emergence of some cutting-edge techniques as a result of the composition of innovations provided by all of these areas. For instance, virtual reality and computational steering have both benefited from the improvements in simulation and HCI; HCI and software engineering have revolutionised the construction of user interface frameworks; space systems engineering has expanded the concepts of model-driven architecture approaches, previously developed by software engineering; and the designing ways of space systems are being changed by modern simulators. Similarly, computer games and virtual reality frameworks have incorporated many of the improvements in simulation, HCI and software engineering, while the combination of simulation, software engineering and space system engineering led to the creation of better spacecraft simulation facilities.

Viewing form this perspective, it is possible to say that the present work expands the state-of-the-art on spacecraft simulation, and consequently on space engineering, by combining the relevant improvements in all these four areas and adding the following contributions:

- A novel steerable simulation facility. A generic framework that allows any model that implements a standardised interface to publish its parameters as *steerable field*, which can be connected to *steering widgets* for online

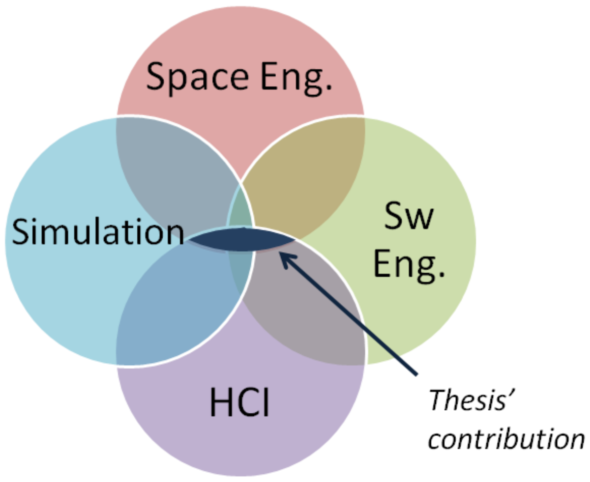

Figure 1.4 - Positioning of the contribution of thesis within the related fields of study.

manipulation. The adoption of meta-modelling concepts makes the steering artefacts portable to different scenarios and reusable in multiple use cases. Furthermore, scheduling parameters can be accessed during execution time via dedicated interfaces of the simulation kernel.

- A new classification of computational steering mechanisms, which is based on the intervention types that the user may apply in the computational model. This organisation supports the specification of design goals of simulation facilities and guides its implementations.

- A new set of tooling for editing and deploying simulation artefacts based on UML.

- The identification of a set of steering widgets for handling parameters common in the space engineering domain, such as quaternions, 3D vectors and Sun position.

- The demonstration of simulation interoperability with a legacy thermal simulator. A synchronous mechanism for interfacing the steerable simulator with a commercial simulator was developed to demonstrate the interoperability of legacy models in a soft real-time scenario. This approach can increase the fidelity of simulations, by expanding the application of complex thermal models to different environments.

- An innovative *Design Pattern* for implementing models described by Ordinary Differential Equations. This generic object-oriented architecture decouples the development of numerical integrators from the simulation models, allowing their assembly in run-time. This solution will typically be used for modelling the orbit and attitude dynamics of the platforms.

1.2.1 Published works

The results of this thesis have been published in the following works:

Articles

- HOFFMANN, L. T.; MOREIRA, C. J. A.; LOPES, I.; HIDALGO, M. A.; LOPES, R. V. F. AMoRe – An Accredited Model Repository Towards the Reuse on AOCS Projects. In: 24th International Symposium on Space Flight Dynamics, Laurel, MD, 2014.
- AZEVEDO, D. R.; HOFFMANN, L. T.; Ambrosio, Ana Maria ; Perondi, L. F. Analysis of the Simulation Model Platform (SMP) Adoption in the Context of INPE Simulators. In: Workshop on Simulation & EGSE facilities for Space Programmes (SESP), Noordwijk, 2012.
- HOFFMANN, L. T.; Perondi, L. F. Mecanismo de um escalonador de tarefas baseado em SMP2. In: I Workshop em Engenharia e Tecnologia Espaciais, São José dos Campos, 2010.
- HOFFMANN, L. T.; Perondi, L. F. Estudo de simuladores computacionais aplicados ao ciclo de desenvolvimento de plataformas orbitais. In: I Workshop em Engenharia e Tecnologia Espaciais, São José dos Campos, 2010.
- BARRETO, Joaquim P.; HOFFMANN, L. T.; Ambrosio, Ana Maria . Using SMP2 standard in operational and analytical simulators. In: SpaceOps, Huntsville, 2010.

Extended Abstracts

- HOFFMANN, L. T.; MOREIRA, C. J. A.; STRIEDER, C.; LOPES, I.; LOPES, R. V. F. Development of a Spacecraft Dynamics Simulator to the Brazilian Multi-Mission Platform MMP. In: Workshop on Simulation & EGSE facilities for Space Programmes (SESP), Noordwijk, 2012.

- HOFFMANN, L. T.; Perondi, L. F. Increasing user Interactivity in Spacecraft Simulations. In: Workshop on Simulation & EGSE facilities for Space Programmes (SESP), Noordwijk, 2012.
- MOREIRA, C. J. A.; HOFFMANN, L. T.; STRIEDER, C.; LOPES, I.; HIDALGO, M. A.; LOPES, R. V. F. Desenvolvimento de um simulador da dinâmica de satélites para a Plataforma Multi-Missão Brasileira. In: XVI Colóquio Brasileiro de Dinâmica Orbital, Serra Negra, 2012.

1.3 Thesis Outline

Spacecraft simulation and computational steering are the two main fields that substantiate the development of the current work with theoretical concepts. For this reason, the state-of-the-art in these areas is presented separately in the next two chapters. Based on them, the role of computational steering in space engineering is discussed and followed by a description of a satellite simulation facility powered by steering mechanisms. The promising applications of the approach and tools proposed in this work are demonstrated by a series of case studies of typical satellite simulation scenarios. Finally, the conclusions and future works are exposed.

The remainder of this document is organised as follows:

- **Chapter 2. Spacecraft Simulation** —This chapter presents the fundamental concepts of computer simulation and the overall architecture commonly adopted by tools in the space engineering domain. The types and applications of spacecraft simulators are described, accordingly to the definitions of the *European Cooperation for Space Standardization* initiative. After, their development requirements are discussed from the viewpoint of the *Simulation Modelling Platform* standard.
- **Chapter 3. User Interactivity and Computational Steering** —The main features of computational steering environments are provided in this chapter, including their relation to the user interactivity concepts. Existing applications and taxonomies are presented.
- **Chapter 4. The Role of Computational Steering in Space Engineering** —In this chapter, the benefits of using the computational steering technique are shown and compared against the traditional post-processed approach. Its adoption in typical space engineering

activities supported by simulation is then discussed. After, a novel computational steering classification is proposed.

- **Chapter 5. A Novel Computational Steering Facility Applied to Spacecraft Simulation** —The common features of steering environments and spacecraft simulators are summarized in this chapter, followed by the identification of the design goals for building the proposed facility. Next, all the components of the software architecture are described, including the tools for developing simulation artefacts and the modules for loading, running, controlling, visualising, and steering the scenarios.

- **Chapter 6. Case Studies** —A series of case studies are presented in this chapter to show the advantages of computational steering within satellite simulation domain. In total, eleven scenarios have been chosen to cover different aspects of user interventions, user interfaces and steering functionalities in representative applications of space engineering. In each case, a brief description of employed simulation components and artefacts is given, in addition to the simulation goal and the characteristics of the modelled problem. The results demonstrate the flexibility of space engineer to online interact with simulation and his/her agility to test new hypothesis as the scenario evolves.

- **Chapter 7. Conclusion** —This chapter summarises the results and consequences of the contributions presented in this thesis and the potential research themes that can be derived for future works.

2 SPACECRAFT SIMULATION

In the context of this thesis, a simulator is any computational system that by means of a formal model is capable of reproducing the behaviour of an entity (GOULD; TOBOCHNIK, 1996). This technique has been widely applicable to better understand phenomena, complex systems, processes, and their relations with other elements of the real world (ADKINS; POOCH, 1977). In the space engineering domain, these tools are admittedly key tools for space systems verification (ECSS, 2009a; ECSS, 2009b; NASA, NATIONAL AERONAUTICS AND SPACE ADMINISTRATION, 2008).

Several simulation use cases are described in the literature that supports different levels and phases of a space mission development. Some of them are applied to specific components of the space system, such as the design and analysis of data communication devices (AGRE et al., 1987; DOWNING, 2006), whereas others cover ground activities, as operator training and procedures validation (WILLIAMS, 1993). High fidelity environments may also assist the assembly, integration and test of hardware devices (SCHENAU et al., 1998; BODIN et al., 2012) or even allow the inclusion of man-in-the-loop of very complex simulations (JOHN et al., 1987).

When the space system embeds some source of autonomous controller, the simulation plays an important role in the process of verification and validation of control laws and performance assessment, since the loop with the plant is usually closed by a virtual environment. Example of these applications includes the construction of orbit and attitude control subsystems (KANG et al., 1995; ELFVING, 1999), evaluation of robotic arm operation (FREUND et al., 2003), and navigation system design for interplanetary mobile robots (ESTLIN et al., 2008).

In the scope of the Complete Brazilian Space Mission, several simulators have been employed for design assessment of space and ground systems of the Data-Collecting Satellite mission. Some examples include the evaluation of power generation architecture (PERONDI, 1987), attitude control algorithms (FERREIRA; CRUZ, 1991), and validation of ground procedures (ORLANDO et al., 1992). A review of operational simulators applied in Brazilian ground segment is presented by Ambrosio et al. (2006).

The increasing number of works published recently shows the continuous interest and relevance of this field (NESNAS, 2007; HASSMANN, 2008; SEBASTIAO et al., 2008; FRITZEN, 2009; FRITZ; ROESER, 2010; REGGESTAD et al., 2011; CAZENAVE; ARROUY, 2012; IRVINE et al., 2013; KRANZ, 2014).

Traditionally, the strategy of building simulators to support space engineering process has been adopted since the early days of space race, wherein, for instance, models executed in analogue computers have been used to assist spacecraft designers from the *National Aeronautics and Space Administration* (NASA), in 60's (JOHN et al., 1987). All the determination for developing new simulation technology since then is now reflected in the vast number of engineering fields that make use of these tools in their processes, such as mission analysis, on-board software development, verification and validation in system and subsystem levels, assembly & integration campaigns, ground teams and astronauts training, support on mission operations, among others (AGRE et al., 1987; NASA, 1989; LICEAGA, 1997; BETTS et al., 2002; PAPASIN et al., 2003; FREUND et al., 2003; PISANICH et al., 2004; NESNAS, 2007; HAMMERS, 2008).

Led by European Space Agency (ESA), significant effort has also been conducted in European community for developing and integrating better simulation tools into the engineering activities, thus enhancing the quality of processes. Historically, independent demands have driven the construction of dedicated applications, particularly oriented for the activities from *European Space Operations Centre* (ESOC) and *European Space Research and Technology Centre* (ESTEC). At the former, the need for a system to validate procedures and to train operators led to the construction of the *Software Infrastructure for Modelling Satellites* (SIMSAT), a package for building operational simulators (WILLIAMS, 1993). In complement, the improvement of environments to facilitate system engineering activities and the design and production of avionics has been the focus at ESTEC.

One of these tools is the *Project Test Bed* (PTB), presented by Franco & Miró (1998) as a multi-purpose simulation and verification platform to support the definition of mission concepts and architecture, in the early phases of space projects. By the adoption of a 3D graphical visualization of simulation outputs, the system provides an intuitive front-end for mission requirements verification. Initially it is applied in the project of PROBA (*Project for On-Board Autonomy*) satellites, but it is intended to be reused in other missions.

In order to achieve such flexibility, PTB is based on a common infrastructure known as *EuroSim*, a real-time framework for building simulations in the space and non-space domains, developed by a consortium of European companies and the National Aerospace Laboratory (NLR, from *Nationaal Lucht-em Ruimtevaartlaboratorium* in Dutch) of the Netherlands. Widely adopted in projects

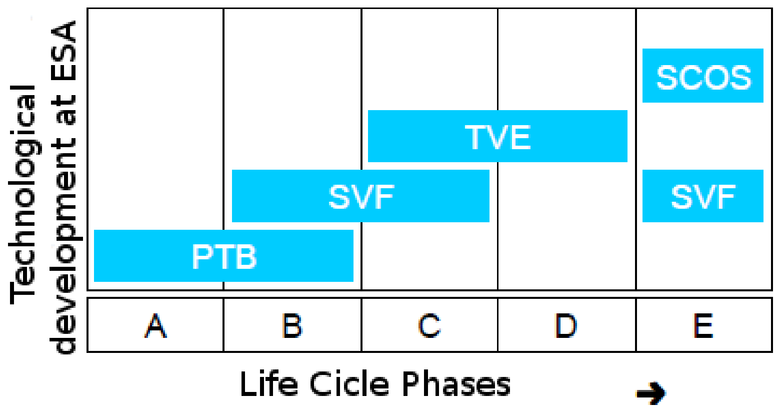

Figure 2.1 - Historical simulation usage in ESA along the spacecraft project's life cycle. Source: Adapted from Timmermans et al. (2001)

at ESTEC, this system provides generic interfaces for model development and integration, scheduling and execution of events, and data presentation (VRIES et al., 2002).

In the same direction of PTB of rationalising infrastructure resources, NLR has proposed the *Test and Verification Equipment* (TVE), a new generation of equipment used to test, verification and validation of XMM and INTEGRAL missions (SCHENAU et al., 1998). TVE comprises a set of hardware and software elements structured in a layered architecture, in which the lowest layer is the front-end interface with the system under test, followed by the communication layer, and finally the test software. The latter embeds the *Programme and Real time Operations SIMulation* (PROSIM), a legacy application.

As the development of TVE progresses, its adoption is expanded to new use cases, covering various phases of project's life time (BROUWER et al., 2000; TIMMERMANS et al., 2001). In order to achieve such level of communality, the facility has combined several existing products to create a flexible and multi-functionality environment. In addition to the PTB and *EuroSim*, the *Software Verification Facility* (SVF) has been used as the on-board computer emulator and the *Satellite Control and Operation System* 2000 (SCOS-2000) as the checkout equipment [1]. The application comprehensiveness of these facilities is illustrated in Figure 2.1, accordingly to the project's life cycle phases.

[1]SCOS-2000 is originally designed to serve as an operational tool for controlling satellites at ESOC

2.1 Simulation Role in Space Engineering Activities

As previously discussed, simulation plays an important role to support space engineering activities in different phases of a space mission. In this section, some examples found in the bibliography are presented.

In the early steps of the project, requirements from stakeholders are identified and mission analysis is performed. Generic-purpose simulators are employed to bring up possible architectures that meet these requirements and to conduct trade-off studies (SCHUMANN et al., 2008; SCHAUS et al., 2010). Typically in this phase, the first studies on orbit definition and attitude type are conducted (CARRARA; MEDEIROS, 1996), (PRUDÊNCIO, 1997), (HASSMANN, 2008). A well-known example of commercial software applied in these activities is the Simulation Tool Kit (STK), but it is also common that customised simulation tools are developed to support the system engineers in these activities (KALDEN et al., 2007; PALOMBA et al., 2008; LIU et al., 2010; TANG; GUO, 2011; KRANZ, 2014).

Moreover, multi-objective optimization tools can be attached to the simulators to automatically search the parameter state space and compare a large number of solutions (CUCO et al., 2008; STUMP et al., 2009; LEGO et al., 2010).

As the project evolves to Phase A, more detailed analysis are done on power, mass, thermal, and communication budget (PERONDI, 1987; LICEAGA, 1997; DEFOUG; ZIMMERMANN, 2006).

In addition, specialized applications can be used to assess the proposed architecture with respect to the scientific goals of the mission, which are known as *end-to-end* simulators and they are focused on modelling payload functionalities and user segment aspects (RAMOS et al., 2008; POLVERINI; LARRIEU, 2008).

When the project enters Phase B, a baseline concept is chosen, the system architecture is defined and the external interfaces among the subsystems are identified. In this phase the development of flight software can be started based on simulation environments that embody hardware emulators of the target computers. Later, in the Phase C, the on-board software is verified and performance campaigns are executed to tune the AOCS parameters (SONDERMANN et al., 2008). Progressively the emulators can be replaced by physical engineering models of the actual on-board computer in order to validate the flight software and its physical interfaces (ELFVING, 1999; KALDEN; IRVINE, 2011).

During the Phase D, the simulation infrastructures adopted in the previous phases may be reused to support the assembly, integration and test (AIT) campaigns and gradually be replaced by the actual subsystems as they are integrated. Moreover, simulation in this phase is a powerful tool to evaluate and define AIT procedures, before the physical models are made available (NEEFS; HAYE, 2010; CADETE et al., 2010).

Previously to the satellite launch and commissioning, distinct simulators are employed to validate ground systems (e.g. satellite and mission control software and ground station devices for tracking, telemetry and commanding)(LAROQUE et al., 2008), operational procedures, and provide a training environment for operators (WILLIAMS, 1993; ORLANDO et al., 1992; FREUND et al., 2003; AMBROSIO et al., 2007; TOMINAGA et al., 2008; PIDGEON et al., 2008; NAYAR et al., 2009; DENNISTON et al., 2012; WERKMAN et al., 2012). The model fidelity adopted in this phase should be the highest as possible, mostly when the simulator will assist the execution of critical task, such as planning of orbital and attitude manoeuvres, fault diagnosis analysis, or validation of on-board patch before upload (REGGESTAD et al., 2011).

Finally, in the end of satellite's life time (Phase F), decommissioning studies can be conducted by simulation tools that compute accurate manoeuvres and define deorbit trajectories and debris impact area (OLIVEIRA, 2009; LING, 2014).

2.2 Architecture and Common Features of Spacecraft Simulation Environments

A spacecraft simulation infrastructure comprises of a facility composed of hardware and software elements that executing a simulation model extracts behavioural information or emulates environmental conditions to test a space system device and operational procedures. From the perspective of software discipline, the architecture of these systems is pretty much the same than other computational applications. Typical requirements commonly present in other domains, such as flexibility, software reuse and interoperability, are also applied to spacecraft simulators (WILLIAMS, 1993; BIESIADECKI et al., 1997; TURNER, 2006; LIM; JAIN, 2009) - and even for on-board software projects (PASETTI, 2002) - and frequently implemented with modern programming languages like C++, Java or .NET. Still, from the space engineering point of view, special care has been given for the development of high fidelity models and reliable infrastructures to facilitate the design, construction and qualification of complex space systems.

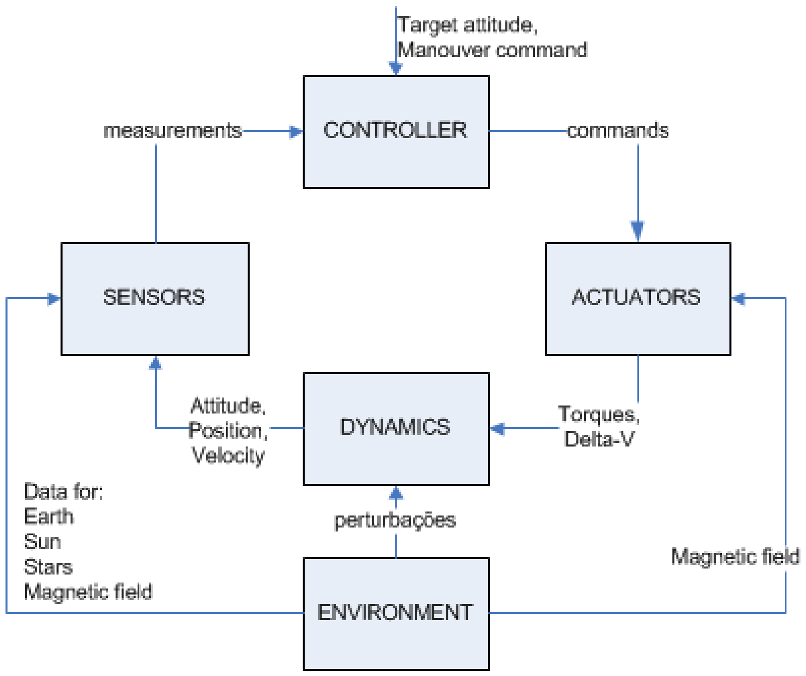

Figure 2.2 - Generic attitude control system and simulated elements.
Source: Adapted from Brouwer et al. (2000)

Since the reproduction of space environment is hard to achieve on the ground, particular attention is given on the construction of simulation facilities to support the development of Attitude and Orbit Control Subsystems (AOCS). The main challenge is accurately simulate the platform dynamics against the environmental perturbations, noisy sensors and actuators and close the loop with the control algorithm. The central feature consists in emulating the sensorial interfaces accordingly to the current simulation state and processing the actuator signals to propagate the next attitude and orbital dynamics state (SCHENAU et al., 1998). The basic architecture is illustrated in Figure 2.2, in which the environmental module provides additional models as required by the scenario (e.g. celestial bodies geometry, solar flux, geomagnetic field, atmospheric drag, environmental radiation, thermal effects, etc.).

Depending on the development stage, real pieces of equipment may be integrated in the facility and replace simulation models for better fidelity or to test physical interfaces and hardware features of avionics. The integration is feasible thanks to auxiliary hardware devices that handle signal conditioning and support the interface with flight equipment. The overall structure of this facility is shown in Figure 2.3 and its often referenced as *Electrical Ground Support Equipment* (EGSE).

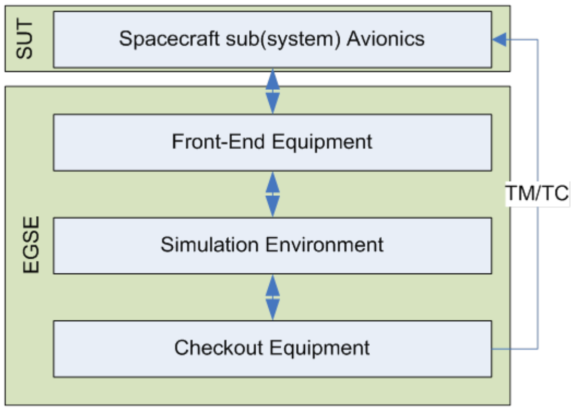

Figure 2.3 - Overall architecture of an avionics testing equipment.
Source: Adapted from Brouwer et al. (2000)

The conceptual architecture of an EGSE is described by Brouwer et al. (2000) as a four tier system, in which the simulation infrastructure becomes one of the multiple components of the environment for testing flight equipment, as illustrated in Figure 2.3. The upper most layer represents the System Under Test (SUT), which can be a single sensor, actuator, on-board computer, or any arrangement of avionics assembled to accomplish the goals of a given test phase. In this setup, the test harness must be as representative as the real environment and for achieving it the flight hardware interacts with the simulation infrastructure through the front-end interface.

Having the same electrical interfaces as the flight hardware, the front-end equipment produces and consumes the same physical stimulus as if the real avionics were connected in the test-bench. For instance, if the AOCS on-board computer is the SUT, than the interface will emulate the sensorial signals and process the commands sent to the actuators. In the case the real sensors or actuators be present in the setup, the electrical front-end may physically stimulate the sensors and monitor the actuators (ELFVING, 1999). Moreover, fault injection may also be introduced by this layer.

The simulation environment is the computational system that contains the infrastructure to close the loop with the system under test, e.g. the spacecraft sub(system) avionics, emulating the platform dynamics and the space environment, as already depicted in Figure 2.2.

Finally, the lowest layer of the conceptual architecture is used to define and automatically control the execution of test procedures and simulation scenarios. The checkout component can also be based on a telemetry and telecommand database and makes use of a base band equipment to directly communicate with the SUT.

When designed in a modular way and adopting modern software engineering techniques, the basic architecture described in this section can be reused in various configurations and serve several scenarios. The flexibility aspects and commonality of simulation facilities are discussed in the next section.

2.3 Towards Software Reuse in Spacecraft Simulation Tools

The increasing number of simulation applications in engineering fields stimulates the pursuit for better and cheaper methods for facilities construction. Whilst simulators streamline the space engineering processes and promote cost reduction, still the development of these tools itself can be expensive. On the other hand, the wide range of application throughout project life time offers an effective opportunity to enhance system communality and rationalise resource usage, hence diluting costs across a broader number of missions.

In this direction, Hendricks & Eickhoff (2005) present the Model-based Development and Verification Environment (MDVE) to support satellite development and verification. The MDVE provides a construction kit, i.e. a set of hardware and software components, which allows a rapid reconfiguration of the environment in different simulation facilities. Accordingly to the tasks to be performed during the project, typically starting in the Phase B, at least the following configurations can be prepared (EICKHOFF et al., 2007; EICKHOFF, 2009):

- Functional Verification Bench: facility to verify critical algorithms, such as attitude and orbit control algorithm, previously designed in environments like MATLAB/Simulink. In this moment, only the algorithm is present in the simulation loop, without any emulation of target computer.

- Software Verification Facility: environment to verify the control algorithm implemented in the target programming language (e.g. C, ADA), which runs over an emulated on-board computer.

- Hybrid System Testbed: this facility mixes software and hardware element in the simulation loop. Usually the sensor, actuator and the plant are simulated in software and the controller runs distributed in a representative hardware. Several levels of fidelity of the computer can be used, from a design to a flight model, which aims to test hardware and software compatibility and their interfaces.

- Electrical Functional Model: is an extension of the previous facility, in which additional hardware devices, i.e. sensor and actuators, can be gradually connected to the on-board computer, replacing the simulated models.
- Spacecraft Simulator for Operations Support: is the environment commonly adopted to verify and validate ground systems used to operate the satellite.

To achieve such degree of reusability, it is recommended that the facility design takes into account the adoption of standard interfaces and best practices for generic software development, like generic programming techniques, meta-modelling methods or component and model-driven architecture approaches.

Regarding the standardisation in modelling and simulation in space engineering domain, the ESA has been ahead in publishing several technical memorandums to guide the construction of infrastructures, development tools and simulation models. Resembling the facility classification proposed by Eickhoff (2009), in the ECSS-E-TM-10-21A (ECSS, 2010a) eight types of simulators are defined: System Concept Simulator, Mission Performance Simulator, Functional Engineering Simulator, Functional Validation Testbench, Software Validation Facility, Spacecraft AIV Simulator, Ground System Test Simulator, and Training, Operations and Maintenance Simulator.

Each facility proposed by ECSS is intended to support space engineering activities concentrated in a specific period of project's life time, as depicted in Figure 2.4. The environment architecture is configured accordingly to the task to be performed and is composed of modular elements, including simulation infrastructure, models, front-end equipment, monitoring & control facility and mission control system. Some facilities have hardware attached to it, whereas others are pure software simulation.

In the same direction, NASA has pointed out the need for simulation tools integration across their programs and projects in their 2010 *Modeling, Simulation, Information Technology & Processing Roadmap* (SHAFTO et al., 2010).

The model reuse is one of the challenges when migrating simulation artefacts from

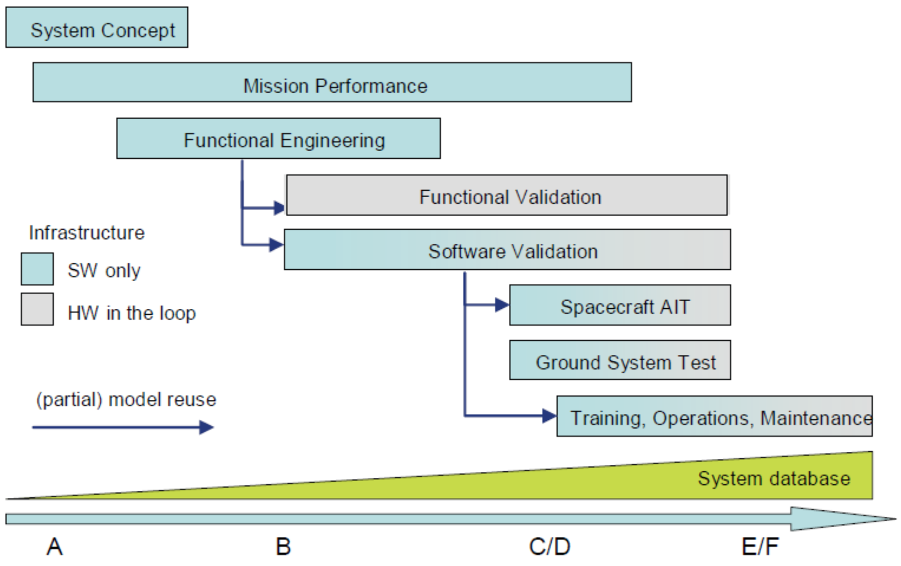

Figure 2.4 - Space engineering activities supported by simulation infrastructures along project's life cycle.
Source: Reproduced from ECSS (2010a)

one facility to another and reconfiguring then to new scenarios or use cases. To easy this task, the *Simulation Modelling Platform* (SMP2) standard formalizes all the software interfaces between the component models and the simulation kernel (ECSS, 2011a).In addition, it provides a platform independent definition language to describe the simulation models, their assemblies and scheduling, and model packages. In addition to enable model interchange among multiple facilities, the standard promotes their platform portability. Moreover, independent groups can work in parallel during the model development, since all simulation components will comply with the same interface. This is especially interesting for suppliers who can deliver both flight equipment and respective simulation model which will be later integrated with other models. This approach enhances the reliability of the models and reduces integration issues, since all models must implement the same communication interface.

Another well-known standard adopted in engineering simulation cases is the *High Level Architecture* (HLA), developed by the USA Department of Defence (DoD) and currently maintained as the IEEE 1516 standard (DAHMANN et al., 1998) (IEEE, 2000) (DoD, 2000). The purpose of this architecture is to integrate a set of distributed and independent systems, called federates, in a central simulation environment, known as federation.

While the HLA focus on interoperability of applications, which can be geographically distributed or a composition of legacy systems, the main goal of SMP2 is ensure model portability. In many space domain applications, a single processing node suffices for executing a simulation scenario (even in real time), thus in a non-distributed environment, SMP2 simplifies the communication interface among models and between models and the simulation kernel. Since the motivation of the current work intervenes precisely in these interfaces, following, the SMP2 standard is presented in more details.

2.4 The SMP2 standard

The first initiative to harmonise activities in European space simulation industry was the version 1 of SMP, named *Simulation Model Portability*. In general, it had basically the same fundamental objectives than nowadays: promote portability and reuse of simulation models (ECSS, 2002). However, it was strongly based on structural programming language concepts, which encumbered the interchange of models, preventing a natural *plug-and-play* usage. It second version, SMP2, object oriented, component based, and model driven architecture concepts have been introduced, hence improving the abstraction level of standard and increasing its flexibility (ARGÜELLO et al., 2000; ECSS, 2011a).

The reuse potentials can be explained from the high-level overview presented in Figure 2.5, which consists in a layered system with different levels of abstraction. The upper layer represents the real world, i.e. the system being modelled and all its components, whose engineering data serves as input to the construction of simulation artefacts. The middle and lower layers are known respectively as *Platform Independent Model* (PIM) and *Platform Specific Model* (PSM), and are the focus of SMP2.

Mainly the purpose of PIM consists in individually specifying simulation models and creating a catalogue, without detailing their implementation to a specific target language or platform. By adopting the inheritance concept from object oriented, different levels of generalization may be modelled, thus leveraging the reuse.

Afterwards, model implementation in a given platform is represented by the PSM layer, in which binary packages are generated with a programming language like C++ or Java.

The definition and instantiation of models are well-split into two phases, represented

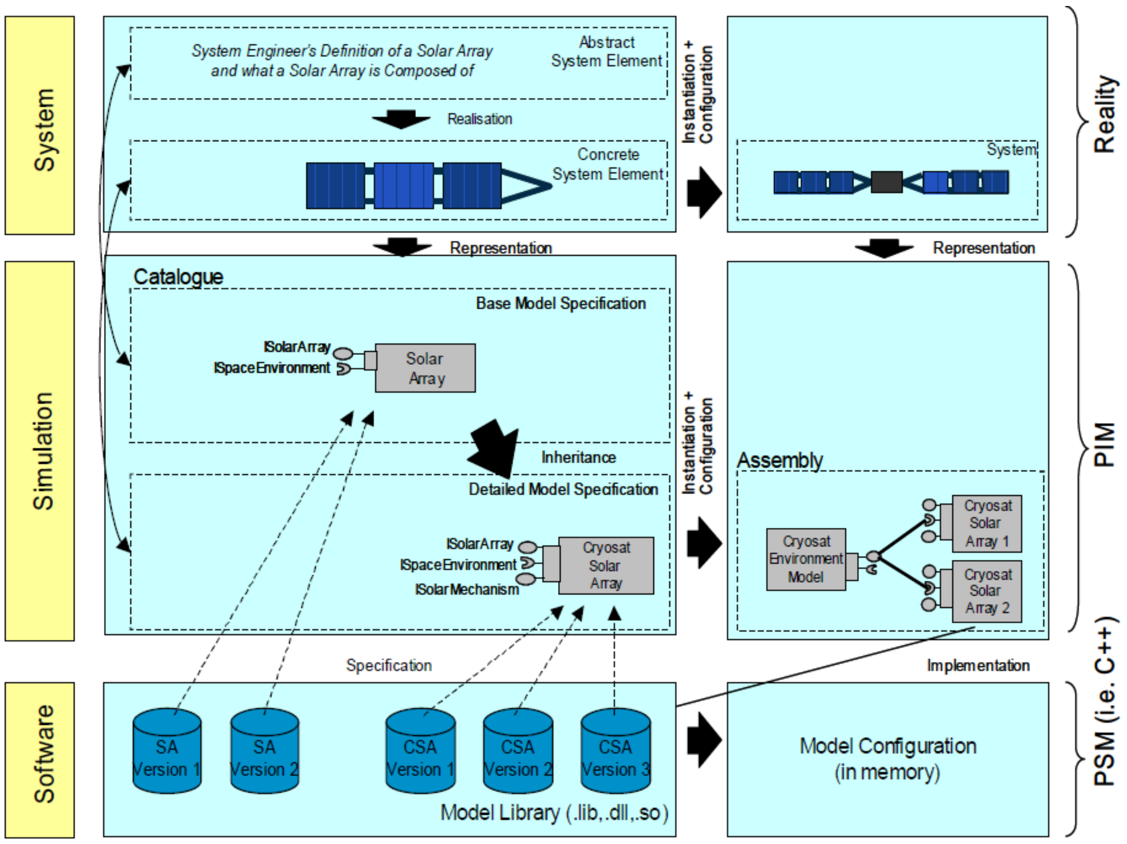

Figure 2.5 - High level overview of SMP2 standard.
Source: Reproduced from ECSS (2010a)

by the left and right columns in Figure 2.5. In run-time, many simulation components can be instantiated and configured from the model described in the catalogue. A meta-model can be used to describe the connections and dependencies of instances and their execution profile in run-time.

Platform independency is accomplished by the adoption of common types and common concepts defined in SMP2 that creates an abstraction layer for the simulation models. All the messages exchanged between models are done through standardized mechanisms, which support communication paradigms as dataflow, event-based, and interface-based. Furthermore, the model-infrastructure interfacing is performed via simulation services. At least, the following services must be provided by the environment:

- *Logger*: provides functions for logging event, error, information messages generated by models;

- *Scheduler*: allows the creation of job queues for executing tasks in predefined instants in simulation time; the model may be invoked by executing entry points (i.e. void/void functions) previously published;
- *Time Keeper*: provides time reference in different formats, such as simulation time, wall-clock time, epoch time, and mission time; the evolution of simulation time may progress in real-time , faster or slower than real-time, as-fast-as-possible (i.e. as result of processing time), or in debug mode;
- *Event Manager*: implements mechanisms for global event registration and notification;
- *Link Registry*: : keeps track of model links and references to others, in order to control the assembly consistence whenever a component is removed from simulation;
- *Resolver*: is a directory service for retrieving run-time references to simulation components.

Currently, few simulation infrastructures fully implement the SMP2 interfaces, but as more simulation tools and reference architecture become available (SEBASTIAO et al., 2008; WALSH et al., 2010), the standard is becoming popular in space projects and expanding its adoption outside European community (NEMETH; DEMAREST, 2010; REW et al., 2010; ZHANG et al., 2011). Examples of the well-known infrastructures in this direction are EuroSim (VRIES; MOELANDS, 2008a; VRIES; MOELANDS, 2008b; DUTCH SPACE, 2006), SIMSAT (SEBASTIAO; NISIO, 2008; WHITTY, 2010), Basilis (DELATTE; MANON, 2008; QUARTIER; MANON, 2013), and SimTG (EISENMANN; CAZENAVE, 2008; ZANON; MORSCHER, 2010; CAZENAVE; ARROUY, 2012).

In addition to compliant infrastructures, complementary tools are being produced to improve the simulation development process and increase productivity. An example of such software is the *Model-Oriented Software Automatic Interface Converter* (MOSAIC), an utility to automatize the algorithm translation from scripts like Matlab/Simulink/Stateflow into *EuroSim* or SMP2 formats (LAMMEN et al., 2002; LAMMEN et al., 2010).

Another example is the *Simulation & Visualization* tool (SimVis) for rapid simulation development to assist concurrent engineering studies, in system conception activities. By gathering system parameters in a spreadsheet from a concurrent engineering environment, a wizard assists the user to generate simulation code compliant to SMP2 standard. This approach showed to be an effective process to automatize the reconfiguration of simulation models from an existing catalogue and perform visual simulations for mission analysis in a short span time (KALDEN et al., 2007).

3 USER INTERACTIVITY AND COMPUTATIONAL STEERING

Accordingly to Parker et alii, the simulation activity involves the following steps: construction of a model of the physical problem domain; application of boundary conditions; development of a numerical approximation to the governing equations; computation; validation; and understanding the results (PARKER et al., 1998). In the field of computational simulation, interpreting the output can be as complex as modelling the problem itself. In these cases, a visualization system can guide the user to analyse data and to understand the simulated system. Notably when the nature of data is three dimensional (3D), its use led to an intuitive and accurate interpretation of simulation results (CHATEL et al., 2006). In other cases, specific domain tools can automatize the data processing and present the information in a structured format. In a satellite domain, for instance, this could imply the representation of an attitude quaternion by plotting the equivalent Euler angles or even by orienting a sophisticated 3D model of the body in a graphical scene.

In addition to assist the interpretation of data, a well-tailored visualisation system can also ease the identification of errors, frequently caused by modelling mistakes or imprecise numerical computation. By monitoring intermediate results, the user can avoid the propagation of gross errors in the simulation.

Nevertheless, in many applications, simulation and visualization software demands significant computational resources. Due to the numerical complexity of the models or to the huge amount of data to be handled, sometimes the analysis of the results have to be done afterwards the simulation has ended. This two steps approach was common in the past, when computational platforms were less powerful.

Nowadays, leveraged by the computational growth, new hardware interfaces and software architectures, it became more usual to attach visualization systems directly to the simulation, in order to readily display the updated results. Moreover, the infrastructures are more interactive, providing the user with capabilities to act in the running simulation and to monitor its evolution at the same time.

In the software context, an interaction technique is defined as “a method allowing a user to accomplish a task via the user interface” by Bowman et al. (2004). This is “the mutual response of computer and user on each other’s actions” (COOMANS; TIMMERMANS, 1997). In order to make it possible, specialized software and hardware components translate the information between the real and virtual world.

More specifically in the field of scientific visualization, this concept is often known as *computational steering*, defined by Marshall et alii as “the interactive control of a computational model during execution while viewing the results of the calculation graphically”. Gottlieb et al. (2001) point that steering can be done in two direction: *forward steering*, when the scientist changes the input parameters in the simulation to observe the output; and *inverted steering*, in the case the derived behaviour is provided and then the computational system searches for the possible input parameters in the space-state to match the given output.

In early 90’s, Marshall et alii implemented a steering mechanism for studying the effects of storms on the Lake Erie (North America). This fluid dynamics problem is described as a 3D turbulence model and executed in a computational grid, in which the user can control parameters, such as heat flux or wind direction and velocity, while observing the impact on the water temperature, velocity and level, represented by a colour contour scheme. In their work, three types of visualization techniques are identified, wherein each of them provide different levels of user interactivity: post-processing, tracking and steering. (MARSHALL et al., 1990).

In the first approach, illustrated in Figure 3.1-a, all the input data is previously configured before the simulation starts. After the simulation finished executing, the output data is processed by a visualization tool. During the data analysis, the user has some flexibility to change parameters in order to adjust the data extraction algorithms or the presentation format. The *post-processing technique* can be time consuming in many simulation domains, which applications can take several hours or even days to execute. Occasionally, during the examination of results, the user may realize that an error was introduced in the input data and the whole process should be restarted.

With the attachment of the visualization system to the simulation, named *tracking technique*, the user is able to follow the results as they are being produced (Figure 3.1-b). This is an important step to increase the interactivity and reduce the risk on rework, but the simulation flux can only be controlled by script mechanisms, whereby the user must foresee all the decision to be taken during the execution time.

Steering is the highest level of interactivity, allowing the user to make on-line changes in the simulation (Figure 3.1-c). Clearly, this approach has several advantages when compared to the previous ones. It sustains the model exploration and allows the efficient interpretation of simulation data in a reasonable level of abstraction. By controlling the course of the scenario and testing *what-if* hypothesis, the scientist

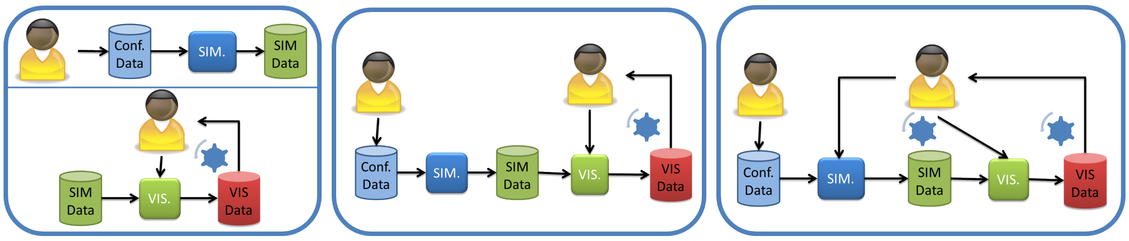

(a) Post-processing (b) Tracking (c) Steering

Figure 3.1 - Types of visualization techniques with different levels of user interaction in scientific simulations.
Source: Adapted from Marshall et al. (1990)

can easily gain insight on system behaviour. For optimization applications, the user can guide the simulation for a faster convergence.

3.1 Related Work

Since Marshall et alii work, many computational steering environments have been developed. Accordingly to Parker et al. (1997), the software architecture is used to "integrate computational components in a manner that allows the efficient extraction of scientific information and permits changes to simulation parameters and data in a meaningful way".

Most of the pioneer environments, such as *Visualization and Application Steering Environment* (VASE) (HABER et al., 1992), *Program and Resource Steering System* (Progress)/Magellan (VETTER; SCHWAN, 1995), *Computational Steering Environment* (CSE) (WIJK; LIERE, 1997; LIEREA et al., 1997), *Collaborative User Migration, User Library for Visualization and Steering* (CUMULVS) (KOHL; PAPADOPULOS, 1995), and *VIsualization of massively Parallel simulation algorithms for Extended Research* (VIPER) (RATHMAYER; LENKE, 1997), have been based on previous experiences of building computational tools to address scientific and engineering problems. Commonly, the solutions implied the implementation of numerical methods, like Discrete Element Method (DEM), FEM (Finite Elements Method), Finite Difference Method (FDM) or those others applied to the fields of fluid dynamics, solid mechanics and molecular dynamics. Consequently, in order to support intensive computation and generation of massive data required by these methods, the environments were frequently distributed and executed over high-performance platforms (e.g. grids and parallel machines).

Visualization systems for generic purpose could be attached to these platforms and among the available tools were *Khoros* (RASURE; WILLIAMS, 1991), *Advanced Visualization System* (AVS®) (ADVANCED VISUAL SYSTEMS INC., 1992), *Data Explorer®* (LUCAS et al., 1992), *VISualization, Animation, and Graphics Environment* (VISAGE) (SCHROEDER et al., 1992), *IRIS Explorer®* (FOULSER, 1995) and *Visualization Toolkit* (VTK) (SCHROEDER et al., 1996), some of them providing 2D and 3D graphical and animation outputs.

Thus, in that period the developments focused on incorporating steering capabilities in the existing simulation/visualization distributed architectures. The main strategy was to implement a code annotation mechanism, with which the legacy source codes could be manually instrumented to invoke functions provided by a steering library (PARKER et al., 1997).

A comparison of scope, architecture and user interface of these early systems can be found in the survey done by Mulder et al. (1998b). In the work, they observe that the computational steering system can be classified in three groups: application specific, domain specific and generally applicable.

A generally applicable computational steering environment is presented by Parker & Johnson (1995). The SCIRun implements a Problem Solving Environment (PSE), wherein a dataflow architecture allows the connection of generic modules to create a new application (PARKER et al., 1997; PARKER et al., 1998). By means of a Graphical User Interface (GUI), the user visually programs the application and defines the dataflow network. A special module, called Salmon, provides simulation interactivity by a direct image manipulation interface (JOHNSON et al., 1999). The performance and flexibility of the environment is demonstrated in applications of torso defibrillator design (medicine), solving rendering equation for global illumination model (computer graphics), wrapping a legacy Computational Fluid Dynamics (CFD) library, and pollutant distribution (atmospheric diffusion) (PARKER, 1999). Originaly the SCRun was designed to be a multi-threaded application, but then Miller et al. (1998) proposed a distributed architecture to the environment.

The dataflow paradigm is also adopted in the CSE of Wijk and Liere to connect the simulation with the GUI in a flexible way, implementing a Parametrized Graphics Object scheme. In edit-mode, graphical objects (i.e. widgets) are created and placed into the GUI. Each object is then mapped to a simulation variable, respecting their degree of freedom. Afterwards, in run-time, the researcher steers the simulation by directly manipulating the graphical objects (WIJK; LIERE, 1997; WIJK et al., 1997).

Later, this concept is improved in the VISSION system, with the employment of oriented object techniques and the addition of a process to automatically map 3D widgets to compatible ports in a dataflow network (TELEA, 1998; TELEA; WIJK, 1999).

In gViz project, a library was developed to support visualization and computational steering in heterogeneous grid environments (BRODLIE et al., 2004). The network of simulation model is described in terms of software architecture and lately allocated to physical resources in the grid. This mapping is done using a markup language, the skML, which allow the on-line collaborative visualization of simulation results by simultaneous participants (DUCE; SAGAR, 2005).

The development of collaborative environments was also exploited in the TeraGyroid experiment, a project that demonstrated intercontinental grid simulations for a large-scale lattice-Boltzmann applications (PICKLES et al., 2004). In that case, the RealityGrid project provided the toolkits to implement the distributed and collaborative environment. For a successful parameters space exploration, a checkpoint mechanism allowed the scientists to compare the evolution of scenarios, using commands to save and recovery the state of simulation. The communication infrastructure was based on Web services and implemented SOAP (PICKLES et al., 2005). Later on, the ubiquitous interaction in the ReallityGrid was demonstrated by user interfaces implemented in handheld devices (i.e. PDA and Smartphones) (HOLMES; KALAWSKY, 2006).

Parallel computing in grid environments were also investigated to increase rendering time of visualization systems. Esnard et al. (2006) developed the EPSN framework to address the bottleneck encountered by sequential visualization tools when processing large datasets. The environment is also a computational steering tool and its potentialities have been demonstrated with an astrophysics simulator for solving an N-body problem of colliding and merging galaxies.

Nonetheless, more recently Linxweiler et al. (2010) have argued that distributed systems can reduce significantly the time response of the simulation and derail many steering applications. To address this limitation, they have proposed a Virtual Fluids Interactive environment that runs on a single desktop equipped with multiple Graphical Processing Units (GPUs). The adoption of these devices are becoming popular for high performance computing applications, since grouped the accelerator cards can achieve processing speeds comparable to grids or supercomputers, with less power consumption and with higher bandwidth when compared to computer network schemes. Implementing a CFD application with lattice-Boltzmann method, Linxweiler et alii claimed to run 3D simulation close to real-time.

Computational steering environments bring capabilities to experts quickly change the simulation course. Although it is convenient for exploring the behaviour of the modelled system, a large number of derived scenarios makes the comparison of the results a complex task. In order to address such volume of information, Waser et al. (2010) have developed a steering application to manage the generation, storage and visualization of alternative scenarios. Extending the *history tree* concept from Brodlie et al. (1993), Waser et al. (2010) implement a mechanism to periodically store states, which can be lately retrieved to restore the simulation back to a given point in time. From each element in state-space, a new event (e.g. steering command) can be inserted to generate a scenario branch. A graphical tree interface guides the user interaction with the simulation and keeps track of all parallel results.

The lack of resources to support the human decision making and comparison of alternative scenarios is also addressed by Coffey et al. (2013). In their system, instead of steering low-level parameters of the simulation, the engineer explores the possible configurations of a medical device design by directly manipulating an output image. The graphical interface abstracts the input parameters of the simulated model (e.g. geometry) and highlights the output properties in the study (e.g. thermal gradient, applied forces). The interaction with the image can apply changes to the input parameters or to the visualization output. In the second case, an inverse design approach is implemented (i.e. inverse steering): a search in the neighbour state-space is performed to find the closest configuration that produces the image distorted by the user.

3.2 User Interactivity Concepts

Several mechanisms can be implemented to provide the user with a flexible interface to change simulation parameters on-the-fly and visualize the results. These mechanisms and the way the user interacts with the simulation are closely related to techniques explored in the Human-Computer Interaction (HCI) research field. Since the early days of computation, the information exchanged between human and machines is being studied in order to understand the user's cognition process and to define best practices for interfaces design.

In the taxonomy for HCI developed by Bernsen (1994), a set of *unimodal representational modalities* are identified, whereby the information can be externalized to the human cognitive system. They are characterized by a combination of *basic features* of communication process, i.e. linguistic/non-linguistic, analogue/non-analogue, arbitrary/non-arbitrary, and static/dynamic; and the possible *media of expression*. For outputting information from the system, graphics (i.e. visual), sound (i.e. acoustics) and touch (i.e. haptic) are used as media of expression, which combined with basic features gives a total of twenty-eight feasible generic unimodal output modalities Bernsen (1994)[1]. In the case of inputting data, thirty classes of generic unimodal input modalities are identified, using the following media of expression: graphics (e.g. video capturing for gesture recognition); sound (i.e. voice input); and kinaesthetic (i.e. body motion reading) Bernsen (1995).

Even though the sensory system comprises additional perceptual qualities to those adopted for the media of expression, Bernsen's taxonomy is still valid nowadays for the great majority of available User Interfaces (UI). Furthermore, it is important to note that two or more generic unimodal modalities can be combined to create multimodal interfaces (e.g. voice input plus gesture recognition).

In the history of HCI techniques evolution, it is possible to distinguish four levels of interactivity: textual, graphical, natural, and immersive. Their popularity is related to the progress of the computational platforms and interface devices in general, but so far, none became completely dispensable.

For the computational steering environments, all of them are important and have advantages over the others, depending on the application domain and the parameter type.

3.2.1 Textual interfaces

Text is a simple way for exchanging information with computers. Usually via a command line interface, the user types a well-formed string to program the machine, which sends back a message in the screen, as illustrated in the Figure 3.2.

They can be harder to use, when compared to other kinds, but easier to extend and frequently preferred by domain experts (FOLEY et al., 1984). In simulation, for instance, textual commands are valuable for programming scenarios, defining scripts, and formally describing verification and validation procedures.

[1]Some arranges are discarded because they don't make sense, e.g. linguistic is always analogue.

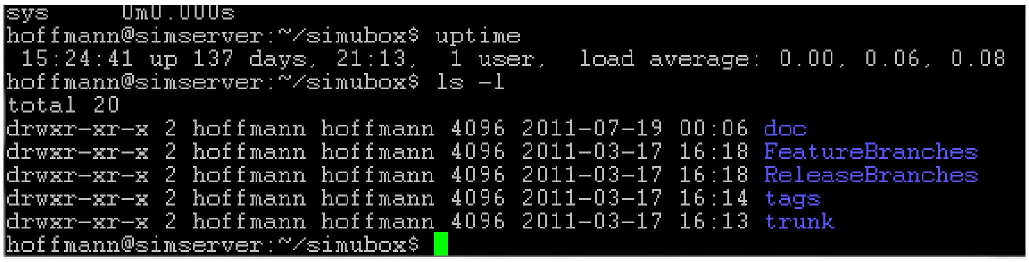

```
sys     0m0.000s
hoffmann@simserver:~/simubox$ uptime
 15:24:41 up 137 days, 21:13,  1 user,  load average: 0.00, 0.06, 0.08
hoffmann@simserver:~/simubox$ ls -l
total 20
drwxr-xr-x 2 hoffmann hoffmann 4096 2011-07-19 00:06 doc
drwxr-xr-x 2 hoffmann hoffmann 4096 2011-03-17 16:18 FeatureBranches
drwxr-xr-x 2 hoffmann hoffmann 4096 2011-03-17 16:18 ReleaseBranches
drwxr-xr-x 2 hoffmann hoffmann 4096 2011-03-17 16:14 tags
drwxr-xr-x 2 hoffmann hoffmann 4096 2011-03-17 16:13 trunk
hoffmann@simserver:~/simubox$
```

Figure 3.2 - A textual interface in which the Bash command processor is used to operate a computational system.

Further, in computational steering, textual interfaces are indispensable for inputting precise values, which can be required for some of engineering parameters (MARSHALL et al., 1990; LINXWEILER et al., 2010).

3.2.2 Graphical user interfaces

Graphical User Interfaces (GUI) are direct manipulation interfaces (MYERS, 1995), more intuitive to operate when compared to command line. Instead of memorizing commands, the user dispatches actions in the computer, searching in the screen for its pictorial representation. It became very popular since the *desktop metaphor* was introduced, making the usage of the operating system analogous to tasks performed daily in an office environment (e.g. creating documents, archiving files, opening a folder, recycling the bin) (LEACH et al., 1997).

The interaction with the virtual system is done using Windows, Icons, Menus and Pointing devices and is known as WIMP paradigm. Buttons, scroll bars, spin boxes, check boxes, dials, among others types of widgets provide specialized means to direct manipulate variables and control the applications. Each widget has geometry and behaviour (CONNER et al., 1992) and is "a way of using a physical input device to input a certain type of value" in the system (MYERS, 1995). An example of such interface is given in the Figure 3.3.

Many programming toolboxes and frameworks have been developed to easy the design and implementation of GUI, by providing generic widget components that can be reused among different projects and use cases. Some examples are Microsoft Foundation Classes (MFC), Motif, Java/Swing, Qt, Gimp Toolkit (GTK) and Windows Forms in .NET (WILKINS et al., 2000; NEC, 1992; ECKSTEIN et al., 1998; BLANCHETTE; SUMMERFIELD, 2006; LOGAN, 2001; RICHTER, 2002). Customized widgets can be extended from those provided in the toolkits or even be entirely new

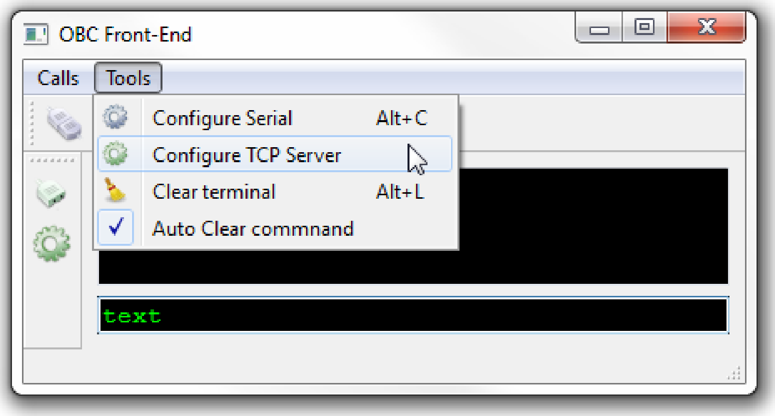

Figure 3.3 - Example of a GUI application containing windows, menus, buttons and other graphical elements.

to meet the requirements of a specialized application. This high level of flexibility leveraged the construction of application with GUI and spread its adoption to many domains. In the computational steering field, a good example of such customization is the *parameter space wheel widget*, described by (COFFEY et al., 2013), with which the user can arbitrarily freeze of weigh parameter values to guide the state-space search in a design optimization application.

Alternatively to the adoption of widgets, the image generated in a GUI can be also directly manipulated. In the work of Chatzinikos & Wright (2001), this approach is used to enable computational steering in scientific simulations and to allow the researcher to interact directly with the image produced by the visualization system. By manipulating the features of different types of image plots or graphs, the expert can change initial and boundaries conditions and extend the problem domain, back into the simulation.

Direct image manipulation techniques are commonly employed in interfaces with 3D graphics, since they implement an intuitive way of interaction with graphical elements that represent objects of real world. Three dimensional user interfaces are a natural enhancement of GUI and they are particularly interesting for dealing with complex geometrical information. Foley et al. (1984) describe six types of user interaction tasks in a computer graphics environment: select, position, orient, path, quantify, and text. Each task can be performed in multiple ways, combining different techniques (e.g. orienting by controlling the angle with a joystick; quantifying by sliding a potentiometer). Complementary to them four controlling task can be executed to modify graphical objects: stretch, sketch, manipulate (i.e. translate or orientate), and shape. Often, the effects of user interaction can be constrained in degrees-of-freedom or to certain limits in the state-space, providing feedback of valid configurations of the modified model. One example of assisting the performance of the task is the as-rigid-as-possible shape manipulation mechanism implemented by Coffey et al. (2013).

3D widgets

Sometimes, the execution of these tasks in the 3D space can be supported by the usage of 3D widgets, which concept is introduced by Conner et al. (1992). In their framework, generic widget objects are implemented to manipulate and modify the properties of 3D objects, for instance a virtual sphere to perform rotations, a snapping widget to do surface-aligned translations, or a colour widget. The relations between objects in the application are controlled by special objects that encapsulate and filter signals from physical devices or simulation algorithm (e.g. collision detection), which makes the configuration of their relationship flexible. The same concept is extended to be applied in simulation steering environments, such as SCIRun (JOHNSON; PARKER, 1994), CSE (MULDER; WIJK, 1995), and VISSION (TELEA, 1998; TELEA; WIJK, 1999).

In the case of SCIRun environment a 3D visualization front-end includes special graphical elements that can be dragged with the mouse. Once these widgets are attached to geometric properties of models, the user can steer the simulation with instantaneous visual feedback from the updated 3D model.

This bi-directional binding between properties of 3D elements and simulation data is also provided by *parametrized geometric objects* from Mulder & Wijk (1995). In their strategy, the geometry of simple objects, such as spheres, cylinders, and boxes, can be defined by the manipulation of graphical control-points (e.g. for controlling the position or radius of a sphere). Changes applied to these points (via mouse or text input) are mapped to variables in the simulation, which can have a predefined degree-of-freedom or be constrained to the values of other control-points (WIJK; LIERE, 1997).

A simple example of a 3D widget is illustrated in the Figure 3.4.

3.2.3 Natural user interfaces

Natural user interfaces have been studied and developed for many years, but only recently multi-touch, motion tracking and voice input techniques are becoming more

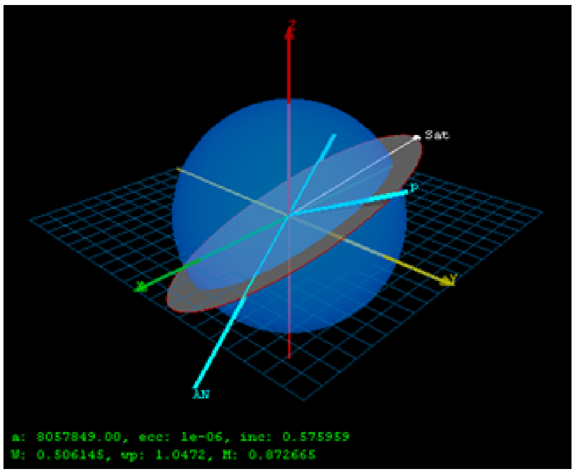

```
a: 8057849.00, ecc: 1e-06, inc: 0.575959
W: 0.506145, wp: 1.0472, M: 0.872665
```

Figure 3.4 - A 3D widget to graphically manipulate orbital parameters.

popular. In general, these interfaces envisage the reuse of human existing skills for content interaction (BLAKE, 2010).

Gestures recognition, i.e. the interaction via the movement of human arm and hand (PAVLOVIC et al., 1997), is a common approach nowadays. Driven by the increasing availability of cheap devices, such as smartphones, MP3 players, modern tablets and seventh generation video game consoles (e.g. Nintendo Wii®, Microsoft Xbox360/Kinetic®), the implementation of this type of interfaces is becoming trivial.

Complementary to the textual and graphical user interfaces, scientific applications could become more flexible to use, exploiting the technological maturity of multi-touch screens, image processing toolkits, and embedded inertial sensors (SCODITTI et al., 2011) applied for the development of natural interfaces.

3.2.4 Immersive environments

The progress of computer graphics and natural UI techniques enabled the construction of simulators that imitates the natural environment, giving to the user a feeling of being completely integrated with the system. The creation of 3D scenes is a key feature, but for some applications, additional feedback can be provided in the form of sound and touch stimulus (or even smell), enhancing the immersion sensation in these environments. The UI can have such level of fidelity that the human sensorial system gets the illusion of being interacting with real objects (COOMANS; TIMMERMANS, 1997; LATOSCHIK, 2005). Frequently, these immersive environments are associated with *Virtual Reality* (VR) systems, in which a synthetic

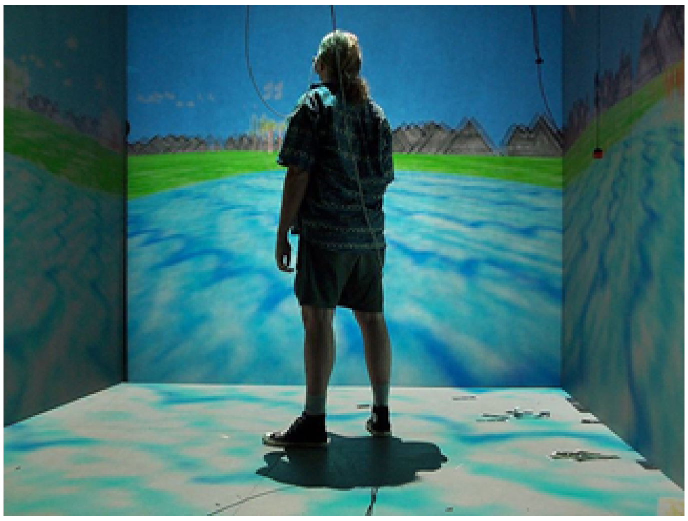

Figure 3.5 - Example of a virtual reality environment.
Source: Adapted from Davepape http://commons.wikimedia.org/wiki/File:CAVE_Crayoland.jpg

world is designed to mimic the real one, but not necessarily with the same physical properties (e.g. the forces of gravity could be altered or simply ignored) (MILGRAM; KISHINO, 1994).

Occasionally, elements from the virtual and real world coexist in the same environment, what have been defined by Milgram & Kishino (1994) as Mixed Reality (MR) that has the virtual and real environment as opposite boundaries. In between these extremities comprises a *virtuality continuum* wherein different levels of virtual and real mixture can occur (e.g. Augmented Virtuality and Augmented Reality).

The most popular VR environments are based on the concept of the CAVE – Audio Visual Experience Automatic Virtual Environment, in which the viewer stands in a room surrounded by projection screens, mounted on the walls, ceiling and floor, resulting in a high degree of immersion and interactive setting, as depicted in the Figure 3.5 (CRUZ-NEIRA et al., 1992). This type of 3D technology has been used in multiple engineering and scientific applications, including those running in computational steering infrastructures (MULDER et al., 1998a; ENGQUIST, 1999; RENAMBOT et al., 2000). Besides the benefits of easing the user perception of 3D information and putting the designer in an active position of simulation, the VR environments also leverages the collaborative work on engineering activities.

In the aerospace domain, immersive simulators are promising tools to anticipate design and process issues and reduce risk in the projects. The Virtual Reality Center[2], from Embraer (SYSTEMS, 2004), and the Collaborative Human Immersive Laboratory, from Lockheed Martin Corp. (CLARK,), are two examples of those environments expected to increase the efficiency in the development of airplanes and satellites.

3.3 Common Functionalities of Computational Steering Environments

Changing simulation parameters during run-time and visually monitoring the effects are the elementary functions of any computational steering environment. Besides that, for many application domains, adjunct features that improve the usability of the system and naturally contribute to the creative process of the user are of great value.

Accordingly to Parker et al. (1998), a typical use case of a computational scientist includes: construction of a model; application of boundary and initial conditions; development of a numerical approximation; computation; validation of results; understanding the results. Consequently, among the data input and visualization mechanisms, a computational steering environment may also integrate components for modelling, computation and data analysis (JOHNSON et al., 1999).

In this section, common functionalities found in the computational steering simulators are discussed. Though the presented features are not an exhaustive list, they are considered to be the most relevant aspects in the context of this thesis.

3.3.1 Comprehensiveness of input commands

Regardless of the user interface type implemented, it is important that all variables in the simulation are accessible, including those internal to the infrastructure and numerical method, such as topology of the model, boundary conditions, integration step, or sample frequency.

As mentioned in section 3.2.1, in some use cases it is desirable to type the precise value for a given parameter, instead of steering it via a graphical widget.

In addition to parameters change capability, many steering applications demand also flexibility to alter the executing source code or to control the computational resource allocation in run-time.

[2]http://www1.embraer.com/english/content/empresa/technology.asp?tela=virtual

3.3.2 Visual feedback

The user shall choose the preferred data visualization technique, accordingly to the problem domain that is being simulated. This may include line graph, surface view, image plots, arrows, streamlines, volume plots, among others (CHATZINIKOS; WRIGHT, 2001). For applications with complex geometry, it is also desirable to have a graphical output with simulated elements modelled as 3D objects.

Regardless of visualization system is employed, it is essential that the impact of modified parameters is rapidly reflected in the graphical user interface, i.e. with low latency and intuitive representation (LINXWEILER et al., 2010). Further, these changes should be easily correlated to updates in the visual output (PARKER et al., 1997). For this, the relation between simulation and visualization data structures must be consistent and the interface metaphor should be intuitive, i.e. easily understood by the scientist. Besides that, the viewer may control the animation of output graphics, in order to better investigate the evolution of simulation time and the behaviour of changes (MARSHALL et al., 1990).

3.3.3 Data abstraction and filtering

Due to the curse of dimensionality or huge amount of data, processing and interpreting the simulation results can turn to be an arduous task, thereby many computational steering environments offer means to abstract and filter data.

For some application domains, a simple parameter grouping mechanism could suffice for handling historic data (MARSHALL et al., 1990), however, for large data sets sophisticated approaches may be required like data reduction techniques (LINXWEILER et al., 2010), map/reduction methods (COSTANZO et al., 2009), or data mining algorithms for clustering and feature extraction (JIANG et al., 2004).

Another efficient way to extract relevant scientific information is to correlate simulation output with graphical visualization. In this direction, Jiang et al. (2004) implement a feature extraction architecture based on rules defined interactively by the user. These features represent attributes of a given region of interest in the space of time-varying data that are mapped into geometrical objects (e.g. ellipsoids). Several levels of abstraction can be selected for visualizing the objects in a graphical scene, wherein the evolution of the features can also be tracked and quantified.

In a more recent work, Mazzeo et al. (2010) have coupled a ray tracing algorithm to a fluid simulation system to directly render visualization frames of the flow field, avoiding the post-processing of large time-varying data sets.

Specifically for the spacecraft simulation domain, a common visualization abstraction is to map the state of simulation (e.g. status of telemetry, critical temperature ranges, or operating modes) to the visual properties of 3D models that represent the affected equipment (DONATI et al., 2004; DURO et al., 2008).

Concerning the evolution visualization of time-varying scenarios, and its generated ramifications, Waser et al. (2010) have implemented *track icons* with thumbnail images of the simulation output on the basis of periodic snapshots. This method showed to be a convenient abstraction tool to provide user with clues on models state along simulation horizon.

3.3.4 Breakpoints

A breakpoint is a statement programmed to suspend the simulation, based on conditions predefined by the user. It can be defined simply as a point in the source code where the execution should hold, just before its execution, or by an elaborated rule that checks the validity of code variables (e.g. the range of some parameter's value). During run-time, the user can choose to enable or disable it.

These mechanisms are commonly employed by software developers to debug the program and in the simulation context this is also convenient to inspect the state of models. By holding the simulation, the researcher can carefully analyse the circumstances that brought the simulation to the current state and then try to correlate the system behaviour with model's parameters.

Breakpoints can be implemented by the simulation infrastructure at the low level of program instructions or be more abstract and operate in the model structure or state.

3.3.5 Snapshot

Snapshot is a key functionality in computational steering to preserve the state of the simulation in a given instant. It is like a "picture" that captures all parameters and internal variables values of the models and, possibly, the state of the kernel. This mechanism serves as a checkpoint in the time-space to which the simulation can be restored any time the scientist wants to investigate the system behaviour from a known state or e.g. from a point where the system dynamics has stabilized (MARSHALL et al., 1990; PICKLES et al., 2004).

Based upon the volume of data required to commit a snapshot, the save operations can be periodically dispatched by the infrastructure or manually invoked by the user. The advantage of having a dataset automatically recorded is to enable a full playback of the simulation and to support the post analysis of temporal data. Further, series of checkpoints can be used to recovery the experiment in the occurrence of a faults (KOHL; PAPADOPULOS, 1995).

3.3.6 Synchronization mechanisms

The computational steering environments may implement mechanisms to guarantee synchronization in the data and control flows. A common approach is to define systematic breakpoints in the simulation, in order to apply the steering inputs and to collect or transfer data when no further computation is being performed (HABER et al., 1992)).

These apparatus can be primarily necessary in distributed applications with parallel or concurrent processing, wherein model intercommunication must also be mediated or the user interaction must take into account certain states of the models (MULDER et al., 1998b).

Another aspect to be respected is the coherence among model states when the user forces values of parameters. In some domains, it only makes sense to modify one variable if another is also updated, e.g. if the pressure changes, then the temperature must be adjusted (PARKER et al., 1997).

3.3.7 Support to application integration

Possibly because of the interest on upgrading legacy systems, code annotation is far the most prevalent mechanism implemented by the precursor steering environments for incorporating application models into the computational infrastructure. By this approach, an existing source code is instrumented with function calls provided by a steering library, which gives access to the application parameters and introduces checkpoints for steering control (LIEREA et al., 1997). Although this is a minimal intrusive approach, it can be cumbersome to manually adapt the code and publish the application parameters, potentially affecting the program legibility.

In contrast to the interoperability with legacy code are the dedicated systems that provide a generic infrastructure to enable the development of new applications. This is the concept adopted by Problem Solving Environment SCIRun, which offers a visual programming interface for connecting application modules in a dataflow scheme (PARKER et al., 1998). Despite of demanding memory resources, dataflow paradigm have been implemented by most visualization systems, since it is quite flexible for connecting independent components and line up processes in a pipeline network.

In fact, flexibility is a key aspect for tailoring tools and promoting software reuse that has been pursued in the very beginning of computational steering applications (MARSHALL et al., 1990). As the software engineering methods has developed over years, the simulation has been upgraded to more advanced architectures, applying object oriented concepts, generic programming techniques, design patterns, among others (TELEA; WIJK, 1999; LINXWEILER et al., 2010; JENZ; BERNREUTHER, 2010).

In addition to the flexibility and integration aspects, it is also important to fulfil special needs that a given application domain may have, such as support to computational resources optimization (BRODLIE et al., 2004), execution of large-scale models in distributed environment (RICHART et al., 2007) or algorithm experimentation.

3.3.8 History log & Playback

Simulation data and event logging is an auxiliary feature, yet important, provided by most computational steering environments. The history database allows the construction of complementary tools for analysing the results of the simulation and comparing different scenarios. When persisted in a formal structure, complex operations of data aggregation (RIBICIC et al., 2013) or data-mining algorithms can be employed to extract information from the modelled system.

For large-scale simulation, it is convenient to have means to select the parameters to be recorded and in which frequency. In order to easy the post processing, a detailed catalogue that describes the data, e.g. meta-data file, should accompanies the archive.

Based upon the historic data, a playback tool can be developed to reproduce the results of the simulation in a lighter way, when compared to the use of snapshots. Still, if a collection of snapshots is available, the expert can choose to restore the simulation in any point of the playback and restart a new execution.

Using this mechanism, the creation of alternative scenarios can grow significantly and make the comparison of results an arduous task. For dealing with this complexity, it is crucial to have some sort of history tree management to control the scenarios and support the analysis process (WASER et al., 2010).

3.3.9 Simulation controllers

Most of the infrastructures provide means to control the simulation run via commands such as *play* (i.e. to start), *pause*, *step*, and *stop* (DUTCH SPACE, 2006). During the execution, the time may progress in different modes: real-time, accelerated and free running (ECSS, 2011b).

In real-time, the time progress accordingly to the computer clock, which can advance close to the pace of the wall-clock (soft real-time). When strict synchronization and low latencies in this clock are required, the simulation is said to be hard real-time (ECSS, 2010a).

For many applications it is desired to execute the simulation slower or faster than real-time, in order to thoroughly follow the dynamics of a fast phenomenon, or conversely speed up the execution to get a wide view of the behaviour. In these cases, the user shall setup an acceleration factor in order to control running speed.

In the free running mode, the execution time is only limited by the processor performance and the simulation runs as fast as possible, until it reaches the end.

Complementary to the breakpoint mechanism, the *pause* and *step* functions allow the user to hold and analyse the execution flow of the simulation. When the execution is based on the scheduling of discrete events, the *step* command could advance the time to the next event in the execution queue. In the circumstance of using a cyclic scheduler, *step* could mean also a jump to the next simulation interval.

Optionally, when the playback mode is implemented, the *play* and *step* commands can work backwards. In this case, an additional command could also be available to immediately jump the simulation to discrete points in time (ANALYTICAL GRAPHICS, INC, 2007).

Depending on the numerical method implemented in the kernel, additional commands could be provided to change the integrator parameters, e.g. internal time step.

3.3.10 Collaborative visualization and steering

In many simulation applications, the effort on understanding complex phenomena can be shared among different scientists. Particularly for multidisciplinary domains, the cooperation of researchers with heterogeneous background can bring different perceptions of the problem and accelerate the state-space exploration (DUCE; SAGAR, 2005; RIEDEL et al., 2008; MALAKAR et al., 2011). For instance, in a collaborative visualization system, all the participants can have the same understanding of the evolution of a dynamic system. Then, starting from a common checkpoint, independent scientists could explore the parameter space in parallel, before they exchange again the results (PICKLES et al., 2004).

For this reason, many research communities are pursuing simulation environments with collaborative visualization and steering capabilities. Still, this requirement poses design challenges for the computational infrastructure, mainly when the system has to handle a huge volume of data or the users and the resources are separated geographically (PICKLES et al., 2004). Further, special attention must be taken to ensure a low latency in the steering commands and to avoid conflicting inputs from concurrent users.

Nowadays the systems are prone to implement collaborative environments based on Web technologies (JIANG et al., 2004; WU et al., 2010; SHU et al., 2011), which enhances the use of steering in ubiquitous applications, but, on the other hand, it rises security issues (HOLMES; KALAWSKY, 2006).

3.4 Computational Steering Applications

Led by the enhancement of simulation techniques and the increasing offer of low-cost hardware, the computational steering has become an important tool in many knowledge fields. This section lists some of the benefited areas and gives a briefly description of application examples found in the literature.

3.4.1 Medicine

Johnson & Parker (1994) have developed a human thorax model, including the epicardium, to simulate bioelectric phenomena and support the design of defibrillator devices. Using a 3D interface, the designer could steer the numerical solver parameters and equipment configuration, such as size and magnitude of shocks.

Defibrillator design is also addressed by Aslanidi et al. (2005). They use the *gViz* steering environment to examine the propagation of electrical waves in ventricular tissues models. By applying current stimulus in different regions of the heart membrane and varying the signal amplitude and area of coverage, the behaviour of re-entrant waves can be investigated. Additionally to the electrical stimulus, pathologies and pharmacology can also be introduced in the model at run-time.

In the field of orthopaedics,Dick et al. (2008) develop a planning system for bone replacement procedures. In their prototype, a 3D model of patient-specific bone assists the surgeon on customising and placing a hip joint implant. At the same time, the stress distribution of the implant in the in-vivo bone can be assessed using a FEM, providing feedback to the optimal design of prosthesis.

Mazzeo et al. (2010) improved a fluid solver to visualize the blood flow in the cerebral vasculature. A ray tracing technique is implemented to achieve high resolution images from the simulation. The physical parameters of neurovascular system can be adjusted in execution time in order to study the hemodynamics behaviour.

3.4.2 Astrophysics

Esnard et al. (2006) implement a steering framework to integrate legacy simulation code (*Gadget2*) and provide parallel graphical visualization of the results. The infrastructure is demonstrated for a simulation of the birth of a galaxy, modelled by a gas cloud.

In a similar application, Costanzo et al. (2009) create a framework to aid astronomers to validate models of Mikyway galaxy structure and evolution against observed data.

The comparison of actual data with simulation output is also provided in the work of (WIJK et al., 1996). Their tool supports the parameter estimation of an atmosphere model for the planet Venus. Using the system, the expert could easily compare the simulation results with light scattering data gathered by the Pioneer Venus Orbiter spacecraft.

3.4.3 Physical Phenomena

An interactive program to simulate grain boundary and fracture phenomena in solids is presented by Merimaa et al. (2000). Before the simulation starts, the parameters of a two-dimensional Lennard-Jones model are configured, which can contains a grain boundary or an initial crack. Then, during run-time, the dynamical behaviour of the system is observed while the researcher stresses the material, by controlling the pressure and temperature parameters in the simulation.

Hecht & Harting (2010) investigate the structural properties formed by solid particles suspended in an aqueous solvent, in response to changes applied to the environmental parameters (i.e. pH-value, salt concentration and volume fraction of the particles).

In the work of Knezevic et al. (2010), a nuclear reactor modeling code is integrated into a computational steering framework bringing flexibility to simulate reactor physics and support the design of power reactors. Among the parameters that can be steered, the researcher can switch between the *Method of Characteristics* and *Nodal Expansion Method* in the simulation.

Stone et al. (2011a) describe the implementation of VMD software package for multi-purpose molecular dynamics simulation. Integrated in an immersive virtual reality environment, with support for multimodal input and haptic feedback, scientist can conduct interactive experiments to explore properties of structures, such as biomolecules or nanomechanical objects.

3.4.4 Environmental and Earth Systems

Brodlie et al. (2004) demonstrate the gViz application in an environmental disaster scenario. By controlling the weather parameters (e.g. wind direction), the scientist can predict the dispersion of a chemical pollutant in the atmosphere.

The motivation in the work of (MALAKAR et al., 2011) is the tracking and visualization of critical weather events. For this they build a framework to run a numerical weather forecast model and simulate the tropical cyclone Aila, formed in 2009. During run-time, climate scientists can specify regions of interest (e.g. low pressure or high vorticity zone) in the visualization system in order to steer parameters to perform a finer level of simulation.

Ribicic et al. (2013) provide a simulation system to examine the uncertainty present in flood situations. In their case study, the consequences of breaches in defence walls are analysed in a 3D model of Cologne city, assuming multiple possible sources of the leak. The strategies to present water to damage the buildings are also evaluated. Among the interaction capabilities in the system is the steering interface to change sand bag properties (e.g. position, orientation and mass), river properties (e.g. velocity and water level), protection properties (height of barriers, breach location), presence of debris (e.g. cars parked on the street).

3.4.5 Simulation-based engineering

Wijk et al. (1997) have developed a design tool to evaluate the mechanical properties (e.g. geometry and material) of wind turbines and their performance against the environmental conditions (e.g. wind profile and terrain roughness).

In the work of Laevsky et al. (1999) a computational steering is applied to predict the flow behaviour of a gob of glass in order to optimize the shape of a mould, used in a process for glass pressing.

A case study is presented by II et al. (2000) to evaluate the protection of critical electronics in the design of missiles. An inverse steering approach is adopted to optimize the presence of hot zones (i.e. regions of local maximum radiation) when the missile casing is exposed to high-power electromagnetic fields. By defining an objective function, the scientist guides the simulation to search the state-space and define the design parameters of missile body.

Borrmann et al. (2008) present an interactive fluid simulator to optimize the layout of operating theaters. The engineers experiment several configurations for the orientation and position of the air conditioning system and operating equipment in the room. By analyzing air flow pattern in a 3D scene, the risk of infections, caused by bad ventilation, is evaluated. Complementary, the tool also contemplates an illumination analysis tool.

A typical civil engineering application for evaluating the vibration comfort in building is presented by Ruess et al. (2009). The simulation of structure responses due to dynamic loading is supported by a framework based on FEM. At run-time, via an interactive interface, the engineer places load sources in a 3D model and analyses their effects on the building structure.

In (WAGNER et al., 2010) a multi-purpose CFD environment is adapted to incorporate steering functionalities. A simple example is given for visualizing the air flow effects when flight control surfaces of an aircraft are adjusted by the user.

An assisted optimization system is improved in the work of Lego et al. (2010) by the implementation of a visual steering mechanism. Based on results provided by state-space search algorithms, a domain expert interactively selects regions of interest using a multidimensional data visualization system to specify where a new local optimization should be performed. The system was coupled to an existing software tool for analyzing launch vehicle and missile configurations, in order to assist engineers in making trade studies on the mission trajectory, cost, schedule and risk.

Using the same concept for guiding the optimization process based on expert preferences, Matkovic et al. (2011) describe a tool used to optimize the design of complex systems in the automotive industry. In the illustrated example, an automatic algorithm explores the state-space to find a geometry configuration of car engine injection system, in order to minimize the presence of pressure oscillations in the common rail system. Then, intermediate solutions can be interactively selected to refine the state-space search.

Finally, the visual steering environment described by Coffey et al. (2013) is applied in the mechanical design of a medical device for performing biopsy surgeries. By exploring the geometrical properties of cannula pieces (e.g. radius, size and length), via the direct interaction with a 3D model, the physical properties of the equipment can be optimized.

3.5 Computational Steering Classifications

In the survey published by Mulder et al. (1998b) three main uses are identified in steering applications: *model exploration*, *algorithm experimentation* and *performance optimization*. The goal of model exploration is to provide insight in the simulation behaviour, by changing model and computational parameters. In the second type, the algorithm experimentation allows the runtime modification of a program structure to compare different pieces of simulation code. Finally, in a performance optimization application, the computational resources are manually allocated to improve the simulation performance.

Alternatively, a bi-dimensional classification is proposed by Parker (1999), wherein the steering tools are distinguished by their *usage type* (equivalent to those classes in (MULDER et al., 1998b)) and *user interaction level*. The interactivity is defined as a continuum were textual, graphical user interfaces, and visual programming languages represent respectively the lowest, middle, and highest levels.

In addition, Lingaraju et al. (2011) classify the steering techniques in two groups: geometrical steering and properties steering. The first is related to changes applied to geometrical properties in the simulation, which can be typically done by user interactions in a graphical scene (e.g. to move an object). The second group comprises the traditional GUI widgets, which modifications directly update a parameter in the simulation.

Analysing the infrastructure functionalities and the applications described in this section, one may conclude that a large set of problems can be addressed by computational steering techniques. Indeed, multiple scientific and engineering simulations can be benefited from steering, especially those which encompass some of the following aspects:

- its physics is modelled by ordinary or partial differential equations;
- the solution belongs to a large state space;
- the employed numerical method involves large scale computation and requires high performance resources (e.g. grids);
- its results are provided after a long execution time;
- its geometric configuration is complex or may be modified during simulation;
- its usage demands the collaboration of different teams; or
- the behaviour of the system and the appearance of events are difficult to predict.

On the other hand, some applications may not take advantage from a computational steering environment, including those whose simulation requires a few seconds to execute, with a tiny space state or whose user interventions take too long to be perceived (CHIN et al., 2003).

In resume, steering is a tool suitable for understanding the behavior and emerging properties of a system, by interactively guiding the course of simulation.

The sequence of events introduced by user in the simulation horizon leads the dynamics to a certain state which would not be achieved, or at least easily performed, by means of a predefined configuration of initial parameters. This sequence could have been programmed by some source of script, but its definition is due to the understanding that the conductor has acquired about the phenomenon dynamics along the simulation evolution.

4 THE ROLE OF COMPUTATIONAL STEERING IN SPACE ENGINEERING

The computational steering technique is adopted by many authors to bring flexibility and efficiency to their simulation activities. Their approach allows the scientists to interact online with an evolving scenario in order to quickly verify the effects of parameter changes on the model behaviour, to easily identify modelling mistakes by means of a visual feedback, to guide the simulation evolution to a given region of interest or to select these regions for further detainment.

In this chapter, the employment of these methods for improving spacecraft simulators in space engineering is discussed. First, a brief analysis of its benefits is done, followed by the introduction of potential applications in space engineering. Finally, a steering classification is proposed based on the type of intervention performed in the computational model, which can be used to guide the design and development of interactive simulations.

4.1 The essence of computational steering efficiency

Among all the benefits pointed in the bibliography, two of them can be emphasised as tacit advantages of computational steering over the traditional post-processed approach: (i) the enhancement of insight as scientist analyses the behaviour of a model and (ii) the time saved in the simulation process.

The idea of these gains is demonstrated by simulation applications from various scientific and engineering domains and often supported by testimonials of specialists who have experienced the steering tools in typical scenarios. Nonetheless, demonstrating the efficiency of these tools is a complex issue and generally the research results are presented qualitatively.

Specially regarding the *enhancement of insight*, comparing computational steering to non-interactive methods requires a deep investigation of the human cognitive process, aiming the comprehension of his or her interaction with the computer. Hence, a common approach in the human-computer interaction field is to conduct a series of interviews with potential users of the system, while a set of representative scenarios are presented to them. However, in order to collect reliable data from use cases, this method must reduce the influence of particular factors during the experimental sections, since the usability of the system could be affected by user's subjective aspects, like the level of expertise on the application domain, the individual familiarity with the problem, level of skill on using computational tools, level of attention during the experiment, among other psychological factors. For this reason, one approach is to maximise the number of users during an evaluation section and obtain average indicators on their interaction behaviour. Still, for many specialised domains, the universe of users can be very limited or the insight characterisation is so subjective and complex to define that the research enters purely in the psychology and human cognition field. Therefore, due to all these aspects the quantitative assessment of these benefits is out of the scope of the presented work.

On the other hand, the demonstration of *time-saving* can be quite direct when comparing two different tools, since the effectivity of using them can be measured in terms of the productivity it provides, which can be seen simply as the ratio of the size of the output to the total effort employed in the process (INTERNATIONAL ORGANIZATION FOR STANDARDIZATION, 2001; PARTHASARATHY, 2007; SUDHAKAR et al., 2012). For instance, the productivity of a certain simulation tool can be expressed by the number of hypotheses verified by a scientist in a given period of time (Equation 4.1):

$$\text{Productivity} = \frac{\text{No. of verified hypotheses}}{\text{Simulation time}}. \tag{4.1}$$

Consequently, the effort for conducting a set of hypotheses verification, measured by means of simulation time, can be assessed for different phases of the simulation session. For instance, in the case of a post-processed approach, the session starts with the configuration of the facility, which can include the implementation or adaptation of a script and the scenario setup, followed by its execution and expert analysis. The timeline of these steps is illustrated in the Figure 4.1. In this example, the script contains the instructions for changing the computational models as the simulation evolves to enable the confirmation (or not) of three hypotheses (H_1, H_2, and H_3).

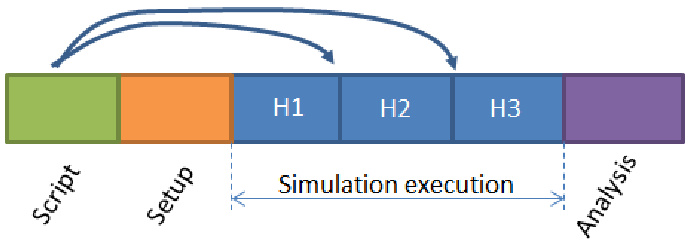

Figure 4.1 - Timeline of sequential steps in a simulation session conduced by a script to perform the verification of three hypotheses.

Contrastingly to a pure sequential method, the computational steering provides the user with the capacity to analyse and alter the evolution of the scenario as it evolves, as shown in Figure 4.2. In these cases, by directly controlling the computational model, the user replaces the script by on-line interventions.

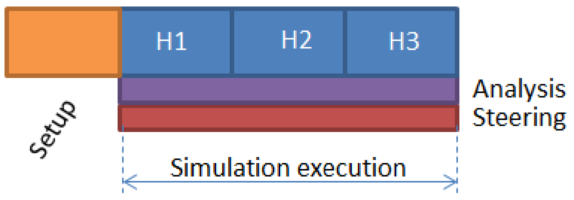

Figure 4.2 - Timeline of action in a simulation session conduced with computational steering to perform the verification of three hypotheses.

Even though the task parallelism provided by computational steering clearly promotes time-saving, one could still argue that the time for analysing the results in both cases can be slightly different, since the cognitive process is non-deterministic. Moreover, the required amount of time to program a script is not directly equivalent to the time used for altering the scenario with a steering interface.

In spite of that, it is common that in real life applications the appearance of new hypotheses occurs just after the scientist has analysed the behaviour of the model and identified a new region of interest to be explored in the state space. This means that conducting the scenario with a script will cause the simulation to be re-executed each time a new hypothesis needs to be checked. In the best case, this would mean running again only the setup step, but in many applications the full simulation horizon is likely to be computed one more time to ensure that the new test starts exactly in the same point in the time-space of the model. The worst case, which results in a progressive increment of processing time, is depicted in Figure 4.3.

Therefore, if the steps that involve a cognitive task are ignored (e.g. writing the script, analysing the results or steering the scenario), the total time required to execute a given number of hypotheses is equivalent to their processing time. Let th_i be the processing time needed to test the *i-th* hypothesis, then the total time to perform three tests using a post-processed approach is given by Equation 4.2:

$$TT_3^{PP} = th_1 + (th_1 + th_2) + (th_1 + th_2 + th_3) = 3.th_1 + 2.th_2 + th_3, \qquad (4.2)$$

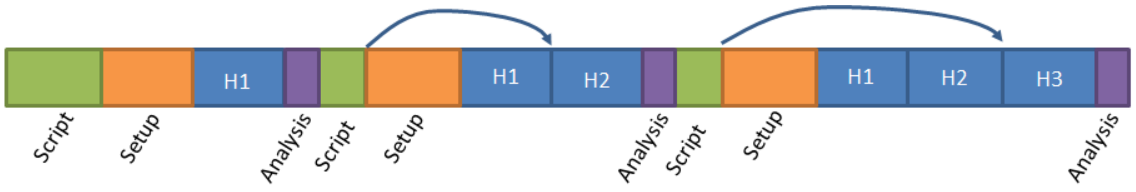

Figure 4.3 - Timeline of step required to verify three hypotheses with adjustments of scenario script.

while for a computational steering method it is given by the Equation 4.3:

$$TT_3^{CS} = th_1 + th_2 + th_3. \tag{4.3}$$

Thus, at least with respect to the processing time, the post-processed approach has clear disadvantages when compared to the computational steering one, as for the generic case of n hipotheses the total time will be:

$$TT_n^{PP} = \sum_{i=1}^{n} (n - (i - 1))th_i \tag{4.4}$$

and

$$TT_n^{CS} = th_1 + th_2 + \cdots + th_n. \tag{4.5}$$

In addition to that, the effects on total simulation time are also susceptible to the characteristics of computational model and its dynamics, which may amplify the contrast between the approaches. For instance, it is evident that the later a non-programmed change needs to be made in the scenario, the longer the overall execution time will be in a post-processed simulator. This is the case when the model behaviour is hard to predict or when the exact moment of intervention cannot be defined in advance and it is likely to be made on user's decision taken during the progression of the simulation. Similarly, a scenario that takes too long to reach a certain state of interest will impact on the user's productivity.

Besides its operational concept and the scenario peculiarities, the efficiency of a computational tool is subjected to the number and the quality of implemented functionalities, including its user interface layer. Looking from a pragmatic perspective, although a clear distinction can be made on steering and post-processed approaches, they are not necessarily conflicting in the context of a simulation environment. On the contrary, facilities providing both interfaces can exploit the best capabilities of each technique and cover distinct use cases. While the first promotes the scientist's immersion into the modelled phenomena, which will foster a continuous and natural flow of mental process, the latter provides complementary functionalities to support the simulation processes. The scripts, for example, play an indispensable role in the automation of scenario generation and execution. Following an activity of model exploration with computational steering interfaces, scripts can be prepared to perform regression testing or further exploration of the state space in a systematic, synchronised and reproducible way. Its application is also preferable for long-term executions, when it is not possible to save and restore the whole state of a simulation, e.g. when physical elements are connected in the environment. In the same manner, data-mining tools can coexist in a hybrid facility to provide extra analysis on results obtained from a steering section.

4.2 Potential applications in space engineering

As modelling and simulation is becoming an indispensable resource on supporting most of the space engineering activities, it is essential to reduce development and operational cost in projects of spacecraft simulation tools. Regarding the construction process, a common approach is to increase the reuse of software components and modelling artefacts, by creating flexible infrastructures and design standards that increase the general commonality of such tools, as proposed by the ECSS–E–TM–10–21 and ECSS–E–TM–40–07 technical memoranda. In addition to that, operational costs can be reduced with the adoption of user interfaces that naturally adheres to the engineer's work methodology, thereby minimising training hours and the required effort to setup the simulation environment.

Similarly to what is already happening in other domains, computation steering can contribute in this direction, providing the fundamental mechanisms to bond highly interactive user interfaces to low level simulation parameters. Its expansion on the fields of space engineering can go alongside the development of simulators that already answer the needs of activities performed along the mission life cycle.

In the very early phases of a space project, when the uncertainty in the mission concept is still high, computational steering can bring great agility to the concurrent engineering process. Changes in the system architecture can be continuously applied in the simulation models, whereby hypothetical concepts that spontaneously appear in the section are rapidly verified. Moreover, budget studies and architectural configurations can be conducted in a cooperative way, promoting a systemic view for trading and awareness of the design.

In the subsequent phases of design and production, computational steering can simplify the way the engineer details the architecture by interactively modifying the simulation scenario and tuning system parameters for consolidating requirements and executing sensitivity or performance analysis. Critical algorithms and on-board software can be exposed to a wide set of environmental conditions set by the designer in order to check their robustness under nominal and contingency circumstances. In the case of non-conformities come to light, the tester can immediately guide the scenario to further debug and investigate the stem from these unexpected behaviours.

Apart from easing the design of space systems, the steering method is also a promising approach for stimulating avionics under test for the purpose of identifying testing strategies, specifying test procedures, and performing verification and validation. Currently, the real time conditions required by hardware-in-the-loop (HITL) environments and the inaccessibility to some of the on-board computer internal variables may impose constraints on the fully employment of computational steering features. Nevertheless, the testing environment is still suitable for implementing steering mechanism and to accommodate user adjustments as new testing ideas emerge in the scenario.

Dynamical changes in the testing conditions are also important functionalities to be explored in the assembly and integration activities of a space system. By rigging simulation tools with computational steering, the quick replacement of real pieces of equipment by virtual models becomes more flexible, easing the gradual substitution of stubs by flight models and supporting the investigations of non-conformities during assembly (e.g. caused by an incorrect harness connection). In addition to that, the whole preparation and validation of procedures can be assisted by 3D virtual models of satellite pieces, thus anticipating mechanical incompatibilities and assuring the feasibility of the tests on physical devices.

Lately, during the operational phase of the space mission, scenarios with dynamic behaviour can be easily prepared for training sessions, exposing the operators with unexpected situations and guiding the simulation evolution depending on their reactions. Furthermore, failure investigations can be efficiently conducted by interactively injecting faults into the simulation models and comparing their results with telemetry data.

On the whole, the computational steering approach may contribute in any simulation that encompasses activities for verifying simulation models and validating the scenario setup, simulation tuning, understanding the system behaviour, designing and verifying a solution, conducting performance analysis and system tuning, specifying and executing test cases and procedures, debugging and investigating malfunction in flight or ground equipment, and training operators.

4.3 A novel computational steering classification

Depending on the type of activity being supported by simulation, different user interventions are expected in the scenario and then distinct steering mechanism may be applied.

As presented in the previous chapter, the computational steering concept can be basically understood as the capability to modify a computational model while its results are being generated and examined. Although simple, this definition is very comprehensive, since various computational aspects may be encapsulated in a single simulation model, i.e. regarding its parameterisation, instrumentation and other characteristics implied by its numerical method. Similarly, the interactive user interface can be derived in multiple mechanisms for accessing the simulation models and displaying the output data. As a consequence of this plurality, and in order to maximize the reuse of a computational steering tool, the software architecture must accommodate a vast range of interaction requirements and be flexible to cover a wide number of use cases.

Aiming to guide the development of such advanced architecture, this work proposes a novel classification for computational steering, based on the type of interventions that a user may apply on the computational model. This organisation assists the identification and construction of mechanisms to support the various aspects of steering within a spacecraft simulation, which may be incorporated by different pieces of software artefacts (i.e. configuration files, simulation kernel, visualisation system or by the model).

Based on taxonomies previously presented in the bibliography, the current extension groups the type of changes made by the user in the following classes:

a) **Behavioural**: are the changes that affect the behaviour of mathematical model or the existing algorithm, which is instrumented to allow steering of its internal parameters. They can be specialised in two sub-types:
    - *Physical parameters*: that represent inherent properties of the modelled physical phenomenon, whose manipulations imply direct

changes on the model behaviour. In most cases, the parameter steering is done by a single change of a variable, provided by a precise text input.

   – *Geometrical parameters*: are those directly associated to the shape and internal structure of a model, but that can indirectly interfere on its behaviour or on the behaviour of other models. They describe the size, position and orientation attributes of an object that may be altered by a precise text input, but typically are manipulated via graphical widgets (especially for 3D domains). Changes on these attributes may propagate the update of other internal variables (e.g. by resizing and object, its volume and surface area will change).

b) **Resolution**: the resolution comprises the level of details that a physical phenomenon is computed by the simulation model. Not only does the model resolution imply on its output precision, but it also affects the computational performance when it is executing. The user may adjust the model resolution in a running simulation in space or time domains.

   – *Spatial resolution*: comprehends the overall structure of the model and the topology that relates its elements or several models. This type of resolution defines the discretisation level of the computational model. The better the spatial resolution, the greater the number of elements and the amount of computational resources.

   – *Temporal resolution*: defines the execution frequency of a simulation model and its internal integration step. A high temporal resolution implies on a small integration step or execution interval, which impacts on the simulation processing time.

c) **Algorithmic**: this type covers the *algorithm exploration* and *algorithm refinement* classes, respectively proposed by Mulder et al. (1998b) and Parker (1999), in which the whole mathematical model may be dynamically replaced by the user. With this type of interventions, new modelling approaches, numerical methods and structures can be verified while the simulation scenario is still running. In the current work, this type of steering assumes that the external interfaces of the model are preserved.

d) **Structural**: comprises the changes on the overall assembly of the scenario, including the composition of models and their interrelations. This may alter the number and types of models instantiated in the simulation and the links that connect them in runtime.

e) **Computational performance**: called *performance optimization* by Mulder et al. (1998b) and *performance steering* by Parker (1999) as , this class of user intervention may improve the allocation of computational resources, such as memory and processor sage, in order to tune the overall performance of the computational models as they are executed.

f) **Data presentation**: are the portions of the steering commands that exclusively affect the way the output data is post-processed and presented to the scientist. It may include the selection of visualisation method (e.g. textual, graphical, or immersive, among others) and related adjustments for defining e.g. colour and texture attributes or the positioning and orientation of 3D cameras. The format for representing scientific data can also be chosen to better display a given property of the system (e.g. field view, geometrical structure, gradients) and processing algorithms may be enabled to filter, fuse or aggregate data from different sources.

5 A NOVEL COMPUTATIONAL STEERING FACILITY APPLIED TO SPACECRAFT SIMULATION

Currently, the SMP2 concepts are becoming a standard in the construction of spacecraft systems simulation and its interfaces are already adopted by some infrastructures, such as *EuroSim*, *SimSat*, *Basilis*, and *SimTG*. In this work, a novel facility is proposed, in which the standard concepts of SMP2 are implemented in harmony with the main steering mechanisms, some of those yet not explored by the existing simulators (e.g. history tree management or on-line control of resource allocation).

In the section 5.1, the design goals of the simulation architecture are summarised, as a result of the key functionalities identified in the works from the literature and in the best practices presented in the technical memoranda ECSS–E–TM–10–21 and ECSS–E–TM–40–07, as discussed in chapters 2 and 3.

Moreover, in the section 5.2, the details of the software design are described, in which an innovative steering layer is proposed (section 5.3) to enable the connection of interface widgets with simulation parameters in a flexible and generic way. In this layer, a special trigger mechanism is implemented to automatically perform state synchronisation of the models, whenever required to maintain the coherence of the simulation after a user interaction occurs.

Following, in the section 5.4, some aspects of the implemented applications are presented, mainly focusing on the overall user interface components, followed by a brief discussion in section 5.5.

5.1 Design Goals

In the Table 5.1, a list of the features commonly implemented by the steering applications and satellite simulators is given. This list is the synthesis of the literature survey performed in this work that will delineate the design goals of the steering facility. For each feature identified, its inclusion in the infrastructure scope is examined envisaging the demonstration of steering approach in the applications of the space engineering domain.

Table 5.1 - Design goals adopted in this work for building a computational steering facility applied to spacecraft engineering.

Feature Type	**Feature**	**Scope**	**Design strategy/rationale**
User interface type and steering approach	Textual	Yes	An extension of `Smp::IForcibleFields` is done to support the steering of model fields in the lower level of the simulator kernel. Based on that, multiple steering front-end can be attached to perform on-line changes on simulation, i.e. from basic text input to graphical approaches, over a TCP/IP bus.
	GUI	Yes	This type of front-end is demonstrated with direct 3D image manipulation and use of 3D widgets.
	Natural I/F	Yes	Customized applications that capture gestures via touch and inertial sensors can be attached to the simulation.
	Immersive	No	The visualization and steering front-end are considered clients of the simulation infrastructure. When available, an immersive environment could be attached to the simulation, probably with tiny modification on the communication interface.
Input commands	Topology and boundary conditions	Yes	Although the infrastructure does not support these feature directly, they can be easily handled by the application models.
	Numerical method parameters	Yes	
	Source code change	Yes	
	Resource allocation control	Yes	This feature is demonstrated by a mechanism that allows the user to reschedule the model's entry points and to control the number of threads used to execute them.

(Continued...)

Table 5.1 - Continued

Feature Type	Feature	Scope	Design strategy/rationale
Visual feedback	Visualization method selection	Yes	The main visualization is performed by independent client application connected to the infrastructure over a TCP/IP bus. Once the communication protocol is implemented in both sides, multiple customized can be adopted.
	Instantaneous feedback	Yes	The communication channel and infrastructure does not imply significant delays on the feedback signal.
Data abstraction & Filtering	Parameters grouping	No	The simulation is an assembly of SMP-like models that can be composed and aggregated in a hierarchical structure. No extra organization is assisted by the infrastructure.
	Data mining	No	These types of pre or post-processing are out of the scope of this work.
	Data reduction	No	
	Data operators (e.g. aggregation)	No	
	3D representation	Yes	External visualization clients can be attached to map model fields into 3D object's properties.
	Track icons	No	This is a desirable function but not essential for the demonstration done in this work.
Breakpoint		Yes	It is possible to hold the execution of the scheduler on the basis of rules applied to the values of published field (i.e. comparing the values against other provided by the user). The mechanism could be easily extended to the execution of entry points.

(Continued...)

Table 5.1 - Continued

Feature Type	**Feature**	**Scope**	**Design strategy/rationale**
Snapshot	Checkpoint	Yes	By using the `Smp::IPublishing` interface the model may indicates the fields that are state or not in the simulation. In special case, models can implement the `Smp::IPersist` interface. The full snapshot archive also includes kernel internal parameters, such as job queue state. This mechanism can be invoked manually by the user or automatically trigged in predefined periods.
	Restore	Yes	All snapshot archives can be used to restore the state a simulation with the very same setup.
Synchronization	Data input	No	Not essential for the current demonstration. All the inputs are handled asynchronously.
	Data coherence	Yes	The model can be notified by an entry point on the event of a parameter modified by user. Via this mechanism, the model has the chance to update any other parameters to keep an internal coherent state.
Application integration	Code annotation	No	The application integration approach uses the SMP2 standard interfaces. It is supposed that all models implement them natively or a wrapper has to be created.
	Visual language	Yes	Since the simulation artefacts follow the SMP2 meta-model, it is strait forward to adapt a UML tool to visually design the components. This is demonstrated in Appendix A.
	Dataflow	Yes	The dataflow integration is supported by the SMP2 field link mechanism.

(Continued...)

Table 5.1 - Continued

Feature Type	Feature	Scope	Design strategy/rationale
	Support for concurrent systems	No	Not crucial for the current demonstration. A single thread suffices for executing the models in the case studies.
	Support for distributed systems (grid)	No	Not essential for the current demonstration. Even there are several modules that are distributed in the facility (e.g. visualization, hardware-in-the-loop, legacy systems), the simulator kernel itself is not distributed. The classes of problems addresses in this work can run in a single processor.
	Framework	Yes	The kernel architecture is designed as a framework for dealing with SMP2 standard interfaces.
History log & Playback	Event log	Yes	The native `Smp::ILogger` service can be used by all simulation models. The interface is extended for internal use of the kernel.
	Data log	Yes	For the demonstration a simple file-based log is implemented.
	Parameter selection	No	Not essential for this demonstration. Currently all parameters are logged in a fixed frequency.
	Frequency selection	No	
	Playback	Yes	A playback module can re-execute scenarios based on historical simulation data.
	History tree management	Yes	At any point in playback time the simulation can be restored from previously stored snapshot and a new scenario branch can be generated. The facility can control these branches in a history tree structure, for future use in playback session.

(Continued...)

Table 5.1 - Continued

Feature Type	Feature	Scope	Design strategy/rationale
Controllers	Play, stop, pause	Yes	The user can hold and resume the simulation as desired.
	Step	Yes	When paused, the step command will advance the simulation to the time of the next job in the queue.
	Backwards	Yes	When executing a playback, the simulation can run in reverse way, i.e. the simulation clock runs backwards.
	Time step control	No	The internal integration time step is implemented by the application model and then out of the scope of the infrastructure. Still, if this parameter is a published field, then it can be steered externally.
	Jump to time	Yes	When executing a playback, the simulation time can be set arbitrary within the limits of the simulation horizon.
	Real time	Yes	The progress of simulation time can be synchronized with the wall clock time. Only soft real-time is supported.
	Accelerated	Yes	Conversely to the real time (RT), the clock can be accelerated or delayed accordingly to an acceleration factor (1: RT; $>$ 1: faster than RT; $>$ 0 and $<$ 1: slower than RT).
	AFAP	Yes	The execution time of all entry points is limit only by the processing performance.
Collaboration	Visualization	Yes	Many visualization clients can be attached to the simulation infrastructure via a TCP/IP bus.
	Async. steering	Yes	Asynchronous steering is the only supported way.

(Continued...)

Table 5.1 - Continued

Feature Type	Feature	Scope	Design strategy/rationale
	Sync. steering	No	Not essential for this demonstration. Many steering clients can connect to the on-going simulation. However there is no explicit synchronization on the commands.
	WAN/Web	No	Not essential for this demonstration. Even the communication within facility is done via TCP/IP links, it is out of the scope of this thesis the study of delays on the communication for links with long distances.
	Ubiquitous	Yes	The use of mobile platforms is demonstrated in the case studies (Chapter 6).

5.2 Computational Steering Facility Architecture

The computational steering facility designed in this thesis comprises an ensemble of hardware and software elements that interoperate in a distributed environment [1].

The overall architecture, illustrated in Figure 5.1, includes a software suite, whose applications are connect by an Ethernet network and provides a set of generic functionalities for simulation modelling, configuration, executing, monitoring & control, visualization and steering. As it can be noticed, many of these components are in common with the reference simulation environments proposed in the ECSS-E-TM-10-21 (ECSS, 2010a) and by Eickhoff (2009).

The *Simulation Infrastructure* is one of the central elements in the architecture and it is in charge of loading and executing the application models accordingly to a predefined scenario. It also closes the loop with the *System Under Test* (SUT), whenever the use case includes an external hardware equipment or on-board computer.

The construction of environmental and application models is supported by

[1] Distributed in the sense each application or piece of equipment may run independently, connected in a network. The simulation infrastructure itself is one of the processing nodes, whose components and models are not distributed.

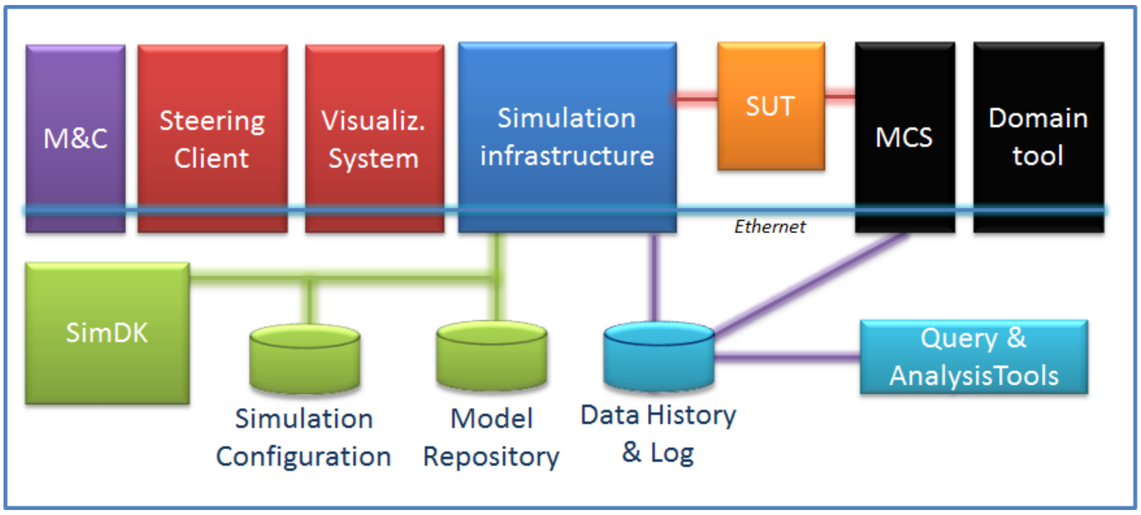

Figure 5.1 - Overall architecture of computational steering facility.

the *Simulation Development Kit* (SimDK) that provides a set of tools for designing, implementing, compiling, and packaging software components. The model packages, their metadata and configuration artefacts are stored by the *Simulation Configuration* database and the *Model Repository*, which serve too as interfaces between SimDK and the infrastructure.

The simulation front-end comprises distributed clients with customized applications for textual, 2D or 3D data visualization or computational steering inputs and they are represented by the Steering Client and Visualization System modules. Moreover, basic *Monitoring and Control* (M&C) actions can be dispatched remotely to guide the simulation execution flow that typically would also include a script mechanism to automate the execution of repetitive test cases. Post-processing can be carried by *Query & Analysis* tools based on data retrieved from the *History & Log* database.

Occasionally, the facility may integrate a *Mission Control System* (MCS) for processing Telemetry & Telecommand, or other ground support equipment. Among the complementary test-bench elements and legacy systems are, for example, the hardware front-ends, *Special Check-Out Equipment* (SCOE), and specialized domain software, such as thermal or mechanical analysis tools.

In order to maximize the simulation infrastructure reuse and ensure flexibility on reconfiguring different scenarios, the simulator kernel is designed as a software framework and is kept generic enough to incorporate any model that conforms to the Appplication Programming Interface (API) specified in the SimDK. To accomplish

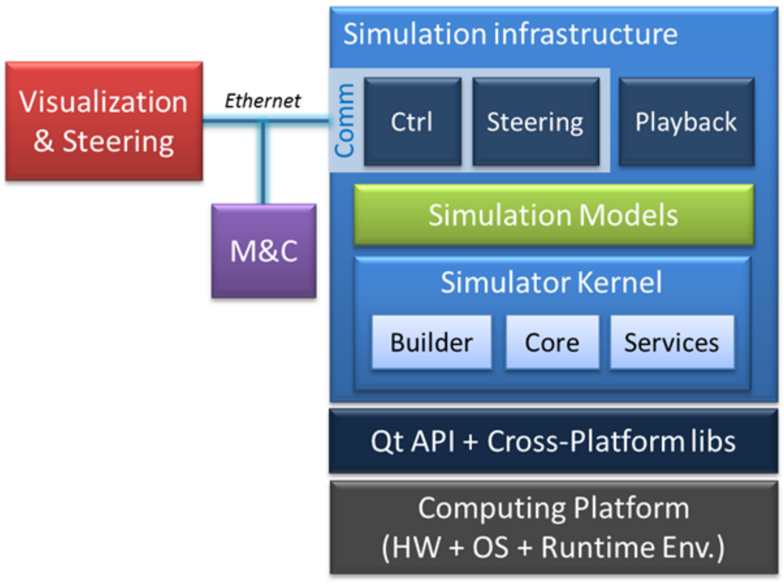

Figure 5.2 - Simulation infrastructure architecture.

this, the environment-model interface is built on the basis of SMP2 concepts, wherein most of mechanisms and data types defined by the standard are implemented in the simulator kernel (ECSS, 2011b).

As presented in Figure 5.2, the infrastructure comprises a set of software modules, in which the kernel plays a central role, providing elementary functionalities for building and running a simulation scenario and supporting cross-platform applications, since it is constructed using Qt Framework (EZUST; EZUST, 2006). The kernel is an independent component provided by the *SimuBox*, a simulation framework built at INPE, in the context of this thesis, that is described later in subsection 5.2.1.

On the top of the kernel, customized modules reside for accessing models' state and functions or commanding the scenario execution. External client applications can connect to the infrastructure – which plays the server side in the communication – thereby monitoring and controlling the simulation remotely. Commands for debugging, saving & restoring snapshots, or steering are also handled by the *Controller and Steering* modules, being the later the focus of the work in this thesis and the main contribution to the architecture proposed in the ECSS-TM-10-21. Besides that, the infrastructure is supplemented with a *Playback* module that runs a simulation scenario from historic and snapshot data.

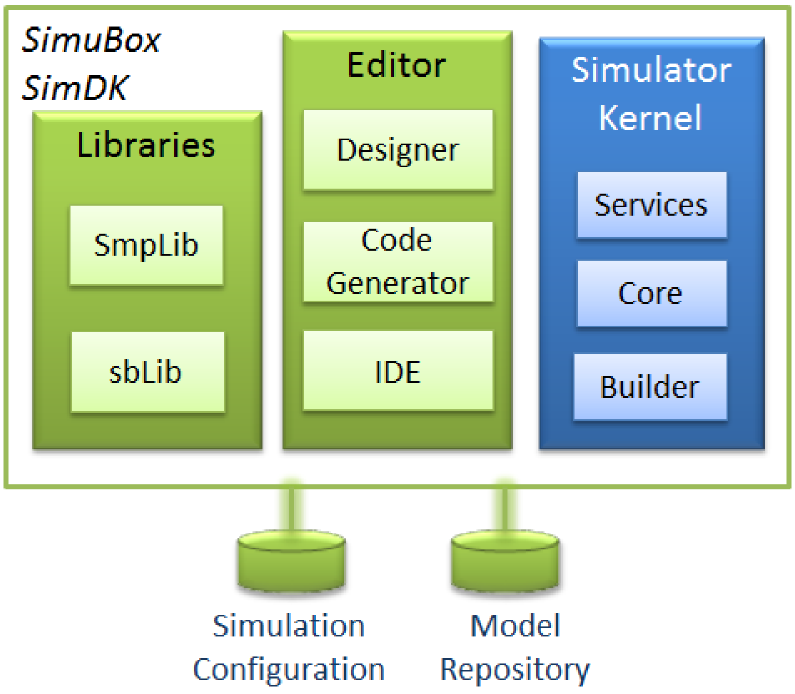

Figure 5.3 - *SimuBox*'s Simulation Development Kit elements.

5.2.1 *SimuBox* Framework

The *SimuBox* is a software framework that aims to be a platform for studying and exploring simulation concepts and related technology within satellite engineering domain. It provides a *Simulation Development Kit* (SimDK) with a set of C++ libraries, editing tools and simulator kernel to support the design and codification of models and simulation applications (Figure 5.3).

Afterwards the ECSS-E-TM-40-07 publication, the project has been motivated to afford simulations with SMP2 models, in order to assess the potentials of the standard. As a result, two libraries have been developed, in collaboration with the software engineering team from *Ground System Development* division at INPE.

The *SmpLib* encompasses the SMP2 component model mapping to C++, with small adaptations. In addition to the codification of interface classes – i.e. header files available from the volume four of the technical memorandum – this library also contains the implementation of exception classes and definition of primitive type in accordance to the computational platform.

Aligned with the concept of a *Model Development Kit* (MDK) (ECSS, 2011c), the

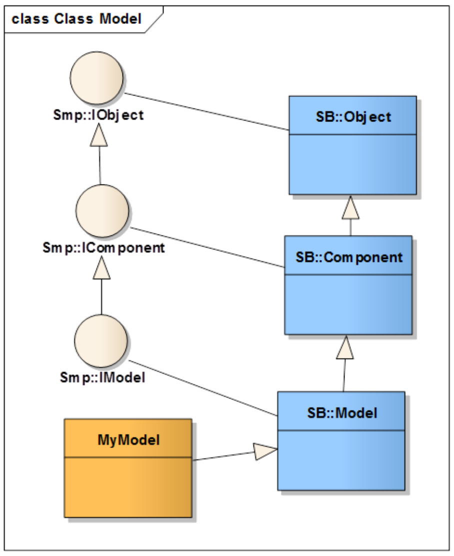

Figure 5.4 - Codification of *MyModel* class supported by *sbLib*.

sbLib provides a default implementation for the interfaces defined in *SmpLib*. This is a convenience mechanism to promote code reuse and to alleviate the programming of classes derived from SMP2 abstract types. For instance, when designing the `MyModel` class in Figure 5.4, one could derive directly from the SMP `IModel` interface and implement all the virtual methods from `IObject`, `IComponent` and `IModel`. Instead of that, deriving from *SimuBox*'s Model, the developer can focus on the codification of the application model, since a default implementation is inherited for the SMP2 interfaces.

In the same direction, the editing tools automate the generation of recurrent code for the models and facilitate their rearrangement in various simulation scenarios. By designing with a diagrammatical tool, the simulation engineer describes the types of models, their instantiations, interconnections, and scheduling for a given application. Later on, the diagrams, which adopt a formal semantic, are exported to a set of metadata artefacts, in accordance to the SMP2 meta-model scheme (i.e. following the XML format for the catalogues, assemblies, packages, and schedules). Moreover, for each model package, corresponding C++ code is produced to enable classes factoring and deployment into dynamic libraries. After these artefacts and binary packages are made available via the *Configuration* database and *Model Repository*, which are described in more details in Appendix A.

The *Simulator Kernel* is delivered as a runtime component compliant with the metadata and model packages produced with the editor and SimDK libraries.

During execution time, configuration files are used to load the binary packages and instantiate the models into the environment. This is done by the *Builder* module, which also interconnects models with interface, data or event links and sets initial values for parameters.

The *Services* module provides common utilities invoked by the models, like Scheduler, Time Keeper, Resolver and Logger defined by SMP2. The implementation of SMP2 `ISimulator` interface and the publication of fields and operations are handled by the *Core* module, which coordinates all the components in the kernel and control the simulation execution state.

In total, the SMP2 standard defines circa 100 types, including interfaces, data types and exception classes. Currently, *SimuBox* has fully implemented over 90 of them.

5.3 Detailed Design of Computational Steering Mechanism

The computational steering facility design takes advantage of mechanisms readily available from the SMP2 standard to implement features such as on-line parameter modification and snapshot. By instantiating SMP2 managed interfaces (e.g. `IManagedModel`, `IEventProvider`, and `IEntryPointPublisher`), simulation components provide access to their operations and fields, consequently allowing other components to change their state. Nevertheless, this access can be constrained and regulated by the simulator kernel, which sometimes avoids the manipulation of these properties. Still, from the perspective of a steering application, it is desirable that every parameter could be accessible, regardless of restrictions applied by the publishing model.

To overcome this limitation, the steering module in the infrastructure implements a different channel for manipulating model field that have been previously published in the simulator kernel. The approach consists on providing *client steering widgets* with direct links to the parameters, allowing their value modification or temporary override. Further, the connection can be ornamented with *adapters* that apply transfer function operations in the steering signal or trigger programmed entry points. The set of components that implement this mechanism is depicted in Figure 5.5 by the elements *widget back-end, adapter, remote widget back-end, steerable fields,* and *adapter catalogue.*

Any *steering widget* connects to the *steering adapters* via the *widget back-end* component, which defines standard interfaces for widgets attach/detach to/from

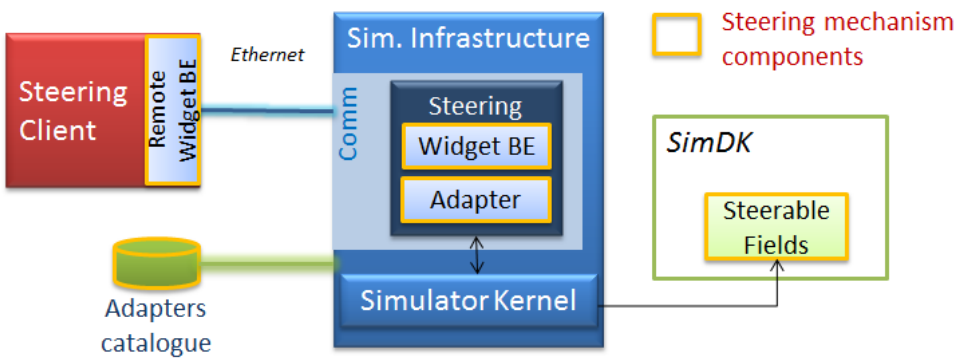

Figure 5.5 - Architecture detailed with components that enable computational steering in the simulation infrastructure: steerable fields mechanism, widget back-end, adapter component and catalogue, and remote widget back-end.

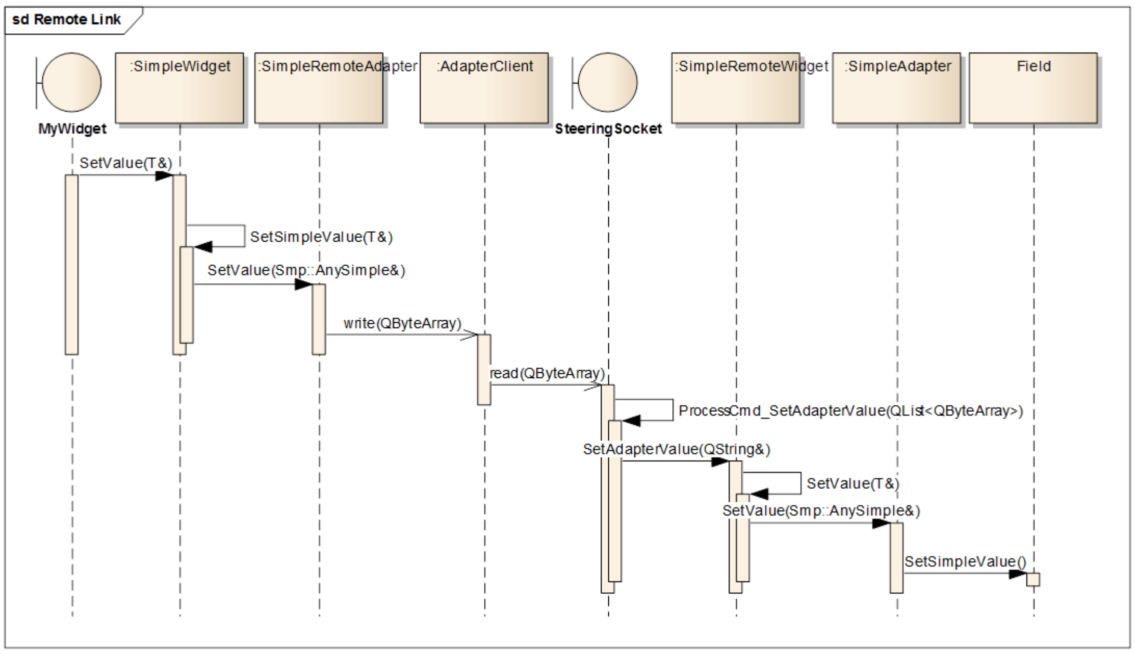

Figure 5.6 - Message invocation sequence originated by a remote adapter over TCP/IP.

adapters and set parameter values. When widgets are deployed in a distributed steering client, the widget-adapter connections are brokered by a specialized widget back-end that communicate with remote adapters over TCP/IP, as detailed in Figure 5.6.

Before the steering signal can be propagated throughout the *adapter* to a field, transfer functions or inhibiting rules may be applied to the value. In the current architecture, this is demonstrated with simple operations to perform scale and bias

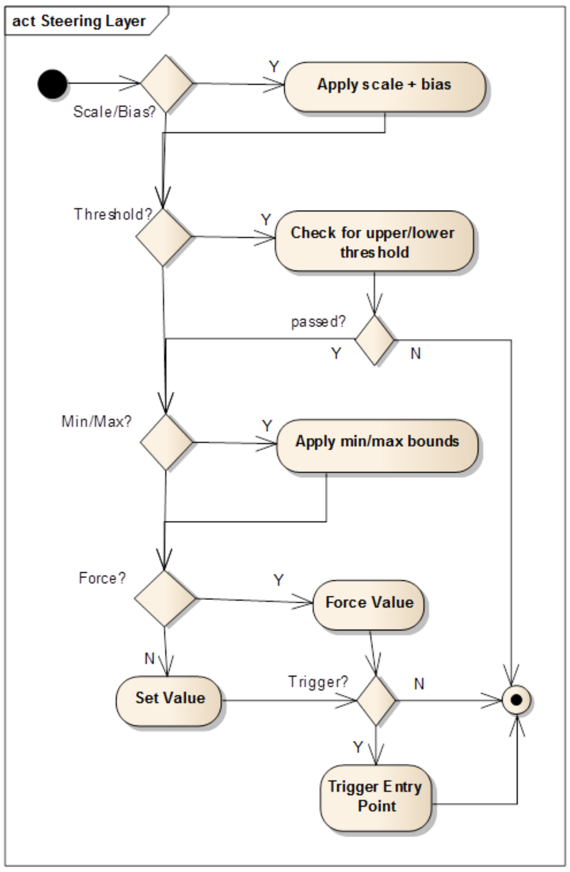

Figure 5.7 - Logical sequence of activities performed by the steering adapter.

gain, to limit the value within a minimum or maximum bound, and to restrict the propagation to a given threshold value. Moreover, the adapter can have an entry point associated, which will be triggered each time the propagation pass/fail criteria of adapter succeed. This mechanism is particularly important to maintain the coherence in the state of model, since the change of some parameter may imply the update of others (e.g. changing some of the orbital parameters will trigger the state vector update). In those situations, the entry point will notify the model to allow its internal reconfiguration. Summarising the adapter behaviour, the overall algorithm is defined by the activity diagram in Figure 5.7.

The structure of widget back-end and adapter components is also described in the class diagram from the Figure 5.8, where the relationship of the classes can be observed. Two interfaces derive from `IWidget` to handle steering connections with simple or array fields, which implementations are done via instantiation of template classes. This generic programming design (i.e. with C++ Standard Template Library) assures great flexibility to specialize the code for dealing with

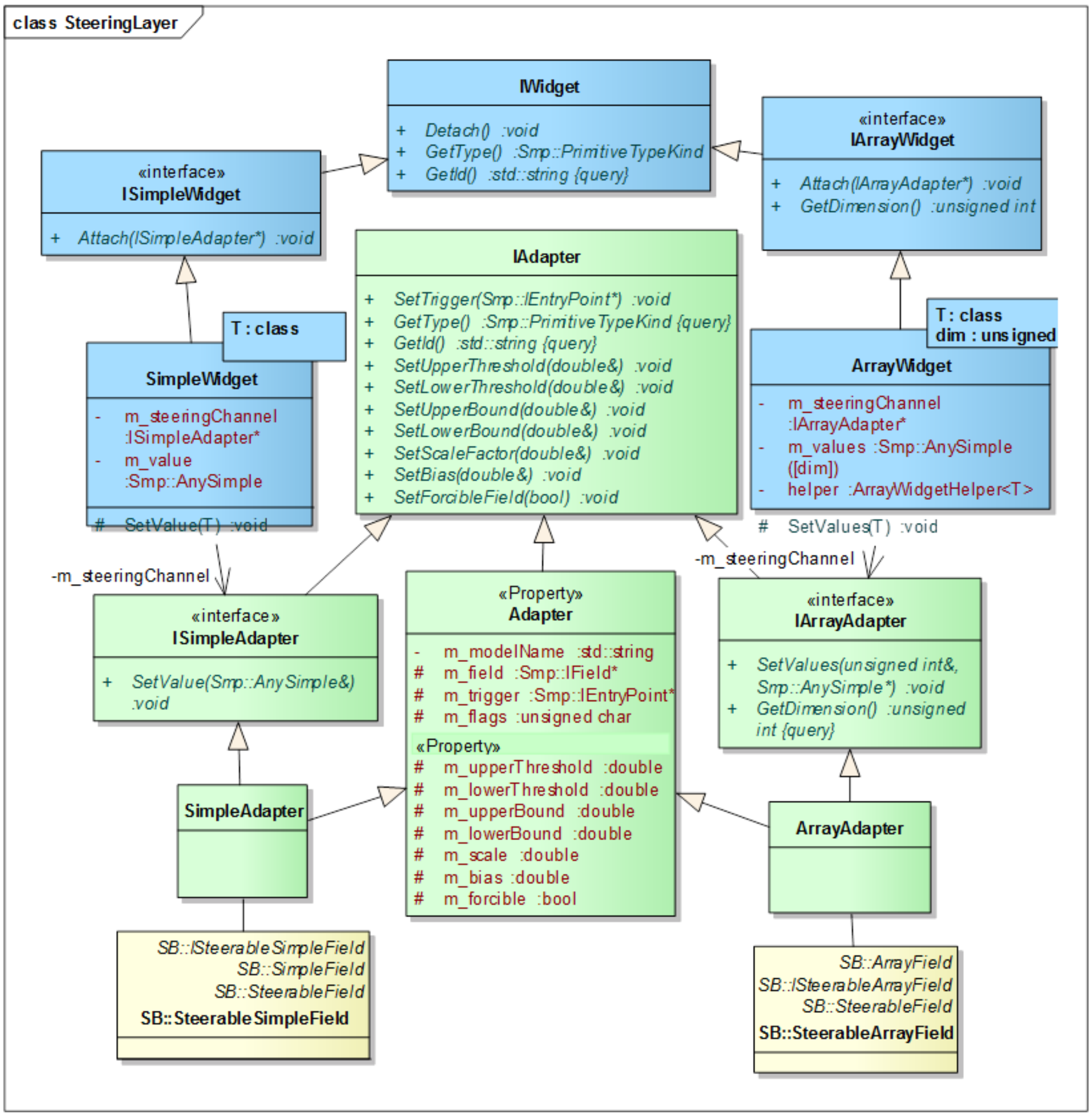
class SteeringLayer
IWidget
+ Detach() :void
+ GetType() :Smp::PrimitiveTypeKind
+ GetId() :std::string {query}
«interface»
IArrayWidget
+ Attach(IArrayAdapter*) :void
+ GetDimension() :unsigned int
«interface»
ISimpleWidget
+ Attach(ISimpleAdapter*) :void
IAdapter
+ SetTrigger(Smp::IEntryPoint*) :void
+ GetType() :Smp::PrimitiveTypeKind {query}
+ GetId() :std::string {query}
+ SetUpperThreshold(double&) :void
+ SetLowerThreshold(double&) :void
+ SetUpperBound(double&) :void
+ SetLowerBound(double&) :void
+ SetScaleFactor(double&) :void
+ SetBias(double&) :void
+ SetForcibleField(bool) :void
T : class
SimpleWidget
- m_steeringChannel :ISimpleAdapter*
- m_value :Smp::AnySimple
# SetValue(T) :void
T : class
dim : unsigned
ArrayWidget
- m_steeringChannel :IArrayAdapter*
- m_values :Smp::AnySimple ([dim])
- helper :ArrayWidgetHelper<T>
# SetValues(T) :void
-m_steeringChannel
-m_steeringChannel
«interface»
ISimpleAdapter
+ SetValue(Smp::AnySimple&) :void
«Property»
Adapter
- m_modelName :std::string
# m_field :Smp::IField*
# m_trigger :Smp::IEntryPoint*
# m_flags :unsigned char
«Property»
# m_upperThreshold :double
# m_lowerThreshold :double
# m_upperBound :double
# m_lowerBound :double
# m_scale :double
# m_bias :double
# m_forcible :bool
«interface»
IArrayAdapter
+ SetValues(unsigned int&, Smp::AnySimple*) :void
+ GetDimension() :unsigned int {query}
SimpleAdapter
ArrayAdapter
SB::ISteerableSimpleField
SB::SimpleField
SB::SteerableField
SB::SteerableSimpleField
SB::ArrayField
SB::ISteerableArrayField
SB::SteerableField
SB::SteerableArrayField

Figure 5.8 - Class diagram of steering layer showing relationship between widgets, adapters and steerable fields.

fields of any SMP2 primitive type and arrays of any size. Still, a *builder* mechanism must checks for type and size compatibility, beforehand a widget can be attached to an adapter.

By default, every field published in the kernel implements a special interface named `ISteerableField`, which extends the SMP2 forcible field concept, used to pin a given field to an arbitrary value. This is a useful strategy to inject failure or to steer the data exchanged between models, even though the forced model remains free to update its fields internally.

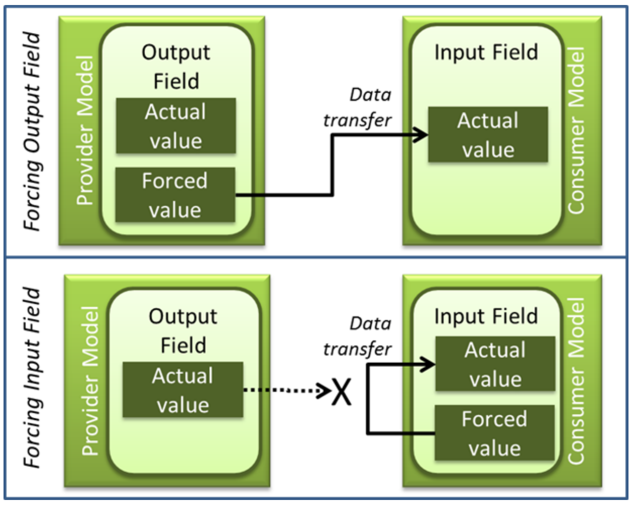

Figure 5.9 - Differences on transferring data from output to input field when their values are forced.

In the dataflow-based assemblies, output fields are linked to inputs and the data transferring is made explicitly by the kernel (i.e. scheduled). Forcing the value of these fields implies two distinct transferring behaviours, as shown in Figure 5.9. When the output field is forced, the failed value is copied to the input field of the consumer model. In this case, the provider may choose to operate over the actual or forced value, since it has directly access to the variables that reside in the model's memory space. Conversely, when the input field is forced, the output value is ignored for data transferring. Instead of that, the failed value in the consumer overwrites the current one.

The class structure for steerable fields is shown in Figure 5.10. As mentioned before, it is based on SMP2 forcible fields, but extended for both types of simple and array fields. Further, the `ISteerableField` interface defines the `OverwriteFieldValue()` service, which is invoked by the field link mechanism, always the input field is forced. This approach has the advantage to rid the consumer model of checking whether the field is failed or not (i.e. using *if* statements or accessing the field via `IManagedModel` interface), thus reducing the computational overhead. Another use to this additional service is to associate the overriding action to an entry point and automatically trigger it before the model is executed (e.g. resetting an internal variable to the forced value on each simulation step).

The last component in the steering architecture is the *adapter* catalogue. This element increases the flexibility of the facility, since various configurations of adapters can be specified for each simulation scenario. To accomplish this, a

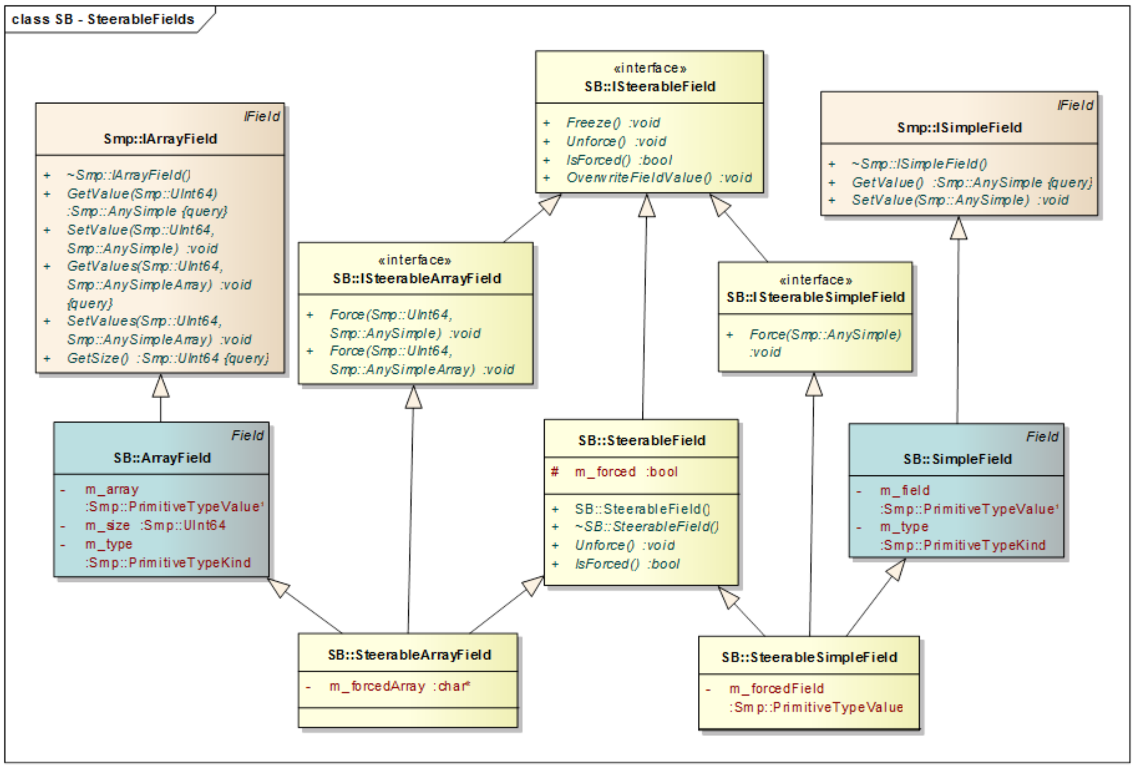
class SB - SteerableFields
«interface» SB::ISteerableField
+ Freeze() :void
+ Unforce() :void
+ IsForced() :bool
+ OverwriteFieldValue() :void
IField
Smp::IArrayField
+ ~Smp::IArrayField()
+ GetValue(Smp::UInt64) :Smp::AnySimple {query}
+ SetValue(Smp::UInt64, Smp::AnySimple) :void
+ GetValues(Smp::UInt64, Smp::AnySimpleArray) :void {query}
+ SetValues(Smp::UInt64, Smp::AnySimpleArray) :void
+ GetSize() :Smp::UInt64 {query}
IField
Smp::ISimpleField
+ ~Smp::ISimpleField()
+ GetValue() :Smp::AnySimple {query}
+ SetValue(Smp::AnySimple) :void
«interface» SB::ISteerableArrayField
+ Force(Smp::UInt64, Smp::AnySimple) :void
+ Force(Smp::UInt64, Smp::AnySimpleArray) :void
«interface» SB::ISteerableSimpleField
+ Force(Smp::AnySimple) :void
Field
SB::ArrayField
- m_array :Smp::PrimitiveTypeValue*
- m_size :Smp::UInt64
- m_type :Smp::PrimitiveTypeKind
SB::SteerableField
# m_forced :bool
+ SB::SteerableField()
+ ~SB::SteerableField()
+ Unforce() :void
+ IsForced() :bool
Field
SB::SimpleField
- m_field :Smp::PrimitiveTypeValue*
- m_type :Smp::PrimitiveTypeKind
SB::SteerableArrayField
- m_forcedArray :char*
SB::SteerableSimpleField
- m_forcedField :Smp::PrimitiveTypeValue

Figure 5.10 - Class diagram with steering mechanism for forcing model parameters.

meta-description of steering channels has to be provided, using a XML format defined by the diagram in Figure 5.11. Reading this artefact on runtime, the simulation infrastructure is able to instantiate the adapter objects accordingly to the features described by the user (i.e. transfer function and rules).

The presented architecture encompasses fundamental steering functionalities to manipulate the simulation scenario via parameters published by the models. The fields are made accessible by the kernel to the steering components and for convenience, all of them are implemented as steerable fields. Further, by delegating the `GetField()` service to the kernel, the model implementing the `IManagedModel` interface does not have to handle forcible flags itself.

Complementarily, customized functionalities can be implemented by systems that run on the top of the infrastructure architecture or are distributed. In this direction, in the next section a suite of applications is presented.

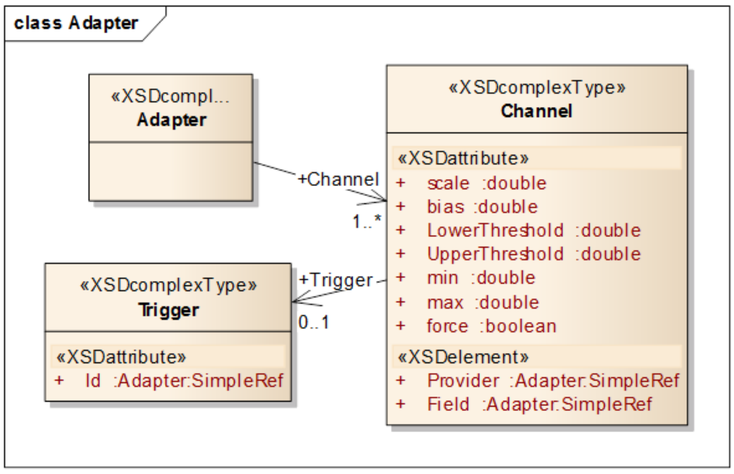

Figure 5.11 - Meta-model adopted to describe steering adapters.

5.4 Implemented Applications

Envisaging the construction of a complete environment, in this section the implementation of various applications of the steering facility is discussed to enable the execution, visualization and steering of satellite simulation scenarios. This is achieved with the development of four distributed modules that interoperate over a TCP/IP bus.

The central element is the simulation controller, which is in charge of loading, configuring and executing the simulation scenarios. From the communication perspective, it plays the server role, to which the client applications connect to.

The simplest client is the simulation monitor that remotely displays graphical and textual information from the on-going simulation. In addition, a second client can be connected to generate graphical 3D images and animation for the scenario. The last implementation presented hereafter is a generic front-end to steer the simulation parameters using dedicated graphical widgets. Every software is developed using Qt framework, which support multi-platforms, including mobile systems.

In addition to that, special-purpose clients may be constructed and connected to the simulation controller as needed by the applications.

5.4.1 Simulation Controller

This application encapsulates the simulator kernel and the infrastructure services, allowing the user to load scenario setup and model packages and control their

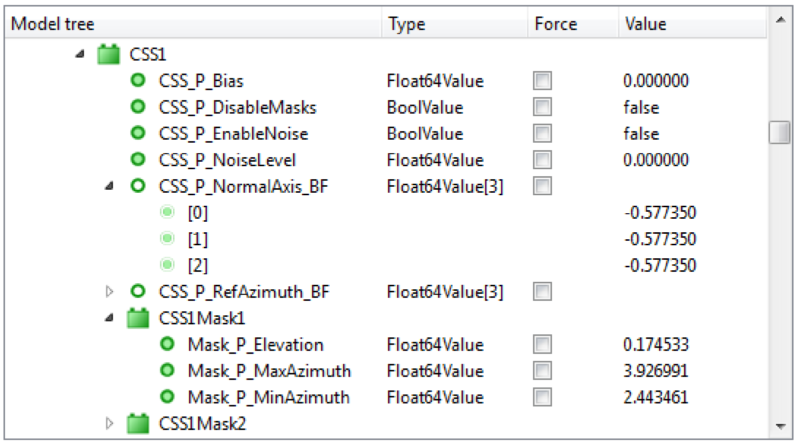

Model tree	Type	Force	Value
CSS1			
CSS_P_Bias	Float64Value	☐	0.000000
CSS_P_DisableMasks	BoolValue	☐	false
CSS_P_EnableNoise	BoolValue	☐	false
CSS_P_NoiseLevel	Float64Value	☐	0.000000
CSS_P_NormalAxis_BF	Float64Value[3]	☐	
[0]			-0.577350
[1]			-0.577350
[2]			-0.577350
CSS_P_RefAzimuth_BF	Float64Value[3]	☐	
CSS1Mask1			
Mask_P_Elevation	Float64Value	☐	0.174533
Mask_P_MaxAzimuth	Float64Value	☐	3.926991
Mask_P_MinAzimuth	Float64Value	☐	2.443461
CSS1Mask2			

Figure 5.12 - Model tree loaded from the simulation configuration and their field values visualization during execution.

execution via a dedicated GUI.

After the environment has been configured, the instantiated model tree can be inspected, as shown in Figure 5.12. The structure can be expanded to explore the model hierarchy and their attributes (i.e. fields and operations). In the same interface, the data types and current values of model fields can be inspected and when the simulation is running the user may choose to change or force their values.

The simulation can be configured to run in the tree modes, described following:

- Soft Real-Time – the simulation time progresses closely to the wall clock time. In contrast to hard real-time, small jitter is tolerated in this mode and violations are only registered and do not invalidate the simulation.
- Accelerated – during the execution the user may choose the speed up the simulation clock or slow down it.
- As-fast-as-possible (AFAP) – the simulation runs free, in the sense it is only limited by the processing time.

Complementary features are provided by the controller application for storing and restoring simulation snapshots, enabling and disabling breakpoints, and displaying event messages generated by the infrastructure and models. The GUI of latter, for instance, is illustrated in Figure 5.13, from which filters can be applied based on message type (i.e. information, warning, error, event or debug).

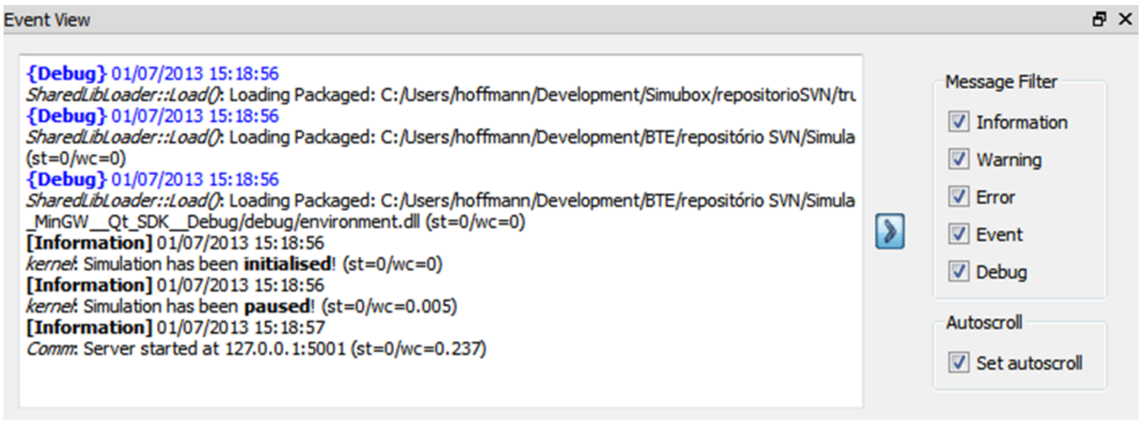

```
{Debug} 01/07/2013 15:18:56
SharedLibLoader::Load(): Loading Packaged: C:/Users/hoffmann/Development/Simubox/repositorioSVN/tru
{Debug} 01/07/2013 15:18:56
SharedLibLoader::Load(): Loading Packaged: C:/Users/hoffmann/Development/BTE/repositório SVN/Simula
(st=0/wc=0)
{Debug} 01/07/2013 15:18:56
SharedLibLoader::Load(): Loading Packaged: C:/Users/hoffmann/Development/BTE/repositório SVN/Simula
_MinGW__Qt_SDK__Debug/debug/environment.dll (st=0/wc=0)
[Information] 01/07/2013 15:18:56
kernel: Simulation has been initialised! (st=0/wc=0)
[Information] 01/07/2013 15:18:56
kernel: Simulation has been paused! (st=0/wc=0.005)
[Information] 01/07/2013 15:18:57
Comm: Server started at 127.0.0.1:5001 (st=0/wc=0.237)
```

Figure 5.13 - Event viewer window used to display messages logged from simulator kernel and model.

More sophisticated functionalities are available for re-executing a scenario in playback mode. In this case, instead of invoking the models, the scenario is reproduced from historic data previously recorded from a regular simulation. Except by the steering interface, the other clients attached to the infrastructure will have the same effect as if the simulation were running in an ordinary mode.

Whenever the engineer wants to change the course of a playback scenario, a branch can be generated within the simulation horizon. This will cause the infrastructure to restore he actual scenario and continues the run from a given point in time.

By commanding branches, derived scenarios can be generated successively from historic data. The result is a history tree whose child leaves define a full scenario based on the composition of all its parents, up to the tree root. This can be clearly visualized in the example given in Figure 5.14, where the history tree for a certain simulation scenario is shown. In the list, each node of the tree is represented by a line in the interface with associated data for a specific period of the simulation. By selecting an entry, a full branch can be restored for playback, as shown by the bars in the *simulation horizon* column, wherein the node (C) will restore a scenario that starts at time 1s in node (A), continues in (B) from 54s to 88s, and finally finish at 121s.

After the history scenario has been loaded, the control pane from Figure 5.15 is used to control the playback execution: (A) contains buttons for forward and backward execution; (B) is the simulation horizon slider that can be used to jump to a certain point in time; (C) is the acceleration factor slider; and finally (D) creates a scenario branch from the current simulation time.

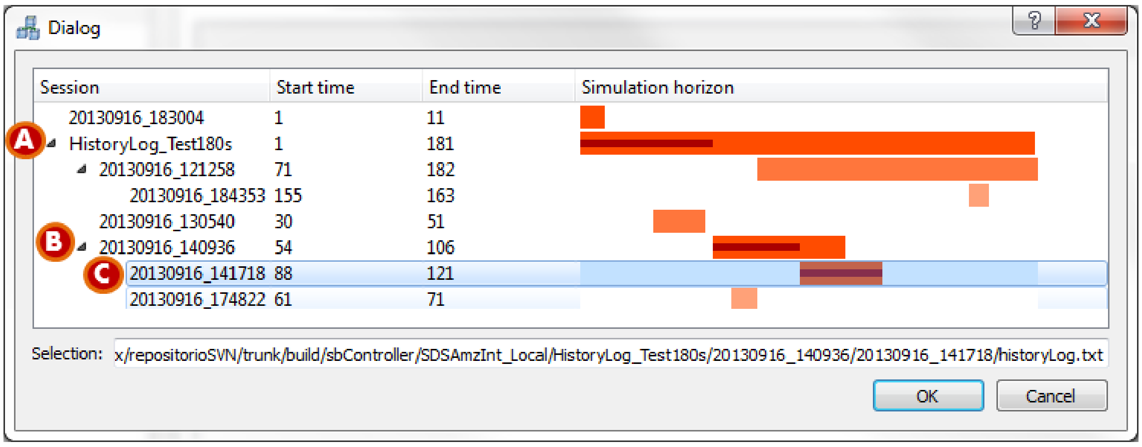
Dialog

Session	Start time	End time	Simulation horizon
20130916_183004	1	11	
HistoryLog_Test180s	1	181	
20130916_121258	71	182	
20130916_184353	155	163	
20130916_130540	30	51	
20130916_140936	54	106	
20130916_141718	88	121	
20130916_174822	61	71	

Selection: x/repositorioSVN/trunk/build/sbController/SDSAmzInt_Local/HistoryLog_Test180s/20130916_140936/20130916_141718/historyLog.txt

OK Cancel

Figure 5.14 - History tree dialog used to load a playback session. The selected scenario is composed of fragments of history data up to a root node. (A) is a root node in the history tree that have been branched to (B) and the latter to (C).

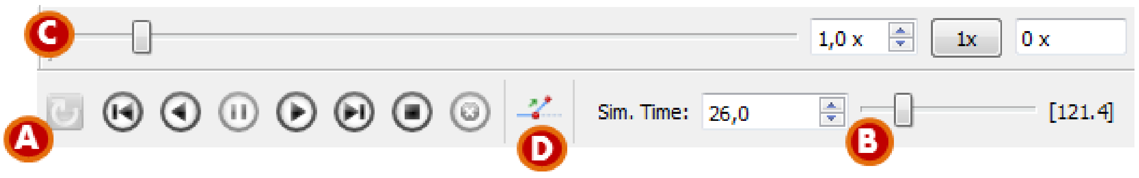

Figure 5.15 - Playback control panel: (A) execution control; (B) simulation horizon slider; (C) acceleration factor slider and edit fields; (D) scenario branch generation.

5.4.2 Simulation Monitoring Client

This client application allows the simulation conductor to remotely monitor the scenario evolution, via numerical and graphical plots information. Except for the latter format, this software is sufficient generic to display the values of any model field published within simulator kernel.

The main window of its GUI is presented in Figure 5.16, wherein basic simulation information is given, as time, name and description, as well as satellite orbital and attitude data. Details about the published fields are available from a list obtained from the simulation infrastructure.

Moreover, simple input commands can be performed by the user, like setting the value of a field or triggering a model's entry point and failures, which can serve as the basis for constructing a M&C application (e.g. with scripting functionalities).

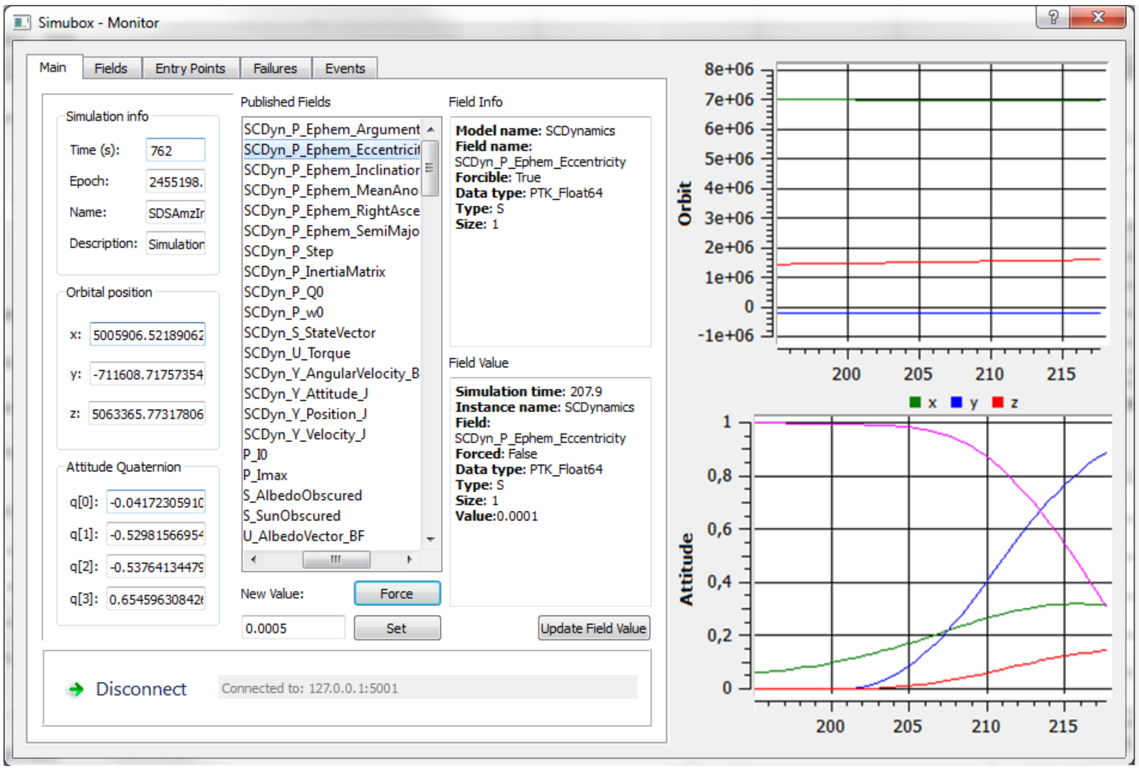

Simulation info

Time (s): 762

Epoch: 2455198.

Name: SDSAmzIr

Description: Simulation

Orbital position

x: 5005906.52189062

y: -711608.71757354

z: 5063365.77317806

Attitude Quaternion

q[0]: -0.04172305910

q[1]: -0.52981566954

q[2]: -0.53764134479

q[3]: 0.65459630842

Published Fields

SCDyn_P_Ephem_Argument
SCDyn_P_Ephem_Eccentricit
SCDyn_P_Ephem_Inclinatior
SCDyn_P_Ephem_MeanAno
SCDyn_P_Ephem_RightAsce
SCDyn_P_Ephem_SemiMajo
SCDyn_P_Step
SCDyn_P_InertiaMatrix
SCDyn_P_Q0
SCDyn_P_w0
SCDyn_S_StateVector
SCDyn_U_Torque
SCDyn_Y_AngularVelocity_B
SCDyn_Y_Attitude_J
SCDyn_Y_Position_J
SCDyn_Y_Velocity_J
P_I0
P_Imax
S_AlbedoObscured
S_SunObscured
U_AlbedoVector_BF

New Value: 0.0005

Field Info

Model name: SCDynamics
Field name:
SCDyn_P_Ephem_Eccentricity
Forcible: True
Data type: PTK_Float64
Type: S
Size: 1

Field Value

Simulation time: 207.9
Instance name: SCDynamics
Field:
SCDyn_P_Ephem_Eccentricity
Forced: False
Data type: PTK_Float64
Type: S
Size: 1
Value:0.0001

Connected to: 127.0.0.1:5001

Figure 5.16 - Main window of GUI for monitoring the simulation, provided by a client application.

5.4.3 Three Dimensional Visualization Client

Mainly for the problems with complex geometry, 3D visualization is an essential tool for assisting the analysis of simulation results. Typically in space engineering domain, a 3D mock-up of spacecraft offers a natural visualization of the system and alleviates the interpretation of attitude and orbit information.

In the proposed steering facility, a generic TCP/IP interface is provided by the simulation infrastructure to attach image generation clients, like Celestia, OpenIGS, STK or even customized applications. In this work, a simple 3D environment is built to demonstrate this interoperability and the benefits of such visualization systems.

The client provides two simultaneous graphical windows to better represent the position and attitude of a Low Earth Orbit (LEO) satellite. The two screenshots captured in Figure 5.17 give examples of the orbit view window, which has the planet Earth as the central object and the celestial sphere as background of the scene. The Earth Centred Inertial system (ECI) is represented by the XYZ axes, respectively painted with Red-Green-Blue (RGB) colours. The direction of the Sun w.r.t. ECI is

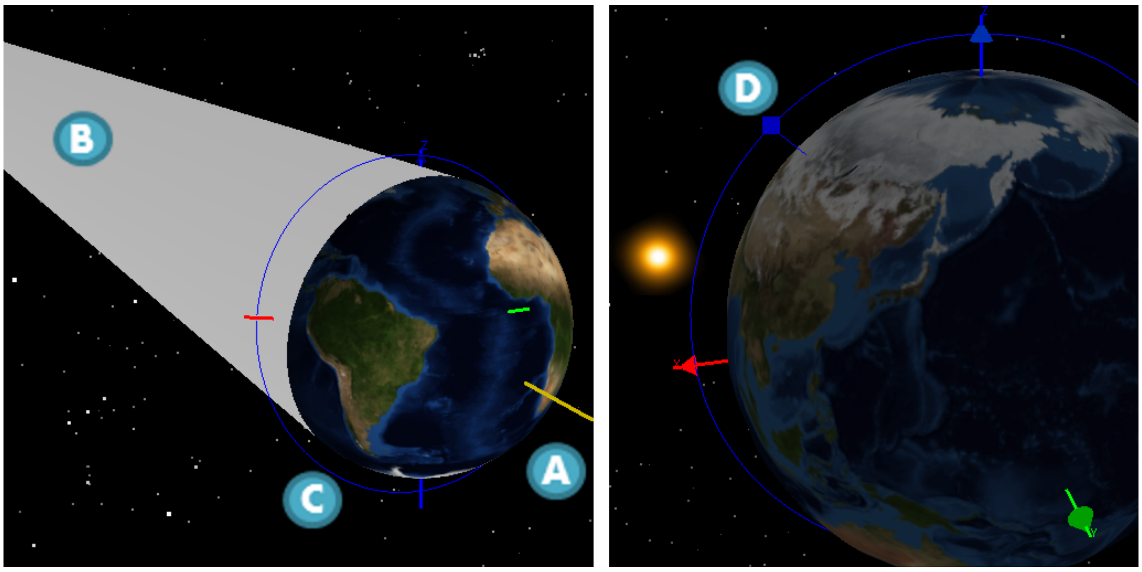

Figure 5.17 - 3D view of spacecraft's orbiting Earth: (A) umbral shadow cone; (B) orbit tube; (C) Sun direction w.r.t. Earth's centre; (D) spacecraft position.

given by the yellow vector (A), whereas the umbral shadow cone is presented as in (B). The orbit tube (C) is shown in scale and provides the current position of the satellite (D). The second view window, illustrated in Figure 5.18, has the 3D model of a satellite as the central body, including its reference frame (A) and body frame (B) [2].

After the connection to the infrastructure has been established, the 3D viewer registers to periodically receive updates of simulation parameters. Some of these values are used to display the Sun and satellite in right position or attitude. Other parameters, such as celestial sphere, are internally computed by the client from initial parameters.

For specialised applications, the client can be updated to exhibit detailed 3D information of satellite's parts.

5.4.4 Computational Steering Clients

Similarly to the visualization clients, different steering front-end applications can be integrated in the facility via a TCP/IP interface. Occasionally, specialized clients will be built as necessary, but herein a generic-use front-end is described and will serve as a platform for assessing various interactivity and connectivity methods.

[2]The texture of Earth's surface is based on the image provided by (STÖCKLI et al., 2005). Credit: Reto Stöckli, NASA Earth Observatory.

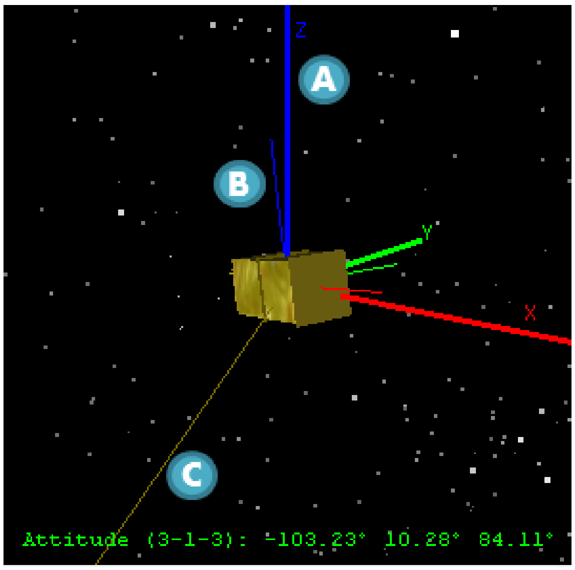

Figure 5.18 - 3D view of spacecraft's attitude: (A) Reference frame; (B) Body frame; (C) Sun direction w.r.t. body's centre.

The client makes use of a factory class implementing an `IWidgetFactory` interface to load any widget implemented with Qt framework. This flexible approach, designed in this work, permits to build a widget repository and dynamically connect them to simulation fields on running time. Furthermore, every component must implement the `IWidgetFactory` interface, which provides access to the data types and dimensions handled by the widget, thus enabling their categorization in equivalence classes.

Once the widget components have been loaded and the simulation fields retrieved, the user can select any combination of them that holds the data type compatibility. The linkage GUI is illustrated in Figure 5.19, wherein a 3D vector widget is connected to the Sun position field. This multi-purpose interface component allow user to graphically manipulate the orientation of a vector in the 3D space, but could be also embedded in other 3D visualization scene. Special purpose widget can be developed and attached as required and this process will be demonstrated in the case study in the Chapter 6.

5.5 Discussion

In this chapter, aspects of the design and implementation of a complete computational steering facility applied to satellite simulation are described. The environment encompasses a set of products for developing and executing models, configuring scenarios and clients for monitoring, visualization and steering.

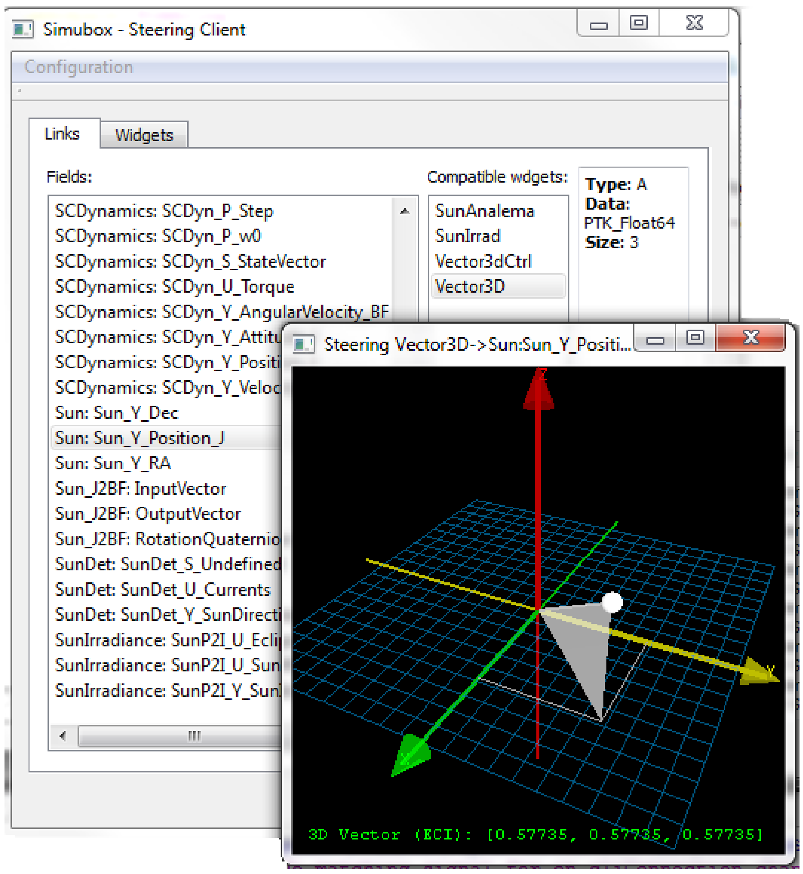
Simubox - Steering Client
Configuration
Links
Widgets
Steering Vector3D->Sun:Sun_Y_Positi...
Z
Y
X

Fields:

SCDynamics: SCDyn_P_Step
SCDynamics: SCDyn_P_w0
SCDynamics: SCDyn_S_StateVector
SCDynamics: SCDyn_U_Torque
SCDynamics: SCDyn_Y_AngularVelocity_BF
SCDynamics: SCDyn_Y_Attitu
SCDynamics: SCDyn_Y_Positi
SCDynamics: SCDyn_Y_Veloc
Sun: Sun_Y_Dec
Sun: Sun_Y_Position_J
Sun: Sun_Y_RA
Sun_J2BF: InputVector
Sun_J2BF: OutputVector
Sun_J2BF: RotationQuaternio
SunDet: SunDet_S_Undefined
SunDet: SunDet_U_Currents
SunDet: SunDet_Y_SunDirecti
SunIrradiance: SunP2I_U_Ecli
SunIrradiance: SunP2I_U_Sun
SunIrradiance: SunP2I_Y_Sun

Compatible wdgets:

SunAnalema
SunIrrad
Vector3dCtrl
Vector3D

Type: A
Data: PTK_Float64
Size: 3

```
3D Vector (ECI): [0.57735, 0.57735, 0.57735]
```

Figure 5.19 - Screenshot of generic steering application with a 3D vector widget connected to the Sun position field.

The simulator kernel is built on the basis of SMP2 concepts, which brings great flexibility to the framework and promotes model reuse over different scenarios. Upon it a novel steering layer is created to enable the manipulation of model parameters during execution time. Moreover, the modular architecture of the infrastructure allows the extension of components, e.g. for enhancing the implementation of a service or adding a new one, and the rearrangement of elements for creating customized products. New widgets, steering and visualization front-ends can be designed to enhance the environment to assist the accomplishment of specialized studies.

In general, the implemented applications embody a set of fundamental capabilities to cover a large number of simulation scenarios, commonly performed along the development of space missions. Nonetheless, the success on using these tools will depend on the establishment of an efficient and lean process for integrating simulation models and configuring new scenarios. Some directions for defining a such process are given in the Appendix A.

6 CASE STUDIES

In this chapter, the application of computational steering to assist space engineering activities is demonstrated in a set of representative satellite simulations. By adopting a tailored user interface, it is shown how a specialist can address the complexity of the scenarios and naturally interact with the computational model to rapidly test hypotheses on the system behaviour and algorithms under very specific conditions.

Among the simulation goals proposed in these case studies are the accomplishment of tasks typically related to the verification of models, consolidation of mission architecture, promotion of awareness of the design & construction, specification of avionic test cases, verification & validation of on-board software (OBSW) systems, and the enhancement of understanding on the system operation as a whole. At the same time these simulations cover a broad number of application types, as discussed in section 4.2, they demonstrate the benefits of the current approach in different circumstances of user interactivity, including all the interventions types (section 4.3), diverse interface paradigms (section 3.2), and the usability aspects of the computational steering mechanisms (section 3.3).

The results are organised in eleven simulation scenarios, as introduced in the Table 6.1, which have been designed and implemented to illustrate real use cases of the steering facility. They have been based on the personal experience of the author working as simulation engineer at INPE, notably: in the customization of the EGSE and the specification of test cases to verify the on-board computer and AOCS of the Brazilian satellite Amazônia-1; participating in the team of the Testing and Verification Device for the Inertial Systems for Aerospace Applications project; and during the exchange program in the EGSE group at ESTEC.

Each scenario consists in an independent simulation session that executes on the basis of a common initial configuration. Accordingly to the hypothesis being tested in a particular instant of simulation, several snippets are extracted from the scenario and described as individual scenes. Furthermore, a video demonstration of the computational steering facility is given in the Appendix E.

For conducting the case studies, a baseline simulation setup is considered and described in the section 6.1. The implementation details of the physical simulation environment is given in the section 6.2, including the specialisation of its graphical front-end. A summarisation of the results is discussed in the last part of this chapter, in section 6.14.

Table 6.1 - Overall description of simulation scenarios presented in this work.

#	Description	Main purpose
1	Model verification	Application of changes on the boundary conditions of a simulation model that computes the position of the Sun to verify and debug its implementation. Use of a direct image manipulation interface to change geometrical parameters of the solar panel.
2	On-board software verification	Guide the simulation state to a point where the on-board software can be assessed and debugged.
3	Analysis of recurrent effects on the dynamics behaviour of the Sun determination algorithm	Search of singular geometrical configurations that causes the system to behaves abnormally.
4	Investigation of on-board Sun determination precision and its impacts on S/C attitude	Fault injection in sensors and configuration of arbitrary geometric conditions to analyse the performance of Sun determination algorithm.
5	Attitude steady state analysis	Performance and robustness analysis of attitude controller subjected to torque perturbation and errors in the computed position of Sun.
6	Performance analysis of HITL implementation	Performance analysis of an independent hardware connected to the simulation loop. Use of natural interface to change simulation parameters and inject torque perturbation in the body's attitude dynamics.
7	Comparison of potential scenarios to support test case specification	Analysis of attitude controller subjected to different initial conditions and comparing the results using the history tree mechanism.
8	Sun determination algorithm experimentation	Assessment of alternative implementations of Sun determination algorithm with on-line replacement of the model.
9	Spatial resolution adjustments	Tuning the resolution of Earth's Albedo model to balance the precision of the simulation and its computational performance.
10	Temporal resolution adjustments	Analysis of a thermal system and verification of a heater's control strategy. Demonstration of interoperability of the steering facility with a legacy system specialised on simulating thermal models. On-line modification of execution frequency of models to balance precision and computational performance.
11	Assisted computational performance optimisation	Simulation scheduling tuning to perform load balancing by changing the number of tasks per processing threads.

6.1 Baseline Simulation Scenario and Models

The characteristics of the baseline scenario consist in a typical closed-loop simulation of an attitude control system. Accordingly to the scenario goal, different components are loaded, configured and assembled into the infrastructure from a model repository. In this work, a set of models have been developed to simulate the behaviours of spacecraft dynamics (i.e. orbit and attitude), common aspects of the space environment, and usual sensors & actuators. Further, some basic functionalities of the on-board computer are implemented to command the orientation of the platform in the space.

Particularly in this work, most of the analyses are focused on a specific component of the flight software, known as *Sun Determination* algorithm and frequently used to determine on-board the direction of the Sun. This type of algorithm is usually deployed as a module of Attitude and Orbit Control Subsystem (AOCS) and plays a fundamental role to provide, for instance, critical information to properly orient the solar panels and maximize the power generation, safely point the spacecraft towards the Sun during contingency modes, and check orbital data consistency.

Besides theoretical methods for determining the Sun versor on-board (e.g. based on ephemeris), several techniques can be used to compute it from data provided by sensors. In the present work, the simulation scenarios are built for a determination algorithm that processes data from eight Coarse Solar Sensors (CSS), which generate electrical current accordingly to the level of light incident on their sensorial planes.

In a typical Earth observing mission, three-axis stabilised and Low Earth Orbit (LEO), the environmental and geometrical aspects that affect the behaviour of the Sun Determination algorithm are manifold. The output current of each solar sensors varies as a function of the incidence angle of light, which primarily comes from Sun, but can also be affected by Earth's Albedo. The direction and the distance of the Sun changes along the year and sometimes it may be eclipsed by Earth, as the satellite goes into the shadows. Further, the incidence on each sensor is subjected to the platform's attitude, which evolves depending on the current control model. Finally, the sensor's Field of View (FOV) may be blocked by mechanical interference with other satellite structural elements, such as antennas, launcher interface, radiators, or Solar Array Generators (SAG).

Accordingly, the provided simulation setup allows the engineer to better understand the behaviour of the algorithm and assess its performance in representative scenarios.

Moreover, the application of the steering facility can be used in several development phases of Sun Determination software. In the early phases of spacecraft conceptual design, the simulation can support the selection of sensor types and the definition of the baseline for their mechanical configuration. As the project is detailed, a functional engineering simulator can be used to assess the performance of the Sun determination algorithm and to validate the mission requirements. After, when the on-board software is being developed, the software verification facility supports the qualification of the algorithm and its integration in the on-board computer. Later, during the satellite operation phase, the simulation environment can provide means for failure investigations and validation of software patches.

For each phase of development, different types of models and fidelity levels are required for building the simulation environment. In a traditional approach (e.g. script based), the specialist implements a set of pieces of software to create a specific-purpose simulation scenario to assist an engineering activity. Often the models are reused only in the level of source code refactoring and hardly shared among engineering teams. Moreover, the execution of a simulation scenario is driven by scripts that are minutely defined before some analysis can be done, which requires previous understanding on the system behaviour, high level of expertise by the simulation engineer and is error pone, thereby often demanding many simulation sessions until the script becomes ready for use.

On contrast, the case studies described herein cover many of these limitations, as the scenarios are implemented and executed in a full featured steering environment. The complex relations of geometrical elements and implications of noises, perturbations, and existing errors to the system behaviour can be readily investigated, as the algorithm designer gains insight into the problem and guides the simulation to test new hypothesis. Some examples of typical questions that may arise are listed next:

- How the Earth's albedo affects the precision of the Sun determination algorithm?
- In which cases the solar panels will obstruct the Sun from the solar sensors?
- Will the permanent shadow masks caused by the mechanical configuration degrade the algorithm performance?
- Will a minimum elevation filter on sensor's FOV influence the trajectory of attitude manoeuvres?

- How much critical is the failure of one or more sensors for the mission?
- What is the impact of Sun determination algorithm performance on the power budget?
- The error on determining the Sun direction could lead to a poor orientation of the SAG that would amplify this error?
- Is there any orbital configuration in which the two solar sensors stays in the panel's shadow when the spacecraft is pointing to Nadir? Would this obstruction affect the manoeuvre performance when reorienting the spacecraft to the Sun?
- Will the algorithm loose performance when running in the embedded platform?

By using the steering approach, the configuration of the running simulation can be modified naturally through a highly interactive interface, without interruption on the creative process of the designer, as demonstrated in the next sections. Before, the following subsections describe in more details the configuration of the simulation environment and composition of scenario to accomplishment the case studies[1].

6.1.1 Dynamics and Environmental models

This package is composed by seven environmental models and a spacecraft dynamics models, which are connected accordingly to the assembly represented in the diagram in the Figure 6.1. The simulation interval starts with the execution of the dynamics component that is responsible to integrate the platform's attitude, modelled as a rigid body[2]. Further, this model also simulates the satellite orbit, which consists simply on propagating the *keplerian* elements (LARSON; WERTZ, 1999), based on the implementation provided by Medeiros & Carrara (2009). The state variables from this model are integrated using an innovative *design pattern*, described in the Appendix B and they are used by the environment module to compute derived parameters related to the plant. In the baseline simulation scenario, the Sun, Earth's Eclipse, geomagnetic field, and Earth's Albedo are generally the available models.

[1]An electronic version of the UML models have been designed with the Enterprise Architect (EA) tool (version 9.0.9) and the full package can be accessed in EA format or standard XMI 2.1 format from the following link: `http://urlib.net/8JMKD3MGP5W34M/3H56LQH/Section6.1_SimulationArtefacts.zip`. A free EA Viewer is available from `http://www.sparxsystems.com/`.

[2]Although modeling the flexible modes of the spacecraft would be important for improving the fidelity of the simulation regarding the dynamics of flexible appendages, such as the solar arrays, the rigid body model suffices to demonstrate the steering functionalities in this work.

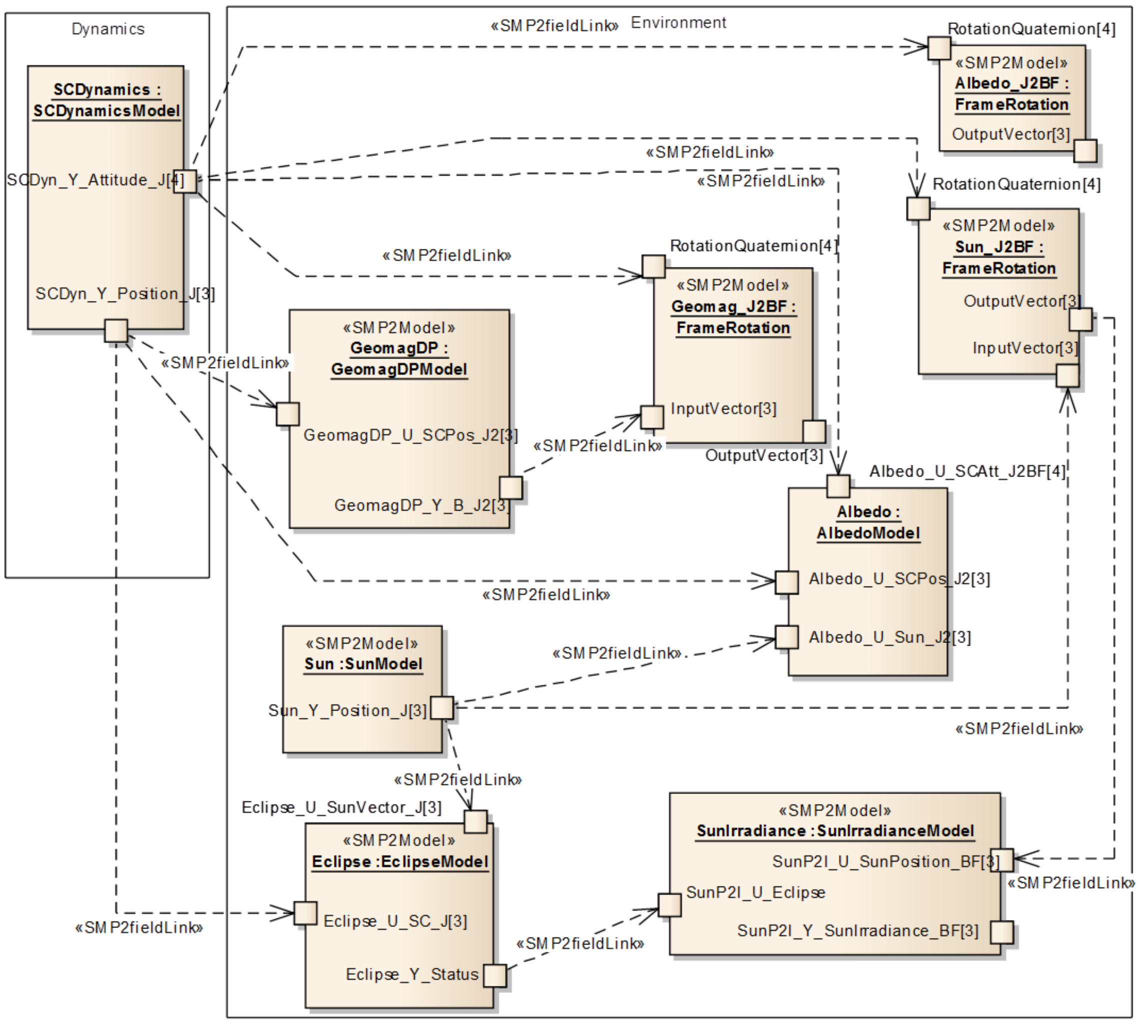

Figure 6.1 - Simulation assembly for the spacecraft dynamics and environmental models.

The `Sun` model is based on the simulation time (directly obtained from the simulation kernel) and implements the algorithm described by Michalsky (1988). In this assembly, the position of the Sun w.r.t. inertial system is then provided to the `Eclipse` model, which uses the position of the spacecraft to check whenever it is in the umbral cone (LONGO; RICKMAN, 1995).

Similarly the Sun position is provided to the `Albedo` model that also uses the body's position and attitude to compute the total amount of Sun light that reaches the satellite after being reflected by the Earth. This model implements a method in which the Earth is discretised in a 2D grid of cells, each of them containing a reflectance index of surface [3], as proposed by Bhanderi (2005) and implemented by Lopes et al. (2011).

Some auxiliary models are instantiated to perform the reference system conversion, e.g. changing data from the inertial frame (w.r.t J2000 epoch) to the body frame that rotates any 3D input vector based on a quaternion. One instantiation of this generic `FrameRotation` model is the `Albedo_J2BF`, which is used to inject a noise albedo vector in the simulation, by accepting an arbitrary input vector in the inertial frame and outputting this vector in the body frame. The same approach is used to convert the Sun and geomagnetic vectors to the body's reference frame.

The `GeomagDP` model implements the algorithm from Finlay et al. (2010) for a given simulation time and orbital position.

Finally, the `SunIrradiance` model merely computes the Sun irradiance that arrives in the spacecraft based on their distance and eclipse condition.

Before the next simulation interval is executed, torques applied on the platform are reefed into the dynamics model. For the sake of simplicity, this is done in the baseline scenario taking directly commanded torque from the controller, without the adoption of any actuators model.

6.1.2 Sensors models

Five types of sensors are implemented in this work. In the Figure 6.2, an assembly diagram is presented for the magnetometer (MGT), gyroscope (Gyro), star tracker

[3]This index is obtained from the database of the Total Ozone Mapping Spectrometer project (BHANDERI, 2005) and consists of several measurements of the Earth reflectance from space. The indexes vary accordingly to the cloud coverage or the presence of ice on the surface, so engineers can load a table for a given date in the database or apply statistics from the values within a period.

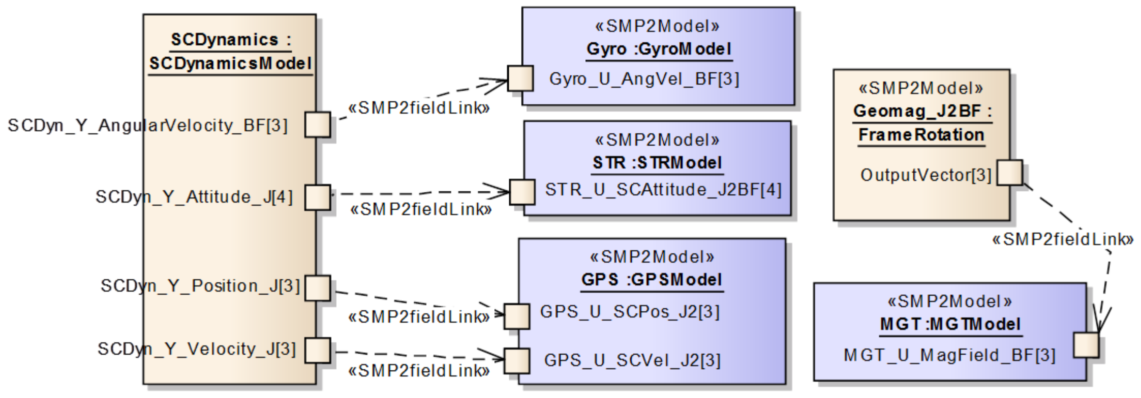

Figure 6.2 - Simulation assembly defining connections between the environmental models and sensors.

(STR), and Global Positioning System (GPS) receptor. In the context of the baseline scenario, these models are implemented just as an interface component for the environmental models and no behavioural code is provided. Yet, their instances are convenient for injecting noise and failures during the simulation runtime.

Regarding the Coarse Solar Sensors (CSS), the concept adopted in this scenario consists in a set of eight photovoltaic cells that generate an electrical current proportionally to the incident light. The sensors are precisely placed on the spacecraft body so the whole sky is coverage and the direction of the Sun can be determined regardless of its position and the attitude of spacecraft. The structural configuration of the body is assumed to be simply as two connected cubes, representing the platform and payload, respectively. In this geometry, the sensor's positions can be roughly described as the eight vertices of a rectangular parallelepiped formed by the two cubes. Further, the boresight axis of each sensor is aligned with the cube's diagonal (i.e. the diagonal formed with their opposite vertex).

In the simulation, the CSS assembly is described by the diagram in the Figure 6.3. The interface with other models is handled by the `CSSAsbShadow` model, which is composed by eight instance of individual solar sensors, each of them containing their own configurations for position and orientation on the spacecraft. Moreover, each CSS can refer to a group of azimuth/elevation mask models that describes fixed regions of sensor's Field of View (FOV) from which the light is blocked, thereby representing, for instance, interferences caused by other mechanical elements (e.g. antennas) previously computed in a Computer-Aided Design (CAD) tool. In addition to these fixed shadow models, the `CSSAsbShadow` also dynamically computes

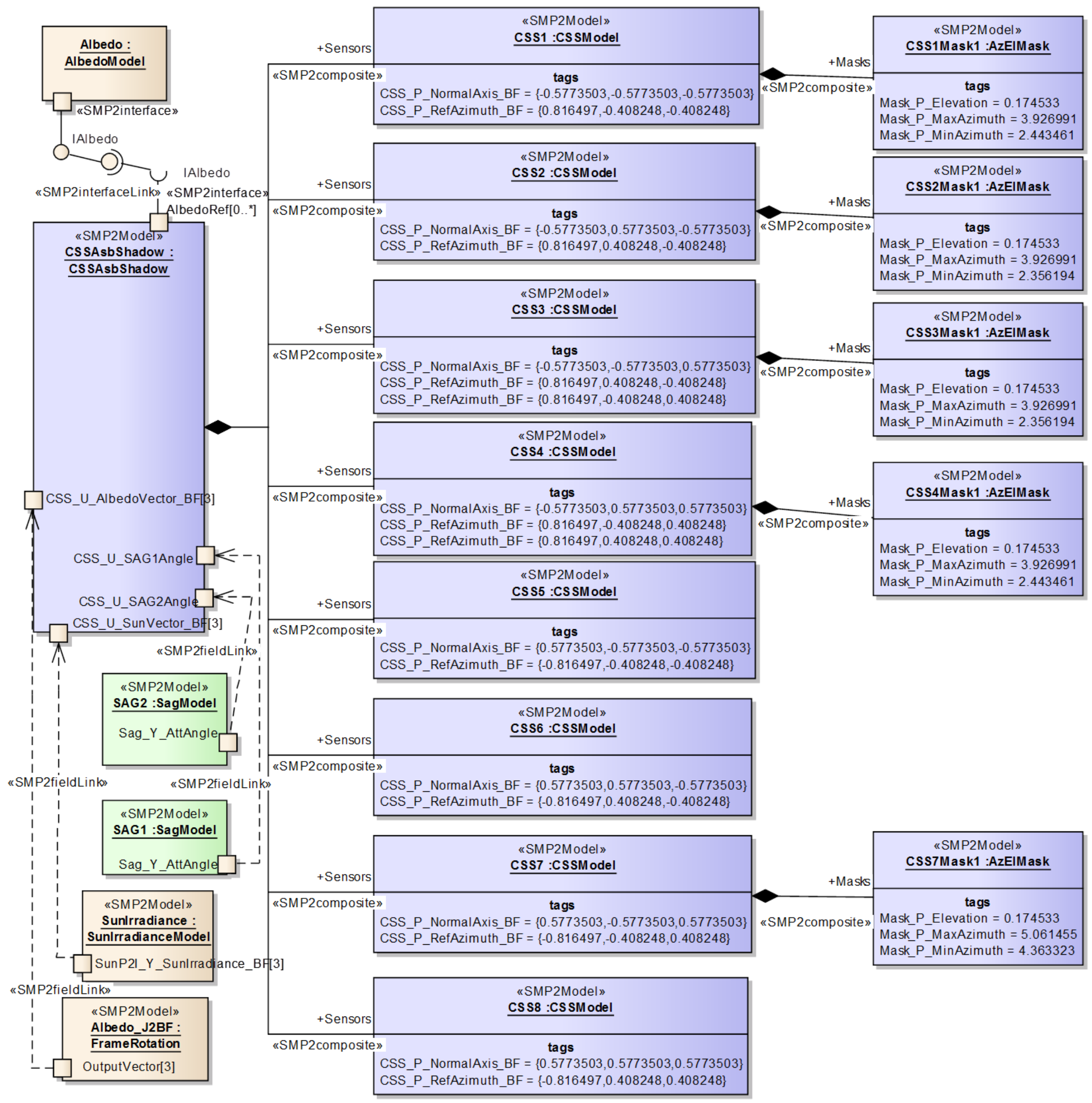
Albedo : AlbedoModel
«SMP2interface»
IAlbedo
IAlbedo
«SMP2interfaceLink»
«SMP2interface»
AlbedoRef[0..*]
«SMP2Model» CSSAsbShadow : CSSAsbShadow
CSS_U_AlbedoVector_BF[3]
CSS_U_SAG1Angle
CSS_U_SAG2Angle
CSS_U_SunVector_BF[3]
«SMP2fieldLink»
«SMP2Model» SAG2 :SagModel
Sag_Y_AttAngle
«SMP2fieldLink»
«SMP2fieldLink»
«SMP2Model» SAG1 :SagModel
Sag_Y_AttAngle
«SMP2Model» SunIrradiance : SunIrradianceModel
SunP2I_Y_SunIrradiance_BF[3]
«SMP2fieldLink»
«SMP2Model» Albedo_J2BF : FrameRotation
OutputVector[3]
+Sensors
«SMP2composite»
«SMP2Model» CSS1 :CSSModel
tags
CSS_P_NormalAxis_BF = {-0.5773503,-0.5773503,-0.5773503}
CSS_P_RefAzimuth_BF = {0.816497,-0.408248,-0.408248}
«SMP2Model» CSS2 :CSSModel
tags
CSS_P_NormalAxis_BF = {-0.5773503,0.5773503,-0.5773503}
CSS_P_RefAzimuth_BF = {0.816497,0.408248,-0.408248}
«SMP2Model» CSS3 :CSSModel
tags
CSS_P_NormalAxis_BF = {-0.5773503,-0.5773503,0.5773503}
CSS_P_RefAzimuth_BF = {0.816497,0.408248,-0.408248}
CSS_P_RefAzimuth_BF = {0.816497,-0.408248,0.408248}
«SMP2Model» CSS4 :CSSModel
tags
CSS_P_NormalAxis_BF = {-0.5773503,0.5773503,0.5773503}
CSS_P_RefAzimuth_BF = {0.816497,-0.408248,-0.408248}
CSS_P_RefAzimuth_BF = {0.816497,0.408248,0.408248}
«SMP2Model» CSS5 :CSSModel
tags
CSS_P_NormalAxis_BF = {0.5773503,-0.5773503,-0.5773503}
CSS_P_RefAzimuth_BF = {-0.816497,-0.408248,-0.408248}
«SMP2Model» CSS6 :CSSModel
tags
CSS_P_NormalAxis_BF = {0.5773503,0.5773503,-0.5773503}
CSS_P_RefAzimuth_BF = {-0.816497,0.408248,-0.408248}
«SMP2Model» CSS7 :CSSModel
tags
CSS_P_NormalAxis_BF = {0.5773503,-0.5773503,0.5773503}
CSS_P_RefAzimuth_BF = {-0.816497,0.408248,0.408248}
«SMP2Model» CSS8 :CSSModel
tags
CSS_P_NormalAxis_BF = {0.5773503,0.5773503,0.5773503}
CSS_P_RefAzimuth_BF = {-0.816497,0.408248,0.408248}
+Masks
«SMP2composite»
«SMP2Model» CSS1Mask1 :AzElMask
tags
Mask_P_Elevation = 0.174533
Mask_P_MaxAzimuth = 3.926991
Mask_P_MinAzimuth = 2.443461
«SMP2Model» CSS2Mask1 :AzElMask
tags
Mask_P_Elevation = 0.174533
Mask_P_MaxAzimuth = 3.926991
Mask_P_MinAzimuth = 2.356194
«SMP2Model» CSS3Mask1 :AzElMask
tags
Mask_P_Elevation = 0.174533
Mask_P_MaxAzimuth = 3.926991
Mask_P_MinAzimuth = 2.356194
«SMP2Model» CSS4Mask1 :AzElMask
tags
Mask_P_Elevation = 0.174533
Mask_P_MaxAzimuth = 3.926991
Mask_P_MinAzimuth = 2.443461
«SMP2Model» CSS7Mask1 :AzElMask
tags
Mask_P_Elevation = 0.174533
Mask_P_MaxAzimuth = 5.061455
Mask_P_MinAzimuth = 4.363323

Figure 6.3 - Simulation assembly defining the composition of eight Coarse Solar Sensor models, their fixed shadow masks and the connections with the environmental and power models.

shadows that are produced by the solar panels, based on their geometry and current orientation.

Aside from the light received directly from the Sun, the CSS models also compute the amount of light reflected by the Albedo into the sensors, and for this purpose an interface link from the `CSSAsbShadow` to the Albedo model is defined in the assembly. Furthermore, it is important to mention that additional sources of light can be introduced in the form of internal random noise or injected externally by the user via the `Albedo_J2BF` component.

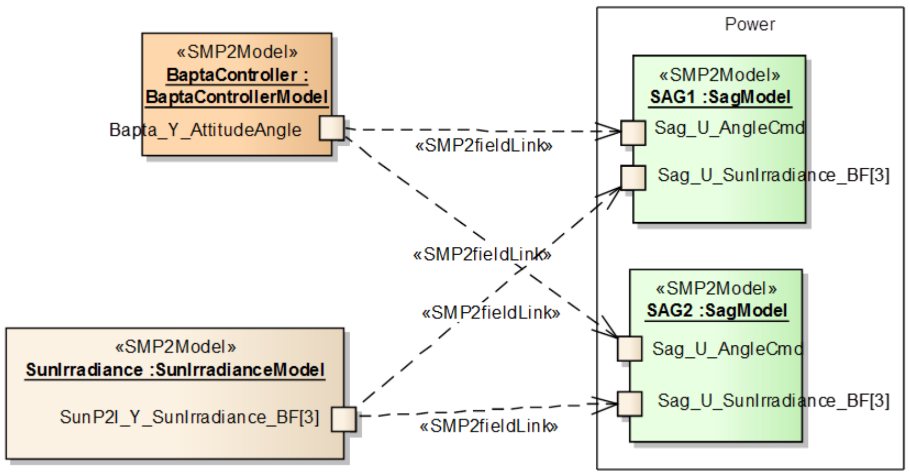

Figure 6.4 - Simulation assembly of power subsystem models and their connections with OBC and environmental models.

6.1.3 Power subsystem models

The power subsystem package comprise merely on models that orient the Solar Array Generators (SAG) accordingly to the commanded angle computed on-board by `BaptaController` model. A nominal output current is computed as a result of the Sun's incidence angle on the panels, but no dynamic behaviour is modelled for the rotation movement[4]. Two independent panels are instantiated in the simulation, as seem in the Figure 6.4.

6.1.4 On-board computer models

In this work, three basic functionalities are provided by the On-Board Computer (OBC): Sun determination, solar panels orientation, and attitude control. The baseline scenario can be loaded as a pure software simulation or with a hardware-in-the-loop configuration. In the first case, the flight algorithms are implemented by regular models, while in the latter they are embedded in an independent hardware platform.

When the software configuration from the diagram in the Figure 6.5 is used, the Sun Determination algorithm is wrapped by a model that processes the eight currents provided by the coarse solar sensors. The Sun versor is computed w.r.t. the body frame, accordingly to the method developed by Lopes et al. (2011), and then

[4]The purpose of SAG model in this work is essentially to demonstrate the feasibility of on-board software to command the orientation of panels and to compute their shadows produced over the solar sensors. In a more sophisticated analysis of spacecraft attitude, the fidelity of the simulation should be improved by modelling the dynamics of the panel's actuators and their flexible modes.

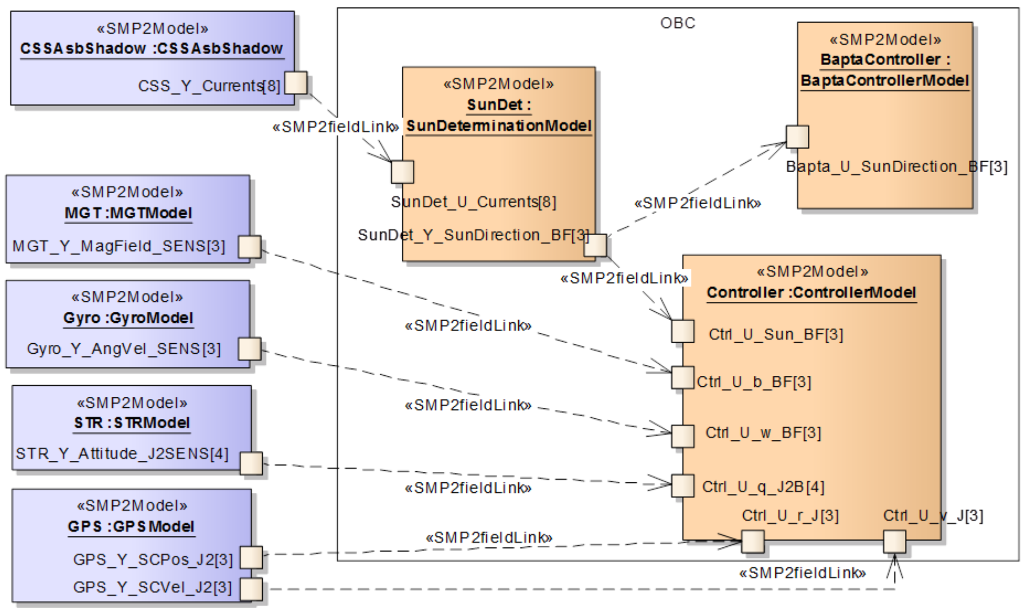

Figure 6.5 - Assembly for the software configuration of the on-board components, which are implemented as simulation models.

made available to the `BaptaController` and `Controller` models. Following, the `BaptaController` is responsible for computing the best orientation angle for the solar panel, so the incident light on the solar arrays maximise the power generation.

The spacecraft attitude is commanded by a proportional-derivative controller, which closes the simulation loop and implements four operational modes. In the simplest, *stand-by mode*, the model executes but no torque is commanded to the actuators [5]. In the *Sun pointing* mode, the satellite is oriented so its X axis is aligned with the Sun versor computed on-board. Next, the *nominal mode* points the Z body axis to the nadir and aligns its X axis with the velocity vector, based on the readings from the STR, MGT, Gyro, and GPS. In addition, the fourth mode, *inertial pointing*, orients the spacecraft accordingly to a quaternion provided by the operator.

Due to the flexibility provided by the assembly artefact, the dataflow scheme used for connecting the models can be easily rearranged to comply with manifold studies. In the hardware-in-the-loop configuration, all the on-board algorithms are replaced by an interface adapter that handles all the communication with the flight software embedded in an external platform. In this additional assembly, defined in the Figure 6.6, all data necessary to the on-board software is gathered by the `ObcIF`

[5]Actually, in the current assembly the torques are directly connect to the spacecraft dynamics model. Yet, the controller can be configured by the user to limit the applied torque.

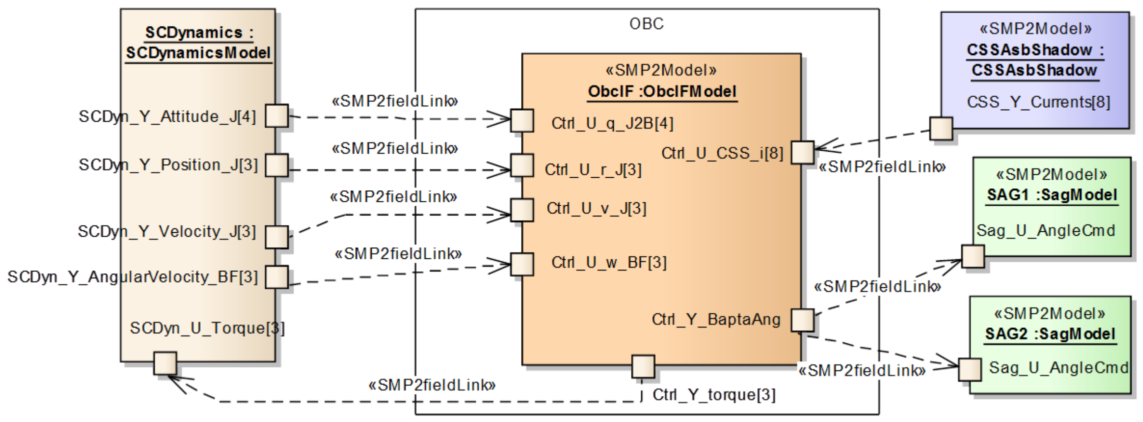

Figure 6.6 - Assembly for the hardware-in-the-loop configuration, in which the on-board components are embedded in an independent platform and all the communicate with the simulation is handled by the `ObcIF` model.

model and forwarded to the hardware. Similarly, the commands sent by the OBC are received by the `ObcIF` and distributed to the corresponding simulation models.

6.2 Computational Steering Facility Implementation

The simulation facility built for conducting the current case studies implements the computational steering architecture proposed in Chapter 5. The software components are deployed in a distributed environment, as illustrated in Figure 6.7, in which the Simulator is the central element of the facility. Attached to it are independent visualization and steering client nodes.

The viewer stations register to the simulation to periodically receive updates on parameter values and display a 3D animation of orbit and attitude dynamics. Several computers can be used for visualization, which can be running in Windows, Linux or OSX platforms.

For closing the interaction loop, the steering clients provide specialized interfaces for changing the scenario parameters as the simulation evolves. In the current studies, general purpose and customized steering widgets have been developed and they are described in more details in the Appendix C. Most of steering interfaces have been implemented for desktops, but some can be running in tablets with Android 4 platform.

In addition to that, the facility supports the execution of flight software in two different setups:

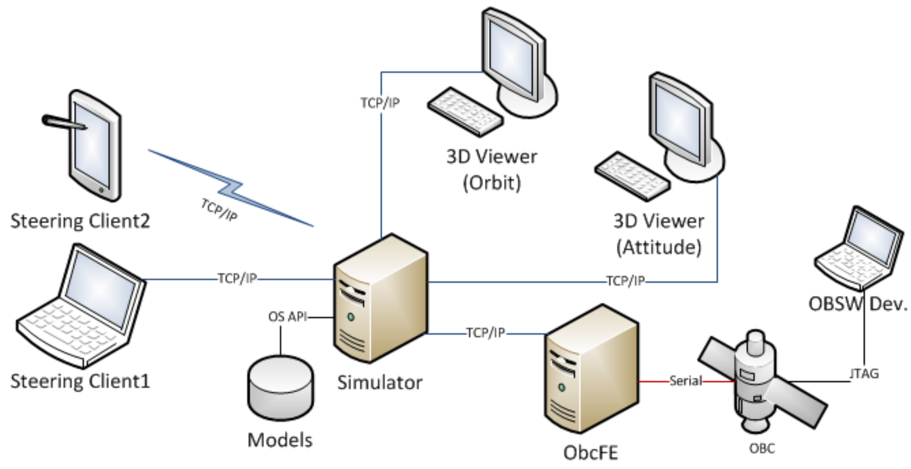

Figure 6.7 - Physical architecture of simulation facility.

- Software Verification Facility (SVF): in which the flight software is implemented as a regular model and the control loop is entirely closed in software; and
- Real-Time Test Bench (RTB): in which the flight software is embedded in an independent hardware platform.

All the simulation models adopted in both setups are available from a model repository and dynamically loaded into the kernel using configuration descriptions provided in assembly files, as previously presented in section 6.1.

It is worth to mention that, in principle, most of the software components could be running in a single workstation. However, in order to point out the roles and communication paradigm of each module, a distributed architecture is adopted. This approach also demonstrates the flexibility on using multiple platforms and combining clients with heterogeneous resources.

For the RTB setup, two additional working stations can also be introduced to perform the front-end interface (ObcFE) with the On-Board Computer (OBC) and to support the on-board software development (i.e. compilers and debugging tools for the embedded software).

The on-board computer is represented by a hardware platform using a microcontroller ARM that runs an embedded code written in C language and communicates with a PC via an USB interface emulating a serial communication. More details on the features of this device are presented in Table 6.2, as provided

Table 6.2 - Features of hardware platform adopted to run the flight software and emulate the on-board computer node.

Name	Stellaris LaunchPad
Vendor	Texas Instruments
Microcontroller	ARM Cortex-M4F processor core
Model	LM4F120H5QR
Processing capacity	80-MHz operation; 100 DMIPS performance 1.25 DMIPS/MHz
FPU	IEEE754-compliant single-precision Floating-Point Unit (FPU). 32-bit instructions for single-precision (C float) data-processing operations
Comm I/F	asynchronous serial communication emulated at 115,200 bps over USB
Program Memory	Flash 256kB
SRAM	32kB
EEPROM	2kB

by its vendor Texas Instruments (TI, 2013).

6.2.1 3D Visualization adopted in the case studies

In order to close the steering loop in the current case studies, the basic 3D visualization application (described in section 5.4.3) is enhanced to provide additional feedback on the behaviour of Sun determination algorithm and the geometry of solar sensors and solar panels. Details of these graphical elements are presented in the scene of the attitude viewer in Figure 6.8. The Solar Array Generators are characterized by two panels (A) that can be rotated around the Y axis (body frame). The normal of each wing is described by a line perpendicular to the panel (B). Eight coarse solar sensors are arranged in the corners of the two cubes that represent the platform and the payload of satellite (1 to 8 in Figure 6.8, in which 3 and 4 are not visible in the image). The geometry of each sensor is defined by a plane (D), a normal vector and a reference azimuth. Moreover, some sensors have shadow masks defined to represent the obstruction in its FOV, caused by the mechanical interference with other static structural elements. For instance, in the detail of the Figure 6.8 the shadow mask (E) for the sensor 6 represents the interference of payload's antenna, which has been previously computed with a CAD tool. The direction of the Sun is depicted by a line with origin in the satellite's body (C) and also by eight lines coming from each solar sensor (F). The later representation helps the user to identify conditions when the solar sensor is

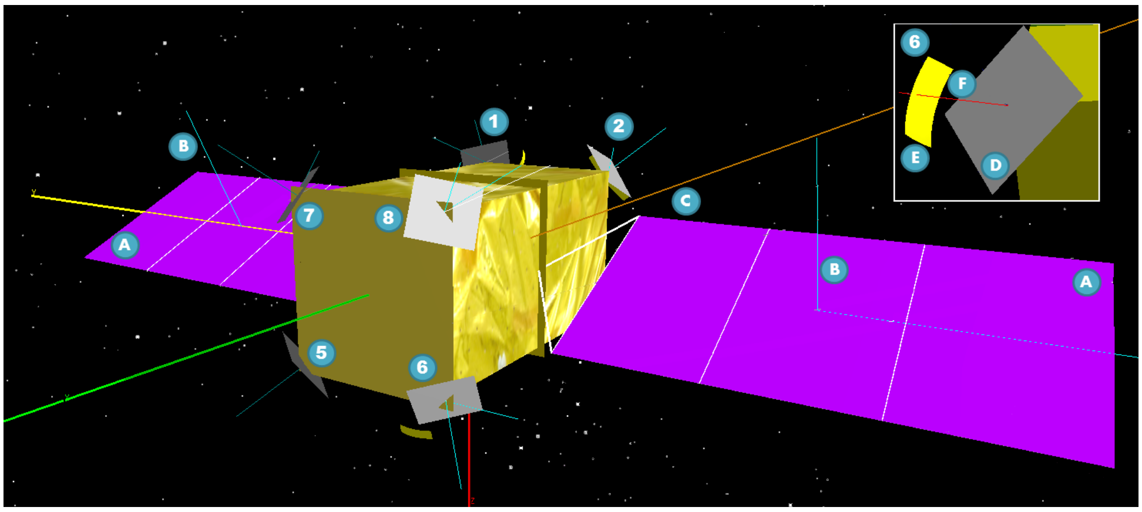

Figure 6.8 - Enhanced 3D visualization system for supporting the steering interactions in the *Sun Determination* case studies. 1-8: coarse solar sensors; A: solar panels; B: normal of solar panels; C: Sun vector (BF); D: sensor's plane; E: shadow mask applied to the sensor; F: Sun vector as seen from the sensor.

obscured by a shadow mask or by the solar panels (dynamically computed based on their geometry and current orientation).

6.3 Scenario 1: Model Verification

This first case study demonstrates the computational steering usefulness on testing the implementation of simulation models. The scenario focuses on the behaviour of the CSS and solar panel components and the consistence of their results in different geometrical configurations. Once checked, the baseline scenario is reliable to support the analysis of shadows produced by the panels on the sensors and its effects on the Sun Determination algorithm.

6.3.1 Scene 1: Verification of shadows produced by Solar Panels on the Coarse Solar Sensors

This scenario begins with a very simple test case to ensure that the shadow model is properly implemented and reliable to be used in more complex configurations. Although the modelling and simulation of the problem might be simple, testing and debugging the implemented model can be tedious and error prone. This is related to the problem's geometry, as the shadows produced by the Solar Panels on the Coarse Solar Sensors have a dynamic behaviour and depends on manifold attributes, like direction of the Sun, current position of satellite in orbit and attitude, orientation of solar panels, and configuration of sensor's fixed shadow masks.

Still, from the point of view of the shadow model, only the Sun's direction and the panel's orientation affect directly the outputs of solar sensors. Thus, the test cases for this model can be created with the definition of various geometrical arrangements of Sun position and solar panel attitude. The expected output of each test case can be visually verified accordingly to the inputted Sun vector w.r.t. body frame (varying it all around $4\pi rad$) and commanding the attitude angle of the panels from 0 to 360 rotation degrees.

By using the computational steering mechanisms the current SVF scenario can be easily configured on runtime to support the execution of these test cases. At first, the spacecraft attitude and the eclipse flag are fixed to not interfere in the simulation results, so the following fields are forced:

- `Eclipse::Eclipse_Y_Status` = false;
- `SCDynamics::SCDyn_Y_Attitude_J` = $\{0, 0, 0, 1\}$.

Two steering adapters are defined to force the `Sun::Sun_Y_Position_J` and `BaptaController::Bapta_Y_CommandedAngle` fields applying values provided by the simulation engineer on the fly with generic steering widgets.

The Figure 6.9 illustrates a sequence of interactions of user with the simulation, in which the steering interfaces are used to verify the correctness of models when the solar panel +Y blocks the Sun on two solar sensors (CSS1 and CSS2). Initially the panel is 180^o oriented and using a 3D vector widget (Figure 6.9-a) the Sun is positioned roughly at $-X+Y$ w.r.t. J2000 frame [6]. As result, from the 3D scene it can be clearly seen that both sensors are in the shadow created by the solar panel, as the sight vector from each sensor's plane to the Sun crosses the structure of SAG (i.e. white lines indicated by the arrows in Figure 6.9-b). This result can be easily compared to the output current from the sensors, in order to check the simulation coherence [7].

In the following intervention in the simulation, the engineer makes use of a simple knob widget to rotate the solar panel Figure 6.9-c) and steer its orientation until both

[6] Since the S/C attitude is aligned with the inertial frame, the Sun vector w.r.t. body frame will be the same. In addition to that, the versor defined with the 3D widget is scaled by $1.5e^{+11}m$ to place Sun approximately at 1AU.

[7] In this scenario the numerical output of models are verified, but these parameters could also be represented as graphical outputs (e.g. color code of the sensor to indicate whether it is illuminated or not).

sensors become illuminated by the Sun Figure 6.9-d). Finally the Sun's elevation is changed towards $+Z$ Figure 6.9-e) and CSS2 becomes again blocked by the panel Figure 6.9-f).

The interaction represented in Figure 6.9 demonstrate the potentials of the computational steering mechanism to rapidly test different hypothesis of model's behaviour when executing a simulation. If desired, many other changes can be done on runtime, such as enabling/disabling fixed shadow masks and redefinition of geometrical parameters.

In addition to that, the adoption of visual interface provides an unambiguous feedback on the modelled geometry, which explicitly reveals contradictions when some model contains implementation errors. In these cases, even a simple signal inversion could be overlooked in simulations with numerical outputs, but readily noticed in the graphical visualization. This approach is illustrated taking as example the faulty code from the Table 6.3. By using the steering environment, the user injected two attitude angles for the -Y solar panel: $+45^o$ and -45^o. From the screenshot in Figure 6.10 it is evident that the CSS6 is blocked by the Sun in the first case and illuminated in the second one. Yet, running the faulty model, the output current of this sensor produces the opposite behaviour.

6.3.2 Scene 2: Direct image manipulation of SAG's geometry

In the current scenario, several geometrical parameters are considered for computing shadows on the coarse solar sensors caused by the solar panels obstructing the Sun. Besides the orientation of the solar panel, spacecraft attitude, position of the Sun, and configuration of sensors, the structure of the solar array generators also interferes directly in the simulation results.

Thus, in this computational steering demonstration, the engineer continuously analyses the behaviour of the shadows as the geometry of the panels are modified. For this purpose, the 3D visualisation system is used both for displaying simulation results and to permit the user to input commands via a direct image manipulation mechanism. A sequence of interactions using this type of interface is given in the Figure 6.11.

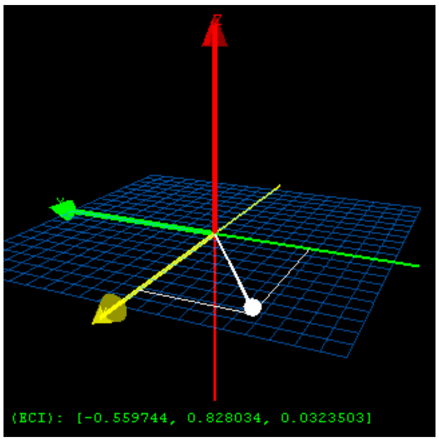
(ECI): [-0.559744, 0.828034, 0.0323503]

(a) The 3D vector widget is used to place Sun at -X+Y.

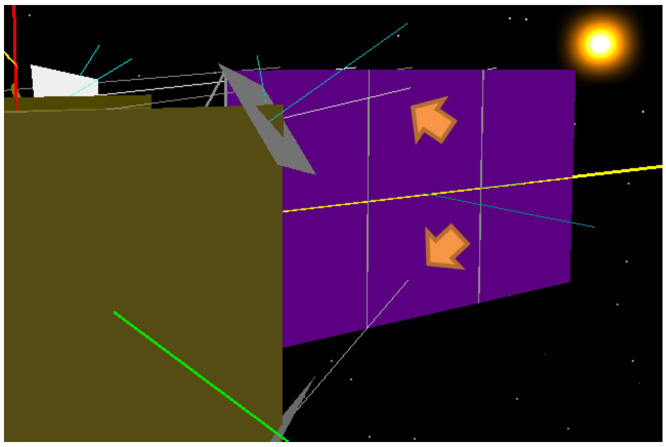
(b) The Sun is blocked by solar panel +Y and both CSS 1 and 2 are in the shadow.

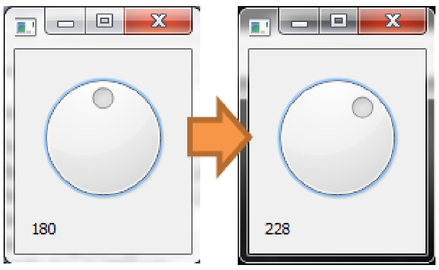

(c) A new orientation is defined for the panels rotating the knob.

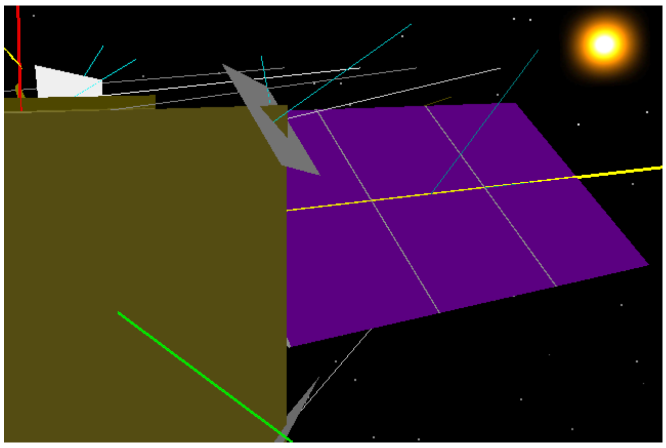
(d) CSS 1 and 2 are illuminated after the panel has been rotated.

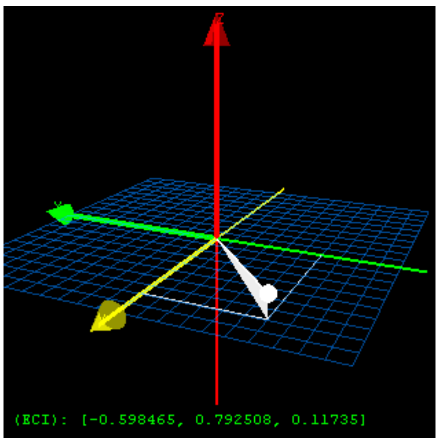
(ECI): [-0.598465, 0.792508, 0.11735]

(e) The elevation of the Sun is changed towards +Z.

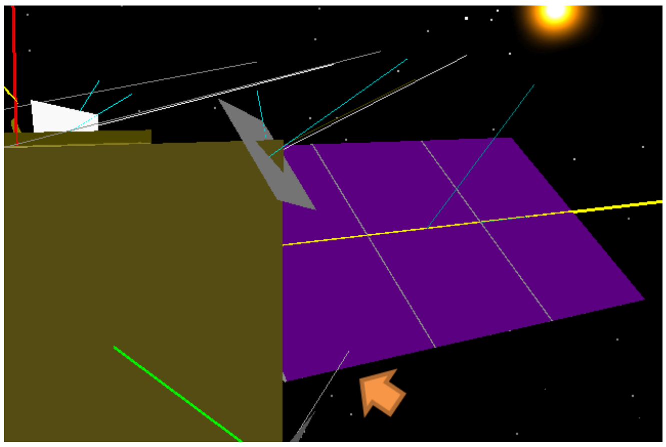
(f) As result of steering input from (e) the CSS 2 became in the shadow.

Figure 6.9 - Sequence of actions for Sun position and solar panel orientation steering and corresponding simulation results.

Table 6.3 - Two C++ implementations of the shadow model. Small errors in the implementation are hard to find by code inspections in contrast to a explicity visual verification in Figure 6.10.

```
/// SAG's geometry
Vector3 P0(
   this->CSS_P_SAGOrigin[0],
   this->CSS_P_SAGOrigin[1],
   this->CSS_P_SAGOrigin[2]);

Vector3 S1(
   this->CSS_P_SAGHeight[0],
   this->CSS_P_SAGHeight[1],
   this->CSS_P_SAGHeight[2]);

Vector3 S2(
   this->CSS_P_SAGWidth[0],
   this->CSS_P_SAGWidth[1],
   this->CSS_P_SAGWidth[3]);

// Panel's normal is computer
after rotation is applied
double rotAngle =
   this->CSS_U_SAG1Angle *
   BTE::toRadian;

if(sag == sag2) {
   P0[1] = -P0[1];
   S2[1] = -S2[1];
   rotAngle =
     -this->CSS_U_SAG2Angle *
     BTE::toRadian;
}

/// Rotate SAG accordingly to the
current attitude
Vector3 axis(0,-1,0); // rotation
axis (-Y: is the axis in which the
angles are measured)

P0 = P0*cos(rotAngle)+ (axis^P0) *
sin(rotAngle) + axis * (axis *
P0)*(1-cos(rotAngle));

S1 = S1*cos(rotAngle)+ (axis^S1) *
sin(rotAngle) + axis * (axis *
S1)*(1-cos(rotAngle));

// Panel's normal
Vector3 N = (S2 ^ S1).unit();
```

```
/// SAG's geometry
Vector3 P0(
   this->CSS_P_SAGOrigin[0],
   this->CSS_P_SAGOrigin[1],
   this->CSS_P_SAGOrigin[2]);

Vector3 S1(
   this->CSS_P_SAGHeight[0],
   this->CSS_P_SAGHeight[1],
   this->CSS_P_SAGHeight[2]);

Vector3 S2(
   this->CSS_P_SAGWidth[0],
   this->CSS_P_SAGWidth[1],
   this->CSS_P_SAGWidth[3]);

// Panel's normal is computer
after rotation is applied
double rotAngle =
   this->CSS_U_SAG1Angle *
   BTE::toRadian;

if(sag == sag2) {
   P0[1] = -P0[1];
   S2[1] = -S2[1];
   rotAngle =
     this->CSS_U_SAG2Angle *
     BTE::toRadian;
}

/// Rotate SAG accordingly to the
current attitude
Vector3 axis(0,-1,0); // rotation
axis (-Y: is the axis in which the
angles are measured)

P0 = P0*cos(rotAngle)+ (axis^P0) *
sin(rotAngle) + axis * (axis *
P0)*(1-cos(rotAngle));

S1 = S1*cos(rotAngle)+ (axis^S1) *
sin(rotAngle) + axis * (axis *
S1)*(1-cos(rotAngle));

// Panel's normal
Vector3 N = (S2 ^ S1).unit();
```

Errors:

(1) In both codes the third index for accessing `CSS_P_SAGWidth` is invalid;

(2) In the left code there is a signal inversion in the operation `CSS_U_SAG2Angle * toRadian`.

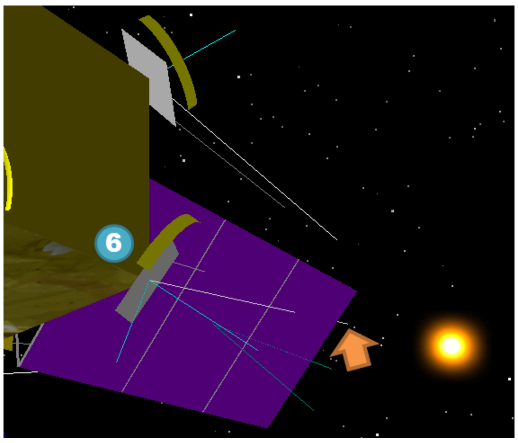

(a) SAG 45^o, view from the sensor 6.

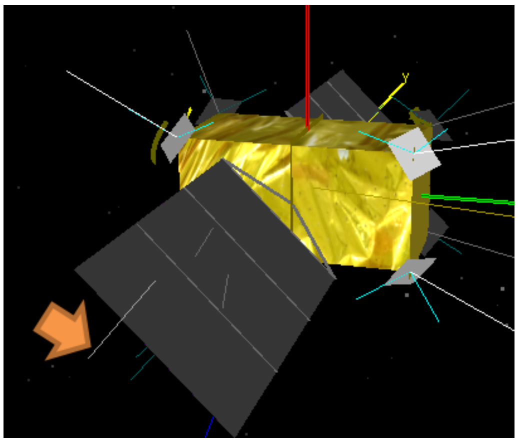

(b) SAG 45^o, view from the Sun.

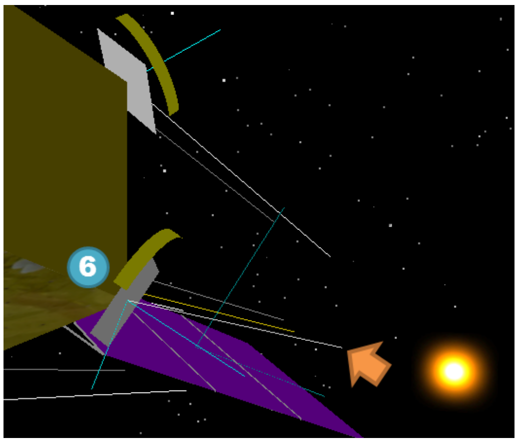

(c) SAG 315^o, view from the sensor 6.

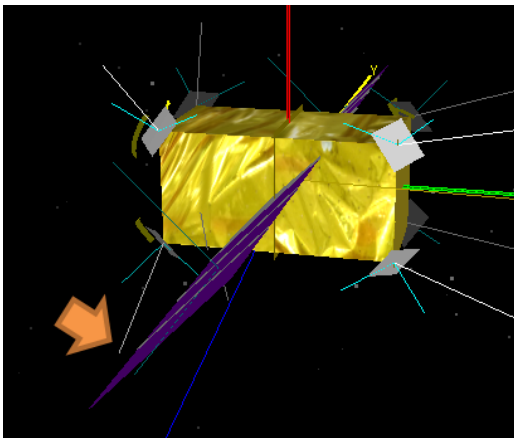

(d) SAG 315^o, view from the Sun.

Figure 6.10 - Assessment of SAG's shadow effect on the Coarse Solar Sensors. The visual output provides a tacit feedback on the model's correctness. When orienting the $-Y$ panel at 45^o it is clear that Sun is being blocked for CSS6 (arrows in a,b) and illuminating it when panel is oriented at 315^o (arrows in c,d).

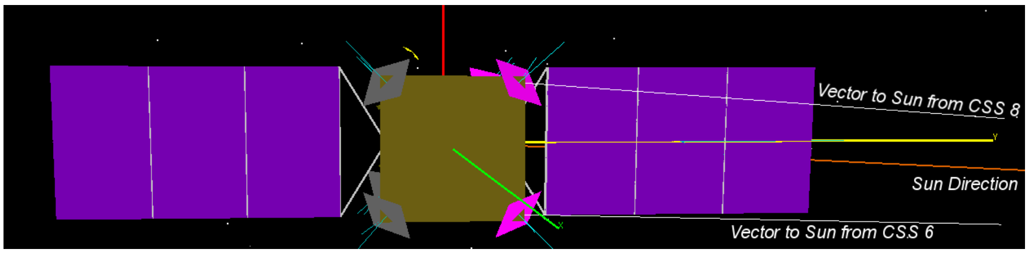

(a) a. In an arbitrary simulation time, the default configuration of panel's geometry produces no shadows on the CSS 6 nor 8.

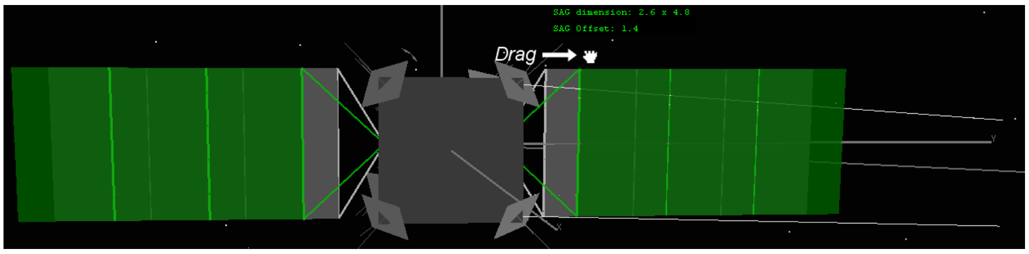

(b) b. The direct image manipulation is enabled and the user drags the solar panels to increase their offset from the spacecraft's body.

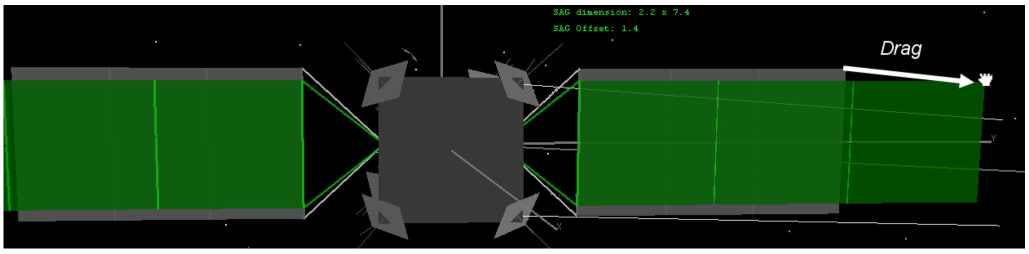

(c) c. A new interaction changes the shape of panels.

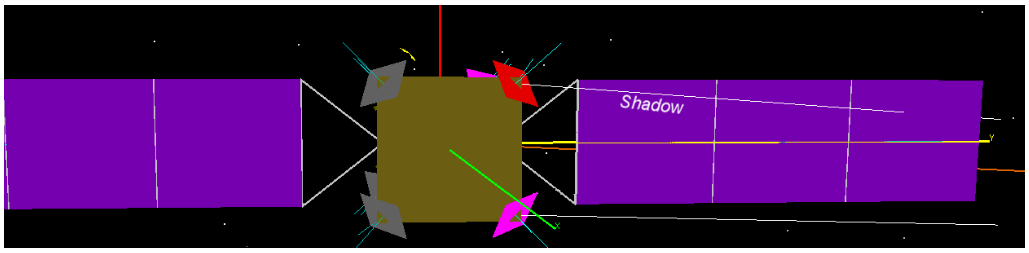

(d) d. The edition mode terminates and the visualisation systems is immediately updated, now with the CSS 8 on the shadows.

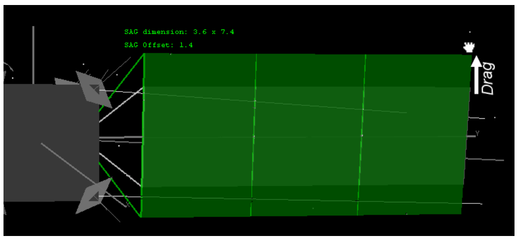

(e) e. Again the image is manipulated to change the panel's height.

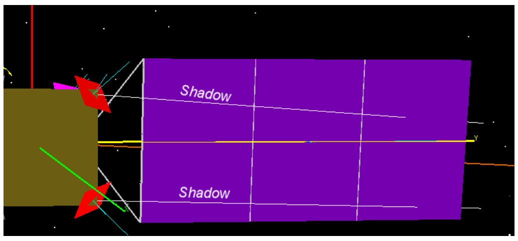

(f) f. The final geometry causes both CSS 6 and 8 to be on shadows.

Figure 6.11 - A sequence of interactions performed to modify the solar panel's geometry and investigate its effects on the shadow model. A direct image manipulation mechanism allows the engineer to steer the simulation parameters with the same 3D visualisation interface.

As represented in the Figure 6.11-a, in a given point in the simulation time, no shadows are being produced on the CSS 6 nor CSS 8. By enabling the geometry manipulation in the 3D image, which is represented by the green objects in the Figure 6.11-b, the engineer uses the mouse device to drag the solar panels and increase their offset from the satellite's body. On the sequence, in Figure 6.11-c, their shape are changed when the width is enlarged and the height slightly reduced. Next, the edition is disabled and the visualization system is immediately updated from the data produced by the modified simulation model. As seen in the Figure 6.11-d, the first set of interventions causes the Sun to be obscured from the CSS 8 point of view, but the CSS 6 remains illuminated. Finally, a new manipulation in the 3D visualization (Figure 6.11-e) increases the height of the panels, producing a shadow also on the CSS 6 (Figure 6.11-f).

Not only is the presented interaction an easy approach to validate model implementations, but it is also a rapid method to test different hypothesis concerning the geometry and mechanical configurations of the satellite. By changing the shape of the solar panel, the associated models can be automatically updated to reflect the new measurements, accelerating, for instance, trade-off analysis such as power subsystem dimensioning and mass budget or power budget and attitude control performance.

Furthermore, the direct image manipulation interface can be extended to support more complex parametric designs, thereby ensuring consistency among technical drawing, visualisation systems and simulation models.

6.3.3 Scene 3: Verification of solar panel's orientation commanded by the Bapta model

Once the shadow model has been verified in the previous scenes, the implementation of on-board software for computing the Sun versor and commanding the orientation of solar panel can be now evaluated. This can be done with the same configuration as before, except by the `BaptaController::Bapta_Y_CommandedAngle` parameter, which now is unforced and is autonomously computed. Still suing the 3D vector widget the user continues on defining the Sun position and observing the behaviour of SAG's orientation as commanded by the on-board software. In Figure 6.12, a sequence of four steering inputs is shown and the corresponding simulation results. It is noticed that so far both Sun determination algorithm and Bapta Controller are executing properly, since the solar panels are being pointed appropriately to the Sun.

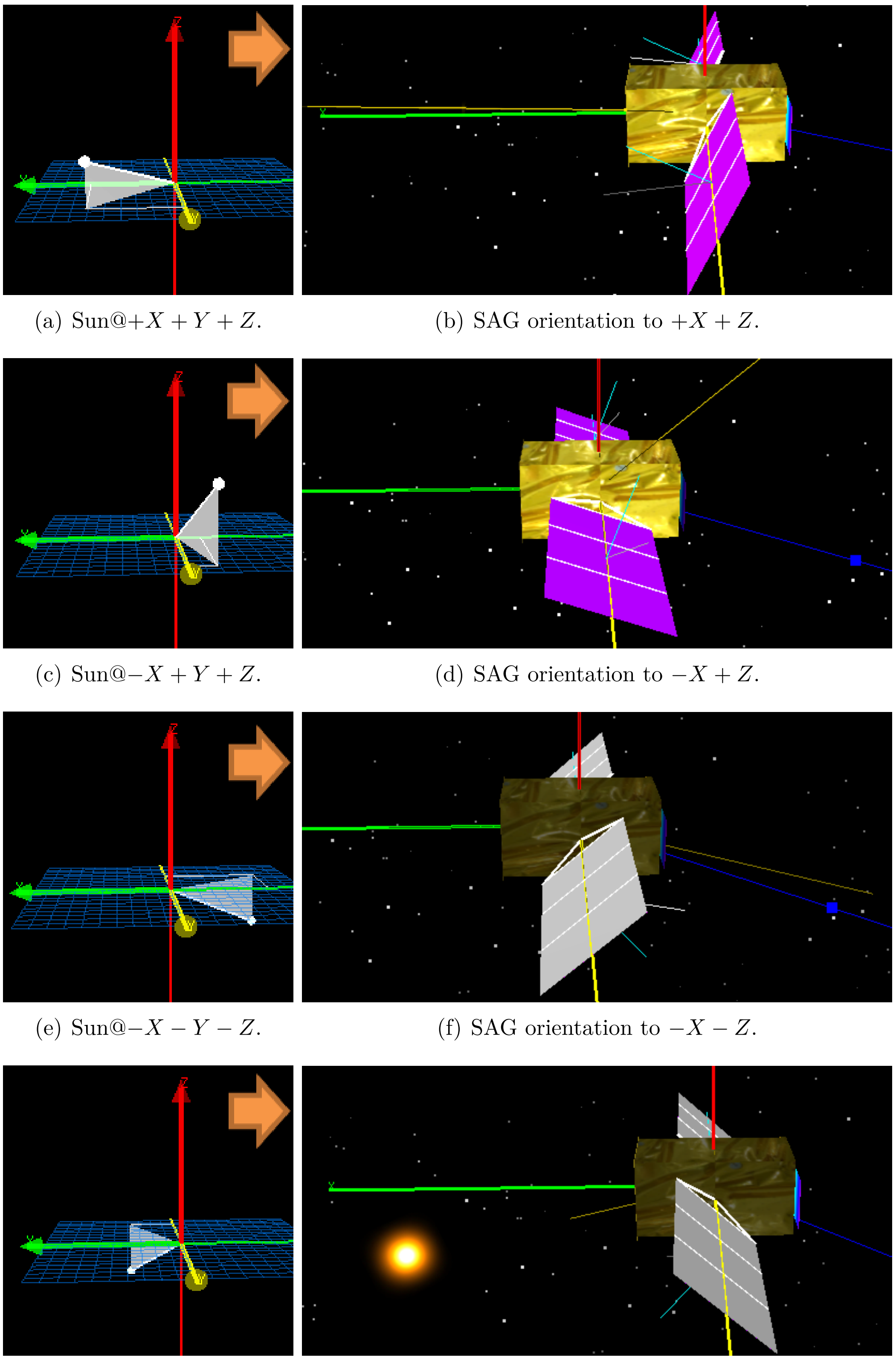

(a) Sun@$+X+Y+Z$.

(b) SAG orientation to $+X+Z$.

(c) Sun@$-X+Y+Z$.

(d) SAG orientation to $-X+Z$.

(e) Sun@$-X-Y-Z$.

(f) SAG orientation to $-X-Z$.

(g) Sun@$+X-Y-Z$.

(h) SAG orientation to $+X-Z$.

Figure 6.12 - Assessing the commanded solar panel's orientation as function of Sun vector.

In this simulation, the on-board computation of Sun versor is based on readings provided by the Coarse Solar Sensors, thereby the performance of Bapta Controller is indirectly influenced by the level of Sun incidence on the sensors. Many hypotheses could rise regarding the possible behaviours of the algorithms due to external noise and environmental changes (e.g. CSS precision, Earth's Albedo interference). As an illustration of the flexibility of steering environment for assessing these scenarios, the Figure 6.13 shows the simulation results when a special-purpose widget is attached to the Sun model and used to steer its position taking into account the expected level of solar irradiance on the sensors (measured in W/m^2). In this complementary test case, by choosing samples from an irradiance profile, which varies along the year as a function of Earth-Sun distance, erroneous results could be identified as a result of solar sensors saturation of under illumination. The simulation outputs in Figure 6.13 indicates that model works well for nominal irradiance limits within an year.

6.4 Scenario 2: On-board software verification

In addition to its flexible interface for verifying the correctness of simulation models, the computational steering also provides a convenient tool for studying the behaviour of space systems and validating their design. In this scenario, this benefit is demonstrated in a case study for testing a module of on-board software, responsible for the *Fault Detection, Isolation and Recovery* (FDIR) functionalities.

Hence, an illustrative implementation of FDIR rules is employed for detecting failures triggered by attitude determination errors, drifts on the spacecraft attitude, or solar panel orientation errors. In this scenario, the engineer is committed to assure that all rules have been properly designed and codified and executed in a full covered simulation.

6.4.1 FDIR component description

The FDIR module comprises a software implementation with a set of rules that monitors the appearance of error events and their evolution to actual fault. This component adopts a simple mechanism to compute the error every time the value of an observed variable exceeds a given threshold. After the error counter has reached a limit, for instance ten times, the associated event is marked as faulty. The same approach is used to restore the flag status when the error disappears after a sequence of verifications.

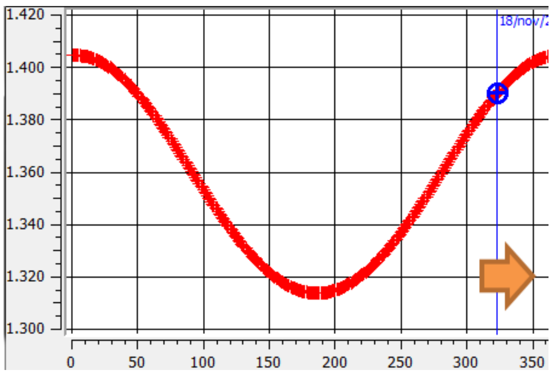

(a) Before December's Solstice.

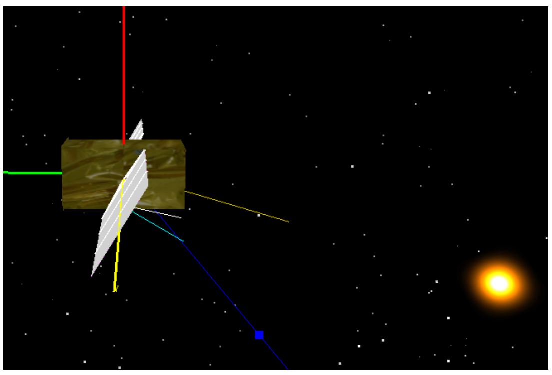

(b) SAG orientation to $-X - Z$.

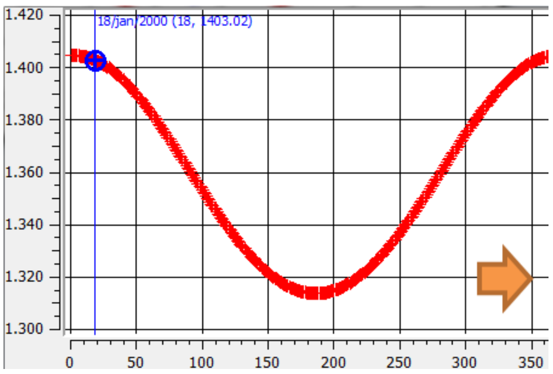

(c) After December's Solstice.

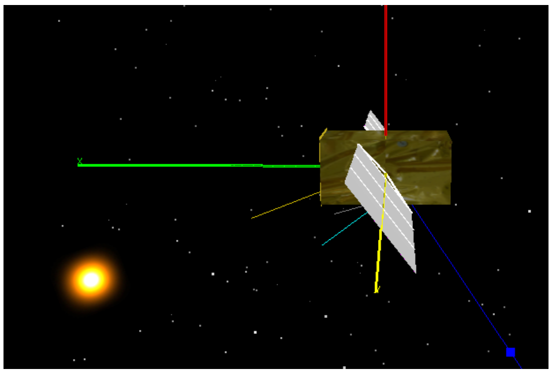

(d) SAG orientation to $+X - Z$.

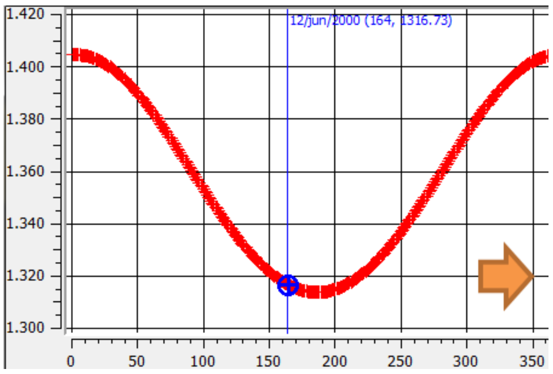

(e) Before June's Solstice.

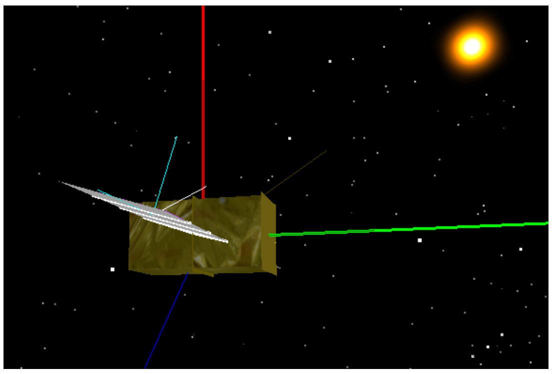

(f) SAG orientation to $+X + Z$.

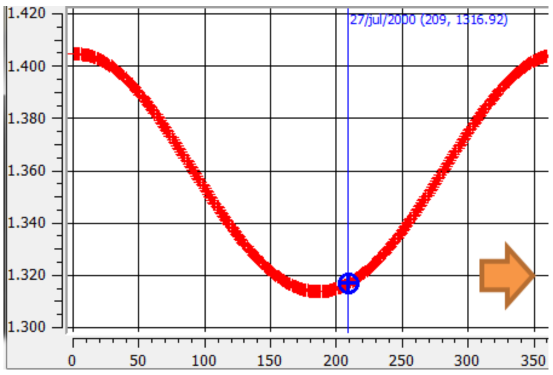

(g) After June's Solstice.

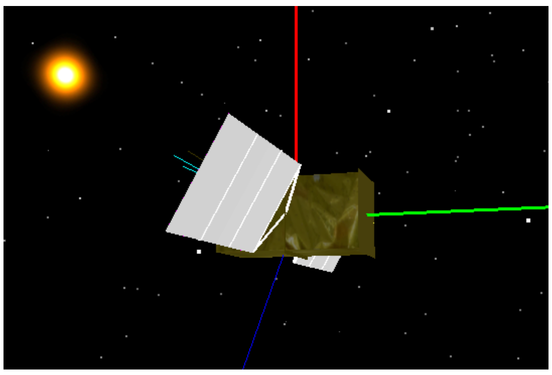

(h) SAG orientation to $-X + Z$.

Figure 6.13 - The usage of special widget for steering the Sun vector with well-defined irradiance levels (between 1310 and 1405 W/m^2).

In this scenario, three types of rules have been defined to execute every second. The first group checks to the accuracy on pointing the spacecraft to the commanded quaternion. The goal is to detect deviations from the pointing target by monitoring the angle between the reference and determined attitude quaternion. A fault flag is enabled if the error event persists more than ten seconds and, in this case, neither isolation nor recovery actions have been programmed. Additionally, the second type of rules monitors the orientation of the solar panels, by detecting any inconsistency on the commanded and the measured orientation angle. Moreover, during the nominal operating mode (i.e. nadir pointing) the angle between the computed Sun and the normal of each solar panel is used to assess the coherence among the sensorial data with respect to the orbital plane. In other words, if the satellite is properly pointing to the nadir and precisely computing the direction of the Sun, it is expected that the beta angle remains within a certain limit.

Finally, the health of the attitude determination module is controlled by the FDIR system to enable its automatic reconfiguration whenever a fail is detected in one of the sensors. This algorithm considers the classic method for combining the measurements from the star trackers, gyroscopes, magnetometers, and solar sensors to build a fault tolerant system for computing the spacecraft attitude. Due to its high precision, the use of star trackers are preferred for providing the attitude, but in case of fails, the data from the solar sensors and magnetometers can be combined in the TRIAD method for computing an approximated attitude. Further, in the absence of these, a valid attitude quaternion can be propagated from the body rates measured by the gyroscope. The set of rules to monitor this service can be represented by the *fault tree diagram* in the Figure 6.14, which is equivalent to the following Boolean expression: $\text{STR} \wedge (\text{MGM} \vee (\text{Eclipse} \vee \text{CSS})) \wedge (Q_{init} \vee \text{Gyro})$. Based on the fails detected in the equipment or environmental conditions, the FDIR commands the attitude determination module to switch between its modes.

Thus, the baseline scenario has been modified to include the new FDIR module and a stub component that mimics the behaviour of an attitude determination component. The sub-assembly of the updated on-board architecture is depicted in the object diagram in the Figure 6.15, in which the control variables and data exchanged between the elements are described.

6.4.2 Overall test procedure and strategies

The on-board software verification strategy comprises on organising the test activities in four phases, accordingly to the FDIR's feature being analysed. As

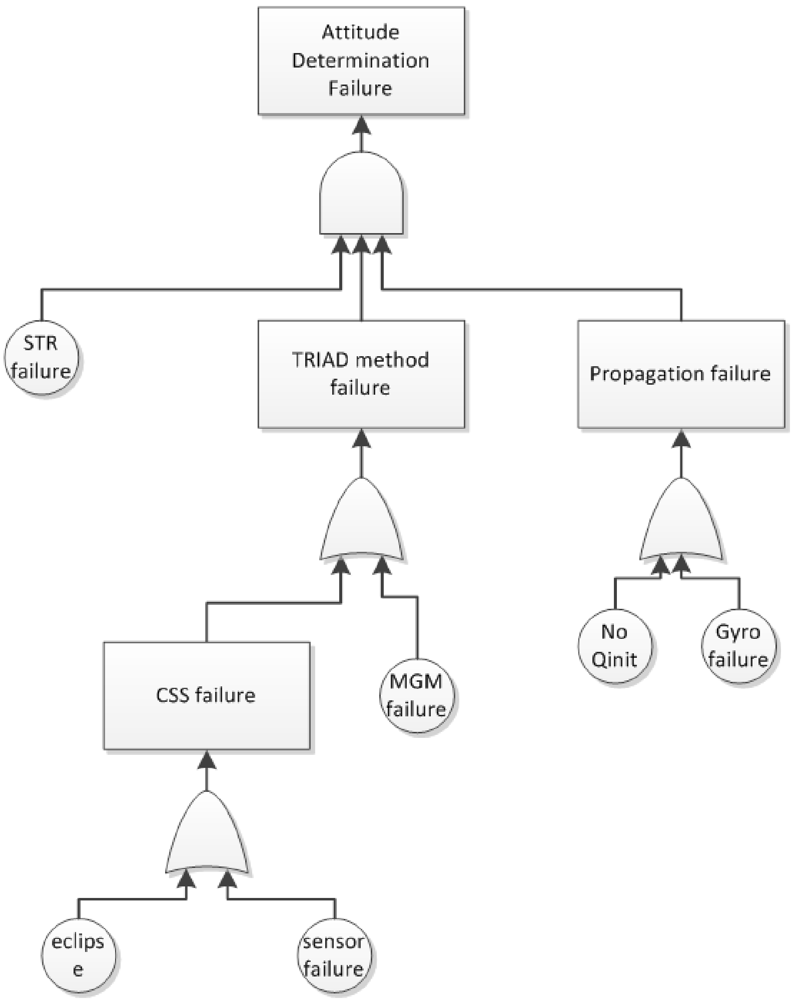

Figure 6.14 - Fault tree diagram of the attitude determination module.

presented in the Figure 6.16, the simulation scenario, which executes in soft real time, begins with a configuration procedure that represents the delay used for the OBC initialisation (i.e. booting & initialisation sequence) and the moment in which the simulation engineer commands the spacecraft to the nadir pointing mode and waits its convergence.

Following the initialisation phase, the first planned test phase ($T1$) consists in steering the Sun position to induce a beta angle error and verify its detection. In order to test all aspects of the FDIR mechanism, it is important that the user toggles the error injection in different time intervals, so the counter that enables and disables the fault flag can be checked.

The second test set related to the solar panels are performed in the $T2$ phase, in which the Sun model is restored to its simulated position and the SAG's orientation

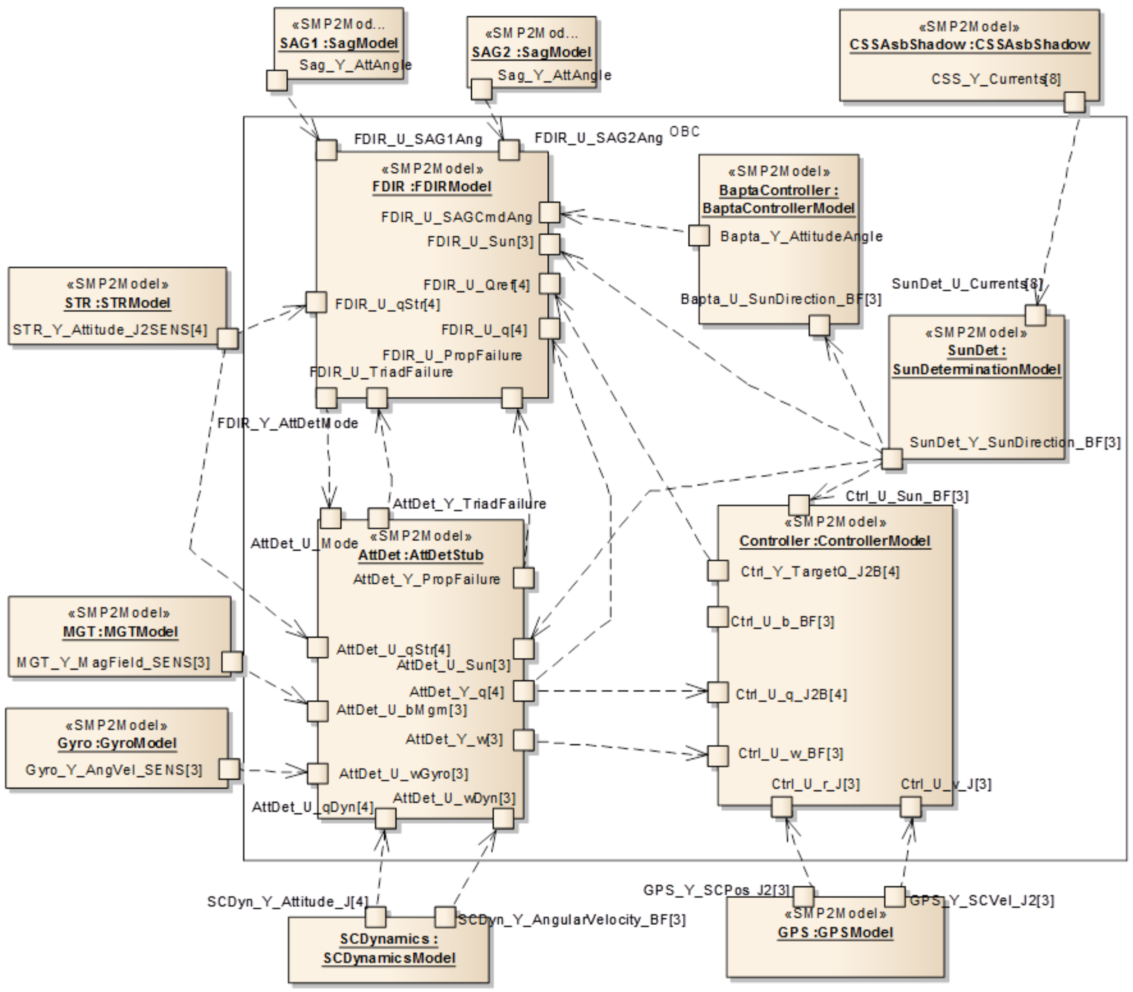

Figure 6.15 - Sub-assembly of the on-board elements containing the FDIR module and a stub for the attitude determination component.

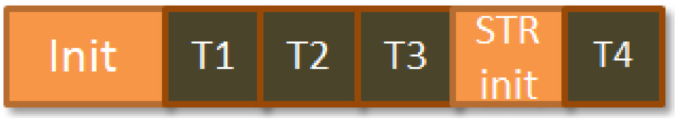

Figure 6.16 - Timeline of testing activities planned in the scenario.

is forced to produce a discrepancy with the commanded signal. In the sequence, the attitude error detection can be verified in the phase $T3$ by injecting noise in the simulation in many different ways. For instance, the torque commanded by the controller can be inhibited in the loop, a perturbation torque can be injected in the attitude dynamics, or the attitude quaternion is simply set to an arbitrary value.

Before the attitude determination module can be checked, in the phase $T4$, another configuration procedure takes place to initialise the star tracker sensor (e.g. representing the time required to acquire the first image and compute the first quaternion). Then, the basic strategy to test the several types of fails that can appear in the attitude determination system consists in setting the low level events from the fault tree diagram to verify all its operating modes.

It is important to note that it would be straightforward to write a script to automate the test that covers all the 64 arrangements of event states in the fault tree or only the minimum cut set that led to a faulty attitude determination module. Nevertheless, in real applications, some combinations are impossible or useless to be tested or simply the number of combinations could be so big that its execution is unfeasible in an acceptable time. Furthermore, the transitions between faulty to normal states must also be verified, which usually requires that a certain order in the test is obeyed. This type of temporal dependency appears, for instance, when testing the attitude determination by gyro propagation, in which an initial quaternion must exist before entering the mode.

For these reasons, in the current scenario a sequence of twelve test cases has been specified for the verification of FDIR rules regarding the attitude determination operation. The execution of the test cases requires the user to change the state of each component in an ordered way, by setting errors or injecting noise in their respective sensors or environmental variables. As described in the Table 6.4, for each combination of states an attitude determination mode is expected to be set by the FDIR service.

Another advantage of using the computational steering environment for executing these test cases is the independence gained by the engineer on deciding whether to interrupt or not a simulation section in the case an unexpected behaviour shows up. Particularly when small mistakes are performed, like a misconfiguration of scenario variables or a forgotten test step, the user can make progresses in the running simulation to fix the problem or to investigate in details a failure if an irrecoverable error occurs (e.g. a bug in the OBSW, an error in the simulation assembly).

Table 6.4 - Sequence of test cases planned to verify the FDIR rules that controls the attitude determination module. For each combination of failures (i.e. failed=T) a determination mode is expected to be set.

#	Failed component						Det. Mode	Remarks
	STR	MGM	Eclipse	CSS	Q_{init}	Gyro		
1	F	F	F	F	F	F	STR	All fine.
2	T	F	F	F	F	F	TRIAD	STR fails.
3	T	T	F	F	F	F	GYRO	MGM fails.
4	T	T	F	F	F	T	NONE	Gyro fails.
5	F	T	F	F	T	F	STR	Restore Gyro and STR. Set invalid Q.
6	T	T	F	F	F	F	GYRO	STR fails.
7	T	T	F	F	F	T	NONE	Gyro fails.
8	T	F	F	F	F	T	TRIAD	Restore MGM.
9	T	F	F	T	F	T	NONE	CSS fails.
10	T	F	F	F	F	T	TRIAD	Restore CSS.
11	T	F	T	F	F	T	NONE	Force eclipse.
12	T	F	F	F	F	T	TRIAD	Unforce eclipse.

Some facets of the flexibility in this environment can be observed from the graphical user interface configured for this scenario and reproduced in the Figure 6.17. At a glance the engineer can monitor various aspects of the orbit and attitude simulation (A) in addition to the fault flags and error event counters in the infrastructure (B). Besides from changing values directly in the model tree (e.g. forcing the eclipse condition), a set of steering widgets are attached to variables of interest for rapid access and manipulation. As illustrated in this snapshot, special interfaces are available for steering the orbital parameters (C), forcing the SAG's orientation (E), injecting rotation rates (F) and attitude quaternions (G) into the body dynamics, and guiding the Sun's position. Moreover, a custom monitor application can be connected to the simulator to process derived output parameters, such as the error between the computed and simulated Sun.

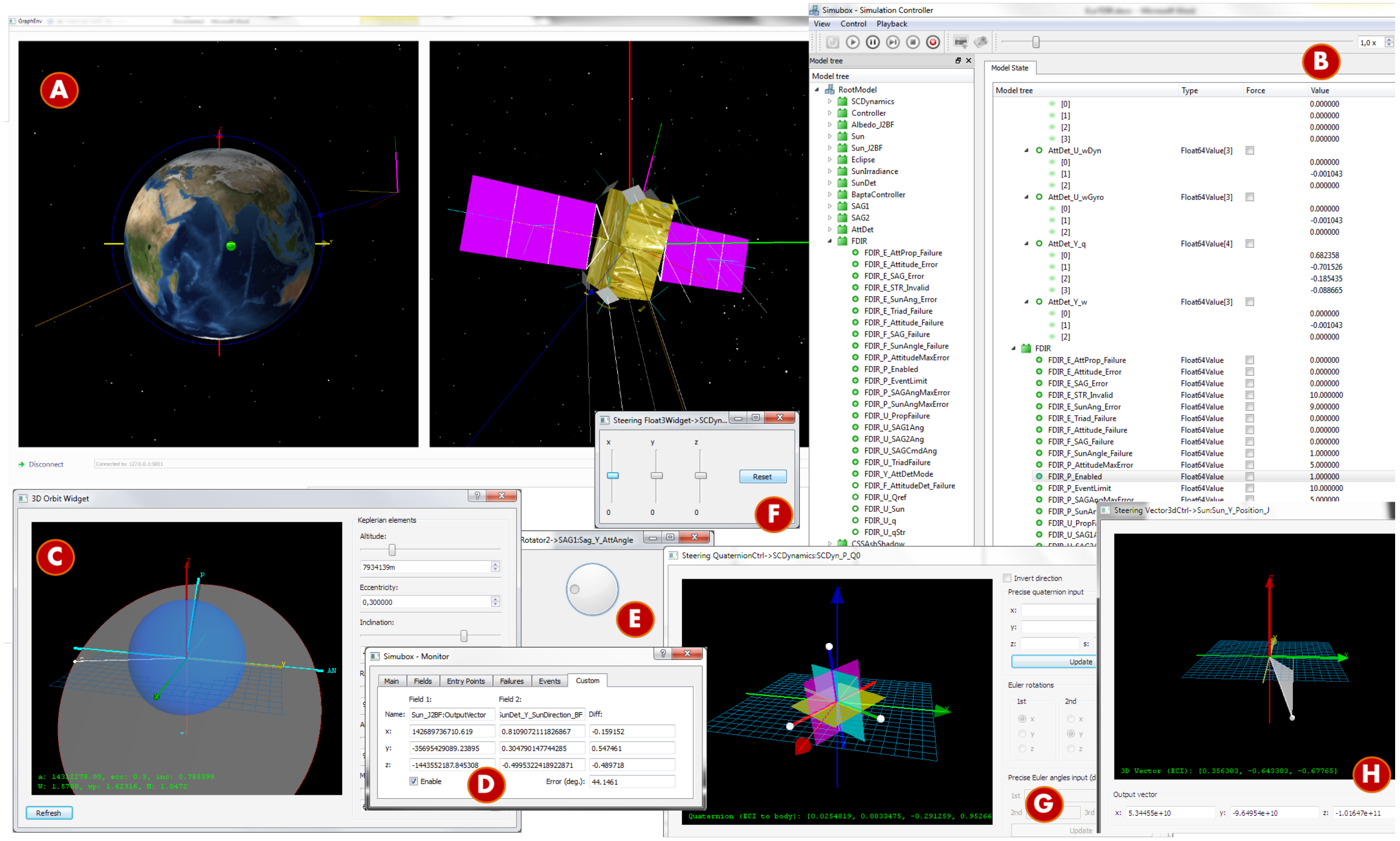
A
B
C
D
E
F
G
H
Simubox - Simulation Controller
View Control Playback
Model tree
Model State
Steering Float3Widget->SCDyn...
Reset
3D Orbit Widget
Keplerian elements
Refresh
Rotator2->SAG1:Sag_Y_AttAngle
Simubox - Monitor
Main Fields Entry Points Failures Events Custom
Steering QuaternionCtrl->SCDynamics:SCDyn_P_Q0
Steering Vector3dCtrl->Sun:Sun_Y_Position_J
Output vector
Disconnect

Altitude: 7934139m
Eccentricity: 0,300000

	Field 1:	Field 2:	Diff:
Name:	Sun_J2BF:OutputVector	SunDet_Y_SunDirection_BF	
x:	142689736710.619	0.8109072111826867	-0.159152
y:	-35695429089.23895	0.304790147744285	0.547461
z:	-1443552187.845308	-0.4995322418922871	-0.489718
✓ Enable		Error (deg.):	44.1461

Quaternion (ECI to body): [0.0254819, 0.0833475, -0.291259, 0.95266

3D Vector (ECI): [0.356303, -0.643303, -0.67765]

Output vector x: 5.34455e+10 y: -9.64954e+10 z: -1.01647e+11

Figure 6.17 - GUI of the computational steering facility used in the on-board software verification scenario: (A) 3D visualisation system; (B) infrastructure; (C) Widget for steering the orbital parameters; (D) Simulation monitor computing the Sun determination error; and widgets to steer the (E) SAG's orientation; (F) body rates; (G) attitude quaternion; and (H) Sun's position.

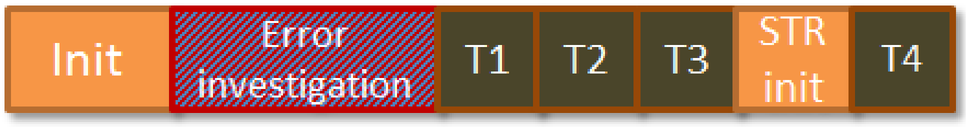

Figure 6.18 - Timeline of testing activities performed in the scenario.

6.4.3 Simulation results

The complete execution of this scenario took approximately half hour. After the initialization phase, which lasted about 200 seconds, the test of Sun angle error rules begins (T1). However, as soon as the FDIR component is enabled, these rules are trigged without any failure injected by the engineer. This behaviour is unexpected, since the maximum angle between the solar arrays and the Sun is 30 degrees, when the spacecraft is pointing to the nadir in the nominal orbit.

Therefore, in this moment the user has to suspend the test procedure to investigate the causes of the FDIR malfunction. Without interrupting the simulation, a set of interactions with the models has brought to light that there was an inversion in the connection between the two solar sensors and the Sun determination OBSW. Then, this mistake is corrected during the execution of the scenario and in the end of the simulation, the actual sequence of activities executed by the user includes the *error investigation phase*, as illustrated in the Figure 6.18.

The user interventions during the error investigation and the activities performed in the remaining phases of this scenario are described in details in the next paragraphs. In addition, the results obtained in the simulation are presented in the Figures 6.19 and 6.20.

6.4.3.1 Error investigation

Before the cause of the Sun angle error has been identified, a set of hypotheses for explaining the source of the fault is proposed to guide the investigation: (i) the orbital parameters are not properly configured in the scenario and the simulated orbit is not the nominal one; (ii) there is a bug in the orbital dynamics or Sun position models; (iii) the CSS models are not correctly implemented; (iv) the Sun determination algorithm is not computing the Sun version precisely; or (v) the OBSW that computes the angles is faulty.

After a quick verification in the 3D orbital visualization system, it is observed that

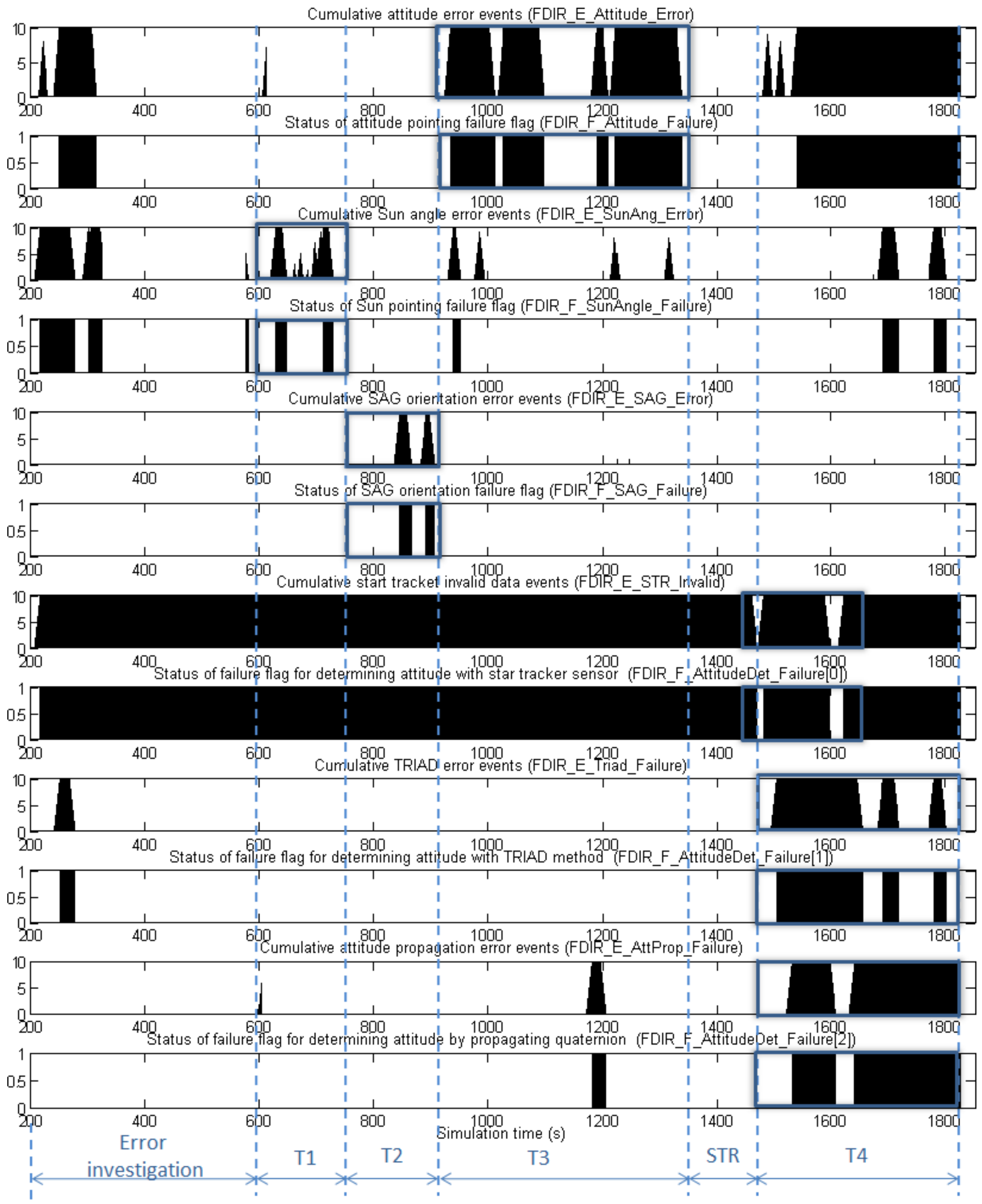

Figure 6.19 - Evolution of error events and fault detection flags in the FDIR along the simulation horizon.

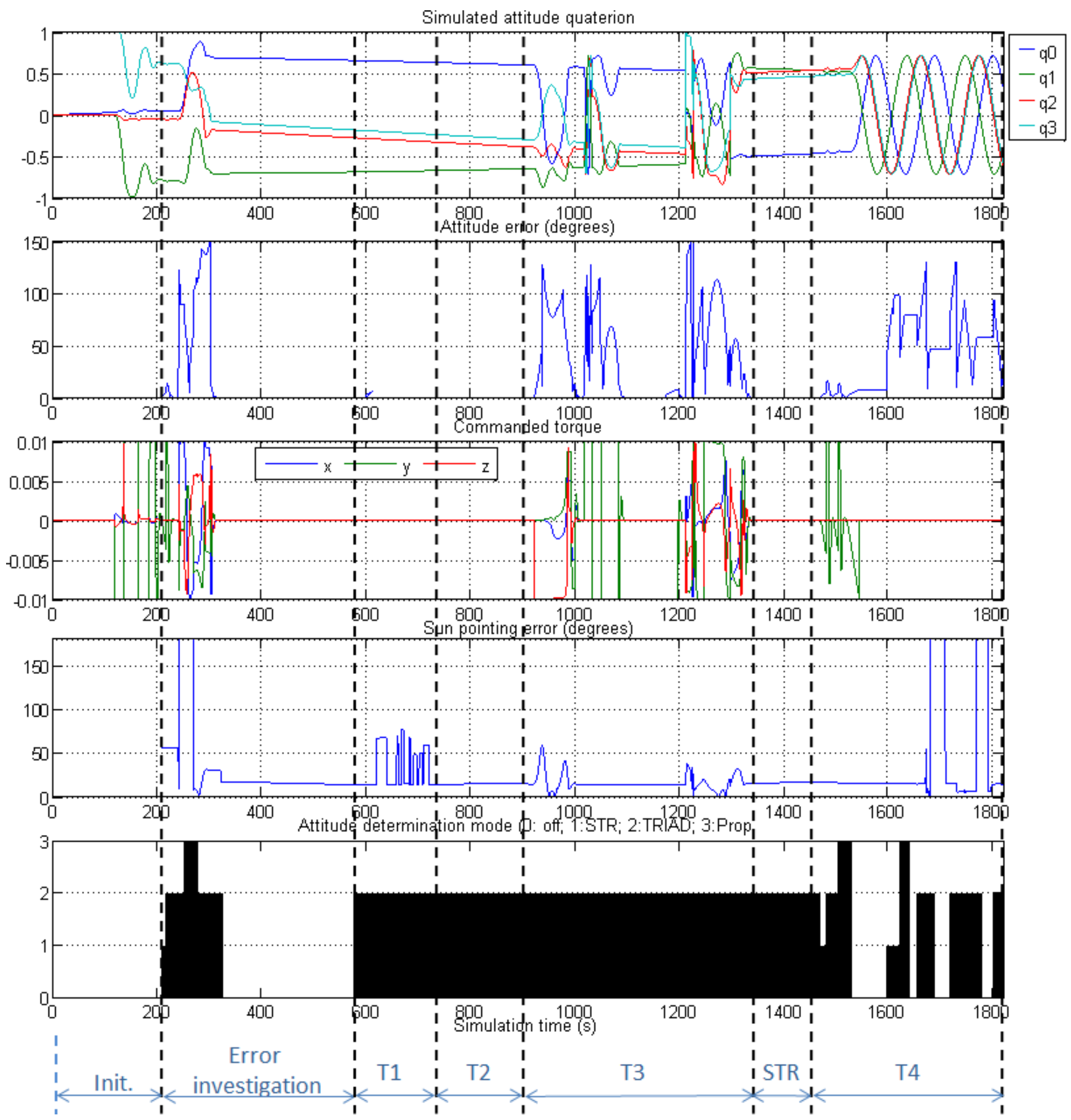

Figure 6.20 - Evolution of control variables used in addition to the visual feedback during the scenario execution.

indeed the simulated orbit is not using the proper parameters, since the simulation configuration file has not been updated with the scenario data. In this case, instead of reloading the simulation, the user readily steers the orbit to the desired position, by rotating the Right Ascension of Ascending Node (RAAN). Unfortunately, this first reconfiguration puts the satellite in the Earth's shadows and the test procedure *T1* cannot start because the fault flag remains enabled. Hence, a second intervention is done to change the argument of perigee.

The initial conditions of the orbital and the results of its reconfiguration are illustrated in the snapshots in the Figure 6.21. In the first orbital configuration (Figure 6.21-a), the angle between its plane and the Sun vector is visibly greater than 30 degrees. In addition, the respective attitude view visually confirms that error in the angle, even if the computed Sun on-board is not precise, in the Figure 6.21-d. After the first change, the satellite becomes clearly in the shadow (Figure 6.21-b) and the Sun cannot be computed on-board (Figure 6.21-e). Finally, after a new correction of orbital parameters, the satellite is illuminated by the Sun, which position is not far misaligned with the orbital plane (Figure 6.21-c).

Nonetheless, from the attitude view in the Figure 6.21-f, it is observed that the difference between the computed and simulated Sun actually has increased. In this moment, the malfunction hypotheses lie on the Sun determination algorithm and its input data. Hence, by using a similar approach for steering the Sun position from the section 6.3, additional verifications are done in the simulation that finally point that output currents from the solar sensors are inconsistent, since an inversion has been made in the assembly of CSS 3 and 7.

Therefore, the correction in the sensorial signals is directly performed in the simulation by the user, thereby adjusting the scenario for continuing with the FDIR test procedures. So far, the attitude correction manoeuvres caused by the scenario interventions are shown in the curves between the 200 and 600 seconds of simulation in the Figure 6.20.

6.4.3.2 T1: Sun angle test

This test comprises on setting the attitude determination to execute on gyroscope propagation mode, forcing the eclipse condition to false, and steering the Solar position to force the incidence angle error. The results of user interaction are shown in the simulation interval from 600s to 730s in the Figure 6.19 and in the Sun pointing error curve in the Figure 6.20.

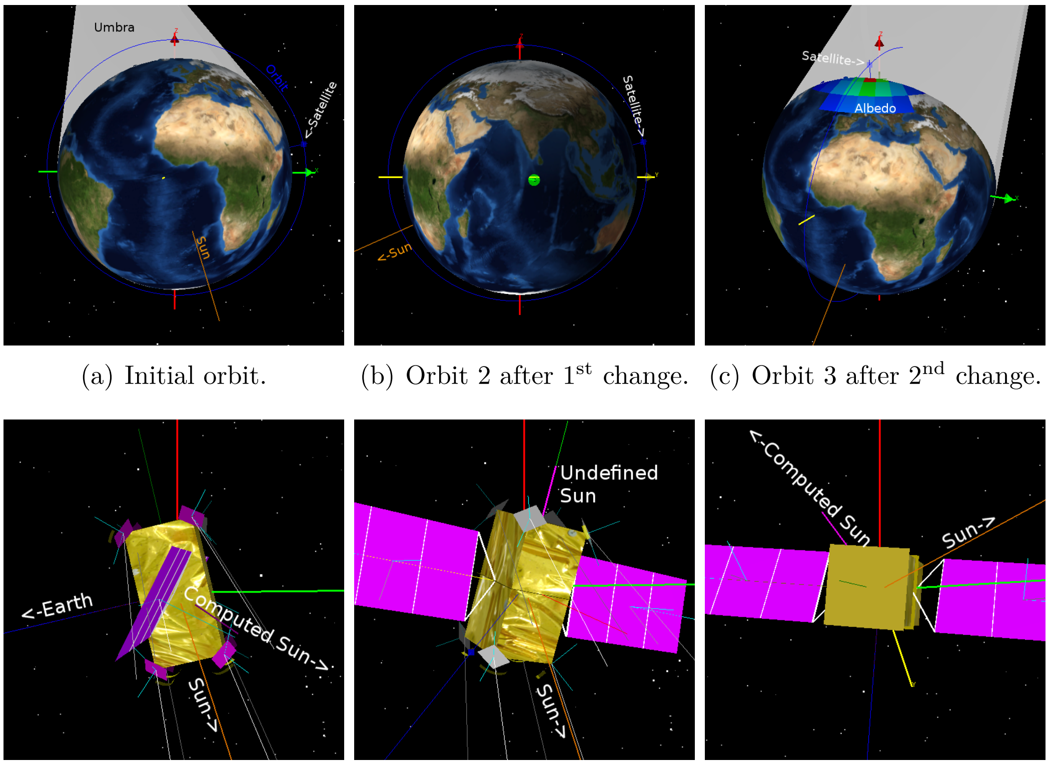

(a) Initial orbit. (b) Orbit 2 after 1st change. (c) Orbit 3 after 2nd change.

(d) Attitude for orbit 1. (e) Attitude for orbit 2. (f) Attitude for orbit 3.

Figure 6.21 - Orbit and corresponding nadir pointing attitudes in the beginning of the scenario and after the 1st and 2nd user interventions.

As the Sun angle reaches the limit defined by the engineer (i.e. 30^o), the error counter increases until the fault flag is triggered by the FDIR algorithm. In order to test the fault cancelation, the Sun is steered close to the nominal position and as seem in the graphics, the error counter decreases until the fault flag becomes disabled. Moreover, during this test the user injects the angle error but removes it before the fault is triggered to verify the counter mechanism. This error intermittence is observed in the Figure 6.19 by the oscillation in the counter, in which the fault only becomes enabled again when it reaches ten consecutive occurrences.

6.4.3.3 T2: SAG orientation test

A similar strategy is used to trigger the FDIR rules regarding the SAG orientation error. However, in this case the user intervention simply consists in forcing the orientation of the solar panels, thereby simulating a malfunction of the controlling mechanism. The evolution of the respective error counter and fault flag can be seen in the period from 770s to 912s of the scenario in the Figure 6.19.

6.4.3.4 T3: Attitude error test

Several types of error can be injected to test the rules that monitor the loss of attitude accuracy. In this test case, in the instant 920s a perturbation torque is inserted in the spacecraft dynamics model, which causes the attitude to drift from its commanded position. In this moment, the rise of attitude error can be observed in the Figure 6.20 in addition to the torques commanded by the controller to correct the deviation. As a result of the orientation error, the fault flag is eventually triggered, as presented in the Figure 6.19.

After the perturbation is removed, the controller finally corrects the attitude and the fault disappears. Then, in the instant 1118s the signals from the controller to the dynamics model are inhibited and the spacecraft starts to drift again.

When the attitude is established again by enabling the controller, the engineer tries another type of failure injection by steering the attitude quaternion directly in the spacecraft dynamics models. The results for this approach as shown in the graphics between the simulation time 1209s and 1350s in the Figures 6.19 and 6.20.

6.4.3.5 T4: Attitude determination test

Following to the initialisation of the star tracker sensor, the last set of tests covers the operation modes of the attitude determination component, from the instant 1458s until the end of the simulation, as shown in the Figures 6.19.

The sequence of interventions follows the procedure previously defined in the Table 6.4. As illustrated in the Figure 6.20, initially the attitude determination uses the data provided by the STR (i.e. mode 1) and then the engineer provokes the automatic change to the TRIAD method (i.e. mode 2), by setting an error in that equipment (i.e. forcing an invalid output quaternion). Next the MGM is failed (i.e. annulling the measured output vector) and the OBSW begins to propagate the attitude using the gyroscopes (i.e. mode 3). In this moment, an additional error in the gyroscopes causes the attitude determination to fail and then the user turns-off the controller.

Accordingly to the fault tree, the failure in the mode 3 can also be provoked by the unavailability of an initial quaternion (Q_0) that must be propagated. Hence, the engineer sets the Q_0 to an invalid value and restore the nominal states of STR and Gyro, thereby switching to the mode 1 again. As expected, a new STR fault leads the OBSW to the mode 3, since the Q_0 is updated with the last valid quaternion.

In the last part of the test procedure, the GYRO is failed and the MGM is restored to induce the change to mode 2. The complete coverage of possible fault events in the attitude determination is done to provoke the failure of TRIAD method, by injecting errors in the CSS and next forcing a eclipse condition.

6.4.4 Discussion

The current scenario demonstrates the computational steering approach for testing OBSW artefacts, commonly conducted in the scope of activities of subsystem designers and software developers, in which both the correctness of the implementation and the configuration of the testing environment are verified. By interacting with the simulation via the steering mechanisms, the engineer could guide the scenario to a state of interest to validate the test procedure or to identify the ideal condition for performing the software verification.

Thus, in contrast to a script approach, several hypotheses could be online tested and deviations from the original testing procedures could be adjusted, avoiding the simulation re-initialisation. In a real application scenario, for instance with hardware-in-the-loop, the re-execution of the scenario for updating the script each time an error comes up, could represent additional man-hours, particularly if the equipment start-up requires a long initialisation sequence or time-consuming manoeuvring and filter convergences are involved. In the illustrated scenario, the initialization phase would be executed at least five times for accommodating two orbital corrections, performing the error investigation, and finally running the simulation with the proper configuration.

Furthermore, as the simulation evolves, it is likely that new parameterisation mistakes and configuration issues in the test procedure appears, increasing the chances to reinitialize the scenario, especially when the test specification is not yet mature. In the example of the *T4* procedure, this could have happened if a STR initialisation parameter had been forgotten or if the satellite had entered in eclipse exactly in the moment the TRIAD method would be tested.

6.5 Scenario 3: Analysis of recurrent effects on the dynamics behaviour of Sun Determination Algorithm

One of the remarkable benefits on using a computational steering environment refers to its flexibility on exploring the space state of dynamic phenomena and transient regions. In addition to all the parameter complexity for tuning the *Sun*

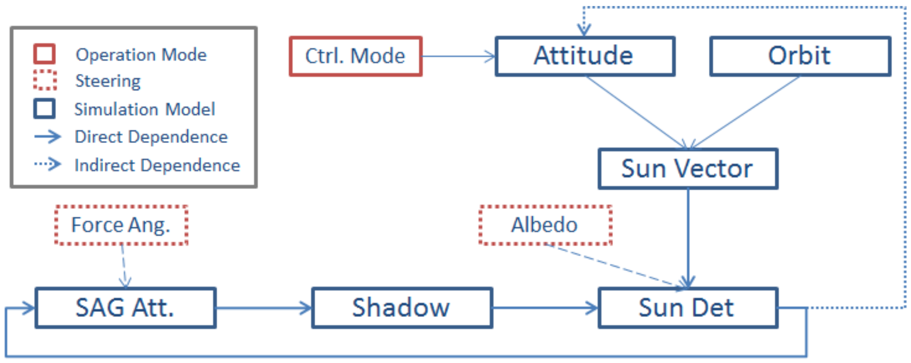

Figure 6.22 - Dynamic dependencies of simulation models for the *Sun Determination* scenario and some possible user interactions.

Determination algorithm, its behaviour is particularly hard to predict in some scenarios, due to the interdependence of variables, in which emerging properties may appear.

In fact, the Sun vector computed on-board will be used to orient the solar panels and possibly the satellite attitude, which in turn will eventually affect the determination of Sun vector itself. Consequently, the impacts on computing the Sun's direction imprecisely would cause recurrent effects on this determination and potentially amplify the error, in a given scenario condition.

This dynamic relation is depicted in the general diagram in Figure 6.22, in which the computations are performed as follows: (1) the Sun w.r.t. body frame is simulated accordingly to the spacecraft attitude and position; (2) , the Sun Vector is determined on-board from the solar sensors readings; (3) this vector is then used to orient the solar panels; and (4) the orientation of solar panels may produce shadows over the sensors used for computing the Sun on-board. On the top of that, the behaviour of the models may also be influenced by user interactions, which can, for example, cause the control mode to change, inject albedo noise on the sensors, force the orientation of solar panels, or alter any parameter in the running simulation.

As a result of this type of scenarios, questions like this may arise: *Is there any case that an injected noise on the solar sensors would imply an imprecise orientation of the solar panels, which in its turn would deteriorate the Sun Determination performance? Would this effect be critical to the mission?*

Testing this kind of hypothesis would require a tangle of statements in a script based simulator, in order to cover many conditions and search for a geometrical configuration in which the situation in the first question satisfies. On the other hand, by using a steering interface, the engineer can simply guide the simulation to that state.

Therefore, this approach is demonstrated by using the baseline scenario to answer the exposed question. During its execution, a steering widget is connected to the solar sensor models so noise can be injected by the engineer in the form of Earth's Albedo. At the same time, the Sun is forced to be positioned in a way that one of the solar sensors stays in the shadow of a solar panel wing. In addition, the eclipse condition is forced to *false* and the attitude is frozen to easy the analysis of the geometry.

As the simulation runs, the engineer keeps experimenting new positions for the Sun, which causes the Sun versor to be recomputed and the SAG reoriented, in the next simulation step. The Figure 6.23-a captures the instant that an arbitrary position of the Sun is set ($azimuth = 70^o$ and $elevation = -2^o$) and the solar panel is oriented at 130^o.

Initially in this investigation, four solar sensors are receiving direct Sun light and the error on Sun determination is nearly zero (the two lines in the graphical scene representing the simulated Sun in orange and computed Sun in pink are aligned). After the solar panel is reoriented to 174.17^o one sensor becomes blocked, but with the three remaining sensors a precise Sun determination is still performed (Figure 6.23-b). However, when a small Albedo is introduced by the user at azimuth -27^o and elevation 38^o, the error on Sun determination increases by 4 degrees (Figure 6.23-c), which causes the reorientation of the panel. Finally, with a different SAG's attitude a new solar sensor is obscured, raising the error to 30^o (Figure 6.23-d).

This sequence of steering and simulation steps demonstrates how a recurrent effect on the behaviour of the models can be reproduced and analysed. The detailed outputs for each scenario step is given in Table 6.5. It is observed that the resulting error on determining the Sun direction on-board may not be critical for controlling the attitude when the pointing mode does not depend on Sun's position, e.g. when the S/C is oriented to the Nadir. In this case, the most affected performance could be the power generation subsystem, which would not be maximizing the incidence of light. Nevertheless, in the case the computed Sun is being compared to a vector obtained from a theoretical method, the resulting discrepancy could trigger more critical actions from e.g. the FDIR system.

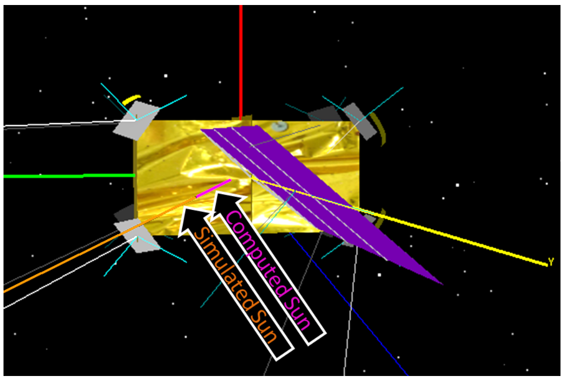

(a) Sun at $azimuth = 70^o$ and $elevation = -2^o$ is defined and no error is observed.

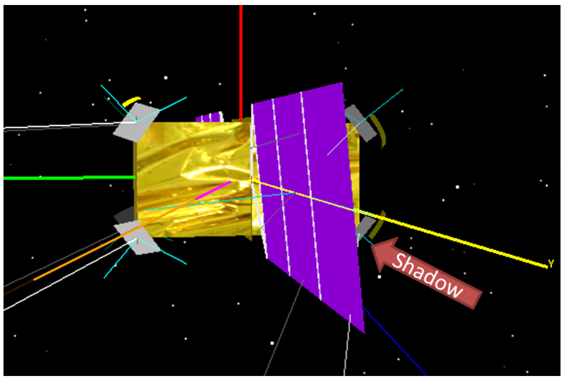

(b) The new orientation of SAG produces shadow on the CSS2.

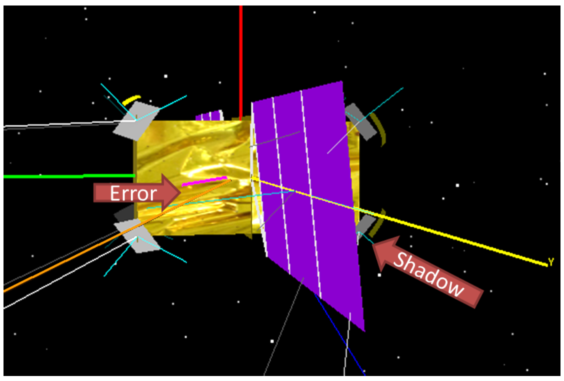

(c) Noise is introduced on solar sensors in the form of Earth's Albedo and a small error is observed.

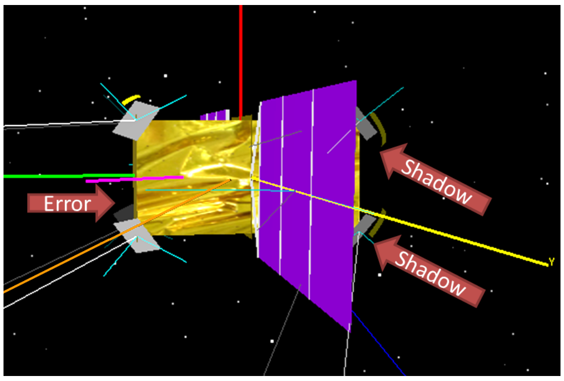

(d) The new orientation of SAG amplifies the error on Sun determination because a new solar sensor is blocked.

Figure 6.23 - Investigation of a recurrent effect on Sun Determination error when a given Sun/SAG geometry exists and an Earth's Albedo vector is injected on the solar sensors.

Table 6.5 - Output parameters of models in a sequence of four simulation steps after an arbitrary position of Sun is defined.

Parameter	step (a)	step (b)	step (c)	step (d)
SAG orientation	130^o	174.17^o	174.17^o	181.55^o
CSS1	0	0	0	0
CSS2	0.3630	*shadow*	*shadow*	*shadow*
CSS3	0	0	0	0
CSS4	0.3229	0.3229	0.3229	*shadow*
CSS5	0	0	0.1889	0.1889
CSS6	0.7556	0.7556	0.7556	0.7556
CSS7	0	0	0.0712	0.0712
CSS8	0.7155	0.7155	0.7563	0.7563
Sun Detetermination Error	0^o	0^o	4.24^o	30.07^o
SAG Commanded Angle	174.17^o	174.17^o	181.55^o	180.76^o

Step (a) Sun at $azimuth = 70^o$ and $elevation = -2^o$ is defined.
Step (b) The new orientation of SAG produces shadow on the CSS2.
Step (c) Noise is introduced on solar sensors in the form of Earth's Albedo.
Step (d) The new orientation of SAG amplifies the error on Sun determination.

6.6 Scenario 4: Investigation of on-board Sun determination precision and its impacts on controlling spacecraft attitude

It is learned from the previous case studies that the error on Sun determination overcomes four degrees when only two solar sensors are being illuminated by the Sun. Based on this fact, a system designer might wonder: *What would be the impact of Sun determination error when manoeuvring the spacecraft towards the Sun? Would the solar panel attitude influence on this manoeuver? Is there any preferred strategy for orienting the panel in this control mode?*

To answer these questions and other hypothesis related to the effects of Sun determination algorithm on the attitude control, the first step is to better understand the geometry of the problem, at the time an attitude manoeuvring from Nadir pointing to Sun pointing is performed. *Is there any situation in which the satellite is nominally pointing to the Nadir and there are two solar sensors being obscured by the solar panels? In addition to that, will these sensors remain on shadow during a manoeuvre to point the X body axis to the Sun?*

One possible configuration for these conjectures is depicted by the scheme in Figure 6.24, in which the Sun pointing manoeuvring would require a spacecraft rotation around its axis Z. Taking these configuration as the bounding conditions

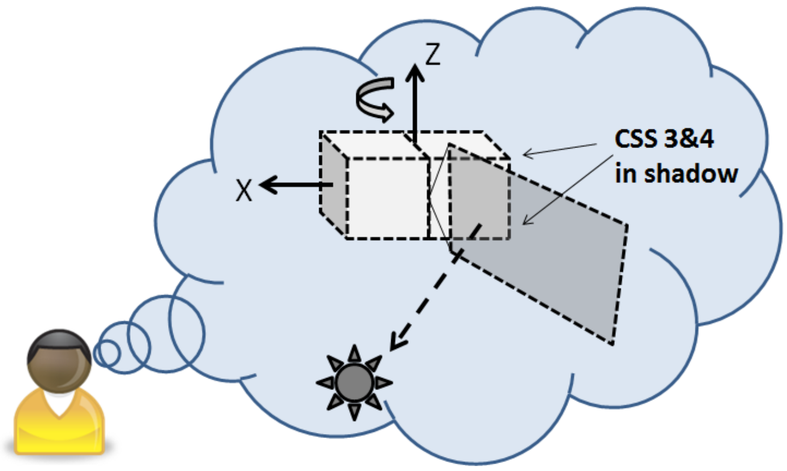

Figure 6.24 - Scheme of target geometrical configuration for investigation of control behaviour when manoeuvring from Nadir to Sun pointing.

for the simulation, the performance of attitude control algorithm could be compared in multiple conditions, i.e., with manifold strategies for orienting the solar panels (fixed or not), different torque profile of actuators, and constraints or failure applied to the coarse solar sensors.

Thus, during the evolution of the simulation, the typical interaction made by the engineer would include the steering of the following parameters:

- Solar panel orientation: force to an arbitrary attitude, bypassing the commanded value from the on-board software; change the dimensions of the structure;
- Earth's Albedo: injection of a vector with different levels of intensity;
- Attitude control: command a different mode and target; change the gains;
- Orbit: change on Keplerian elements, forcing a geometry configuration (e.g. eclipse, period, angle of the Sun);
- Sun position: alter the direction and distance of the Sun;
- Eclipse: force the satellite to be always illuminated or in the shadow;
- Shadow masks: change the azimuth/elevation profile of shadow masks attached to the solar sensors; enable or disable masks;
- Attitude dynamics: inject perturbation torques;

- Sensors: inject noise and induce failures.

The state space search for configuring the scenario starts with a sequence of interactions to adjust the orbital parameters, using a custom 3D steering widget for visualising the *Keplerian* elements. Some steps in this process are highlighted in Figure 6.25, which starts with a polar LEO, in which spacecraft is aligned with the inertial frame of reference (Figure 6.25-a).

The first user interaction consists in commanding the satellite attitude to the Earth pointing mode. As a result, after a few seconds of simulation, the body's Z-axis is pointing to Nadir and the X-axis is aligned with the velocity vector, as seen in Figures 6.25 *a* and *c*.

The adopted strategy for achieving the desired geometry from the Figure Figure 6.24 is to adjust the orbit and place the satellite in a position that its Z-axis is perpendicular to the Sun vector. The first attempt has brought the satellite close to the North Pole, but after steering the orbital parameters (Figure 6.25-d) it is observed that the satellite comes into an eclipse region (Figure 6.25-e/f). Thus, again using the 3D widget ((Figure 6.25-g), the orbit is changed to place the satellite close to the South Pole (Figure 6.25-h). Even though the angle between Sun Vector and Z-axis is close to the desired configuration, some refinements in the geometry are still required, so the final orientation of the Sun and solar panels produces shadows on two coarse solar sensors. This final adjustment is illustrated in Figures 6.25-j/k/l.

It is important to notice that as the simulation keeps running and the satellites orbits the planet, this geometrical arrangement will dismantle. Hence, for the sake of future scenario reconstruction, a snapshot is recorded to preserve the simulation state and restore the initial conditions of the scenario.

In the next sections, this snapshot is used to restore the initial conditions of the scenario just before the manoeuvring from Nadir to Sun pointing is commanded, so the effect of different environmental conditions and controlling strategies can be compared. The Table 6.6 summarises the configuration of eight scenes configuration for assessing the manoeuvring behaviour, in which the following parameters have been experimented [8]:

[8]The scenario results are also documented in the video available in the following link: `http://urlib.net/8JMKD3MGP5W34M/3H56LQH/Section6.6_Scenario4.wmv`.

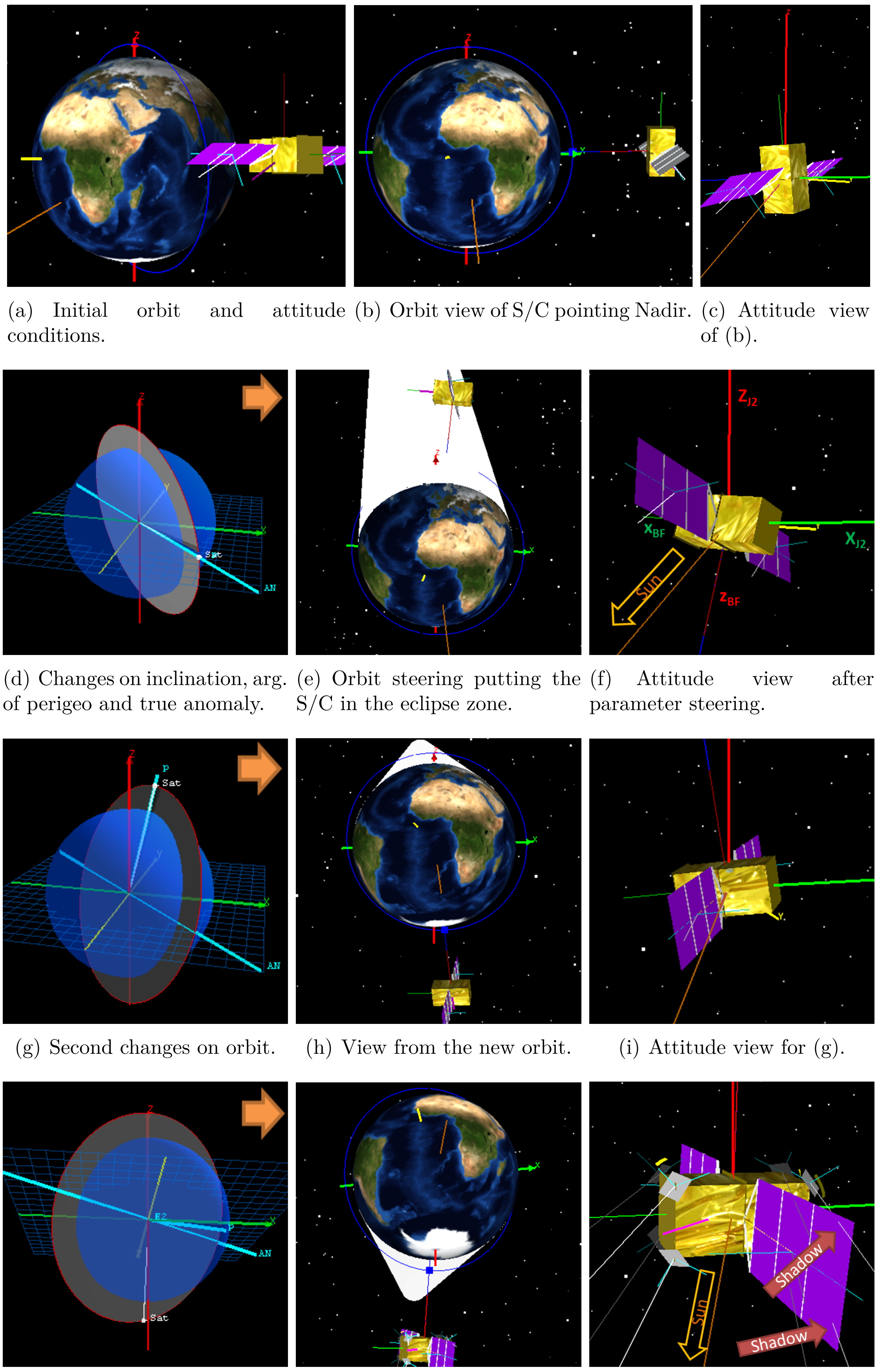

(a) Initial orbit and attitude conditions. (b) Orbit view of S/C pointing Nadir. (c) Attitude view of (b).

(d) Changes on inclination, arg. of perigeo and true anomaly. (e) Orbit steering putting the S/C in the eclipse zone. (f) Attitude view after parameter steering.

(g) Second changes on orbit. (h) View from the new orbit. (i) Attitude view for (g).

(j) Final orbit adjustments. (k) Final orbit view. (l) Obtained attitude geometry.

Figure 6.25 - Orbital parameters steering for searching to a simulation state to comply with the geometrical configuration from the Figure 6.24.

Table 6.6 - Parameter variation for comparing nine scenarios of Nadir to Sun pointing manoeuvring.

#	SAG Orient.	Torque Limit	CSS Min. Elev.	CSS Failure
a	$\sim 180^o$ (auto)	Unlimited	0^o	none
b	90^o (fixed)	Unlimited	0^o	none
c	180^o (fixed)	Unlimited	0^o	+X+Y-Z
d	180^o (fixed)	5Nm	0^o	+X+Y-Z
e	$\sim 180^o$ (auto)	5Nm	0^o	none
f	90^o (fixed)	5Nm	0^o	none
g	$\sim 180^o$ (auto)	Unlimited	20^o	none
h	$\sim 180^o$ (auto)	5Nm	20^o	none

- **SAG Orientation**: due to the geometrical arrangement, it is likely that two solar sensors stay in shadow when the panel attitude is automatically commanded. Thus, different attitude configurations are investigated to better understand the effects of the shadows.

- **Torque limitation**: currently the controlling strategy applies ideal torques to the plant and no actuators have been modelled. Designing the controller is out of scope of this scenario, but it would be interesting to see on the manoeuvring trajectory when the applied torque is limited to a certain value.

- **CSS Minimum Elevation**: so far, the performance of solar sensors is ideal, producing outputs without noise and for any positive elevation of the Sun. In practice, small elevations are too noisy and should be discarded by the Sun determination algorithm, since the Sun incidence is closely aligned to the sensor's plane. For this reason, the effects of a minimum elevation should be analysed.

- **CSS Failure**: the impact of a single solar sensor failure is investigated. The failure is injected by applying a bias to its output current, making its value equal to zero.

6.6.1 Scene 1: manoeuvre *a*

The trajectory of the first Sun pointing manoeuvre is illustrated by the sequence of images in Figure 6.26. In the beginning of the attitude correction (at simulation time=314s), the shadow of +Y solar panel on two sensors cause the error on the

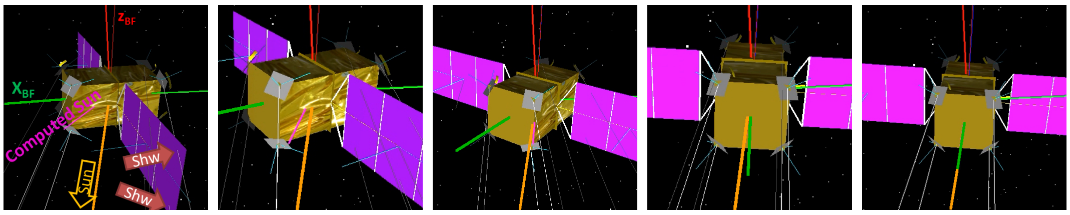

(a) $t = 314s$ (b) $t = 316s$ (c) $t = 317s$ (d) $t = 322s$ (e) $t = 330s$

Figure 6.26 - Evolution of Sun pointing manoeuvre representing 16 seconds of simulation time.

computed Sun to be higher than 20^o. Although this error is big, the computed direction of manoeuvre remains coherent and as the X-axis is aligned towards the Sun, this error is gradually reduced (Figure 6.26-b). During the Z-axis rotation, both -X+Y+Z and -X-Y+Z solar sensors remain on the shadow, however at simulation time 317s the Sun determination error decreases close to zero, because two new solar sensors become illuminated by the Sun (Figure 6.26-c). As a consequence, the maximum overshooting in the movement is not significant (Figure 6.26-d) and due to the ideal controller that applied unlimited torque in the plant, the whole manoeuvre is performed in a few seconds (Figure 6.26-e).

The behaviour of the controller and the performance of Sun determination algorithm can be easily observed with the animation provided in the 3D scene. Even though, complementary information is given in Figure 6.27, in which the profile of attitude quaternion, commanded torque, sun determination error, number of illuminated solar sensors, and sun pointing error can be compared as the simulation time evolves.

6.6.2 Scene 2: manoeuvre *b*

In this second configuration, the attitude of solar panels is fixed in 90^o, so four solar sensors are illuminated by the Sun during the whole trajectory of manoeuvre. From the Figure 6.28 it can be observed that the Sun determination error is reduced close to zero from the very beginning of the simulation. Still, due to the unconstrained level of torque applied in the control, the total time elapsed for performing the attitude correction is nearly the same from the previous configuration.

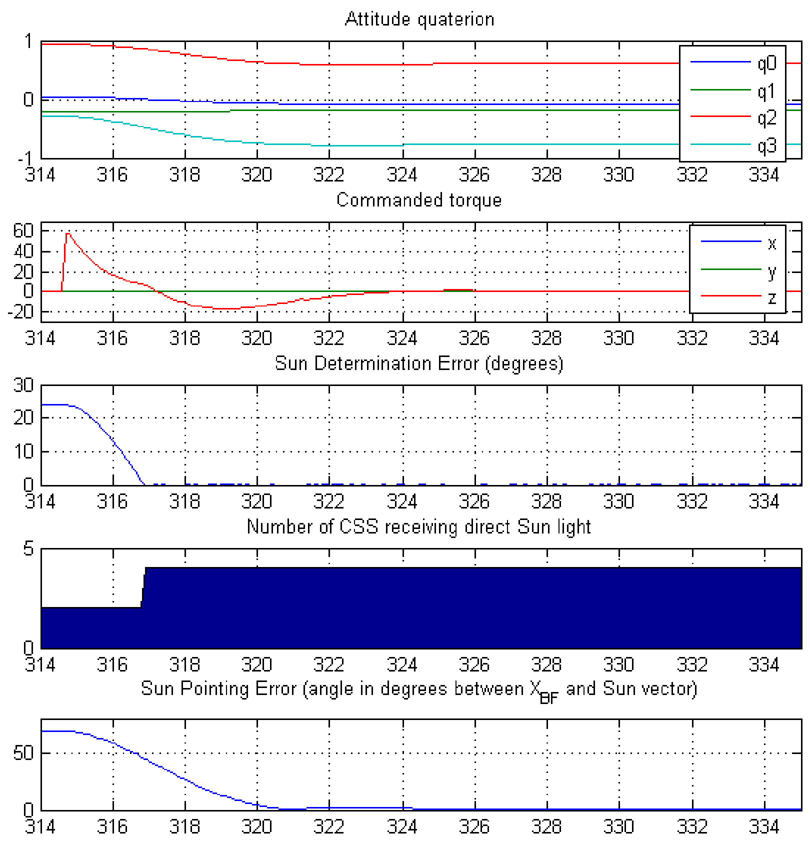

Figure 6.27 - Behaviour of Sun pointing manoeuvre *a* (*SAG Orient.*=180^o; *Torque=unlimited; CSS Min. Elev.*=0^o; *none CSS Failures*).

6.6.3 Scene 3: manoeuvre *c*

In this configuration, a failure is injected in the solar sensor +X+Y-Z, resulting in a spurious output from Sun determination algorithm, since only one sensor is being illuminated by the Sun in the beginning of the manoeuvre. As observed from the Figure 6.29, the direction of the computed Sun will force the attitude correction to a wrong direction.

Nevertheless, the curves in Figure 6.30 show that even the Sun determination error starts high, as the attitude of spacecraft changes, additional solar sensors become illuminated by the Sun and the error decreases. As a result, the controller rapidly corrects the trajectory to the direction of the simulated Sun. This recovery is clearly seen after the simulation time has reached 316s, when the number of illuminated sensors increase, the Sun determination error decreases and the commanded torque changes axes. Again, the short duration of manoeuvre is related to the unlimited torque applied in the dynamics.

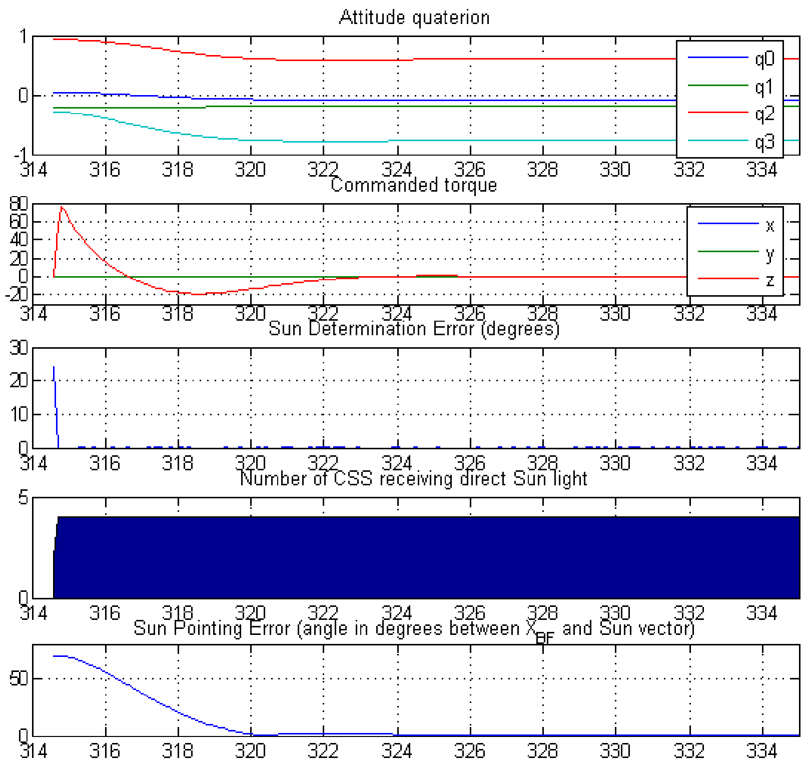

Figure 6.28 - Behaviour of Sun pointing manoeuvre *b* (*SAG Orient.*=90^o*; Torque=unlimited; CSS Min. Elev.*=0^o*; none CSS Failures*).

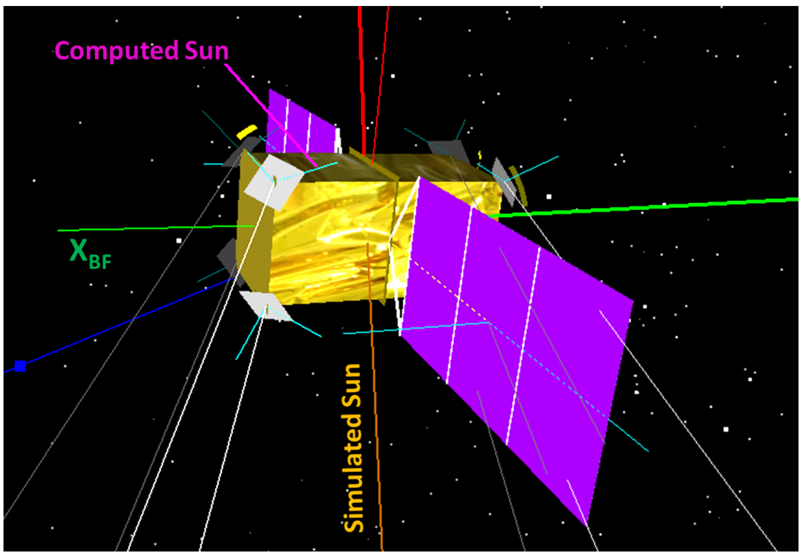

Figure 6.29 - Sun determination error when a failure is injected in solar sensor +X+Y-Z.

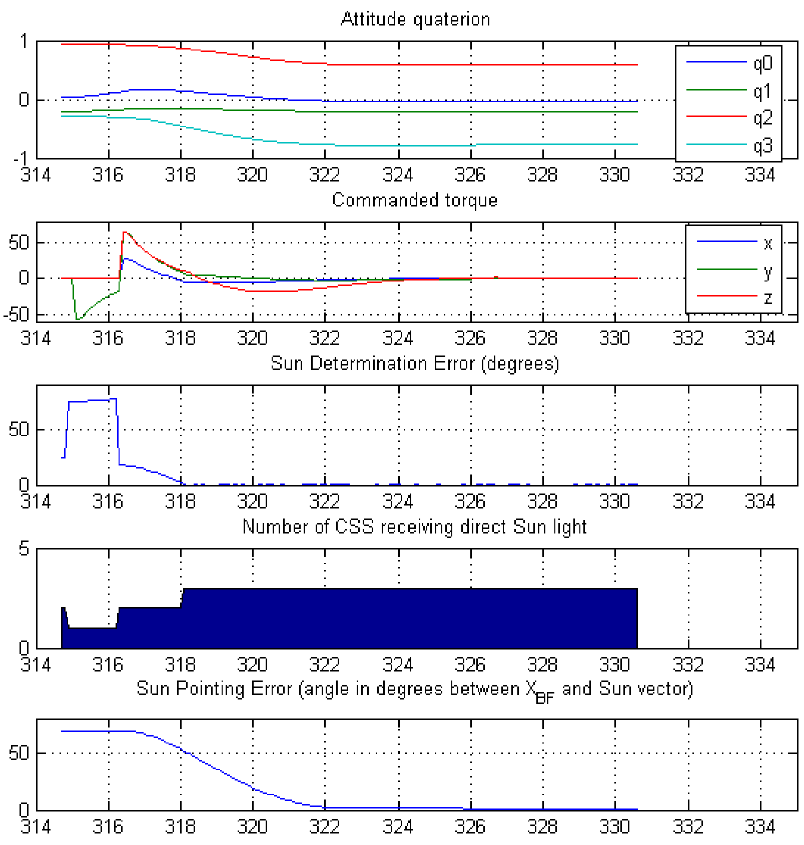

Figure 6.30 - Behaviour of Sun pointing manoeuvre *c* (*SAG Orient.*=180^o; *Torque=unlimited; CSS Min. Elev.*=0^o; *Failure applied to +X+Y-Z sensor*).

6.6.4 Scene 4: manoeuvre *d*

Complementing the analysis of the previous configurations, a limit of 5Nm is applied to the norm of the commanded torque vector. As expected, with smaller torques being introduced in the plant, the pointing convergence takes longer and the overshooting is higher (Figure 6.31).

6.6.5 Scene 5: manoeuvre *e*

A similar behaviour of overshooting is observed when limiting the torque and removing the failure on the solar sensor, as seen in Figure 6.32. Although, since the manoeuvre now starts to the right direction, the total time required to stabilise the attitude is smaller.

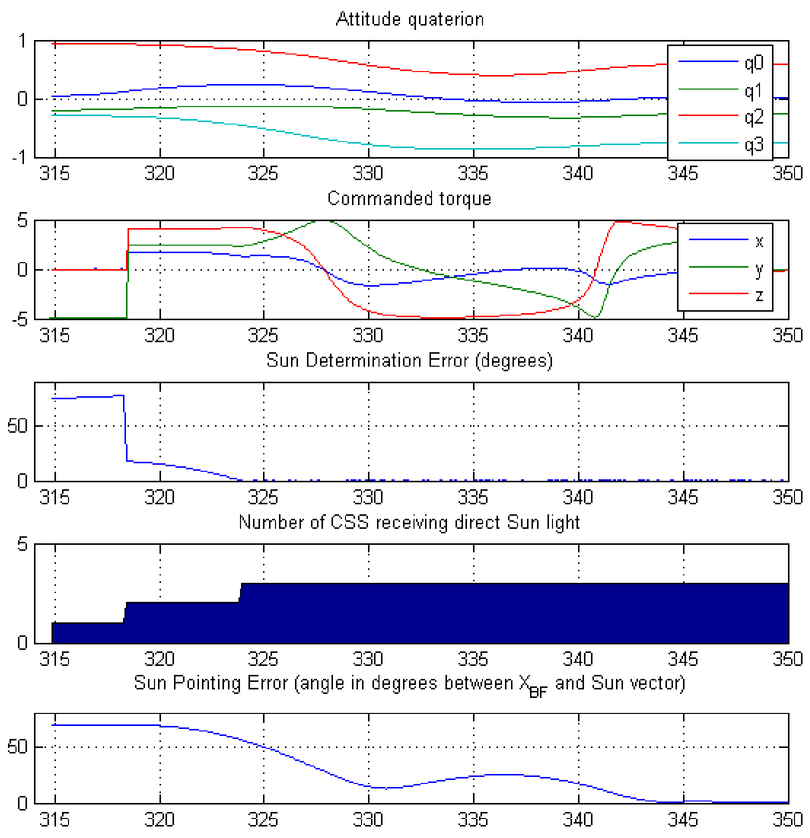

Figure 6.31 - Behaviour of Sun pointing manoeuvre *d* (*SAG Orient.*=180^o; *Torque=limited to 5Nm; CSS Min. Elev.*=0^o; *Failure applied to +X+Y-Z sensor*).

6.6.6 Scene 6: manoeuvre *f*

This addition simulation with torque limitation is done to compare the behaviour of the systems when the solar panels are 90^o oriented and four sensors are used to compute the Sun versor on-board. The observed overshooting is basically the same, which indicates that in these cases an adjustment of controller's gains would be necessary (Figures 6.33 and 6.34).

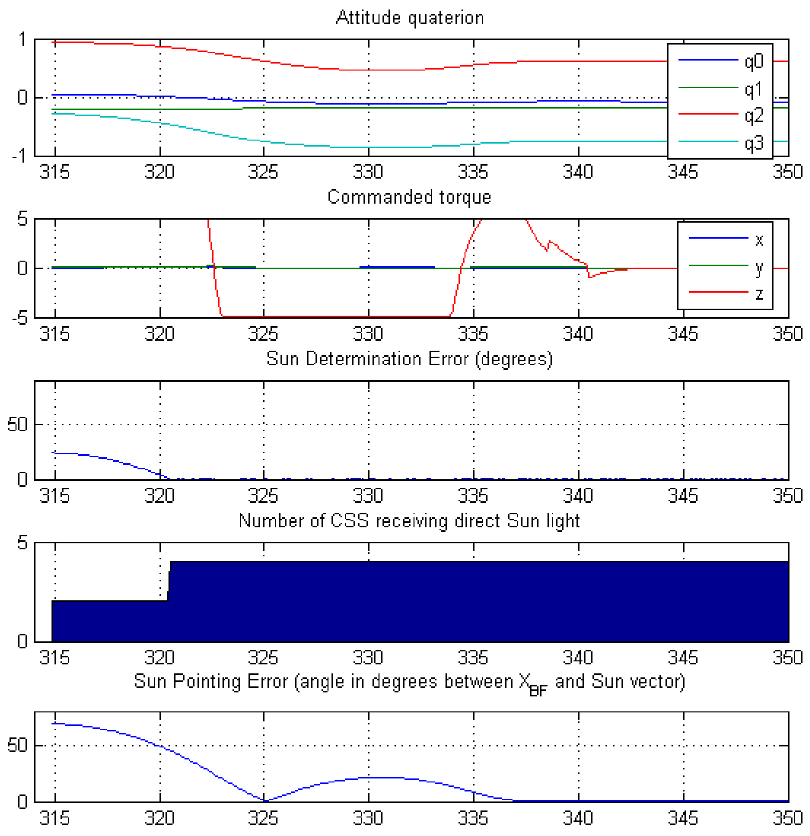

Figure 6.32 - Behaviour of Sun pointing manoeuvre *e* (*SAG Orient.*=180^o; *Torque=limited to 5Nm; CSS Min. Elev.*=0^o; *none CSS Failures*).

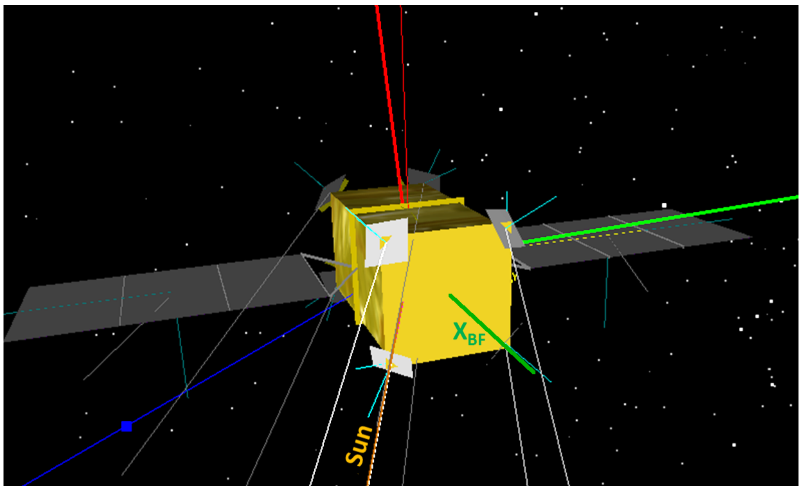

Figure 6.33 - Instant of maximum overshooting when performing a Sun pointing manoeuvre with limitation on applied torque.

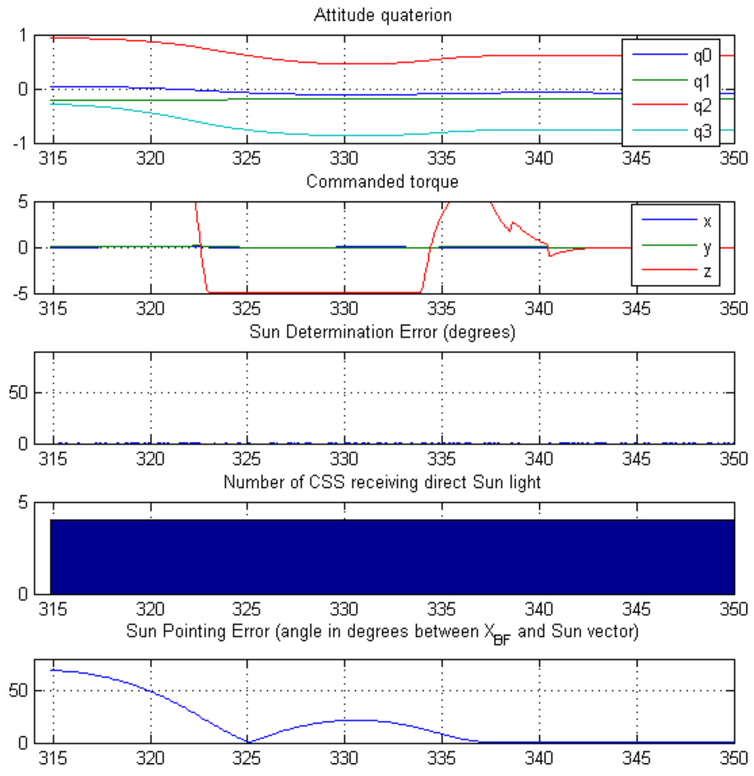

Figure 6.34 - Behaviour of Sun pointing manoeuvre *f* (*SAG Orient.*=90^o; *Torque=limited to 5Nm; CSS Min. Elev.*=0^o; *none CSS Failures*).

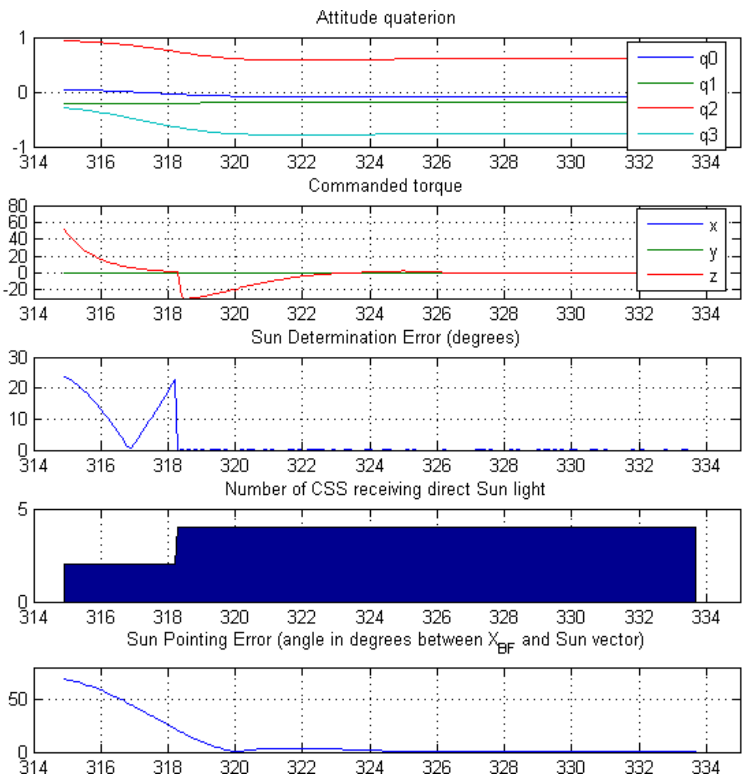

Figure 6.35 - Behaviour of Sun pointing manoeuvre *g* (*SAG Orient.*=180^o; *Torque=unlimited; CSS Min. Elev.*=20^o; *none CSS Failures*).

6.6.7 Scene 7: manoeuvre *g*

In this configuration, an elevation mask of 20^o is configured for all coarse solar sensors. As an effect, it takes longer for four sensors be used on Sun determination, during the manoeuvre. As it can be seen in the curves from the Figure 6.35, the sun determination error even increases after 317s and only when four sensors are used (after 318s), the controller starts to break the satellite commanding a $-Z$ torque. Still, the total time required to point the spacecraft to the Sun is small due to the application of unlimited torque.

6.6.8 Scene 8: manoeuvre *h*

In this last analysis of Sun pointing manoeuvre, the torque is again limited to 5Nm and the 20^o elevation mask is applied to the solar sensors, complementing the previous run. In this case, the overshooting in Figure 6.36 is clearly greater than the configuration from configuration in item 6.6.5, in which the torque limit is applied, but no elevation mask is used. It is explained by the delay on using four sensors to determine the Sun, increasing the error and making the controller to decelerate the

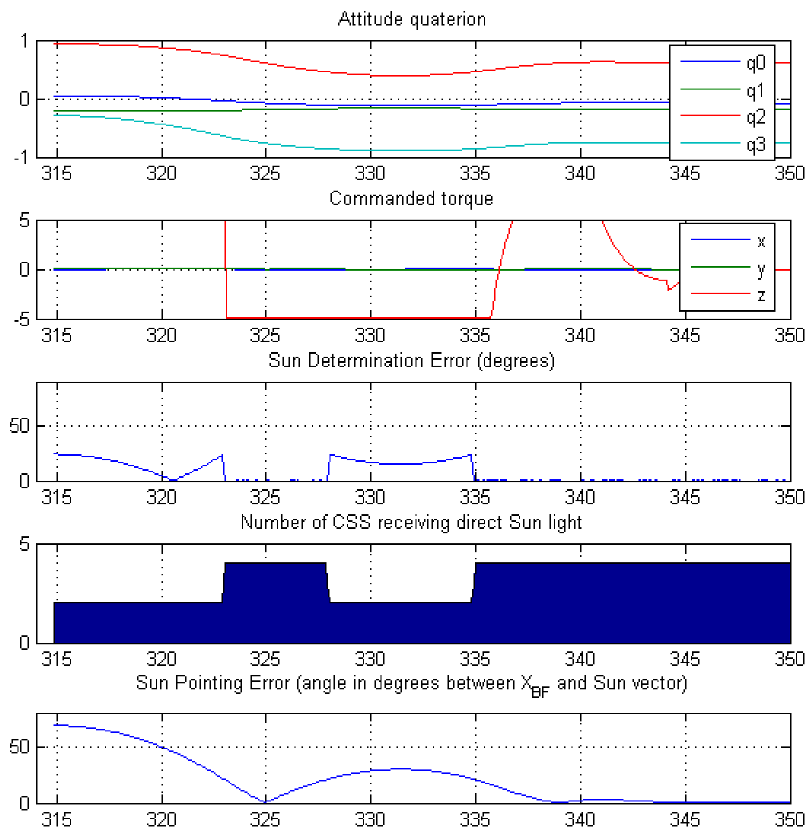

Figure 6.36 - Behaviour of Sun pointing manoeuvre *h* (*SAG Orient.*=180^o; *Torque*=*limited to 5Nm; CSS Min. Elev.*=20^o; *none CSS Failures*).

spacecraft later.

The 3D scene in Figure 6.37-a indicates how the Sun determination error influences the overshooting in the controller, by providing it with a imprecise reference. A similar effect happens when the controller starts to correct its position back, rotating the spacecraft along -Z-axis (Figure 6.37-a).

6.7 Scenario 5: Steady State Analysis

After the features and behaviour of Sun pointing manoeuvre has been investigated, another point of interest is the control stability of the platform against environmental perturbations and equipment failure. To demonstrate the flexibility of computation steering facility, in this scenario three types of user interactions are done in the running simulation: (1) introduction of noise in the solar sensors in the form of Earth's Albedo; (2) injection of perturbation torque in the platform; and (3) failure injection in two solar sensors. The simulation results for these three cases are presented next.

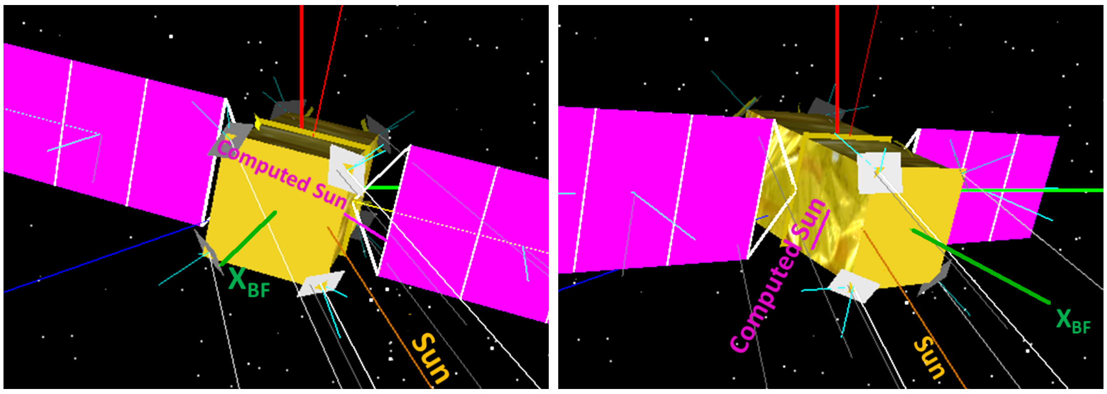

(a) (b)

Figure 6.37 - Overshooting in the manoeuvre caused by the imprecise on-board determination of Sun, when a elevation mask of 20^o is applied to the solar sensors.

6.7.1 Scene 1: Albedo Noise

For injecting an arbitrary vector representing Earth's Albedo, the engineer can use a 3D vector widget and scale it accordingly to the desired level of reflected light. In the current simulation, a level of $100W/m^2$ has been used, which introduces a direct error on Sun Determination algorithm and consequently causes an equivalent bias in the attitude control. The Figure 6.38 shows three instants when the Albedo vector is redefined. After it is removed, the attitude error decreases near zero.

6.7.2 Scene 2: Perturbation noise

Differently from the previous type of noise, the insertion of an external torque makes the controller to constantly compensate the forces. For injected torques smaller than 2Nm, the Sun pointing error is kept under 2^o, as seen in Figure 6.39.

6.7.3 Scene 3: Solar Sensors failure and recovery

The last investigation on the attitude control stability comprises on gradually failing coarse solar sensors that are being used to compute the direction of Sun. From the results presented in Figure 6.40, it can be observed that the algorithm is robust for a single failure, but the pointing accuracy cannot be maintained when a second failure occurs. Still, in the case the failure disappears (e.g. a redundant equipment is switched on), the attitude control is recovered.

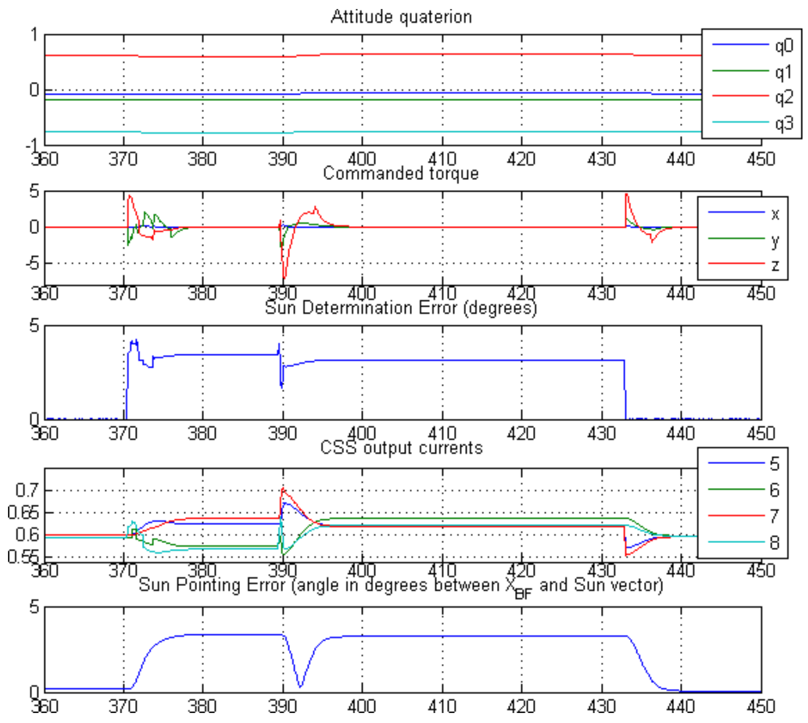

Figure 6.38 - The effects of noise insertion in the solar sensor models in the form of Earth's Albedo in the attitude control.

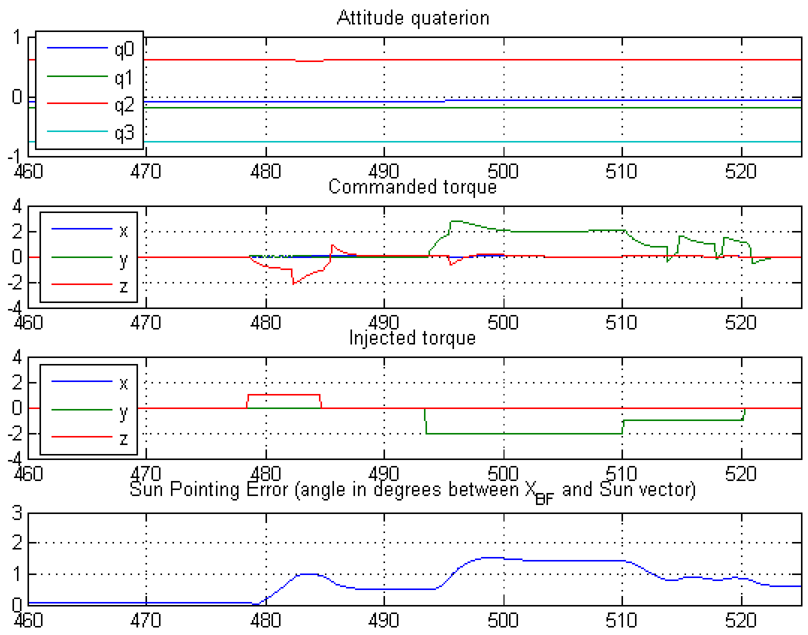

Figure 6.39 - The effects of external torque insertion in the attitude control.

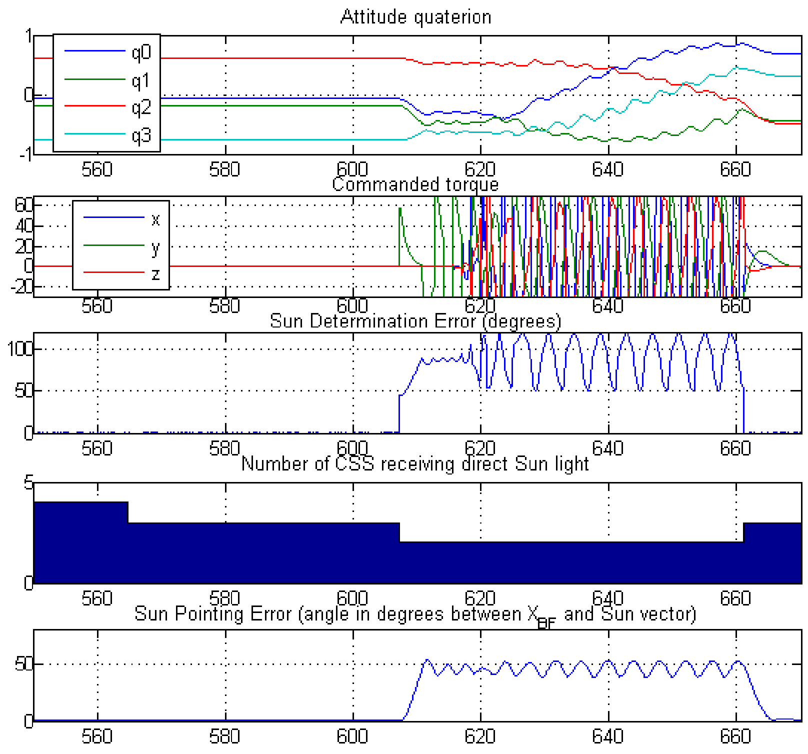

Figure 6.40 - The effects of failures on 1 and 2 solar sensors in the attitude control.

6.8 Scenario 6: Hardware-in-the-loop simulation for assessing the performance of the embedded attitude controller

In the current demonstration, the on-board software models are replaced in the simulation environment by an interface component that communicates with an external hardware (i.e. the `ObcIF` model). This independent device executes an embedded version of the Sun determination algorithm, bapta control and attitude control algorithms, which communicates with the simulation facility in soft real-time through a serial channel. By closing the simulation loop with a hardware representing the on-board computer, the performance of the flight software can be evaluated in a more realistic environment and effects such as signal propagation delays and precision of floating point representation can be analysed. The computational steering interface is still valid for controlling the model parameters which are not embedded in the hardware. The results of a typical scenario execution is given in Figure 6.41. In this example, the user injects perturbation torques in the beginning of the simulation to put the spacecraft in a tumbling state, using a gestures interpretation interface described in the Appendix C.

At the instant 60s the controller is commanded to stabilize the platform and point the spacecraft to the Sun. In this moment, it can be observed that the commanded torque has a typical staircase profile due to the fact that the execution cycle of the embedded controller is set to 1 second. The delay on the communication and the discretization of the torque signal increases the overshooting effect in the manoeuvre, but eventually the pointing error converges close to zero. In the graphical animation this slower convergence is clearly observed, even when an unlimited torque is applied in the dynamics. A similar behaviour is seems when the Nadir pointing mode is commanded around the simulation time 90s. Since in this mode the control is done in three-axes, the convergence is even slower.

6.9 Scenario 7: Comparison of potential scenarios to support test case specification

The focus in this case study is to analyse the spacecraft attitude in the end of a simulation, as a consequence of changes imposed to the computational model along the scenario evolution. The comparison of the final simulation state is supported by a *historic tree* service that manages the creation of scenario branches based on user interventions. Hence, in this section, the performance of an attitude control subsystem that orients the spacecraft towards the Sun is verified in various environmental and operational circumstances, which represents, for instance,

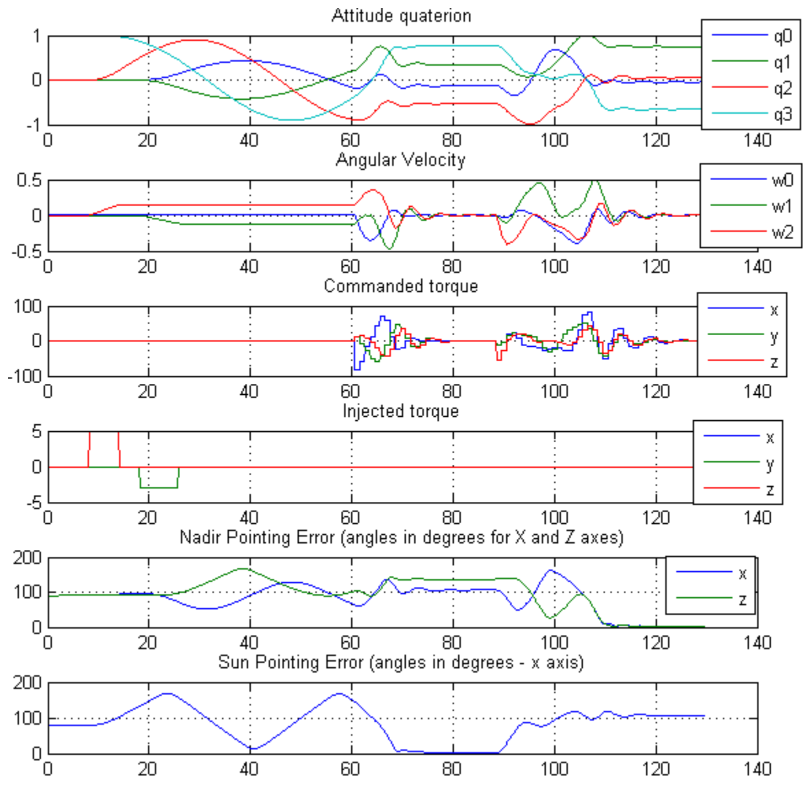

Figure 6.41 - Manoeuvre profile for pointing the spacecraft to the Sun and then to the Nadir, using a controller embedded in a distributed hardware platform.

different deployment conditions that the controller has to deal with.

Each test conducted by the engineering comprises a 300 seconds simulation that starts with the same initial conditions. After processing, the data is reloaded and executed in playback mode for visual analysis. Then, from any point in the historical data, the user may decide to restore the simulation from a snapshot and derive the scenario into a new test case branch, in which additional adjustments can be applied. In the context of a detumbling and Sun acquisition application, typical verifications that need to be carried out by the specialist include the variation of initial orientation and body rates, status of sensors and actuators, orbital position, and illumination conditions, among others.

In this scenario, the baseline configuration has been adjusted to include the model representing a set of three reaction wheels (RW), which are orthogonally arranged. The links among the models that close the loop of attitude dynamics are defined in the Figure 6.42. It is observed int this assembly that the commanded torque is sent to the RWs that compute the actual torque applied in the plant and their angular momentum. By default, every RW produces a maximum torque of 0.5 Nm and their

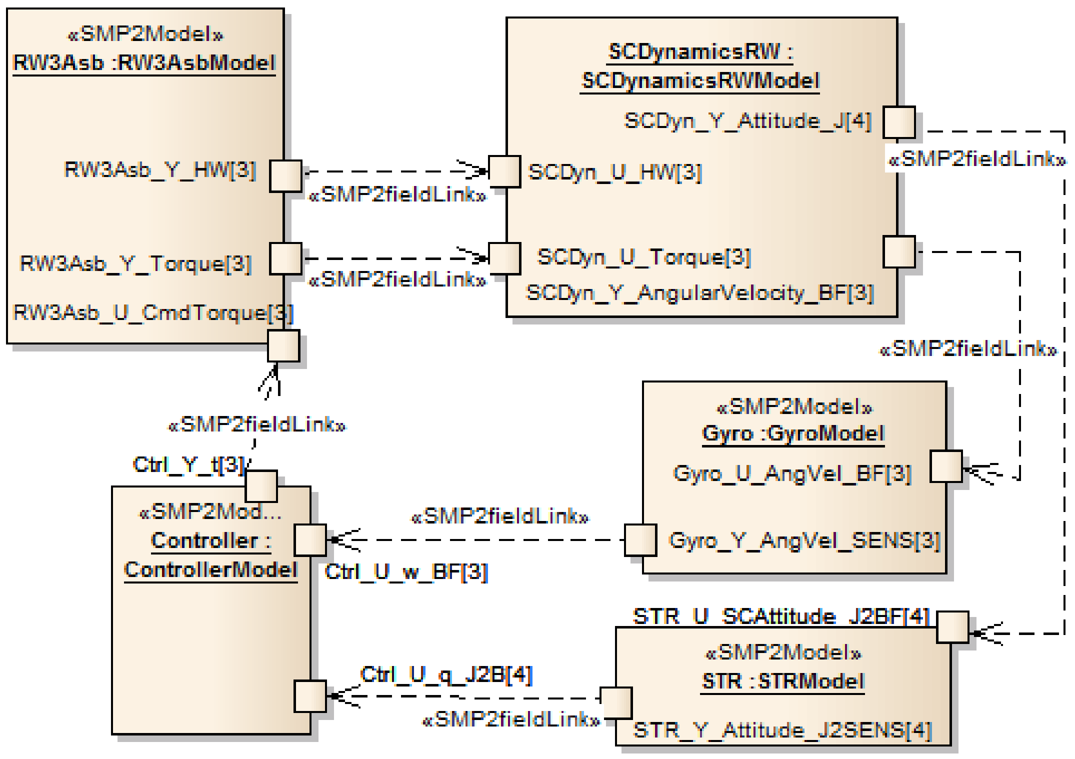

Figure 6.42 - Updated simulation assembly with reaction wheels models closing the attitude dynamics loop.

speeds are limited to 6000 revolutions per minute (RPM). At $t = 4s$, the controller is switched to point the spacecraft X-body axis to the Sun.

The complete set of branches generated in this study is described in the Table 6.7. The root node is a reference scenario that orients the satellite in about $90s$, whose execution is performed with a default configuration and without user intervention. Based on these results, the specialist derives new scenarios to test additional hypotheses. For example, in the first level derivation (i.e. 0.1), the satellite attitude is steered to verify the manoeuvre behaviour beginning from a different initial orientation. The branch creation is only limited by the system memory and hence a historical tree of multiple levels can be defined.

For each branch listed in the Table 6.7, the test goals are presented together with the adopted steering strategy and a brief description of the obtained results. During the simulation playback, the manoeuvre trajectory is analysed from the 3D attitude animation, but here the Sun pointing error evolution can be compared in the curves provided in the Figure 6.43 and Figure 6.44.

Table 6.7 - Description of test cases executed in the scenario branches and observed results.

Scenario	#	**Test case**	**Steering Actions**	**Results**
0.0	0	Reference scenario	None	Attitude converges in about 90s.
0.1	1	New initial orientation, in which the X-body axis is aligned with the orbital velocity vector.	Set q	Attitude converges slightly faster when compared to the reference scenario.
0.1.1	2	Same orientation as (1), but now with a residual angular velocity along X (e.g. imposed by the launcher).	$w_x = 0.8$ (7.6 RPM)	The overshooting are smaller but the convergence takes longer.
0.1.2	3	Same orientation as (1), but now with a residual angular velocity along $-Y$.	$W_w = -0.8$ (7.6RPM)	Could not converge within the horizon.
0.1.2.1	4	Adjust the controller gain to improve convergence.	Set gain = 1000.	Converges but a noise is observed.
0.1.2.2	5	Reduce the controller's gain.	Set gain = 500.	Converges faster.
0.2	6	Set initial orientation to point X-body axis to the opposite direction of the Sun.	Set q.	As expected, the convergence takes longer than ref. scenario.
0.2.1	7	Inject a residual angular velocity along X.	$W_x = 0.8$ (7.6RPM)	The rates are dumped and the body is oriented towards Sun, but in the end of the simulation the error was still > 36 degrees. RW reached $RW_x = -1500$ and $RW_y = 1600$ RPMs.

(Continued...)

Table 6.7 - Continued

Scenario	#	**Hypothesis**	**Steering Actions**	**Results**
0.2.1.1	8	Adjust the controller gain to improve convergence.	Set gain = 500.	Converges, but RW reached $RW_x = -1900$ and $RW_y = 2200$ RPMs.
0.2.1.1.1	9	Increase the speed of RW_x to force its saturation and see if the controller enters in stand-by mode.	$RW_x = -5000$ RPM)	The controller becomes unstable, because it keeps commanding the other wheels, thus accelerating the platform indefinitely. A protection in the OBSW should be implemented.
0.2.1.1.2	10	Instead of saturating the RW_x, just freezes its speed.	Freeze RW_x	The platform has almost stabilized, but the convergence was not possible. A redundant RW should be used.
0.2.2	11	What is the effect of saturating a RW in the middle of the manoeuvre?	In the instant 30s, when the controller is using most the RW_y, it is saturated.	The controller keeps commanding RW_y but the S/C remains nearly stable.

(Continued...)

Table 6.7 - Continued

Scenario	#	**Hypothesis**	**Steering Actions**	**Results**
0.2.3	12	And what if the S/C enters in eclipse in the middle of the manoeuvre?	At $t = 30s$ the eclipse condition is forced and restored 30s later.	Just after entering in eclipse, the controller is suspended. The S/C remains rotating around Y and the error increases. Back to light, the S/C is oriented to Sun.
0.2.4	13	What are the albedo effects to the manoeuvre?	Set albedo std=2. Place S/C over a strong reflectance area. (RAAN: 95^o, AP:-135^o)	The albedo model is recomputed at $t = 10s$, producing noise to CSS 5 and 8 and an error of 27^o in Sun Det. The attitude error is $> 36^o$ in the end of simulation.
0.2.4.1	14	During the manoeuvre, what is the effect of introducing noise in a CSS that is facing Earth?	At $t = 19s$ inject random noise ($\mu = 0.1$) and bias (0.2) in CSS_5.	The final attitude error increases to $> 50^o$.
0.2.4.2	15	What would be the results of a CSS assembly inversion (e.g. made in AIT)?	Swap CSS 1 and 6 signals	Final attitude error around 36^o
0.2.4.2.1	16	And if the albedo noise is removed but the inversion from (15) remains?	Cancel albedo at $t = 22.5s$.	The results are even worse than (15), since the attitude oscillates.
0.2.4.3	17	And if the inversion is done between CSS 7 and 8?	Swap CSS 7 and 8 signals	Final attitude error $> 40^o$

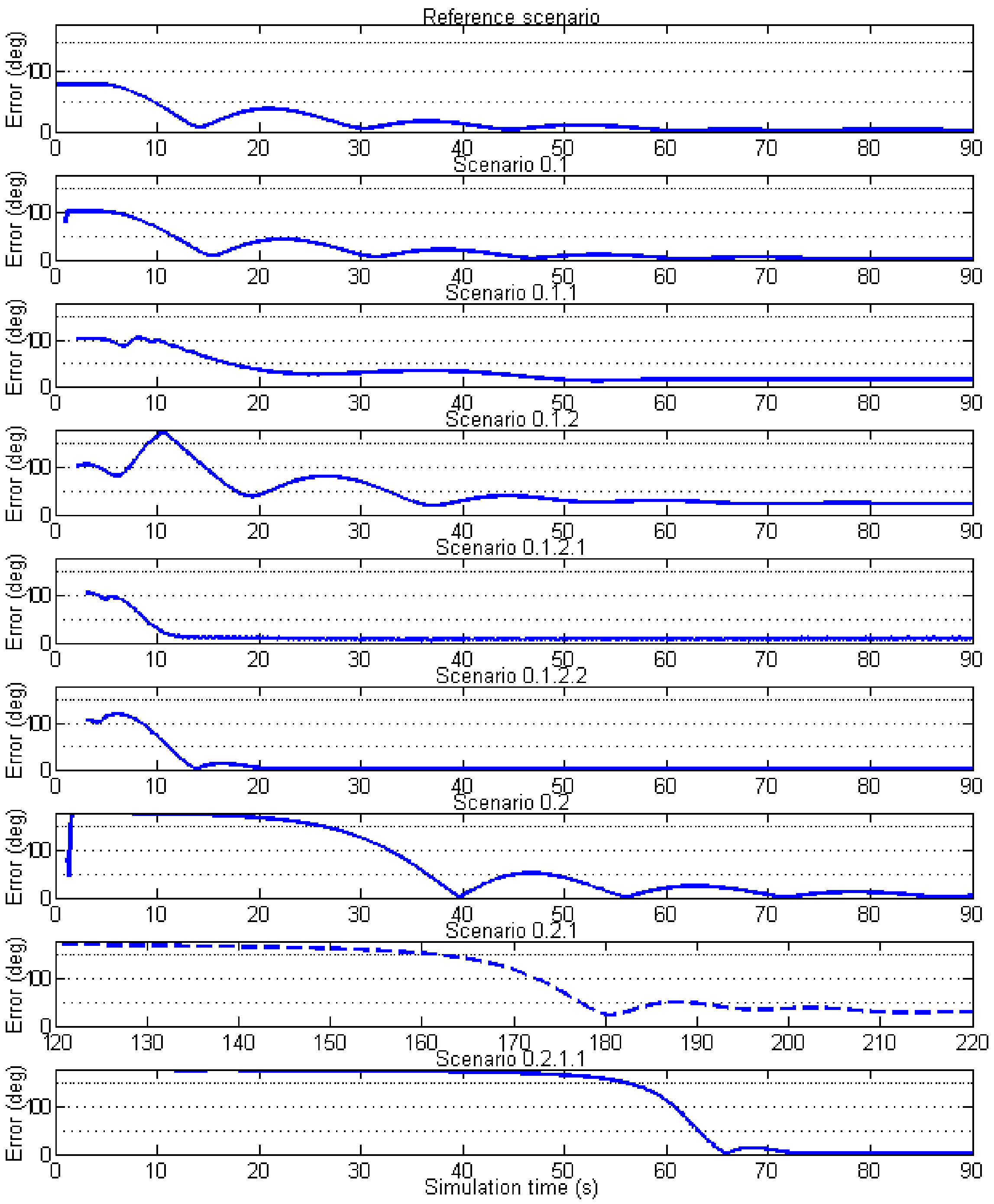

Figure 6.43 - Sun pointing error curves for the first half of scenario branches.

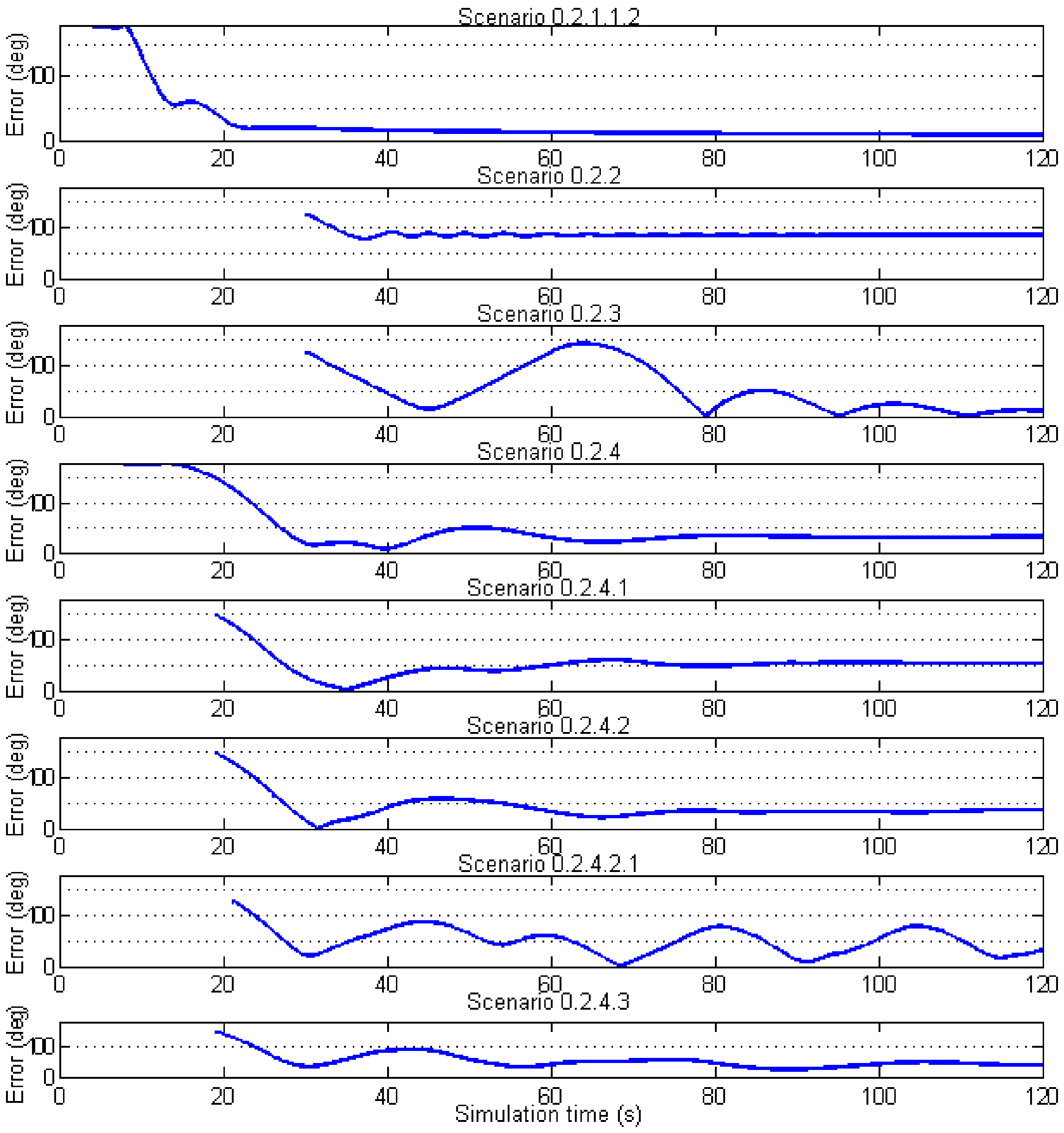

Figure 6.44 - Sun pointing error curves for the second half of scenario branches.

The full historic tree is illustrated in the Figure 6.45-a, wherein the derivations occurred until the instant $t = 4s$ represent the interventions applied before the manoeuvre start. An equivalent graphical representation is provided to the engineer for loading a path of historical data into the playback simulator, as depicted in the GUI in the Figure 6.45-b. After selecting a given node (e.g. 0.2.4.2.1), the parent nodes are automatically identified up to the root scenario and new derivations can be performed from different nodes, accordingly to the simulation interval they represent (e.g. from 0.2.4 if $t = 10s$).

In complement to the benefits of online intervention already shown in the previous case studies, the history tree and automatic snapshot mechanisms allow the generation of scenario ramifications and comparison of their evolution as a natural product of user's cognitive process. In addition to the verification of system behaviour against the baseline design, in the current demonstration the computational steering is presented as a pragmatic tool for specifying test cases and consolidating avionics validation plans, since this type of activities requires the examination of unlikely situations, though possible, in which a robust equipment must be prepared. In this direction, steering plays an important role on easing the understanding of the effects of singular configurations, thus guiding the definition of relevant test conditions.

Therefore, many other analyses could have been performed in this section, such as the power consumption of each manoeuvre or the stability of control during several orbits. Naturally, this approach is limited to the capacity of saving and restoring the whole computational state in the simulation environment, which may not be the case of some physical elements present in the scenario (e.g. the environmental temperature, the power level available for a device, or the OBC's operating mode). Still, in the case of a HITL setup, the history tree feature could be adopted if an automatic OBC reconfiguration functionality is available in conjunction to the snapshot mechanism.

6.10 Scenario 8: Sun determination algorithm experimentation

In most cases, steering the models parameters suffices for exploring the state space in a simulation scenario and analysing the behaviour of the modelled phenomenon. However, this type of user intervention may be limited when the internal parameters of a model have not been exposed to the simulation infrastructure or the whole logical structure of the algorithm needs to be modified.

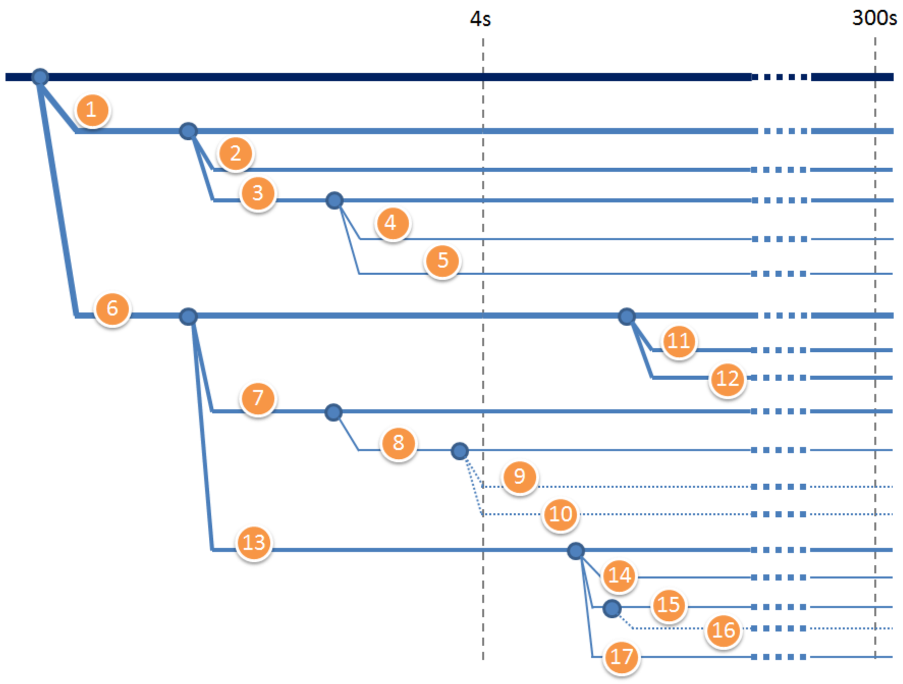

(a) General scheme.

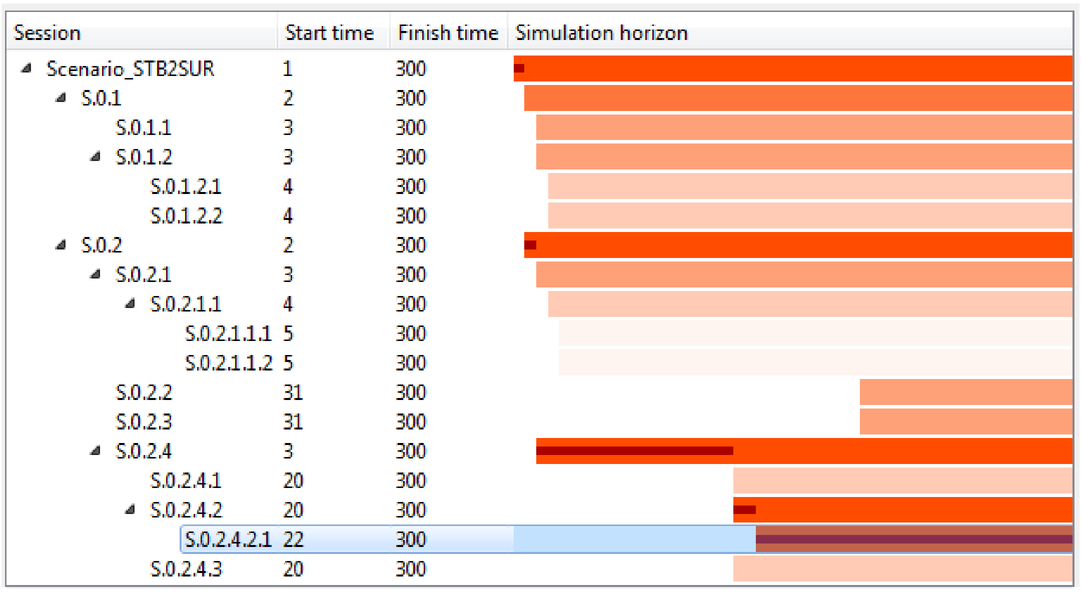

Session	Start time	Finish time	Simulation horizon
Scenario_STB2SUR	1	300	
S.0.1	2	300	
S.0.1.1	3	300	
S.0.1.2	3	300	
S.0.1.2.1	4	300	
S.0.1.2.2	4	300	
S.0.2	2	300	
S.0.2.1	3	300	
S.0.2.1.1	4	300	
S.0.2.1.1.1	5	300	
S.0.2.1.1.2	5	300	
S.0.2.2	31	300	
S.0.2.3	31	300	
S.0.2.4	3	300	
S.0.2.4.1	20	300	
S.0.2.4.2	20	300	
S.0.2.4.2.1	22	300	
S.0.2.4.3	20	300	

(b) GUI for playback loading.

Figure 6.45 - Historic tree representing the scenario branching.

This aspect of steering, when the model's source code itself can be modified or changed during the simulation execution, is called by many authors as *algorithm experimentation*. In the context of space engineering domain, this capability can be useful in many application that an algorithm requires to be debugged, corrected or tuned, or event to compare different computational approaches to address a given situation in the simulation, without the need to reset the scenario after every test.

In this section, this functionality is demonstrated by applying online modifications in the internal structure of the *Sun Determination* algorithm. Therefore, the original C++ implementation of that model is replaced by a wrapper code that invokes an external sun determination algorithm implemented in MATLAB®. Once the SMP2 interfaces of the `SunDet` model is preserved, the simulation assembly can be reused as is and the only difference from the baseline scenario is the interpretation of an *m–file* script, by the MATLAB engine (MATHWORKS, 2014), each time the model's update entry point is executed.

This interoperation with MATLAB needs no further modification in the simulation infrastructure and it has the advantage to allow changes in the script during the scenario execution from a simple text editor.

In the case of the Sun Determination algorithm, many adjustments can be applied, for instance, to analyse the effect of a current threshold on its performance, since it is known that small incident angles of light in the solar sensor's plane produces a noisy signal. Additionally, the whole script can be replaced to evaluate different types of algorithms.

Therefore, the steering facility setup illustrated in the Figure 6.46 is employed by the algorithm designer to assess the sun determination error when different elevation masks are configured in the algorithm. Further, the classical matrix inversion method is momentarily replaced by an artificial neural network algorithm [9] (HAYKIN, 1998). Attached to the simulation, two steering widgets allow the user to explore different configuration of the Sun incidence and inject arbitrary albedo vectors. As the Sun versor is continuously determined from the CSS currents, both simulated and computed positions are displayed in the 3D visualization system and the error is automatically calculated by a simulation monitor.

[9] In this demonstration, a multi-layer perceptron network containing 50 units in a single hidden layer has been employed. The network has been trained with the backpropagation algorithm using a training set of 860 CSS currents, randomly selected from a simulation of the spacecraft pointing to the Nadir from one day simulation. The total sum of squared errors in the output layer after the training was 0.0696 degrees.

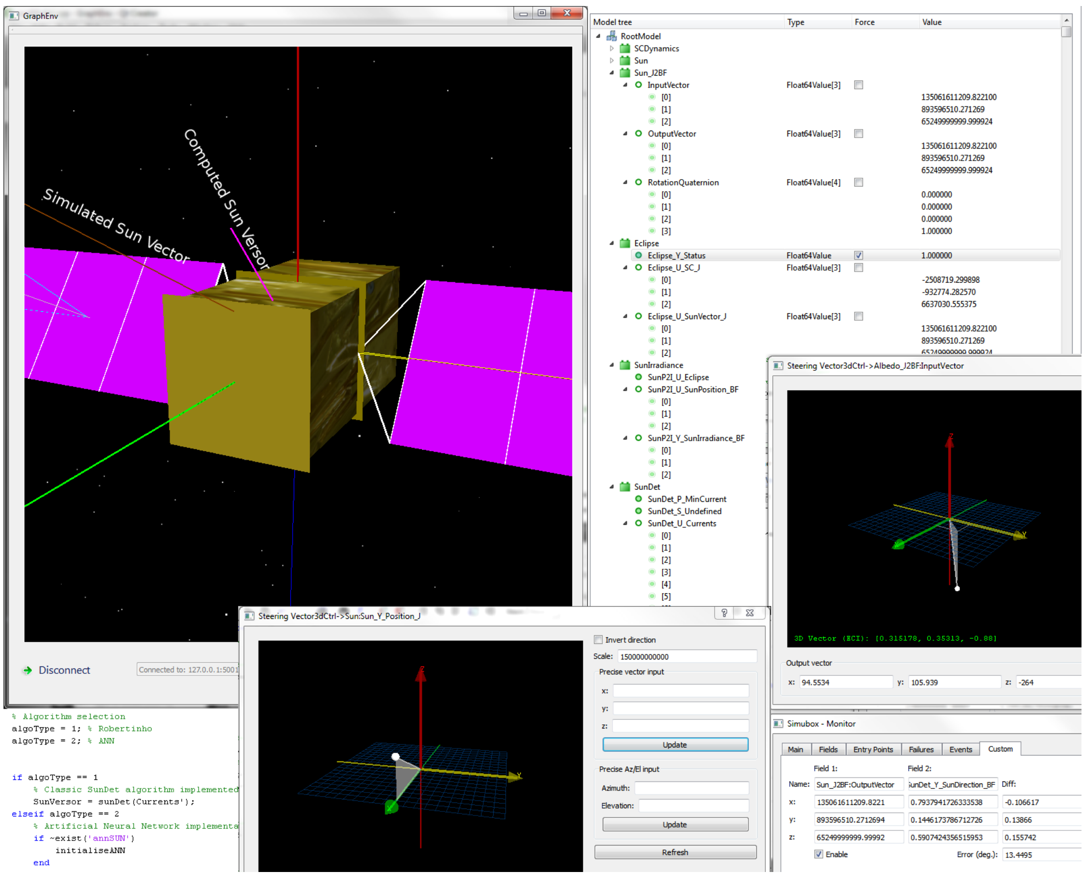

```
% Algorithm selection
algoType = 1; % Robertinho
algoType = 2; % ANN


if algoType == 1
    % Classic SunDet algorithm implemented
    SunVersor = sunDet(Currents');
elseif algoType == 2
    % Artificial Neural Network implementa
    if ~exist('annSUN')
        initialiseANN
    end
```

```
Model tree                    Type              Force   Value
RootModel
  SCDynamics
  Sun
  Sun_J2BF
    InputVector               Float64Value[3]   ☐
      [0]                                               135061611209.822100
      [1]                                               893596510.271269
      [2]                                               65249999999.999924
    OutputVector              Float64Value[3]   ☐
      [0]                                               135061611209.822100
      [1]                                               893596510.271269
      [2]                                               65249999999.999924
    RotationQuaternion        Float64Value[4]   ☐
      [0]                                               0.000000
      [1]                                               0.000000
      [2]                                               0.000000
      [3]                                               1.000000
  Eclipse
    Eclipse_Y_Status          Float64Value      ☑       1.000000
    Eclipse_U_SC_J            Float64Value[3]   ☐
      [0]                                               -2508719.299898
      [1]                                               -932774.282570
      [2]                                               6637030.555375
    Eclipse_U_SunVector_J     Float64Value[3]   ☐
      [0]                                               135061611209.822100
      [1]                                               893596510.271269
      [2]
  SunIrradiance
    SunP2I_U_Eclipse
    SunP2I_U_SunPosition_BF
      [0]
      [1]
      [2]
    SunP2I_Y_SunIrradiance_BF
      [0]
      [1]
      [2]
  SunDet
    SunDet_P_MinCurrent
    SunDet_S_Undefined
    SunDet_U_Currents
      [0]
      [1]
      [2]
      [3]
      [4]
      [5]
```

```
3D Vector (ECI): [0.315178, 0.35313, -0.88]
```

Output vector

x: 94.5534 y: 105.939 z: -264

	Field 1:	Field 2:	
Name:	Sun_J2BF:OutputVector	SunDet_Y_SunDirection_BF	Diff:
x:	135061611209.8221	0.7937941726333538	-0.106617
y:	893596510.2712694	0.1446173786712726	0.13866
z:	65249999999.99992	0.5907424356515953	0.155742

[✓] Enable   Error (deg.): 13.4495

Figure 6.46 - Computational steering facility for assessing different implementations of the Sun Determination algorithm.

The worst Sun determination errors observed during a simulation section are summarised in the Table 6.8. The algorithm begins with an ideal implementation that process all current signals coming from CSS, i.e. without minimum elevation filter. In that case, no significant error is observed if no albedo noise is injected. By applying a $300W/m^2$ albedo vector, the error increases up to 14.92 degrees.

As the algorithm is re-programmed to discard CSS readings bellow a minimum light incidence angle, the error gradually grows, reaching 38.48 degrees with an elevation mask of 30^o, with albedo interference. Still, in a particular case of using an elevation mask of 20^o, the presence of albedo has decreased the error, since its contribution to the CSS currents has cancelled the effect of the elevation filter in some cases.

Following, in the same simulation section, the script of the algorithm is completely replaced by an artificial neural network implementation. In this case, the results show a determination error around 4 degrees without albedo and 32.06 degrees with albedo, but only in favorable geometry conditions. That means that steering the

Table 6.8 - Worst sun determination errors (in degrees) observed during the state space exploration and algorithm experimentation scenario.

CSS minimum elevation mask (degrees)	**0**	**20**	**30**
Without albedo	0.02	18	36.88
With albedo	14.92	11	38.48

Sun to a position where the neural network has not been trained (i.e. far from the nominal nadir oriented orbit), the error reached almost 89 degrees. In this point, the algorithm designer could decide to keep training the neural network in a broader range of configurations or restore back the traditional algorithm.

Apart from testing the feasibility of Sun determination algorithms, this scenario illustrates the flexibility to experiment various approaches and implementations in a running simulation. Specific geometrical configuration can be rapidly accomplished to test the performance of the system in very specific situations (e.g. checking the angle between two sources of light), bringing insight into the development of the algorithm. Further, in the presence of erroneous code, computational steering provides a ready to use interface for debugging the model in the very same simulation state that the error has appeared.

6.11 Scenario 9: Spatial resolution adjustment

It is common that during the construction of a scenario, a trade between fidelity and computational complexity must be done to allow the execution of a simulation in a given platform within a reasonable time or to meet specific computational performance requirements. Therefore, in some use cases the adoption of simplified mathematical models reduces significantly the time required to process the simulation, without compromising its overall quality. On the other hand, low resolution models may hide details of a complex behaviour that should be well investigated, thus requiring the modification of the scenario to better describe the phenomenon.

In this work, the capability of adjusting the spatial resolution of models while the simulation is executing is one of the interactive aspect to be addressed with computational steering mechanisms. Hence, in the current section, this type of intervention is applied using the baseline scenario to study the characteristics of the albedo and its implications in the solar sensors behaviour.

As previously described in section 6.1, the albedo is modelled as a set of discrete cells that defines the reflectance index of Earth's surface for a given region of the globe. Index tables are drawn from daily observational data that can be loaded individually or combined with statistical operations for a given period. For instance, due to short term variations in the atmosphere, applying low-pass filters in a temporal series of index data is a common approach to model cloudy regions. Moreover, averages indexes can also be computed to model seasonal changes when the rain, ice formation, and snow accumulation vary periodically within a year.

The albedo grid resolution impacts differently on the model fidelity, depending on the region. The average reflectance of cloudy areas, for instance, results in cell clusters with fuzzy delineation, which are less affected by a low resolution discretization. On the other hand, the precision of the index on the surface may be more susceptible to the spatial resolution, since land features, such as mountain belts or the land coverage in general, usually have a well-defined edge and a contrasting spectral property.

Due to all these characteristics of the albedo, the simulation engineer must be able to naturally adjust the model parameters, especially when unexpected behaviour appears and needs to be better analysed. In the computational steering facility, the baseline scenario is loaded with a low resolution configuration and then enhanced as required by the user.

Moreover, during the interaction a custom user interface for displaying the albedo model is provided by the visualization system, in which the engineer can toggle between multiple layers on the 3D Earth representation, as presented in the Figure 6.47. In the first option, the raw reflectance index table can be used to paint the globe with a false colour representation (i.e. blue is low reflectance and red is high reflectance). In the Figure 6.47-a an arbitrary table is loaded, wherein the Antarctica continent is clearly identified from its high reflectance caused by the ice coverage. Next, the visualization of the albedo as computed in the simulation can be enabled to better analyse the relation between Sun's position and reflectance table, as shown in the Figure 6.47-b. Further, the region of albedo that is seen from the spacecraft is represented by a third layer in the visualization system, using a normalised colour scheme (Figure 6.47-c). Any of these layers can be displayed simultaneously and overlapped with partial transparency, as illustrated in the Figure 6.47-d.

Furthermore, from a steering widget, the engineer can define the reflectance index in the grid by selecting and combining tables previously computed and loaded in

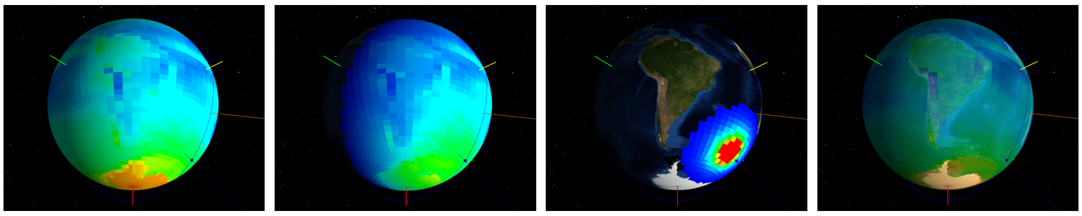

(a) Raw reflectance index table. (b) Simulated albedo (c) Portions of the albedo as seen from the spacecraft. (d) Reflectance table overlapped with surface texture.

Figure 6.47 - Earth's Albedo visualization layers in the 3D display system.

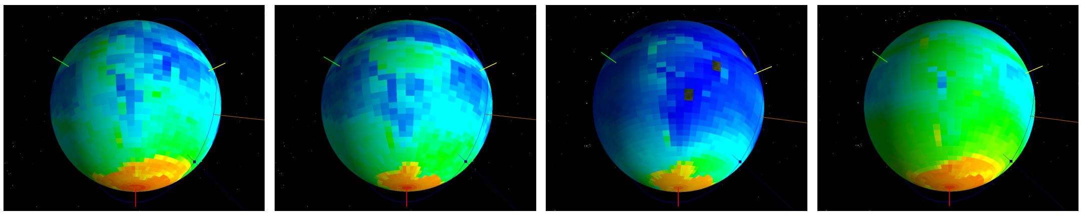

(a) Sep.'05 average. (b) Mar.'05 average. (c) Annual average $+1\sigma$ (d) Annual average -1σ

Figure 6.48 - Online selection and combination of reflectance index tables.

the simulation. In the Figure 6.48 some examples of this online intervention are provided. The average tables for September and March of 2005 are respectively shown in the first two images (Figures 6.48-a & b), wherein the variation in the ice coverage can be easily observed around Antarctica. Another contrasting change in these images is the cloud coverage on the Amazon rainforest, which is larger during the wet season (i.e. March). Any of pre-loaded tables can be combined and in the Figure 6.48-c the user subtracts the annual average with its standard deviation and in the Figure 6.48-d adds them.

The analyses performed in this section consider the spacecraft operating in the nominal mode (i.e. S/C pointing Z-axis to nadir and aligning X-axis with the velocity vector), in a low orbit. The first advantage of using the steering environment in this scenario is demonstrated by the enhancement of insight into the problem's geometry. Without the 3D animation feedback, the relation of the sensors with the albedo is not always simples to realise, since their boresight are not perpendicular to the body1s panels. Still, by steering the visualization system, the engineer confirms, for instance, that it is possible that all solar sensors receive simultaneously light from albedo, even if in small quantities.

This observation is evidenced with the geometrical configuration represented in the Figure 6.49, wherein the satellite is pointing to nadir and orbiting an illuminated region of the Earth, towards the ascending node (i.e. from south to north pole). From the 3D model, it is clear that the CSS 6 and 5 receives direct light from the Sun, while sensors 3, 4, 7, and 8 from albedo. In addition to that, the simulation results have shown that the sensors 1, 2, 5, and 6 also receives light from albedo, as seen from the images of the visualisation system reproduced in the Figure 6.50. In this simulation instant, the representation of albedo regions visible to each sensor confirms that even those positioned on the $-Z$ side of the body will see a portion of the Earth's surface far in the local horizon (Figures 6.50-a,b,e,f), while the others will receive albedo close from the sub-satellite point. This is explained by the orientation of the sensors and by the low altitude orbit that makes the angular diameter of the Earth large from the spacecraft's point of the view.

The effects of Sun light and the albedo coming from each cell in the grid are combined by the sensors that produce a current between 0 and $1mA$, accordingly to the incident angle of each source. As example, the corresponding output currents for the instant illustrated in the Figure 6.50 are the following: $CSS_1 = 0.1422$; $CSS_2 = 0.3917$; $CSS_3 = 0.2294$; $CSS_4 = 0.2277$; $CSS_5 = 0.6762$; $CSS_6 = 0.9275$; $CSS_7 = 0.2088$; $CSS_8 = 0.2091$. As a consequence of the noise introduced by the albedo, the error on computing the Sun on-board is approximately 12 degrees. As a comparison, if in this moment the user add to the reflectance table one standard deviation the error increases over 18 degrees. Similarly, if the one standard deviation is subtracted from the current reflectance table, the error drops to less than 6 degrees.

In addition to the variations in the Sun determination error caused by the use of an extreme or conservative reflectance table, the accuracy of the on-board algorithm is also subjected to the region of the albedo grid, in which the satellite is. This behaviour is analysed by the user as the sub-satellite point crosses a region with steep variations in the albedo, referenced in the Figure 6.51-a. Using a low resolution albedo model, as shown in the Figure 6.51-b, the western coast of South America is not well-defined and the transition of the albedo indexes from the sea areas to the Andes peaks is abrupt, causing the error to suddenly change from 10 to 10.6 degrees. By increasing the spatial resolution of the albedo model (Figure 6.51-c) and steering the satellite's orbit back to the previous position, the observed error ranges from 9.8 to 11 degrees, but with a smooth transition as the icy peaks are crossed.

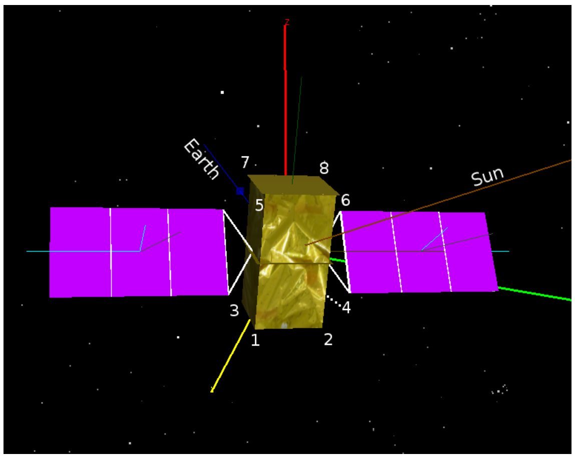

Figure 6.49 - Identification of solar sensors and visualization of the spacecraft's attitude during the albedo analysis scenario.

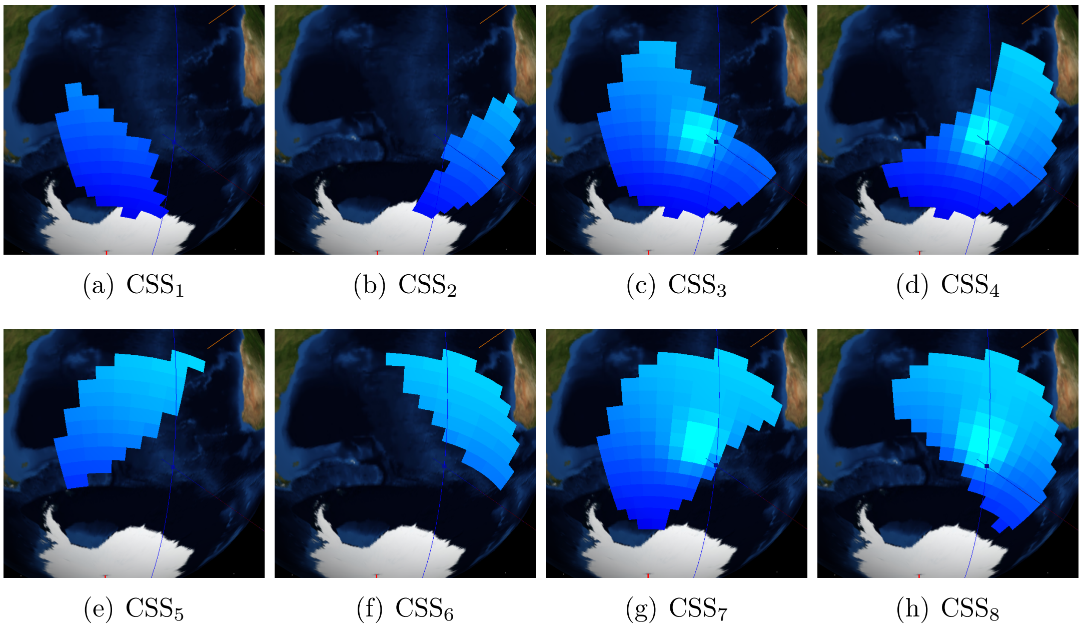

Figure 6.50 - Albedo cells as seen from each CSS, as the spacecraft points to nadir.

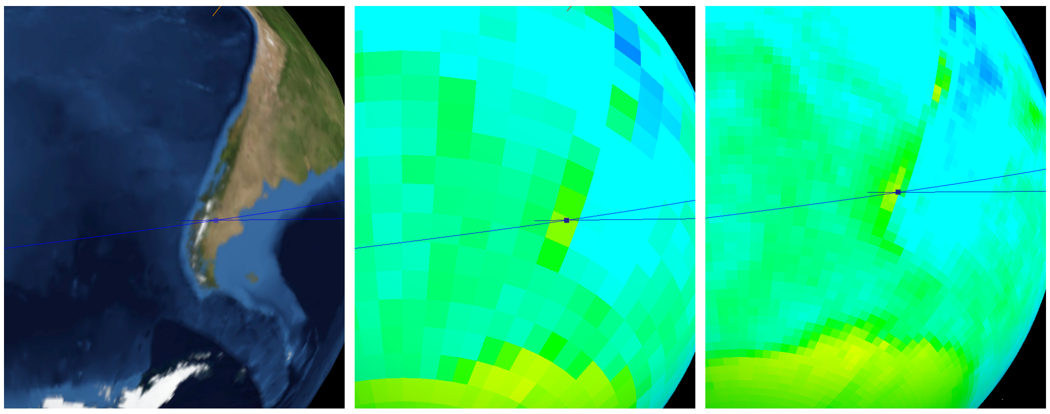
(a) S/C orbital position (b) Albedo visualisation layer with low resolution. (c) Albedo visualisation layer with high resolution.

Figure 6.51 - Comparison of spatial resolution configured in the albedo model, as the spacecraft orbits over the South America.

Although these variations in the Sun determination error are relatively small, the capability to enhance the simulation resolution provides a flexible environment for performing more accurate analysis on the error propagation effects, for instance, on the stability of the attitude control or the solar panels orientation.

Moreover, in the implemented scenario, the spatial resolution is inherent to the albedo model, which is manipulated via the control parameters that define the discretization of the grid (i.e. delta latitude and longitude). In a more complex modelling, this mechanism can be adapted to allow the user to select the regions in which the resolution should be improved, producing a multi-scale grid.

6.12 Scenario 10: Temporal resolution adjustment

Another important aspect regarding the computational models resolution is related to the time domain. It is needless to say that dynamic systems evolve differently over the time and while some behaviours change quickly in a short period of time, others are observed only after a long simulation.

Sometimes, this diversity on dynamics occurs in the same simulation scenario, imposes a challenge to the scientist when choosing a proper simulation step. If in one hand, a small step for all models enhances the observation of first order effects in the dynamics, on the other hand a bigger step may reduce significantly the simulation processing time.

Hence, a straightforward approach would be to re-execute the simulation horizon several times, adjusting the integration step always a given phenomenon wants to be investigated in more details. Nonetheless, by using a computational steering interface, the user is free to decide on adjusting these parameters while the simulation is running and the results are being analysed.

In this direction, the current section demonstrates the applicability of changing the integration step and the scheduling profile in a spacecraft simulation, while the scenario evolves, wherein two distinct thermal systems are used. For supporting the modelling activity, the commercial tool SINDA/FLUINT is employed, which is an equation solver for general purpose network analyses, well-known in the thermal domain (CULLIMORE et al., 2005). In this environment, pieces of equipment or physical objects are modelled by a set of nodes, each of them containing thermal properties (e.g. conductivity, emissivity, and absorptivity of the material) and exchanging heat with other nodes via conductors that represent the heat flow by radiation or conductance. Moreover, boundary nodes can be described in the network and thermal load may be applied to the individual nodes.

In order to allow the online manipulation of properties in the SINDA/FLUINT models, a new interoperability mechanism is implemented in the *SimuBox* facility, whose details are given in the Appendix D. In addition to that, the baseline scenario has been modified to include a new instance for the thermal models, as presented next.

6.12.1 Thermal models

The thermal scenario is built with two independent networks modelled in the SINDA/FLUINT, whose temperature of nodes can be read in the *SimuBox* side. Furthermore, environmental information, such as spacecraft orbit, Sun position, and Eclipse condition can be sent to the models running in the SINDA/FLUINT simulation.

In the *SimuBox* side, the interoperability channel is handled by the SMP2 Thermal model, as presented in the Figure 6.52, which is connected in a new assembly derived from the baseline scenario. As a regular component in the infrastructure, this model is scheduled and executed from its main entry point (i.e. `Update()` method). In addition, the parameter `Thermal_P_SimTimeStep` is used to control the simulation step in the SINDA/FLUINT execution, which can be changed by the user. However, in this case, a specialised trigger must be used in the steering adapter layer to ensure

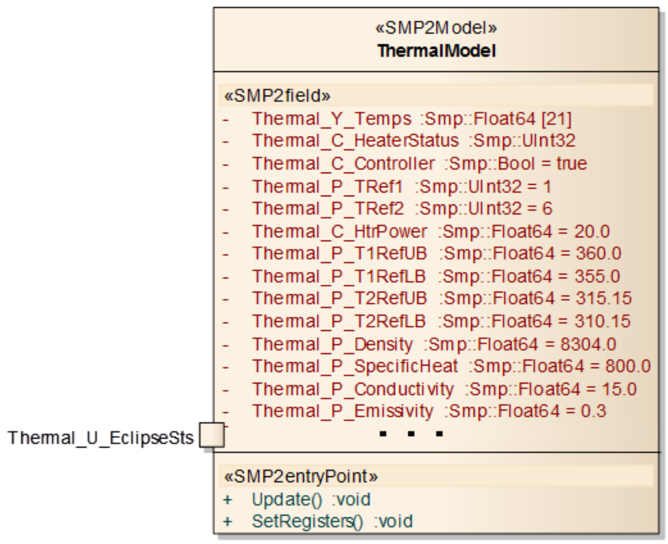
«SMP2Model»
ThermalModel
«SMP2field»
- Thermal_Y_Temps :Smp::Float64 [21]
- Thermal_C_HeaterStatus :Smp::UInt32
- Thermal_C_Controller :Smp::Bool = true
- Thermal_P_TRef1 :Smp::UInt32 = 1
- Thermal_P_TRef2 :Smp::UInt32 = 6
- Thermal_C_HtrPower :Smp::Float64 = 20.0
- Thermal_P_T1RefUB :Smp::Float64 = 360.0
- Thermal_P_T1RefLB :Smp::Float64 = 355.0
- Thermal_P_T2RefUB :Smp::Float64 = 315.15
- Thermal_P_T2RefLB :Smp::Float64 = 310.15
- Thermal_P_Density :Smp::Float64 = 8304.0
- Thermal_P_SpecificHeat :Smp::Float64 = 800.0
- Thermal_P_Conductivity :Smp::Float64 = 15.0
- Thermal_P_Emissivity :Smp::Float64 = 0.3
. . .
Thermal_U_EclipseSts
«SMP2entryPoint»
+ Update() :void
+ SetRegisters() :void

Figure 6.52 - SMP2 Thermal model responsible for handling the communication with the SINDA/FLUINT simulation.

the consistency in the simulation step and the Thermal model scheduling. In other words, every time this parameter is changed by the user, the `Update()` entry point is properly rescheduled in the simulation kernel.

As described next, a heated bar and an isothermal tank are modelled in the SINDA/FLUINT environment and during the simulation, its intermediate results are read by the SMP2 Thermal model to update its internal temperature variables. Similarly, the environmental conditions and the heater state are periodically updated in the SINDA/FLUINT networks by the model in the *SimuBox* side.

6.12.1.1 Heated Bar

The first system modelled in SINDA/FLUINT represents the behaviour of a heated bar, which is $0.5cm$ tick, $5cm$ wide, and $10cm$ long. As illustrated in the Figure 6.53-a, four-fifths of the bar are fully insulated from the environment and the other $^1/_5$ is exposed to the outer space. The bar is modelled as a network of 500 nodes connected in series with a heater attached to its insulated end.

The initial temperature in the bar is assumed to be 293.15^oC and as the simulation evolves the heat starts to flow from the inner nodes to the outer ones, by conduction, and from there it is irradiated to the deep space. A full list of the parameters used in the thermal modelling is given in the Table 6.9.

The objective in this illustrative problem is to control the temperature in the middle

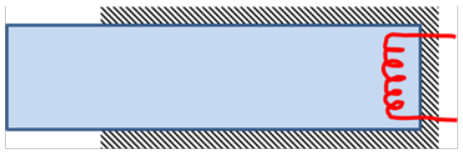

(a) The bar is $^4/_5$ fully insulated and has a $20W$ heater attached to one of its end.

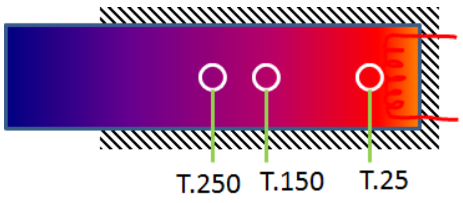

(b) The set point temperatures is set to the T.250 node, based on the reading of two termistors located at T.150 and T.25 nodes.

Figure 6.53 - Illustration of the heated bar's geometry.

Table 6.9 - Physical properties and geometrical variables of the heated bar model.

Parameter Type	**Parameter**	**Value**
Thermal	Initial temperature $[^oC]$	293.15
	Density (ρ) $[kg/m^3]$	8304
	Specific heat (Cp) $[J/kg-K]$	800
	Conductivity $[W/m-K]$	15
	Emissivity (ϵ)	0.3
Network topology	# Nodes	500
Geometry	Thickness $[m]$	0.005
	Width $[m]$	0.050
	Length $[m]$	0.100
Environmental	Heater power $[W]$	20

```
Heater status = ON, if STS1 = true and STS2 = true;
                OFF, otherwise.
$ Init vars
STS1 = STS2 = true
STS1_UB = 360
STS1_LB = 355
STS2_UB = 315.15
STS2_LB = 310.15

$ Ctrl Loop
If (T.150 > STS1_UB) then
   STS1 = false
Else if( T.150 < STS1_LB) then
         STS1 = true
endif

If (T.25 > STS2_UB) then
   STS2 = false
Else if( T.25 < STS2_LB) then
         STS2 = true
endif
```

Figure 6.54 - Algorithm for controlling the temperature in the middle of the heated bar.

of the bar (represented in the SINDA/FLUINT by the T.250 identifier) between 280 and 300 Celsius degrees, by switching the heater *on* and *off*. From the engineer point of view, the thermal behaviour in the bar must be understood in order to dimension the heater and to design the control law.

The control algorithm is implemented by the SMP2 Thermal model, in the side of the *SimuBox* simulation. By default, the heater has $20W$ of power and the temperature control in the bar must be done from the readings of two thermistors, which are located in the position of the bar represented by the nodes T.25 and T.150, as shown in the Figure 6.53 [10]. The adopted control strategy is the *bang-bang*, in which the heater is turned on when temperatures at T.25 and T.150 are respectively lower than 310.15 and 355 degrees, and turned off if either T.25 is higher than 315.15 or T.150 is higher than 360 degrees. Furthermore, the heater shall not be turned on if the temperature at T.1 is higher than 385 Celsius degrees. This algorithm is given in the Figure 6.54.

[10]The locations of the thermistors do not have any engineering meaning and they are chosen just to increase the dynamics of this illustrative problem.

Table 6.10 - Physical properties and geometrical variables of the isothermal tank model.

Parameter Type	**Parameter**	**Value**
Thermal	Initial temperature $[^oC]$	0.00
	Density (ρ) $[kg/m^3]$	8304
	Specific heat (Cp) $[J/kg-K]$	800
	Conductivity $[W/m-K]$	10
	Emissivity (ϵ)	$[0.6, 0.7]$
	Absorptivity (α)	0.98
Network topology	# Nodes	1
Geometry	Radius $[m]$	0.1
Environmental	AM0 $[W/m^2]$	1370

6.12.1.2 Isothermal Tank

The second thermal model represents an isothermal sphere of $10cm$ radius, whose mass is represented by a single diffusive node in the network. This node is then connected to a boundary node representing the deep space, which heat flow by radiation is equal to the product of the material emissivity (ϵ), Stefan-Boltzmann constant, and area (i.e. the surface of the sphere). The sphere is subjected to thermal loads by radiation coming in the form Sun light and is equal to the product of its absorptivity (α), incident area (i.e. area of the circle), and solar flux (e.g. $1370W/m^2$).

In spite of its topological simplicity, this problem exemplifies the potentials of connecting SINDA/FLUINT legacy models to the spacecraft simulation, since in this scenario, the tank is assumed to be in the orbit and its thermal load updated accordingly to the orbital position, eclipse condition and Sun distance.

The complete list of parameter values used in this model, which can also be changed during the simulation, is presented in the Table 6.10.

6.12.2 Scenario results

The dynamics are very contrasting in the presented thermal models. While the temperature in the bar changes significantly in few seconds (particularly in the nodes next to the heater), the temperature in the tank varies slowly over the spacecraft orbit, which takes approximately six thousands seconds. Due to these differences on the time scale, the user can take advantages of adjusting the temporal resolution of the computational models as needed.

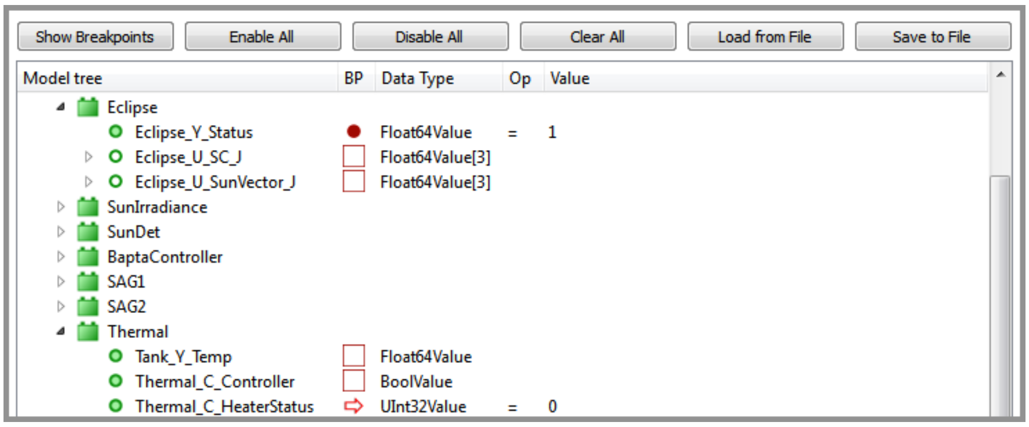

Model tree	BP	Data Type	Op	Value
Eclipse				
Eclipse_Y_Status	●	Float64Value	=	1
Eclipse_U_SC_J	☐	Float64Value[3]		
Eclipse_U_SunVector_J	☐	Float64Value[3]		
SunIrradiance				
SunDet				
BaptaController				
SAG1				
SAG2				
Thermal				
Tank_Y_Temp	☐	Float64Value		
Thermal_C_Controller	☐	BoolValue		
Thermal_C_HeaterStatus	⇨	UInt32Value	=	0

Figure 6.55 - Grahical User Interface of the *SimuBox* application for setting simulation breakpoints.

In the current scenario, the default configuration schedules the thermal models to execute cyclically every ten seconds and the orbital dynamics ten times a second (i.e. every hundred milliseconds). The simulation starts with the tank approximately in the middle of the eclipse period, so no thermal loads are being applied. The investigation on the variations of its temperature requires at least a full orbit. Hence, as the scenario evolves, the engineer uses a simple slide bar widget attached to the orbital model to reschedule its update entry point to a cycle of ten seconds. This change allows the user to accelerate the simulation clock over 10 times, reducing the processing time of a complete orbit to less than 10 minutes, without significantly compromising the simulation precision [11].

Conversely, ten seconds is proportionally a long period for the bar model, since in this time span the control algorithm may switch the heater a couple of times. Still, due to its initial temperature, it is expected that the heater in the bar model remains off, until the extra heat slowly dissipates out. Thus, the user's strategy is to set a simulation breakpoint to hold on its execution as soon the heater is turned on, thereby enabling the analysis of temperature in more details. In the Figure 6.55, the GUI for setting the breakpoint is given, which also contains a breakpoint for indicating the moment the tank comes out the Earth's shadow.

The heater is turned on for the first time at the simulation clock $t = 1000s$. After the simulation has been suspended the user steers the thermal model's update entry point to execute at $1Hz$. In this moment, what interests most in the control of the

[11]The impact on executing the orbit model will produce in the worst case an error of 10 seconds for computing the eclipse condition, which is acceptable in the context of a complete orbit that lasts $6,000s$.

heater is when the T.25 node is close to 360 degrees. Thus the simulation is resumed and a new breakpoint is set to interrupt the scenario again, after the heater is turned off.

Around the $t = 1057$ the simulation is paused and the user focus on the behaviour of the controller and the temperature gradient at the bar. The simulation is resumed, but the clock is set to run slower than the real time. The evolution of the temperature can then be visualized in a false colour animation, as illustrated in the sequence of images captured in the Figure 6.56. For instance, in the instant $t = 1080$ the red colour in the right of the bar indicates the heater is turned on and applying thermal loads. As it became off few seconds later, the temperature decreases as the heat flows from the right to the left, until the heater is turned on again around $t = 1095$. This switching behaviour can be observed in the visualization system until the temperature in the middle of the bar reaches its set point temperature close to 290^oC at $t = 3044s$.

The proper operation of the thermal control system is confirmed by the temperature profile shown in the graphical plot in the Figure 6.57, in which the control nodes T.25 and T.150 are kept within the limits, while the target node T.250 slowly converges to the set point.

Following the analysis of the heated bar model, the engineer concentrates on the isothermal tank model and speed up the simulation execution, by steering back its entry point to a ten seconds cycle and accelerating the simulation clock by a factor of ten.

After the first orbit, the periodic behaviour of the thermal system is confirmed: the heat in the tank is dissipated until it becomes illuminated and absorbs thermal energy from the Sun; once it re-enters the eclipse, the heat starts to dissipate again. Thus, in the end of the second orbit, the user interferes in the scenario, by changing the material emissivity from 0.7 to 0.6, causing the mean temperature in the Tank to increase.

The results of this dynamics for the first three orbits are presented in the sequence of images in the Figure 6.58. Each row of images (Figure 6.58-a to d) shows the temperature of the tank at different instants of a complete orbit. The columns (e.g. Figure 6.58-a, c, and i) compare the temperature of the Tank in approximately the same orbital position. Hence, it is observed from the false colour scheme that temperature profile, which is also shown in the graphic in the Figure 6.59, reaches

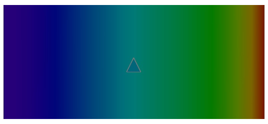
(a) $t = 1080s$; On

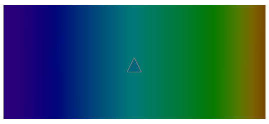
(b) $t = 1083s$; Off

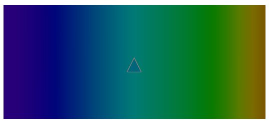
(c) $t = 1086s$; Off

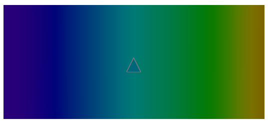
(d) $t = 1089s$; Off

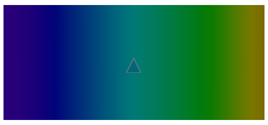
(e) $t = 1092s$; Off

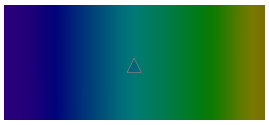
(f) $t = 1094s$; Off

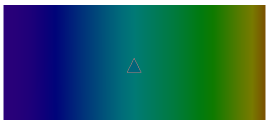
(g) $t = 1095s$; On

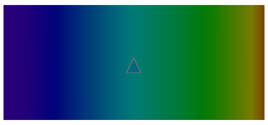
(h) $t = 1096s$; On

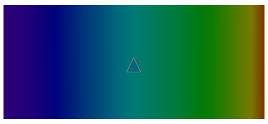
(i) $t = 1098s$; On

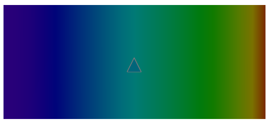
(j) $t = 1100s$; On

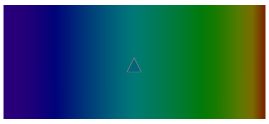
(k) $t = 1102s$; On

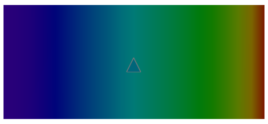
(l) $t = 1104s$; On

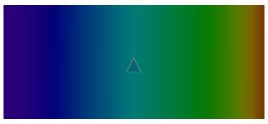
(m) $t = 1105s$; Off

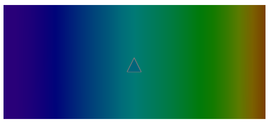
(n) $t = 1106s$; Off

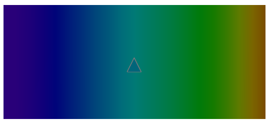
(o) $t = 1108s$; Off

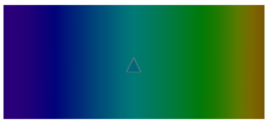
(p) $t = 1110s$; Off

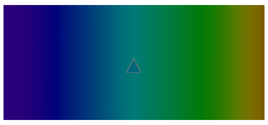
(q) $t = 1112s$; Off

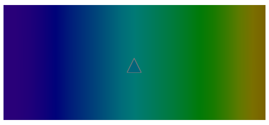
(r) $t = 1114s$; Off

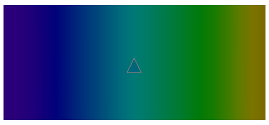
(s) $t = 1116s$; Off

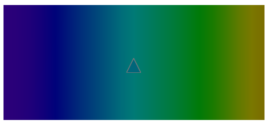
(t) $t = 1118s$; Off

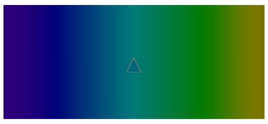
(u) $t = 1121s$; Off

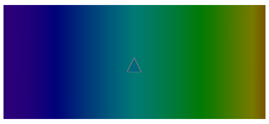
(v) $t = 1122s$; On

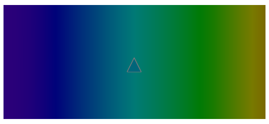
(w) $t = 1123s$; Off

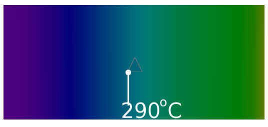

(x) $t = 3044s$

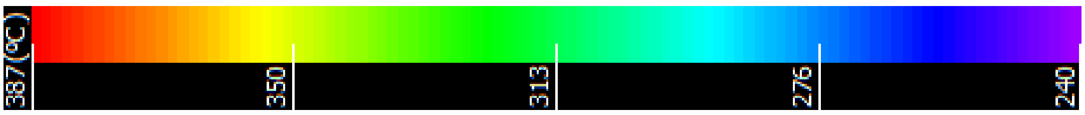

(y) False color legend for displaying bar's temperature.

Figure 6.56 - A sequence of images captured from the custom visualisation system attached to the *heated bar* model.

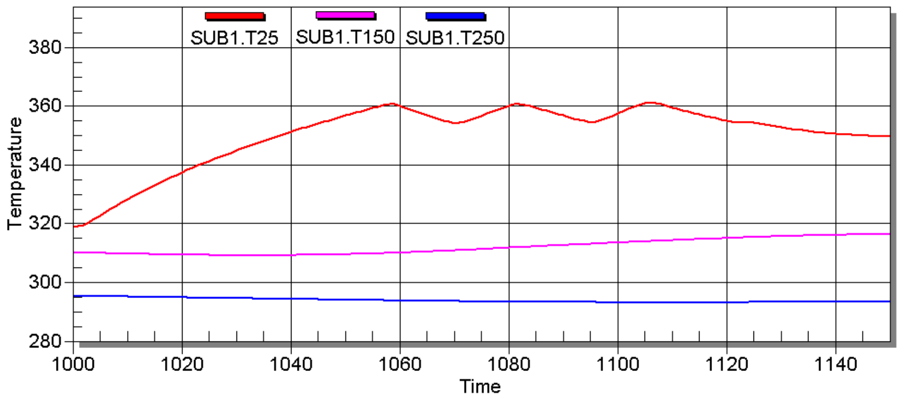

Figure 6.57 - Temperature profile of the control and target nodes.

its minimum just before the end of eclipse and the maximum just before the eclipse. Furthermore, by adjusting the emissivity coefficient, the lower limit of the temperature in the end of the eclipse ($t = 13,500$) is slight higher than in the previous orbits. Similarly, in the end of illumination period ($t = 17,500$), the tank has been heated up to 1.5^oC, in contrast to 0.5^oC before.

Therefore, from the presented scenario, it is evident that the computational steering approach brings flexibility to the simulation environment and increases the efficiency in the engineer's activity, since both processing time and accuracy of the model is sensitive to the execution cycle adopted. The dependence of these variables is shown in the Figure 6.60, in which the processing time of a set of simulation runs is compared against various scheduling profiles. In this test, the execution of the thermal model each second led to a processing time just below the wall-clock time, once the simulation horizon is set to $500s$. As the execution interval increases, the processing time quickly drops, reaching $43s$ for cycle of $10s$.

Although these performance figures depend on many factors (e.g. computational platform, communication infrastructure, and the topology of thermal models), it is clear that the capability on changing the model's temporal resolution during its execution is an advantageous benefit for studying different aspects of a dynamic phenomenon. Moreover, this mechanism can be complemented by the use of breakpoint and time acceleration functionalities provided by the simulation infrastructure.

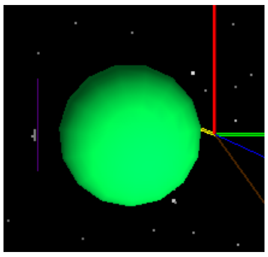
(a) Initial condition; $\epsilon = 0.7$

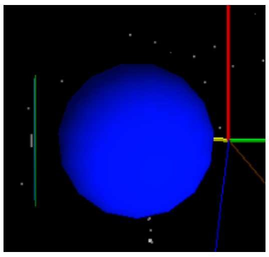
(b) ☾ ^{1}; $\epsilon = 0.7$

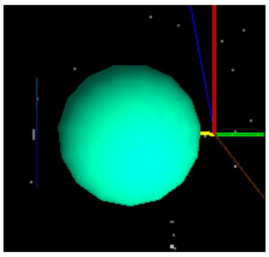
(c) ○^{1}; $\epsilon = 0.7$

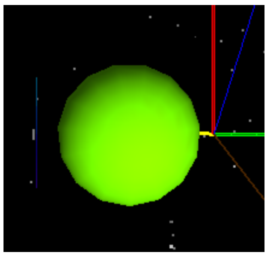
(d) ☽^{1}; $\epsilon = 0.7$

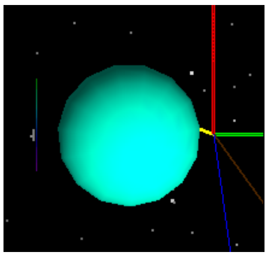
(e) ●^{1}; $\epsilon = 0.7$

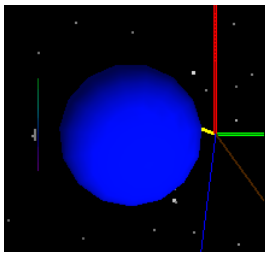
(f) ☾ ^{2}; $\epsilon = 0.7$

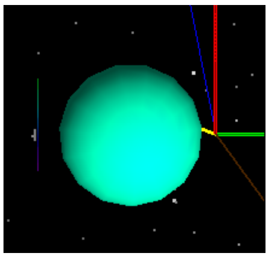
(g) ○^{2}; $\epsilon = 0.7$

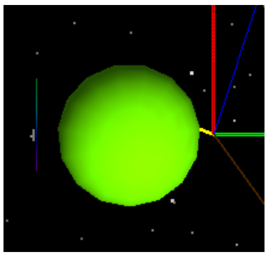
(h) ☽^{2}; $\epsilon = 0.7$

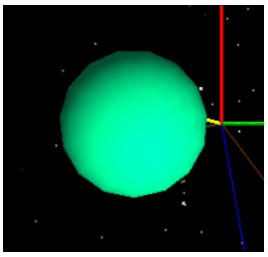
(i) ●^{2}; $\epsilon = 0.6$

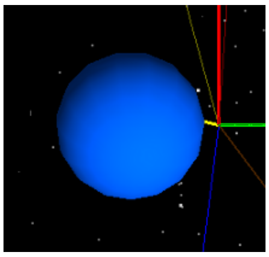
(j) ☾ ^{3}; $\epsilon = 0.6$

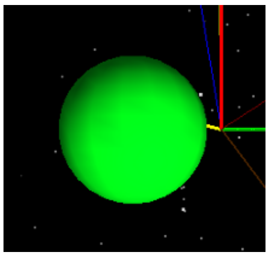
(k) ○^{3}; $\epsilon = 0.6$

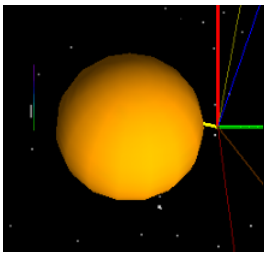
(l) ☽^{3}; $\epsilon = 0.6$

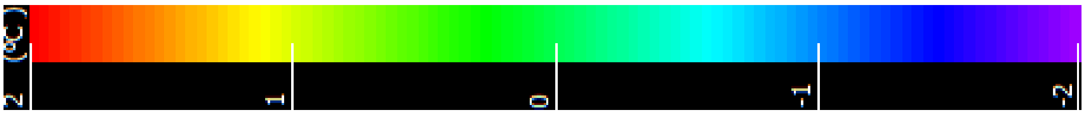

(m) False color legend for displaying tank's temperature.

Figure 6.58 - A sequence of images from visualisation system attached to the *isothermal tank* model. The following symbols apply: (☾) is the end of the eclipsed period; (○) is the middle of the illuminated period; (☽) is the beginning of the eclipsed period; (●) is the middle of the eclipsed period. The suffix is the number of the orbit.

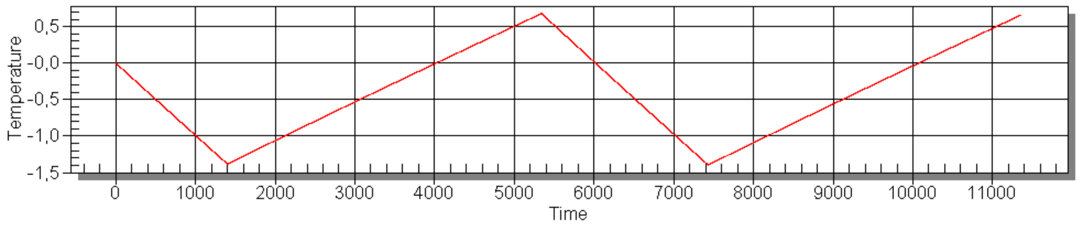

Figure 6.59 - Temperature profile of the tank during the first three orbits.

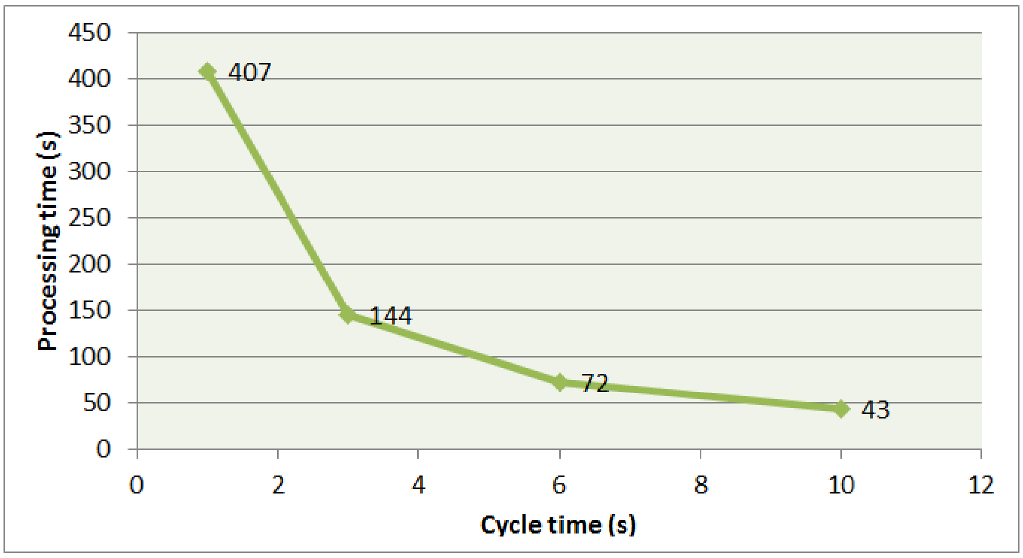

Figure 6.60 - The relation between the executing frequency of a model and the processing time of a simulation with 500s of horizon.

6.13 Scenario 11: Assisted computational performance optimisation

In this last scenario, the baseline configuration is used to demonstrate how the computational performance of a spacecraft simulation can be online adjusted by user intervention.

Frequently, the configuration of a simulation scenario must comply with timing restriction, in other to ensure e.g. its real time execution. In other cases, i.e. in non-real time simulations, the adjustment of parameters in a complex computational model can reduce significantly the processing time, as already discussed in the previous section.

Tuning the performance of a simulation, generally involves the configuration of a scheduling, in which not only is the frequency of model invocation programmed, but also their interdependence must be obeyed in the form of an oriented graph. Depending on the computational platform resources and on the simulation infrastructure characteristics, the designer can avail the scenario of optimisation opportunities, by adopting concurrent programming techniques (i.e. threads) and distributed processing environments to reduce the model's total processing time.

In this performance optimisation task, computational steering offers an alternative interface, whereby the engineer can balance the computational load in threads or processing nodes and guide the scheduling to a configuration that meets the timing requirements during the scenario execution.

In this sense, the current scenario illustrates how an increase in the computational complexity of the Albedo model can be compensated by balancing the simulation tasks in different threads. By default, the following tasks from the baseline scenario are scheduled to execute at $10Hz$, in a single thread: *Environment*, *Sensors*, *Power*, *OBC*, *Dynamics*, *AlbedoMain*, and *AlbedoSC*. Each of the tasks contains a group of entry points respective to their package of models, except by the Albedo model, whose execution can be divided in two parts: *AlbedoMain* computes the Earth surface grid illuminated by the Sun; and *AlbedoSC* marks which of the illuminated cells are visible from the spacecraft [12].

Therefore, during the simulation execution, the engineer monitors the computational performance and decides whether adjustments in the scheduling or model resolution are necessary. In the demonstration presented herein, the goal is to maintain the total processing time of a simulation cycle under $100ms$, thereby ensuring a performance close to the soft real time. Hence, besides changing the number of cells in the Albedo grid, the user can also trade the performance by creating and removing new processing threads and moving the simulation tasks into them.

In order to apply changes in the computational model, the customised interface presented in the Figure 6.61 is used. For each simulation cycle, statistics from the processing time of individual threads are provided, supporting the user decision on managing the number and load of threads. In the illustrated example, by dragging & dropping the *AlbedoSC* task, its execution is moved from the thread 1 to the empty thread 2. The same interaction can be done for defining the order of the tasks within a thread. Further, the number of threads that can be created is limited only to the resources of the operating system and it is up to the user make this decision based on the number of the available processors.

In the baseline scenario, the default Albedo model is discretised with a resolution of 1 degree of latitude and 5 degrees of longitude, resulting in a grid of 12960 points. In this work, the simulation runs in a single microcomputer Dell Vostro 3500 platform, executing Windows(R) 7 Professional 64 bits (SP1) in a multi-processed Inter(R) Core(TM) i5 CPU M 460 @2.53GHz with 4 GB of RAM.

[12]To be rigorous, the execution of *AlbedoMain* and *AlbedoSC* tasks are dependent of environmental and dynamics models and their concurrent execution may led to results slightly different each run. Still, in the context of this scenario, which executes the tasks at $10Hz$, these imprecisions are not relevant, since the variations of the spacecraft orbit and the Sun position in one simulation cycle are small when compared to the resolution of the grid in the albedo Model.

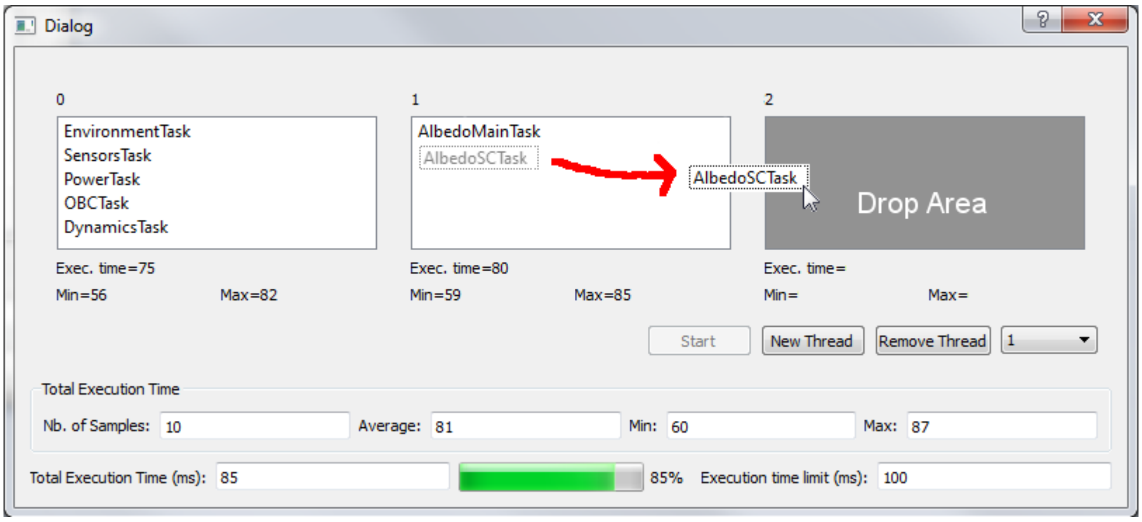

Figure 6.61 - Graphical user interface for steering the computational load of processing threads in the simulation.

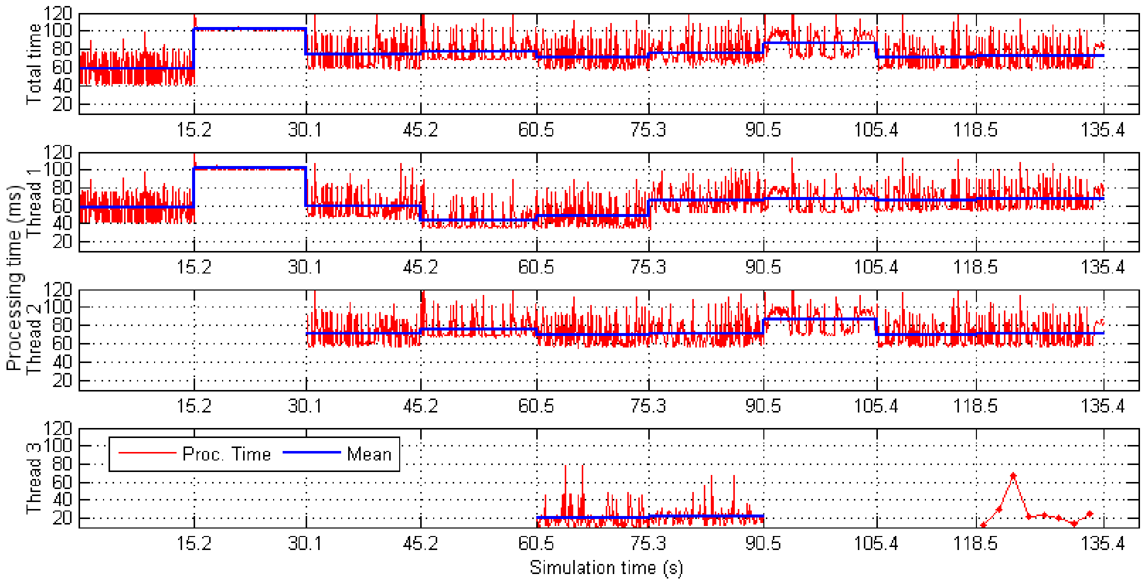

Figure 6.62 - Total processing time of each simulation cycle and over the simulation horizon.

The obtained processing times of the models in this scenario are summarised in the Figure 6.62. Along the simulation horizon, eight user interventions are done and they are represented in the graphic by the simulation time they have occurred.

In the first 15.2 seconds of simulation, the models execute in a single thread, resulting in a total processing time within the range of $40ms$ and $80ms$, with some spikes up to $100ms$ and an average of $60ms$.

After the first user intervention, the longitude resolution of the albedo model is enhanced to 2^o and the total number of cells in the grid is then increased to 32400. As a result, the computational performance of the model is immediately impacted and the average processing time rises to $100ms$.

Envisaging to keep the target under $100ms$, at $t = 30.1s$ the simulation conductor moves the *AlbedoMain* task to a new thread, which causes the average to be reduced to $80ms$. Although the threads may execute simultaneously, it is important to observe in the graphic that the total processing time is not the simple sum of the processing time of each thread, since the addition of threads imposes an overhead in the system. Therefore, several interactions are performed to better understand the computational complexity of each task and their overhead contribution.

At 45.2 seconds, the *AlbedoSC* task is also moved to the thread 2, decreasing the processing time in thread 1, but increasing the overall processing time. Next, in the instant $60.5s$, this very same task is migrated to a new thread 3, occasioning a tiny reduction in the average processing time.

So far in the scenario evolution, the orbital geometry caused the sub-satellite point to be close to the terminator[13], which reduces the total area of albedo as seem from the spacecraft and consequently the computational complexity of the *AlbedoSC* task. For this reason, in the instant $75.3s$, the engineer steers the orbit to ensure that the satellite receives more light from the albedo, as illustrated in the snapshots in the Figure 6.63. As a result, the average of the total processing time increases again (but still below $80ms$), mostly because of the contribution of CSS models in thread 1 those now have to process a larger number of albedo cells.

Additional investigations are done by the user, after moving the *AlbedoSC* task back into thread 2 ($90.5s$), which deteriorates the performance. Then, in the instant $105.4s$ the frequency of this task is reduced to $0.5Hz$ and finally in the simulation time $118.5s$ it is moved again to the thread 3.

In the whole, this type of computational steering brings enormous flexibility to the simulation engineer, since not only the computational performance can be adjusted by changing the scheduling profile, but also the contributions of each model to the complexity of the simulation can be analysed and adjusted to meet the requirements of the scenario.

[13]The line that separates the illuminated and the dark side of the Earth.

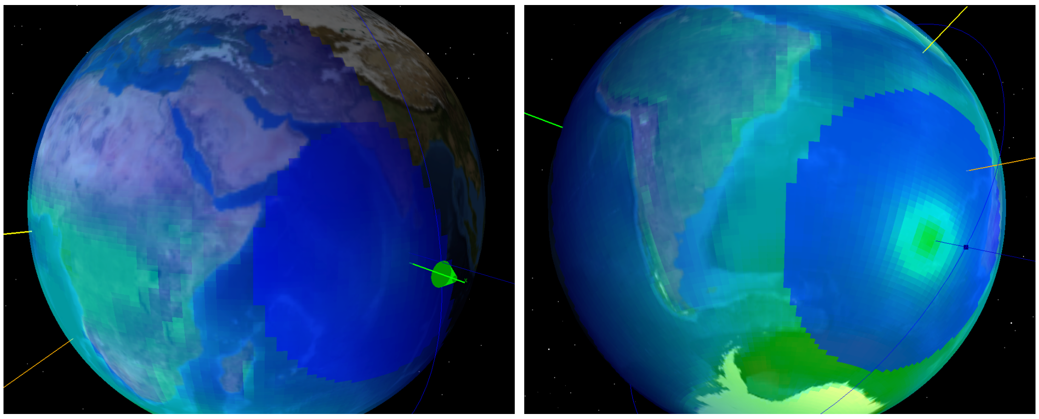
(a) The blue half-circle show the albedo reaching the satellite when its sub-satellite point is close to the terminator.

(b) When the sub-satellite point is close to the midday, a full circular regions of albedo is reflected to the satellite.

Figure 6.63 - Comparison of the albedo amount reaching the spacecraft when its sub-satellite point is close to the terminator and when its is not.

6.14 Results Discussion

The simulation results presented in the case studies have demonstrated the benefits of computational steering techniques in the context of space engineering activities from different perspectives of user intervention types, steering mechanisms, user interface paradigms, and application classes. Theses aspects have been covered by eleven scenarios as listed next:

- *Scenario 1*: Model verification;
- *Scenario 2*: On-board software verification;
- *Scenario 3*: Analysis of recurrent effects on the dynamics behaviour of the Sun determination algorithm;
- *Scenario 4*: Investigation of on-board Sun determination algorithm precision and its impacts on controlling S/C attitude;
- *Scenario 5*: Attitude steady state analysis;
- *Scenario 6*: Performance analysis of HITL implementation;
- *Scenario 7*: Comparison of potential scenarios to support test case specification;
- *Scenario 8*: Sun determination algorithm experimentation;

- *Scenario 9*: Spatial resolution adjustments;
- *Scenario 10*: Temporal resolution adjustments; and
- *Scenario 11*: Assisted computational performance optimisation.

Accordingly to the classification proposed in the section 4.3, the physical parameters and data presentation steering are by far the most common types of user intervention performed in the described scenarios. The complete relation between the steering classes and the case studies is summarised in the Table 6.11, in which all the classes have been fully covered by at least one scenario, except for the structural changes type. The latter requires an assembly manipulation mechanism not yet implemented by the infrastructure, but whose advantages have been demonstrated by the swap of CSS models in the case study (7).

During the simulations, the visual feedback has been confirmed as a fundamental feature in a steering facility. The awareness on the problem's geometry brought by the tool is shown in several results, for instance, in the verification of the models that computes dynamically the shadow on the solar sensors produced by the solar panel, as a result of S/C attitude and Sun position. Moreover, the selection of data post-processing method is also an important functionally and has been used in the scenario (11) for defining the period in which the mean processing time of threads is computed.

Table 6.11 - User intervention type versus case studies.

Intervention	**Type**	**Case Study**										
		1	**2**	**3**	**4**	**5**	**6**	**7**	**8**	**9**	**10**	**11**
Behavioural	Pysical params.	Y	Y	Y	Y	Y	Y	Y	Y	Y	Y	
	Geometrical params.	Y	Y	Y	Y			Y	Y	Y		Y
Resolution	Spatial									Y		P
	Temporal										Y	P
Algorithm experimentation									Y			
Structural								P				
Performance optimisation												Y
Data presentation		Y	Y	Y	Y	Y	Y	Y	Y	Y	Y	Y

Y: demonstrated; P: partially demonstrated (only some aspects).

Furthermore, the flexibility demonstrated in the simulation activities has been improved by complementary steering mechanisms. In addition to the execution and time control used in all simulations, the *breakpoint* feature is shown in the scenario (9) and the *auto-snapshot*, *playback*, and *history tree* in the scenario (7). The manual invocation of the *snapshot* is also made in the scenario (3) and (4), thus ensuring the repetition of simulation conditions and simplifying the comparison of scenarios evolution against parameters exploitation and their impact on the system performance.

Most of these features are handled by the steering adapter layer developed in the simulation infrastructure. By extending SMP2 interfaces, this layer has taken advantage of existing mechanisms for accessing the model's attributes and operations. In this context, the trigger mechanism has been vital for maintaining the coherence between model parameters, as illustrated in the adjustment of orbital parameters and the steering of attitude dynamics' state vector.

In other cases, like in performance optimisation and temporal resolution adjustments, new interfaces have been defined by the simulation kernel, accordingly to the metadata provided in the scheduling. Further, the model implementation has to be prepared for manipulation (e.g. publishing configuration fields) and in the limit they will implement their own steering interfaces, as presented in the scenario of algorithm experimentation (8).

In the steering environment, another key feature for promoting efficiency in the interaction process is the usability of the front-end. Basically in all the scenarios, customised 3D widget have been used to easy the translation from engineering values into simulation parameters. In this direction, the direct image manipulation interface in the scenario (1) has demonstrated the potentials of the parametric design integration with the simulator. Moreover, the user experience with the computational model can be enhanced by the adoption of natural interfaces, as presented in scenario (6) and (7) with gestures interpretation, and immersive environments.

Nevertheless, the standard widgets in the graphical user interface are still a valid and useful approach for steering the model parameters and input precise values. Even a pure textual interface should be available for complex changes, such as algorithm experimental as presented in the scenario (8).

Table 6.12 - Types of simulation applications covered by the case studies.

Application Type	**Case Study**										
	1	**2**	**3**	**4**	**5**	**6**	**7**	**8**	**9**	**10**	**11**
Modelling verification and scenario coherence	Y										
Simulation tuning									Y	Y	Y
System, architecture or component conception & design	Y							Y		Y	
Design verification		Y		Y	Y	Y	Y				
Performance analysis / System tuning			Y	Y	Y	Y	Y		Y		
Test cases specification		Y	Y	Y	Y		Y				
System debugging / Fault analysis		Y									

In general, the purpose of all case studies is to understand some aspect of model or system behaviour and to continuously assess the simulation consistency in a flexible and agile way. Yet, the main goal of each scenario can be grouped accordingly to the types presented in the Table 6.12. This classification confirms the comprehensiveness of potential applications to adopt steering techniques, thereby covering a broad number of activities along the mission life cycle, as previously discussed in the section 4.2. Besides the presented use cases, conceptual design activities, typically performed in the early phases of a space mission, such as selection of mechanical configurations, definition of algorithms and design of control strategies, could also be benefited by computational steering simulations. Furthermore, at the other end of project life time, the interactive exploration of parameter state can support fault diagnosis analysis to accelerate the identification of problems in the space system or create dynamic simulation scenarios for operator training purposes.

Thanks to a high level abstraction layer implemented by the facility, the steering mechanisms could be reused in every study case. The required effort for reconfiguring the scenarios may be considered high when compared to specific-purpose simulators used in very simple analysis (e.g. for creating a coverage mapping of solar sensors, as the Sun directions varies along $4\pi rad$). Still, as the complexity of the simulation increases, which frequently appears in real life projects, this extra effort is significantly diluted and smaller when compared to the work necessary to codify monolithic applications. This can be observed from the SVF and RTB setups, when only eight redefinitions of field links permitted the integration of hardware-in-the-loop.

Nonetheless, it is important to note that for some applications, a more complete computation model may be required to simulate dynamic behaviours with more fidelity, as in the case of high frequency phenomena of actuators or flexible appendages. Although these models are not necessarily an impediment to apply the computational steering approach, they often imply the raise of computational complexity in the simulation, thereby limiting some functionality (e.g. real time simulation) or degrading the interaction experience (i.e. increasing the feedback latency, which would require a more sophisticated synchronisation mechanism for handling the user commands).

Nonetheless, it is important to note that for some applications, a more complete computation model may be required to simulate dynamic behaviours with more fidelity, as in the case of high frequency phenomena of actuators or flexible appendages. Although these models are not necessarily an impediment to apply the computational steering approach, they often imply the raise of computational complexity in the simulation, thereby limiting some functionality (e.g. real time simulation) or degrading the interaction experience (i.e. increasing the feedback latency, which would require a more advanced synchronisation mechanism for handling the user commands).

Regarding the state space exploration, it is observed that when searching for a specific condition in the simulation (e.g. in the case of manoeuvring the satellite towards the Sun with two sensors in the shadows), the steering mechanism provides a suitable interface for rapidly configure the scenario. Especially when the behaviour of the system is still unknown, this approach has clear advantages when compared to analytical methods or simulations programmed by scripts, as discussed in section 4.1. Moreover, as the number of parameters in a given scenario increases, resulting in the problem known as curse of dimensionality, the user interaction approach shows to be an effective complementary tool to actively explore the simulation state space and conduct trade-off analyses.

On a sporadic basis, various existing spacecraft simulators may implement some aspects of computational steering, particularly with respect to the visualisation of 3D digital mock-ups. Therefore, it is expected that the current work contributes to enhance the level of user interactivity in space engineering simulations, by providing a reference infrastructure for advanced steering facilities.

7 CONCLUSIONS AND FUTURE WORKS

This work has presented a novel approach for addressing the design and execution of satellite simulation scenarios, by employing computational steering concepts to enhance the level of user interactivity with the computational model. On the context of space mission projects, simulation systems constitute a fundamental tool for supporting several engineering activities and, in this direction, the results of this work has contributed to expand the applicability of simulators and improve the space engineering practices towards more agile processes.

Among the benefits brought by this technique, the results have shown how the insight into the modelled problem can be promoted by enabling the simulation engineers to guide the progression of the scenario. Moreover, the low level access to the simulation parameters provides more flexibility on studying the behaviour of complex systems, bringing efficiency to their activities.

As a consequence of the continuous interaction with the computational model, the users can naturally perform simulation consistence checking, explore the simulation state space, and test new hypothesis as their understanding on the system evolves. In this process, complementary to the traditional data presentations in graphical plots, the 3D visual displays have confirmed to be a fundamental feedback to allow the engineers to rapidly assimilate simulation outputs, especially when complex geometry is involved, improving the design awareness. As opposite to a script programming environment, the presented approach saves simulation time and simplifies the model parameterisation and control.

Based on a new computational steering classification, which organises the various facets of the concept according to the type of user's intervention, a set of illustrative scenarios have been configured to demonstrate the potentials of this interaction technique. The case studies have been inspired in real life problems and have covered multiple functionalities of computational steering environments and simulation applications, such as model verification, behaviour investigation, performance analysis, mission and system design, on-board software development and verification, test case specification, and computational performance optimisation.

In addition to those use cases, the development of a highly flexible infrastructure facilitates its application in most engineering activities assisted by simulation, including those performed for mission conception, design & construction of flight units, AI&T, operators training, anomaly investigations, and deorbit planning, among others. This is possible due to the adoption of metadata programming techniques and the extension of SMP2 mechanisms to promote the reuse of simulation artefacts and facilitate the instrumentation of models with steering capabilities.

Furthermore, a set of innovative steering widgets have been proposed for handling specialised types of parameters, which can be dynamically connected to the running simulation via a flexible adapter layer. This scheme contributes for the investigations on the field of human-computer interaction and supports the construction of more intuitive user interfaces in applications customised for the space engineering domain.

Another productivity aspect observed regards the level of usability provided by the facility for adapting the framework for new applications. In many generic software development projects, coding the configuration artefacts can be as cumbersome as designing a new product from scratch, if automation tools are not available under a well-defined workflow. For this reason, taking the SMP2 workflow and its tool-chain as a reference model, this work has defined a suite of editors and development kits to allow the formal definition of models and scenario configurations, from which simulation artefacts and wrappers code can be automatically generated. In addition to that, since SMP2 concepts are compatible with UML, the adoption of a commercial Computer-Aided Software Engineering tool to describe models and scenarios has proven to be an appropriate method for documenting simulation artefacts. Hence, the availability of a tool-chain is a key factor to promote reuse and to spread the additional effort of building steering capabilities among multiple use cases. At the same time, the automation provided by these workbenches ensures repeatability of processes, thus increasing the reliability of simulation applications.

Essentially, the simulation is present in activities from all phases of a space mission. It is clear that different simulation problems requires distinct approaches and, in this sense, computational steering may not be suitable for every application, especially in very simple scenarios and with models of predictable behaviour. Still, multiple combinations of steering features will meet a vast number of simulation use cases, when scenarios with highly dynamic behaviour, recurrent effects, and state space exploration exist.

Ultimately, the results presented in this work can be applied beyond space system engineering field, as the adopted simulation concepts are sufficiently generic to be used in other areas. Thus, in order to accomplish this, further improvements may be carried into the facility, as discussed next.

7.1 Future works

The implemented steering mechanisms in this work have demonstrated the advantages of incorporating user interactivity interfaces in spacecraft systems simulators. Still, many improvements in the software architecture could be considered to extents its flexibility and applicability.

One of them concerns the direct manipulation of all model mechanisms defined by SMP2. So far, the developed prototype deals mainly with simulation assemblies that connect models using field links. Although the dataflow paradigm suffices for modelling most of the scenarios, the architecture should also enable steering via other model interfaces like events, operations, and exposed failures. Moreover, the assembly itself could be modifiable in runtime, allowing the engineer to redefine model associations and connections, and possibly the number of instances in the simulation. In this functionality, the use of SMP2 *Link Registry* service and the reconnecting state should be considered.

Additionally, the popularization of the presented approach will depend also on the development (or adoption) of an efficient communication architecture to easy the interoperability of the infrastructure with existing systems, such as visualization toolkits, specialised domain tools or customised steering clients.

Regarding the visualization, which is a fundamental feature for steering environments, new studies should exploit the cutting-edge technology in the HCI field to enhance the user's front-end with immersive and natural interfaces.

Further, the computational steering of 3D elements in the simulation could also be improved by the integration of modern Computer-Aided Design (CAD) tools, taking advantage of their parametric design capabilities. The drawing representations could be linked in both environments then constrained by parametric relations defined by the user. Once the drawing is updated in any of the applications, the changes are propagated bi-directionally to ensure the whole model consistency. For instance, the dimensional parameters of a solar panel in the simulation could be automatically updated from notifications triggered by modifications done in the CAD, and vice-versa.

Nevertheless, the parameters coupling of SMP2 and CAD models is out of scope of existing standards and some effort on harmonizing their meta-models must be done to easy this integration. In this sense, geometric attributes, such as position, relative orientation, size (scale), shape, and appearance (colour, texture) could be formalized in the Simulation Model Definition Language. On the simulation side, these parameters could facilitate the creation of specialized mechanism to model geometrical relations (e.g. mechanical interference and collisions or position and relative distance of sensors and actuators) and to associate the model state to its visual representation (e.g. changing colours). On the user interface side, steering widgets could directly be given access to the interfaces implemented by models (i.e. entry points, fields, operations, failures). Moreover, this level of standardisation would enable the creation of editing and automation tools, based on the same catalogue source.

Furthermore, the use of other communication schemes could be considered for connecting the distributed elements in the steering facility, such as those implemented by protocols of Service Oriented Architecture or High-Level Architecture, since in the presented prototype, the integration of visualization systems, steering clients and legacy systems has been done over a TCP/IP channel, using an ad-hoc protocol. In this evaluation, the adopted communication architecture shall:

- guarantee enough data throughput for real-time simulations;
- implement the data-exchange in both directions;
- be flexible to attach different types of clients; and
- be prepared to synchronise commands from different sources of steering widgets (i.e. support user collaboration in the environment).

Finally, the usability of the steering environment for space engineering applications could be assessed from the perspective of different user profiles and disciplines by applying multidisciplinary methodologies from areas such as human-computer interaction, psychology, software and systems engineering.

REFERENCES

ADKINS, G.; POOCH, U. W. Computer simulation: a tutorial. **Computer**, IEEE Computer Society, Los Alamitos, CA, USA, v. 10, n. 4, p. 12–17, 1977. ISSN 0018-9162. 15

ADVANCED VISUAL SYSTEMS INC. **AVS user's guide**. Waltham, 1992. 32

AGRE, J. R.; CLARKE, J. A.; ATKINSON, M. W.; SHAHNAWAZ, I. H. Computer simulation of communications on the space station data management system. In: CONFERENCE ON WINTER SIMULATION, 19., 1987, Atlanta. **Proceedings...** Atlanta, 1987. p. 809–818. 15, 16

AMBROSIO, A.; CARDOSO, P.; ORLANDO, V. Brazilian satellite simulators: Previous solutions trade-off and new perpectives for the cbers program. In: SPACE OPERATIONS CONFERENCE, 2006, Rome. **Proceedings...** Rome, 2006. 15

AMBROSIO, A. M.; GUIMARÃES, D. C.; BARRETO, J. P. Satellite simulator requirements specification based on standardized space services. In: LOUREIRO, G.; CURRAN, R. (Ed.). **Complex systems concurrent engineering**. São José dos Campos: Springer-Verlag, 2007. p. 175–183. 19

ANALYTICAL GRAPHICS, INC. **STK fundamentals**. Exton, PA, 2007. 670 p. User Manual. 9, 46

ARGÜELLO, L.; MIRÓ, J.; GUJER, J.; NERGAARD, K. SMP: A step towards model reuse in simulation. **ESA bulletin**, v. 103, p. 107 – 111, 2000. 25

ASLANIDI, O.; BRODLIE, K.; CLAYTON, R.; HANDLEY, J.; HOLDEN, A.; WOOD, J. Remote visualization and computational steering of cardiac virtual tissues using gViz. In: E-SCIENCE ALL HANDS MEETING, 2005, Nottingham. **Proceedings...** Nottingham, 2005. p. 6. 47

BAI, X.; WU, X. A simulation and visualization platform for fractionated spacecraft attitude control system. In: INTERNATIONAL CONFERENCE ON MECHATRONICS AND AUTOMATION, 2011, Beijing. **Proceedings...** Beijing: IEEE, 2011. p. 2033 –2038. ISSN 2152-7431. 9

BALCI, O. Principles and techniques of simulation validation, verification, and testing. In: ALEXOPOULOS, C.; KANG, K.; LILEGDON, W. R.; GOLDSMAN, D. (Ed.). **Proceedings...** Arlington, 1995. p. 147–154. 6

BERNSEN, N. O. Foundations of multimodal representations: a taxonomy of representational modalities. **Interacting with Computers**, v. 6, n. 4, p. 347 – 371, 1994. ISSN 0953-5438. Available from Internet: <http://www.sciencedirect.com/science/article/pii/0953543894900086>. 35

_____. **A taxonomy of input modalities**. Roskilde, Denmark, 1995. 11 p. Technical Report. Available from Internet: <ftp://ftp.mrc-cbu.cam.ac.uk/amodeus/taxmod/tm_wp22.rtf>. 35

BETTS, B. J.; MUNDO, R. D.; ELCOTT, S.; MCINTOSH, D.; NIEHAUS, B.; PAPASIN, R.; MAH, R. W. A data management system for international space station simulation tools. In: INTERNATIONAL CONFERENCE APPLIED SIMULATION AND MODELING, 2002, Crete. **Proceedings...** Crete: IASTED, 2002. p. 500–504. 9, 16

BHANDERI, D. D. V. **Spacecraft attitude determination with Earth albedo corrected Sun sensor measurements**. Thesis (PhD) — Aalborg University, Aalborg, Denmark, 2005. 95

BIESIADECKI, J.; HENRIQUES, D.; JAIN, A. A reusable, real-time spacecraft dynamics simulator. In: DIGITAL AVIONICS SYSTEMS CONFERENCE, 16., 1997, Irvine, CA. **Proceedings...** Irvine, CA: AIAA/IEEE, 1997. v. 2, p. 8.2 –8–8.2–14. 19

BLAKE, J. **Natural user interfaces in .NET**. e-book: Manning, 2010. 39

BLANCHETTE, J.; SUMMERFIELD, M. **C++ GUI programming with Qt 4**. Upper Saddle River, NJ: Prentice Hall PTR, 2006. ISBN 0-13-124072-2. 36

BODIN, P.; NYLUND, M.; BATTELINO, M. Satsim - a real-time multi-satellite simulator for test and validation in formation flying projects. **Acta Astronautica**, v. 74, n. 0, p. 29 – 39, 2012. ISSN 0094-5765. Available from Internet: <http://www.sciencedirect.com/science/article/pii/S009457651100350X>. 15

BORRMANN, A.; WENISCH, P.; EGGER, M.; TREECK, C. van; RANK, E. Collaborative computational steering: Interactive collaborative design of ventilation and illumination of operating theatres. In: INTELLIGENT COMPUTING IN ENGINEERING, 2008, Plymouth. **Proceedings...** Plymouth, 2008. 50

BOWMAN, D. A.; KRUIJFF, E.; JR., J. J. L.; POUPYREV, I. **3D user interfaces**: theory and practice. Boston: Addison-Wesley, 2004. 29

BRODLIE, K.; POON, A.; WRIGHT, H.; BRANKIN, L.; BANECKI, G.; GAY, A. GRASPARC-a problem solving environment integrating computation and visualization. In: CONFERENCE ON VISUALIZATION, 1993, San Jose, California, USA. **Proceedings...** San Jose: IEEE, 1993. p. 102–109. 34

BRODLIE, K.; WOOD, J.; DUCE, D.; SAGAR, M. gViz: visualization and computational steering on the grid. In: COX, S. J. (Ed.). **Proceedings...** Nottingham, 2004. p. 54–60. 33, 45, 49

BROUWER, M.; CASTELIJN, A.; SCHENAU, H. van I.; OVING, B.; TIMMERMANS, L.; ZWARTBOL, T. Developments in test and verification equipment for spacecraft. In: INTERNATIONAL WORKSHOP ON SIMULATION FOR EUROPEAN SPACE PROGRAMMES, 2000, Noordwijk. **Proceedings...** Noordwijk, 2000. p. 21. 17, 20, 21

CADETE, R.; DURO, N.; ARAÚJO, B.; PEREIRA, J. iMoted 3D virtual reality solution for assembly, integration and test of the space segment. In: INTERNATIONAL WORKSHOP ON SIMULATION & EGSE FACILITIES FOR SPACE PROGRAMMES, 11., 2010, Noordwijk. **Proceedings...** Noordwijk: ESA, 2010. p. 8. 2, 19

CARRARA, V.; MEDEIROS, V. M. Posicionamento ótimo de painéis solares em satélites solsíncronos. In: REUNIãO ANUAL DA SBPC, 38., 1996, Curitiba. **Proceedings...** Curitiba, 1996. 18

CAZENAVE, C.; ARROUY, W. Implementing SMP2 standard within SimTG simulation infrastructure. In: SIMULATION AND EGSE FACILITIES FOR SPACE PROGRAMMES, 12., 2012, Noordwijk. **Proceedings...** Noordwijk, 2012. 15, 27

CERQUEIRA, C. S. **Emprego de técnicas de realidade virtual em interação em simuladores operacionais de satélites**. 179 p. Dissertação (Mestrado) — Instituto Nacional de Pesquisas Espaciais (INPE), São José dos Campos, 2014-02-17 2014. Available from Internet: <http://urlib.net/sid.inpe.br/mtc-m21b/2014/03.24.13.39>. Cited 06 nov. 2014. 9

CHATEL, F. M.; WUESTEN, H.; MIHAIL, G. Simple attitude visualisation tool for satellite operations. In: SPACE OPERATIONS CONFERENCE, 2006, Rome. **Proceedings...** Rome, 2006. 9, 29

CHATZINIKOS, F.; WRIGHT, H. Computational steering by direct image manipulation. In: VISION MODELING AND VISUALIZATION CONFERENCE, 2001, Stuttgart, Germany. **Proceedings...** Stuttgart, 2001. p. 455–462. 37, 42

CHIN, J.; HARTING, J.; JHA, S.; COVENEY, P. V.; PORTER, A. R.; PICKLES, S. M. Steering in computational science: mesoscale modelling and simulation. **Contemporary Physics**, Taylor and Francis Ltd, v. 44, n. 5, p. 417–434, 2003. ISSN 0010-7514. 52

CLARK, S. **Virtual reality aids Lockheed Martin satellite builders**. Available from Internet: <http://www.spaceflightnow.com/news/n1101/25chil/>. Cited 24 Nov. 2011. 41

COFFEY, D.; LIN, C.-L.; ERDMAN, A. G.; KEEFE, D. F. Design by dragging: An interface for creative forward and inverse design with simulation ensembles. **IEEE Transactions on Visualization and Computer Graphic**, v. 19, n. 12, p. 2783–2791, Dec. 2013. 34, 37, 38, 51

CONNER, B. D.; SNIBBE, S. S.; HERNDON, K. P.; ROBBINS, D. C.; ZELEZNIK, R. C.; DAM, A. van. Three-dimensional widgets. In: SYMPOSIUM ON INTERACTIVE 3D GRAPHICS, 1992, New York, NY. **Proceedings...** New York, 1992. p. 183–188. 36, 38

COOMANS, M. K. D.; TIMMERMANS, H. J. P. Towards a taxonomy of virtual reality user interfaces. In: CONFERENCE ON INFORMATION VISUALIZATION, 1997, London. **Proceedings...** London: IEEE, 1997. p. 279–284. ISSN 1093-9547. 29, 39

COSTANZO, A. di; JIN, C.; VARELA, C. A.; BUYYA, R. Enabling computational steering with an asynchronous-iterative computation framework. In: INTERNATIONAL CONFERENCE ON E-SCIENCE, 2009, Washington, DC, USA. **Proceedings...** Washington: IEEE Computer Society, 2009. p. 255–262. 42, 48

COURTER, B. **Simulation-driven product development**: will form finally follow function? Concord, MA, 2009. Technical Report. 7

CRUZ-NEIRA, C.; SANDIN, D. J.; DEFANTI, T. A.; KENYON, R. V.; HART, J. C. The CAVE: Audio visual experience automatic virtual environment. **Communications of the ACM**, ACM, New York, NY, USA, v. 35, n. 6, p.

64–72, June 1992. ISSN 0001-0782. Available from Internet: <http://doi.acm.org/10.1145/129888.129892>. 40

CUCO, A. P. C.; SOUZA, F. L. de; VLASSOV, V.; NETO, A. J. S. Multi-objective design optimization of a new space radiator. In: INTERNATIONAL CONFERENCE ON ENGINEERING OPTIMIZATION, 2008, Rio de Janeiro. **Proceedings...** Rio de Janeiro, 2008. 18

CULLIMORE, B. A.; RING, S. G.; JOHNSON, D. A. **SINDA/FLUINT general purpose thermal/fluid network analyzer**. Littleton, Colorado, 2005. 1191 p. Users Manual. 165, 233

DAHMANN, J. S.; FUJIMOTO, R. M.; WEATHERLY, R. M. The DoD high level architecture: an update. In: WINTER SIMULATION CONFERENCE, 1998, Washington, DC. **Proceedings...** Washington, 1998. v. 1. ISBN 0-7803-5133-9. 24

DEFOUG, S.; ZIMMERMANN, S. PowerCap, electrical power system simulator for a spacecraft. In: CHANGES IN AERONAUTICAL AND SPACE SYSTEMS: CHALLENGES FOR ON-BOARD ENERGY, 2006, Avignon. **Proceedings...** Avignon, 2006. 18

DELATTE, B.; MANON, F. BASILES on its way up to a wide-spread simulation service. In: INTERNATIONAL WORKSHOP ON SIMULATION FOR EUROPEAN SPACE PROGRAMMES, 2008, Noordwijk. **Proceedings...** Noordwijk, 2008. 27

DENNISTON, J.; UHLIG, T.; GOSLING, A. Columbus desktop trainer: an alternative solution to operations training. In: INTERNATIONAL CONFERENCE ON SPACE OPERATIONS, 12., 2012, Stockholm. **Proceedings...** Stockholm, 2012. 19

DICK, C.; GEORGII, J.; BURGKART, R.; WESTERMANN, R. Computational steering for patient-specific implant planning in orthopedics. In: BOTHA, C.; KINDLMANN, G.; NIESSEN, W.; PREIM, B. (Ed.). **Proceedings...** Delft, 2008. p. 83–92. 48

DoD. **High level architecture run-time infrastructure**: RTI 1.3-next generation programmer's guide. Alexandria, 2000. Technical Report. 24

DONATI, A.; MARTÍNEZ-HERAS, J.; NUNES, P.; TORRÃO, R. Virtual reality for monitoring spacecraft thermal subsystem. In: INTERNATIONAL

CONFERENCE ON SPACE OPERATIONS, 2004, Montreal, Canada. **Proceedings...** Montreal, Canada, 2004. p. poster 270–120. 9, 43

DOWNING, N. Virtual MIL-STD-1553. In: DIGITAL AVIONICS SYSTEMS CONFERENCE, 25., 2006, Houston, TX. **Proceedings...** Houston: IEEE/AIAA, 2006. p. 1–8. Available from Internet: <http://ieeexplore.ieee.org/ielx5/4106227/4106228/04106309.pdf?isnumber=4106228>. 15

DUCE, D.; SAGAR, M. skML: a markup language for distributed collaborative visualization. In: LEVER, L.; MCDERBY, M. (Ed.). **Proceedings...** Canterbury, 2005. Available from Internet: <http://www.comp.leeds.ac.uk/vvr/gViz/publications/skML_EGUK05.pdf>. 33, 47

DURO, N.; CADETE, R.; SOUSA, A. Immersive remote control devices applied in space. In: INTERNATIONAL WORKSHOP ON SYSTEM & CONCURRENT ENGINEERING FOR SPACE APPLICATIONS, 3., 2008, Rome. **Proceedings...** Rome, 2008. p. 3. Available from Internet: <http://www.evolve.pt/images/immersive-remote-control-devices-in-space.pdf>. 2, 43

DUTCH SPACE. **EuroSim Mk4.0 software user's manual**. Leiden, 2006. 49 p. User Manual. 27, 46

ECKSTEIN, R.; LOY, M.; WOOD, D. **Java swing**. Sebastopol: O'Reilly, 1998. 1227 p. (The Java serie). ISBN 1-56592-455-X. 36

ECSS. **Space project management**: project phasing and planning. Noordwijk, The Netherlands: European Cooperation for Space Standardization (ECSS), April 1996. 269 p. Superseded Standard ECSS-M-30A. Available from Internet: <http://www.ecss.nl>. 6

______. **Simulation model portability**: handbook. Noordwijk: European Cooperation for Space Standardization (ECSS), 2002. Technical Report. 25

______. **Space engineering**: verification. Noordwijk, The Netherlands: European Cooperation for Space Standardization (ECSS), March 2009. Standard ECSS-E-ST-10-02c. Available from Internet: <http://www.ecss.nl>. 7, 15

______. **Space product assurance**: software product assurance. Noordwijk, The Netherlands: European Cooperation for Space Standardization (ECSS), 2009. Standard ECSS-Q-ST-80C. Available from Internet: <http://www.ecss.nl>. 15

_____. **Space project management**: project planning and implementation. Noordwijk, The Netherlands: European Cooperation for Space Standardization (ECSS), March 2009. 269 p. Standard ECSS-M-ST-10C. Available from Internet: <http://www.ecss.nl>. 5, 6

_____. **Space engineering**: system modelling and simulation. Noordwijk, The Netherlands: European Cooperation for Space Standardization (ECSS), April 2010. Technical Memorandum ECSS-E-TM-10-21a. Available from Internet: <http://www.ecss.nl/>. 1, 8, 23, 24, 26, 46, 69

_____. **Space engineering**: verification guidelines. Noordwijk, The Netherlands: European Cooperation for Space Standardization (ECSS), December 2010. Standard ECSS-E-HB-10-02A. Available from Internet: <http://www.ecss.nl>. 7

_____. **Space engineering: Simulation modelling platform**: principles and requirements. Noordwijk, The Netherlands: European Cooperation for Space Standardization (ECSS), January 2011. v. 1A, 49 p. Technical Memorandum ECSS-E-TM-40-07. Available from Internet: <http://www.ecss.nl>. 3, 24, 25

_____. **Space engineering: Simulation modelling platform**: component model. Noordwijk, The Netherlands: European Cooperation for Space Standardization (ECSS), January 2011. v. 3A, 269 p. Technical Memorandum ECSS-E-TM-40-07. Available from Internet: <http://www.ecss.nl>. 46, 71

_____. **Space engineering: Simulation modelling platform**: SMP usage. Noordwijk, The Netherlands: European Cooperation for Space Standardization (ECSS), January 2011. v. 5A, 129 p. Technical Memorandum ECSS-E-TM-40-07. Available from Internet: <http://www.ecss.nl>. 72, 217

EICKHOFF, J. **Simulating spacecraft systems**. Berlin: Springer, 2009. 22, 23, 69

EICKHOFF, J.; FALKEB, A.; RÖSER, H.-P. Model-based design and verification–state of the art from Galileo constellation down to small university satellites. **Acta Astronautica**, v. 61, p. 383–390, 2007. 22

EISENMANN, H.; CAZENAVE, C. SimTG: successful harmonization of simulation infrastructures. In: INTERNATIONAL WORKSHOP ON SIMULATION FOR EUROPEAN SPACE PROGRAMMES, 2008, Noordwijk. **Proceedings...** Noordwijk: ESA, 2008. 27

ELFVING, A. The attitude and orbit control of XMM. **ESA bulletin**, v. 100, p. 6, 1999. 15, 18, 21

ENGQUIST, E. Steering and visualization of electro-magnetic simulations using the Globus implementation of a computational grid. In: SIMULATION AND VISUALIZATION ON THE GRID, 1999, Stockholm, Sweden. **Proceedings...** Stockholm, 1999. 40

ESNARD, A.; RICHART, N.; COULAUD, O. A steering environment for online parallel visualization of legacy parallel simulations. In: INTERNATIONAL SYMPOSIUM ON DISTRIBUTED SIMULATION AND REAL TIME APPLICATIONS, 10., 2006, Malaga, Spain. **Proceedings...** Malaga, 2006. 33, 48

ESTEFAN, J. A. **Survey of model-based systems engineering (MBSE) methodologies**. Pasadena, CA, 2008. 70 p. Technical Report. 5, 7

ESTLIN, T.; CASTANO, R.; GAINES, D.; BORNSTEIN, B.; JUDD, M.; ANDERSON, R. C. Enabling autonomous science for a Mars rover. In: SPACE OPERATIONS CONFERENCE, 2008, Heidelberg, Germany. **Proceedings...** Heidelberg, 2008. 15

EZUST, A.; EZUST, P. **An introduction to design patterns in C++ with Qt 4**. Upper Saddle River, NJ, USA: Prentice Hall PTR, 2006. ISBN 0-13-124072-2. 71

FERREIRA, L. D. D.; CRUZ, J. J. da. Attitude and spin rate control of a spinning satellite using geomagnetic field. **Journal of Guidance, Control, and Dynamics**, v. 14, n. 1, p. 216–218, 1991. 15

FINLAY, C. C.; MAUS, S.; BEGGAN, C. D.; BONDAR, T. N.; CHAMBODUT, A.; CHERNOVA, T. A.; CHULLIAT, A.; GOLOVKOV, V. P.; HAMILTON, B.; HAMOUDI, M.; HOLME, R.; HULOT, G.; KUANG, W.; LANGLAIS, B.; LESUR, V.; LOWES, F. J.; LÜHR, H.; MACMILLAN, S.; MANDEA, M.; MCLEAN, S.; MANOJ, C.; MENVIELLE, M.; MICHAELIS, I.; OLSEN, N.; RAUBERG, J.; ROTHER, M.; SABAKA, T. J.; TANGBORN, A.; TOFFNER-CLAUSEN, L.; THÉBAULT, E.; THOMSON, A. W. P.; WARDINSKI, I.; WEI, Z.; ZVEREVA, T. I. International geomagnetic reference field: the eleventh generation. **Geophysical Journal International**, Blackwell Publishing Ltd, v. 183, n. 3, p. 1216–1230, 2010. ISSN 1365-246X. Available from Internet: <`http://dx.doi.org/10.1111/j.1365-246X.2010.04804.x`>. 95

FISCHER, P.; WOLFF, R.; GERNDT, A. Collaborative satellite configuration supported by interactive visualization. In: AEROSPACE CONFERENCE, 2012, Boston. **Proceedings...** Boston: IEEE, 2012. p. 1–11. ISSN 1095-323X. 2

FOLEY, J.; WALLACE, V.; CHAN, P. The human factors of computer graphics interaction techniques. **Computer Graphics and Applications, IEEE**, v. 4, n. 11, p. 13–48, Nov. 1984. ISSN 0272-1716. 35, 37

FOULSER, D. IRIS explorer: a framework for investigation. **SIGGRAPH Computer Graphics**, ACM, New York, NY, USA, v. 29, n. 2, p. 13–16, May 1995. ISSN 0097-8930. Available from Internet: <http://doi.acm.org/10.1145/204362.204365>. 32

FRANCO, R.; MIRÓ, J. The project test bed and its application to future missions. **ESA bulletin**, v. 95, p. 5, 1998. 16

FREUND, E.; ROSSMANN, J.; TUMER, C. Application of robotic mechanisms to simulation of the international space station. In: INTERNATIONAL CONFERENCE ON INTELLIGENT ROBOTS AND SYSTEMS, 16., 2003, Las Vegas. **Proceedings...** Las Vegas: IEEE/RSJ, 2003. Available from Internet: <http://ieeexplore.ieee.org/ielx5/8832/27971/01249624.pdf?arnumber=1249624>. 1, 15, 16, 19

FRITZ, M.; ROESER, H.-P. Low cost control and simulation environment for the 'Flying Laptop', a university microsatellite. In: SPACE OPERATIONS CONFERENCE, 2010, Alabama. **Proceedings...** Alabama, 2010. 15

FRITZEN, P. Model driven development of simulators. In: EUROPEAN GROUND SYSTEM ARCHITECTURE WORKSHOP, 2009, Darmstadt, Germany. **Proceedings...** Darmstadt, 2009. 15

FRITZEN, P.; SEGNERI, D.; PIGNEDE, M. SWARMSIM - the first fully SMP2 based simulator for ESOC. In: INTERNATIONAL WORKSHOP ON SIMULATION & EGSE FACILITIES FOR SPACE PROGRAMMES, 11., 2010, Noordwijk. **Proceedings...** Noordwijk, 2010. 217

GAO, P.; YANG, D.; SHEN, M.; GUO, X.; YU, H.; ZHAO, Y.; XU, Z. Space situation simulation and visualization based on OGRE. In: INTERNATIONAL CONFERENCE ON FUZZY SYSTEMS AND KNOWLEDGE DISCOVERY, 8., 2011, Shanghai. **Proceedings...** Shanghai: IEEE, 2011. v. 4, p. 2566–2569. 9

GENTINA, J. **Desenvolvimento e simulação da lógica embarcada para manobras de rendezvous e docking da plataforma orbital recuperável SARA**. Dissertação (INPE-16692-TDI/1636) — Instituto Nacional de Pesquisas Espaciais, São José dos Campos, 2010. 9

GIBBONS, J. Datatype-generic programming. In: BACKHOUSE, R.; GIBBONS, J.; HINZE, R.; JEURING, J. (Ed.). **Spring School on Datatype-Generic Programming**. Springer-Verlag, 2007, (Lecture Notes in Computer Science, v. 4719). Available from Internet: <`http://www.cs.ox.ac.uk/jeremy.gibbons/publications/dgp.pdf`>. 3

GOTTLIEB, E.; HARRIGAN, R.; MCDONALD, M.; OPPEL, F.; XAVIER, P. **The Umbra simulation framework**. Albuquerque, New Mexico, USA, 2001. 17 p. Technical Report. Available from Internet: <`http://umbra.sandia.gov/pdfs/resources/framework.pdf`>. 30

GOULD, H.; TOBOCHNIK, J. **An introduction to computer simulation methods**: applications to physical systems. New York: Addison-Wesley, 1996. 695 p. 15

HABER, R.; BLISS, B.; JABLONOWSKI, D.; JOG, C. A distributed environment for run-time visualization and application steering in computational mechanics. **Computing Systems in Engineering**, v. 3, n. 1–4, p. 501 – 515, 1992. ISSN 0956-0521. Available from Internet: <`http://www.sciencedirect.com/science/article/pii/0956052192901356`>. 31, 44

HAMMERS, S. R. Virtual satellite. **NASA Tech Briefs**, p. 1, 2008. 16

HAO, H.; PEI, C.; YONGKANG, S.; CHAO, H. Real time three-dimensional simulation platform for satellite mission analysis. In: IEEE CONFERENCE ON INDUSTRIAL ELECTRONICS AND APPLICATIONS, 6., 2011, Singapore. **Proceedings...** Singapore: IEEE, 2011. p. 2593–2598. ISSN pending. 9

HASSMANN, C. H. G. **Simulação e visualização da atitude de satélites com painéis articulados**. Dissertação (INPE-15398-TDI/1412) — Instituto Nacional de Pesquisas Espaciais, São José dos Campos, 2008. Available from Internet: <`http://urlib.net/sid.inpe.br/mtc-m18@80/2008/11.20.15.44`>. 9, 15, 18

HAYKIN, S. **Neural networks**: a comprehensive foundation. 2nd. ed. Upper Saddle River, NJ, USA: Prentice Hall PTR, 1998. ISBN 0132733501. 157

HECHT, M.; HARTING, J. Using computational steering to explore the parameter space of stability in a suspension. In: NAGEL, W. E.; KRöNER, D. B.; RESCH, M. M. (Ed.). **High Performance Computing in Science and Engineering '09**. Stuttgart: Springer Berlin Heidelberg, 2010. p. 33–48. ISBN 978-3-642-04665-0. 48

HENDRICKS, R.; EICKHOFF, J. The significant role of simulation in satellite development and verification. **Aerospace Science and Technology**, v. 9, n. 3, p. 273–283, 2005. Available from Internet: <http://www.sciencedirect.com/science/article/B6VK2-4FJGSRK-1/1/8673dd244330ec9368c0e1ecd142c92f>. 1, 22

HOLMES, I. R.; KALAWSKY, R. S. The RealityGrid PDA and smartphone clients: developing effective handheld user interfaces for e-science. In: CO, S. J. (Ed.). **Proceedings...** Nottingham, 2006. p. 502–509. 33, 47

IEEE. **IEEE standard for modeling and simulation (M&S) high level architecture (HLA)**: framework and rules. New York, 2000. 27 p. Standard. Available from Internet: <http://ieeexplore.ieee.org/servlet/opac?punumber=7179>. 24

II, J. E. S.; LANZAGORTA, M.; MAXWELL, D.; KUO, E.; UHLMANN, J.; ANDERSON, W.; SHYU, H.-J.; SMITH, W. A computational steering system for studying microwave interactions with missile bodies. In: VISUALIZATION, 2000, Salt Lake City, Utah, USA. **Proceedings...** Salt Lake City: IEEE Computer Society Press, 2000. p. 441–444. 50

INTERNATIONAL ORGANIZATION FOR STANDARDIZATION. **IEC 9126-1**: software engineering-product quality-part 1. Geneva, Switzerland, 2001. 32 p. Technical Report. 54

IRVINE, M.; FRITZEN, P.; ELLSIEPEN, P. Trends in european space simulation: standards, architectures and tools across the mission lifecycle. In: INTERNATIONAL CONFERENCE ON RECENT ADVANCES IN SPACE TECHNOLOGIES, 6., 2013, Istanbul. **Proceedings...** Istanbul, 2013. p. 1163–1167. 15

JENZ, D.; BERNREUTHER, M. The computational steering framework Steereo. In: STATE OF THE ART IN SCIENTIFIC AND PARALLEL COMPUTING, 2010, Reykjavik. **Proceedings...** Reykjavik, 2010. p. 4. Available from Internet: <http://vefir.hi.is/para10/extab/para10-paper-42.pdf>. 45

JIANG, L.; LIU, H.; PARASHAR, M.; SILVER, D. Rule-based visualization in a computational steering collaboratory. In: BUBAK, M.; ALBADA, G.; SLOOT, P.; DONGARRA, J. (Ed.). **Proceedings...** Krakow, Poland: Springer Berlin Heidelberg, 2004, (Lecture Notes in Computer Science, v. 3038). p. 58–65. ISBN 978-3-540-22116-6. 42, 47

JOHN, R. H. S.; MOORMAN, G. J.; BROWN, B. W. Real-time simulation for space station. **Proceedings of the IEEE**, v. 75, n. 3, p. 383–398, 1987. 15, 16

JOHNSON, C.; PARKER, S. G. A computational steering model applied to problems in medicine. In: SUPERCOMPUTING, 1994, Washington, DC, USA. **Proceedings...** Washington: IEEE Press, 1994. p. 540–549. 38, 47

JOHNSON, C.; PARKER, S. G.; HANSEN, C.; KINDLMANN, G. L.; LIVNAT, Y. Interactive simulation and visualization. **Computer**, IEEE Computer Society Press, Los Alamitos, CA, USA, v. 32, p. 59–65, Dec. 1999. ISSN 0018-9162. Available from Internet: <http://portal.acm.org/citation.cfm?id=619046.621358>. 32, 41

KALDEN, O.; FRITZEN, P.; KRANZ, S. SimVis a concurrent engineering tool for rapid simulation development. In: RECENT ADVANCES IN SPACE TECHNOLOGIES, 3., 2007, Istanbul. **Proceedings...** Istanbul, 2007. p. 417 –422. 18, 28

KALDEN, O.; IRVINE, M. ATB - an AOCS test bed simulation framework. In: INTERNATIONAL CONFERENCE ON RECENT ADVANCES IN SPACE TECHNOLOGIES, 5., 2011, Istanbul. **Proceedings...** Istanbul, 2011. p. 480 –484. 18

KANG, J.-Y.; KIM, J.-M.; CHUNG, S. J. Design and development of an advanced real-time satellite simulator. **Electronics and Telecomunications Research Institute Journal**, v. 17, n. 3, p. 14, 1995. Available from Internet: <http://etrij.etri.re.kr/Cyber/servlet/GetFile?fileid=SPF-1044878134030>. 15

KIMURA, K. Satellite orbit analysis and design by virtual reality. In: SPACE OPERATIONS CONFERENCE, 1998, Tokio. **Proceedings...** Tokio, 1998. 1, 9

KNEZEVIC, J.; HERNÁNDEZ, H.; FOGAL, T.; JEVREMOVIC, T. Visual simulation steering for a 3D neutron transport agent code system. In: INTERNATIONAL NUCLEAR AND RENEWABLE ENERGY CONFERENCE, 2010, Amman, Jordan. **Proceedings...** Amman, 2010. p. 5. 49

KOHL, J.; PAPADOPULOS, P. A library for visualization and steering of distributed simulations using PVM and AVS. In: DONGEN, V. V. (Ed.). **Proceedings...** Montreal, 1995. p. 243–254. 31, 44

KRANZ, S. System concept simulation for concurrent engineering. In: SYSTEMS ENGINEERING AND CONCURRENT ENGINEERING FOR SPACE APPLICATIONS, 2014, Stuttgart. **Proceedings...** Stuttgart: ESA, 2014. 15, 18

LAEVSKY, K.; TELEA, A.; MATTHEIJ, R. An interactive visualization tool applied to the simulation of glass pressing. **Computing and Visualization in Science**, v. 4, n. 1, p. 31–40, 1999. 50

LAMMEN, W.; MOELANDS, J.; WIJNANDS, Q. Push and pull of SMP2 compliant models: new developments in automated model transfer with MOSAIC from the user perspective. In: INTERNATIONAL WORKSHOP ON SIMULATION & EGSE FACILITIES FOR SPACE PROGRAMMES, 11., 2010, Noordwijk. **Proceedings...** Noordwijk: ESA, 2010. p. 8. 27

LAMMEN, W.; NELISSE, A.; DAM, A. ten. MOSAIC: Automated model transfer in simulator development. In: WORKSHOP ON SIMULATION FOR EUROPEAN SPACE PROGRAMMES, 2002, Noordwijk. **Proceedings...** Noordwijk, 2002. 27

LAROQUE, C.; PECCHIOLI, M.; SEBASTIAO, N. First experience on using SMP2 for the virtual space system for ground data system validation. In: INTERNATIONAL WORKSHOP ON SIMULATION FOR EUROPEAN SPACE PROGRAMMES, 2008, Noordwijk. **Proceedings...** Noordwijk: ESA, 2008. 19

LARSON, W. J.; WERTZ, J. R. (Ed.). **Space mission analysis and design**. 3. ed. Dordrecht: Kluwer Academic Publishers, 1999. 93

LATOSCHIK, M. E. A user interface framework for multimodal VR interactions. In: INTERNATIONAL CONFERENCE ON MULTIMODAL INTERFACES, 7., 2005, New York, NY, USA. **Proceedings...** New York: ACM, 2005. (ICMI '05), p. 76–83. ISBN 1-59593-028-0. Available from Internet: <`http://doi.acm.org/10.1145/1088463.1088479`>. 39

LAUREL, C. Celestia development status. In: WORKSHOP ON ASTRODYNAMICS TOOLS AND TECHNIQUES, 3., 2006, Noordwijk. **Proceedings...** Noordwijk: ESA, 2006. 9

LEACH, G.; AL-QAIMARI, G.; GRIEVE, M.; JINKS, N.; MCKAY, C. Elements of a three-dimensional graphical user interface. In: HOWARD, S.; HAMMOND, J.;

LINDGAARD, G. (Ed.). **Proceedings...** Sydney, Australia: Springer US, 1997, (IFIP - The International Federation for Information Processing). p. 69–76. ISBN 978-1-4757-5437-7. 36

LEGO, S. E.; STUMP, G. M.; YUKISH, M. Trade space exploration: new visual steering features. In: AEROSPACE CONFERENCE, 2010, Big Sky, MT, USA. **Proceedings...** Big Sky, MT: IEEE, 2010. 18, 50

LICEAGA, C. A. **SPASIM**: a spacecraft simulator. Hampton: NASA Langley Technical Report Server, 1997. Technical Report. 16, 18

LIEREA, R. van; MULDER, J. D.; WIJK, J. J. van. Computational steering. **Future Generation Computer Systems**, v. 12, p. 441–450, 1997. 31, 44

LIM, C. S.; JAIN, A. Dshell++: A component based, reusable space system simulation framework. In: INTERNATIONAL CONFERENCE ON SPACE MISSION CHALLENGES FOR INFORMATION TECHNOLOGY, 3., 2009, Pasadena. **Proceedings...** Pasadena: IEEE, 2009. p. 229 – 236. 19

LING, L. Simulation for prediction of entry article demise (SPEAD): an analysis tool for spacecraft safety analysis and ascentrreentry risk assessment. In: INTERNATIONAL ASSOCIATION FOR THE ADVANCEMENT OF SPACE SAFETY CONFERENCE, 7., 2014, Friedrichshafen. **Proceedings...** Friedrichshafen, 2014. 19

LINGARAJU, G.; NITHIARASU, P.; KUSUMA, M.; GOWDA, R. M. Real-time interactive steerable scientific visualisation of free surface flow in the context of synthetic vision. **Defence Science Journal**, v. 61, n. 4, p. 299–305, 2011. 51

LINXWEILER, J.; KRAFCZYK, M.; TöLKE, J. Highly interactive computational steering for coupled 3D flow problems utilizing multiple GPUs. **Computing and Visualization in Science**, Springer Berlin / Heidelberg, v. 13, p. 299–314, 2010. ISSN 1432-9360. 33, 36, 42, 45

LIU, T.; ZHAO, Y.; XU, S. The designing and realizing of the satellite navigation simulation system visualization software. In: INTERNATIONAL CONFERENCE ON COMPUTER SCIENCE AND INFORMATION TECHNOLOGY, 3., 2010, Chengdu. **Proceedings...** Chengdu: IEEE, 2010. v. 1, p. 71–75. 18

LOGAN, S. **GTK+ programming in C**. Upper Saddle River, NJ: Prentice Hall, 2001. ISBN 978-0-13-014264-1. 36

LONGO, C. R. O.; RICKMAN, S. L. **Method for the calculation of spacecraft umbra and penumbra shadow terminator points**. Houston, Texas, 1995. 41 p. Technical Report. 95

LOPES, R. V. da F.; SILVA, A. R.; RELLOSO, J.; ABSI, G.; JUN, Y. Analysis of albedo effects on coarse sun direction determiation algorithms. In: INTERNATIONAL SYMPOSIUM ON SPACE FLIGHT DYNAMICS, 22., 2011, São José dos Campos. **Proceedings...** São José dos Campos, Brazil, 2011. Available from Internet: <http://issfd.org/ISSFD_2011/S11-Attitude.Dynamics.2-AD2/S11_P2_ISSFD22_PF_050.pdf>. 95, 98

LUCAS, B.; ABRAM, G.; COLLINS, N.; EPSTEIN, D.; GRESH, D.; MCAULIFFE, K. An architecture for a scientific visualization system. In: CONFERENCE ON VISUALIZATION, 1992, Boston, MA, USA. **Proceedings...** Boston: IEEE, 1992. p. 107–114. 32

MALAKAR, P.; NATARAJAN, V.; VADHIYAR, S. S. **A framework for online visualization and simulation of critical weather applications**. Bangalore, Karnataka, India, 2011. 31 p. Technical Report. Available from Internet: <http://www.csa.iisc.ernet.in/TR/2011/1/>. 47, 49

MARSHALL, R.; KEMPF, J.; DYER, S.; YEN, C.-C. Visualization methods and simulation steering for a 3D turbulence model of Lake Erie. In: SYMPOSIUM ON INTERACTIVE 3D GRAPHICS, 1990, Snowbird, Utah, USA. **Proceedings...** New York: ACM, 1990. 2, 30, 31, 36, 42, 43, 45

MARTIN, A. C. M.; CARVALHO, M. M. de. **Avaliação do uso da simulação virtual no processo de desenvolvimento de produtos**. Dissertação (Mestrado) — Escola Politécnica da Universidade de São Paulo, São Paulo, 2005. 7

MATHWORKS. **How can I interface MATLAB code with C, C++, or FORTRAN?** 2014. Online. Available from Internet: <http://www.mathworks.com/support/tech-notes/1600/1622_files/1622_R13.html>. Cited 18 june 2014. 157

MATKOVIC, K.; GRACANIN, D.; JELOVIC, M.; CAO, Y. Adaptive interactivemulti-resolution computational steering for complex engineering systems. In: INTERNATIONAL WORKSHOP ON VISUAL ANALYTICS, 2011, Bergen. **Proceedings...** Bergen, 2011. p. 4. 51

MAZZEO, M. D.; MANOS, S.; COVENEY, P. V. In situ ray tracing and computational steering for interactive blood flow simulation. **Computer Physics**

Communications, v. 181, n. 2, p. 355 – 370, 2010. ISSN 0010-4655. Available from Internet: <http://www.sciencedirect.com/science/article/pii/S0010465509003269>. 42, 48

MEDEIROS, V. M.; CARRARA, V. **PROPAT satellite attitude and orbit toolbox for Matlab**. São José dos Campos, 2009. Software. Available from Internet: <http://www2.dem.inpe.br/val/projetos/propat/default.htm>. Cited 14 june 2012. 93

MERIMAA, J.; PERONDI, L. F.; KASKI, K. An interactive simulation program for visualizing complex phenomena in solids. **Computer Physics Communications**, v. 124, p. 60–75, 2000. 48

MICHALSKY, J. J. The astronomical almanacs algorithm for approximate solar position (1950-2050). **Solar Energy**, v. 40, n. 3, p. 227–235, 1988. 95

MILGRAM, P.; KISHINO, F. A taxonomy of mixed reality visual displays. **IEICE Transactions on Information Systems**, v. 77, n. 12, p. 1321–1329, 1994. 40

MILLER, M.; HANSEN, C.; PARKER, S.; JOHNSON, C. Simulation steering with SCIRun in a distributed environment. In: INTERNATIONAL SYMPOSIUM ON HIGH PERFORMANCE DISTRIBUTED COMPUTING, 7., 1998, Chicago, IL, USA. **Proceedings...** Chicago, 1998. p. 364 –365. ISSN 1082-8907. 32

MULDER, J.; WIJK, J. van. 3D computational steering with parametrized geometric objects. In: CONFERENCE ON VISUALIZATION, 1995, Atlanta, GA, USA. **Proceedings...** Atlanta: IEEE, 1995. p. 304 –311, 466. 38

MULDER, J. D.; LIERE, R. van; WIJK, J. J. van. Computational steering in the CAVE. **Future Generation Computer Systems**, Elsevier Science Publishers B. V., Amsterdam, The Netherlands, The Netherlands, v. 14, p. 199–207, Aug. 1998. ISSN 0167-739X. Available from Internet: <http://portal.acm.org/citation.cfm?id=1707847>. 40

MULDER, J. D.; WIJK, J. J. V.; LIERE, R. V. A survey of computational steering environments. **Future Generation Computer Systems**, v. 13, p. 17, 1998. 32, 44, 51, 60, 61

MUSETH, K.; BARR, A.; LO, M. Semi-immersive space mission design and visualization: case study of the Terrestrial Planet Finder mission. In: VISUALIZATION, 2001, San Diego, CA. **Proceedings...** San Diego, CA: IEEE, 2001. p. 501–599. 1

MYERS, B. A. User interface software tools. **ACM Transactions on Computer-Human Interaction**, ACM, New York, NY, USA, v. 2, n. 1, p. 64–103, Mar. 1995. ISSN 1073-0516. Available from Internet: <http://doi.acm.org/10.1145/200968.200971>. 36

NASA. **Space station simulation computer system (SCS) study for NASA/MSFC**: overview and summary. Huntsville, 1989. v. 1, n. TRW-SCS-89-T7, 62 p. Technical Report. 16

NASA, NATIONAL AERONAUTICS AND SPACE ADMINISTRATION. **Standard for models and simulations**. Washington, DC, 2008. Technical Report. 15

NAYAR, H.; JAIN, A.; BALARAM, J.; CAMERON, J.; LIM, C.; MUKHERJEE, R.; POMERANTZ, M.; REDER, L.; MYINT, S.; SERRANO, N.; WALL, S. Recent developments on a simulator for lunar surface operations. In: SPACE OPERATIONS CONFERENCE, 2009, Pasadena. **Proceedings...** Pasadena: AIAA, 2009. Available from Internet: <http://www-robotics.jpl.nasa.gov/publications/Abhinandan_Jain/2009-LSOSSpaceOps.pdf>. 19

NEC. **Ux software Motif programmer's reference**. Palo Alto, CA: NEC Corporation, 1992. 36

NEEFS, M.; HAYE, M. Flexible hardware in the loop configuration in spacecraft test benches. In: INTERNATIONAL WORKSHOP ON SIMULATION & EGSE FACILITIES FOR SPACE PROGRAMMES, 11., 2010, Noordwijk. **Proceedings...** Noordwijk: ESA, 2010. p. 7. 19

NEMETH, S. M.; DEMAREST, P. Research and development in application of the simulation model portability standard. In: SPACE OPERATIONS CONFERENCE, 2010, Alabama. **Proceedings...** Alabama, 2010. 27

NESNAS, I. Claraty: A collaborative software for advancing robotic technologies. In: NASA SCIENCE AND TECHNOLOGY CONFERENCE, 2007, University of Maryland University College, Adelphi. **Proceedings...** Adelphi, 2007. p. 7. 15, 16

NORRIS, J.; DAVIDOFF, S. NASA telexploration project demo. In: VIRTUAL REALITY, 2014, Minneapolis, MN. **Proceedings...** Minneapolis, MN: iEEE, 2014. p. 183–184. 1

OLIVEIRA, S. B. d. **Fragmentação por ação aerotermodinâmica e predição da área de impacto de um veículo espacial com injeção controlada da**

re-entrada. Thesis (PhD) — Instituto Nacional de Pesquisas Espaciais, São José dos Campos, 2009. 19

ORLANDO, V.; ROZENFELD, P.; MIGUEZ, R. R. B.; FONSECA, I. M. da. Brazilian data collecting satellite simulator. In: INTERNATIONAL SYMPOSIUM ON SPACE TECHNOLOGY AND SCIENCE, 1992, Kagoshima, Japan. **Proceedings...** Kagoshima, Japan, 1992. p. 915–919. 15, 19

PALOMBA, M.; MASSOTTI, L.; AGUIRRE, M.; SILVESTRIN, P. Aocsim: a tool for rapid analysis of satellite dynamics during the early phases of a project. In: INTERNATIONAL WORKSHOP ON SIMULATION ON EUROPEAN SPACE PROGRAMMES, 10., 2008, Noordwijk. **Proceedings...** Noordwijk: ESA, 2008. 18

PAPASIN, R.; BETTS, B. J.; MUNDO, R. D.; GUERRERO, M.; MAH, R. W.; MCINTOSH, D. M.; WILSON, E. Intelligent virtual station. In: INTERNATIONAL SYMPOSIUM ON ARTIFICIAL INTELLIGENCE, ROBOTICS AND AUTOMATION IN SPACE, 7., 2003, Nara, Japan. **Proceedings...** Nara, 2003. Available from Internet: <http://robotics.estec.esa.int/i-SAIRAS/isairas2003/data/pdf/AM52paper.pdf>. 9, 16

PARKER, S.; JOHNSON, C. SCIRun: A scientific programming environment for computational steering. In: SUPERCOMPUTING CONFERENCE, 1995, San Diego, CA, USA. **Proceedings...** San Diego: IEEE/ACM, 1995. p. 52–52. 32

PARKER, S.; JOHNSON, C.; BEAZLEY, D. Computational steering. software systems and strategies. **Computational Science Engineering, IEEE**, v. 4, n. 4, p. 50 –59, Oct.–Dec. 1997. ISSN 1070-9924. 31, 32, 42, 44

PARKER, S.; MILLER, M.; HANSEN, C.; JOHNSON, C. An integrated problem solving environment: the SCIRun computational steering system. In: INTERNATIONAL CONFERENCE ON SYSTEM SCIENCES, 31., 1998, Hawaii. **Proceedings...** Hawaii, 1998. v. 7, p. 147 –156. 29, 32, 41, 45

PARKER, S. G. **The SCIRun problem solving environment and computational steering software system**. Thesis (PhD) — University of Utah, 1999. 32, 51, 60, 61

PARTHASARATHY, M. **Practical software estimation**: function point methods for insourced and outsourced projects. India: Pearson Education, 2007. ISBN 0132702444-BEEPB. 54

PASETTI, A. **Software frameworks and embedded control systems**. Berlin, Germany: Springer, 2002. 293 p. 19

PAVLOVIC, V.; SHARMA, R.; HUANG, T. Visual interpretation of hand gestures for human-computer interaction: a review. **Pattern Analysis and Machine Intelligence, IEEE Transactions on**, v. 19, n. 7, p. 677–695, July 1997. ISSN 0162-8828. 39

PERONDI, L. F. **Análise de potência do satélite de coleta de dados 1 (SCD-1)**. São José dos Campos, 1987. Technical Report. 15, 18

PICKLES, S.; HAINES, R.; PINNING, R.; PORTER, A. A practical toolkit for computational steering. **Philosophical Transactions of the Royal Society A: Mathematical, Physical and Engineering Sciences**, v. 363, n. 1833, p. 1843–1853, 2005. Available from Internet: <`http://rsta.royalsocietypublishing.org/content/363/1833/1843.abstract`>. 33

PICKLES, S. M.; BLAKE, R. J.; BOGHOSIAN, B. M.; BROOKE, J. M.; CHIN, J.; CLARKE, P. E. L.; COVENEY, P. V.; GONZÁLEZ-SEGREDO, N.; HAINES, R.; HARTING, J.; HARVEY, M.; JONES, M. A. S.; MCKEOWN, M.; PINNING, R. L.; PORTER, A. R.; ROY, K.; RIDING, M. The TeraGyroid experiment. In: GLOBAL GRID FORUM, 10., 2004, Berlin, Germany. **Proceedings...** Berlin, 2004. Available from Internet: <`http://www.realitygrid.org/TeraGyroid/04-TeraGyroid-Case-Study-GGF10.pdf`>. 33, 43, 47

PIDGEON, A.; STRAW, S.; IRVINE, M.; BODEMANN, C. Galileo constellation operations simulator. In: SPACE OPERATIONS CONFERENCE, 2008, Heidelberg, Germany. **Proceedings...** Heidelberg, 2008. 19

PISANICH, G.; PLICE, L.; NEUKOM, C.; FLÜCKIGER, L.; WAGNER, M. Mission simulation facility: Simulation support for autonomy development. In: AEROSPACE SCIENCES CONFERENCE, 42., 2004, Reno. **Proceedings...** Reno: AIAA, 2004. 16

PMI. **Project management body of knowledge - PMBOK**. 3rd.. ed. Newtown Square, Pennsylvania: Project Management Institute, 2004. 5

POLVERINI, U.; LARRIEU, V. SIMAGE: from rapid prototyping to end to end performance simulation for imaging payloads. In: WORKSHOP ON SIMULATION FOR EUROPEAN SPACE PROGRAMMES, 10., 2008, Noordwijk. **Proceedings...** Noordwijk, 2008. 18

PRUDÊNCIO, S. V. **Simulação digital em tempo real de um sistema de controle de atitude magnético autônomo de um Satélite**. 170 p. Dissertação (Mestrado) — Instituto Nacional de Pesquisas Espaciais, São José dos Campos, 1997. 18

QUARTIER, F.; MANON, F. Simulation for all components, phases and life-cycles of complex space systems. In: COMPLEX SYSTEMS DESIGN & MANAGEMENT, 4., 2013, Paris. **Proceedings...** Paris, 2013. p. 167–174. 27

RAMOS, J.; MOYANO, R.; ACARRETA, J. OpenSF: a generic framework for end-to-end mission performance simulations. In: WORKSHOP ON SIMULATION FOR EUROPEAN SPACE PROGRAMMES, 10., 2008, Noordwijk. **Proceedings...** Noordwijk, 2008. 18

RASURE, J. R.; WILLIAMS, C. S. An integrated data flow visual language and software development environment. **Journal of Visual Languages & Computing**, v. 2, n. 3, p. 217 – 246, 1991. ISSN 1045-926X. Available from Internet: <`http://www.sciencedirect.com/science/article/pii/S1045926X06800078`>. 32

RATHMAYER, S.; LENKE, M. A tool for on-line visualization and interactive steering of parallel HPC applications. In: INTERNATIONAL PARALLEL PROCESSING SYMPOSIUM, 11., 1997, Genva, Switzerland. **Proceedings...** Genva, 1997. p. 181 –186. 31

REBELO, J.; WIJNANDS, Q.; PACE, F.; BLOMMESTIJN, R. The avionics system test bench, functional engineering simulator: new developments in support of mission and system verification. In: INTERNATIONAL WORKSHOP ON SIMULATION & EGSE FACILITIES FOR SPACE PROGRAMMES, 11., 2010, Noordwijk. **Proceedings...** Noordwijk: ESA, 2010. p. 7. 9

REGGESTAD, V.; PECCHIOLI, M.; MERRI, M. Virtual reality for real operations: developing and using operational simulators. **ESA Bulletin**, v. 148, p. 42–51, 2011. 15, 19

RENAMBOT, L.; BAL, H.; GERMANS, D.; SPOELDER, H. CAVEStudy: an infrastructure for computational steering in virtual reality environments. In: INTERNATIONAL SYMPOSIUM ON HIGH-PERFORMANCE DISTRIBUTED COMPUTING, 11., 2000, Pittsburgh, PA, USA. **Proceedings...** Pittsburgh, 2000. 40

REW, D.; JU, G.; KANG, S.; LEE, S. Conceptual design of korea aerospace research institute lunar explorer dynamic simulator. **Journal of Astronomy and Space Sciences**, v. 27, p. 377–382, dec 2010. 27

RIBICIC, H.; WASER, J.; FUCHS, R.; BLOSCHL, G.; GROLLER, E. Visual analysis and steering of flooding simulations. **Visualization and Computer Graphics, IEEE Transactions on**, v. 19, n. 6, p. 1062–1075, 2013. ISSN 1077-2626. 45, 49

RICHART, N.; ESNARD, A.; COULAUD, O. Toward a computational steering environment for legacy coupled simulations. In: INTERNATIONAL SYMPOSIUM ON PARALLEL AND DISTRIBUTED COMPUTING, 6., 2007, Long Beach, CA, USA. **Proceedings...** Long Beach, 2007. p. 43. 45

RICHTER, J. **Applied Microsoft .NET framework programming**. Redmond, WA: Microsoft Press, 2002. 632 p. 36

RIEDEL, M.; FRINGS, W.; HABBINGA, S.; EICKERMANN, T.; MALLMANN, D.; STREIT, A.; WOLF, F.; LIPPERT, T.; ERNST, A.; SPURZEM, R. Extending the collaborative online visualization and steering framework for computational grids with attribute-based authorization. In: INTERNATIONAL CONFERENCE ON GRID COMPUTING, 9., 2008, Tsukuba. **Proceedings...** Tsukuba: EEE/ACM, 2008. p. 104 –111. 47

RIZE, J.; HOFFMAN, J.; CARPENTER, M.; COHANIM, B. Real-time virtual reality environment for majic attitude control system development and implementation. In: AEROSPACE CONFERENCE, 2014, Big Sky, MT. **Proceedings...** Big Sky, MT: IEEE, 2014. p. 1–11. 1

RUESS, M.; MUNDANI, R.-P.; RANK, E. Computational steering in dynamic structure simulation: an improved communication concept. In: INTERNATIONAL CONFERENCE SCIENCE AND TECHNOLOGY FOR HUMANITY, 2009, Toronto. **Proceedings...** Toronto: IEEE, 2009. p. 497 – 502. Available from Internet: <http://ieeexplore.ieee.org/stamp/stamp.jsp?tp=&arnumber=5444450>. 50

SAGARDIA, M.; HERTKORN, K.; HULIN, T.; WOLFF, R.; HUMMELL, J.; DODIYA, J.; GERNDT, A. An interactive virtual reality system for on-orbit servicing. In: VIRTUAL REALITY, 2013, Orlando, FL. **Proceedings...** Orlando, FL: IEEE, 2013. p. 1–1. ISSN 1087-8270. 1

SCHAUS, V.; FISCHER, P. M.; LüDTKE, D.; BRAUKHANE, A.; ROMBERG, O.; GERNDT, A. Concurrent engineering software development at German Aerospace Center: status and outlook. In: INTERNATIONAL WORKSHOP ON SYSTEM & CONCURRENT ENGINEERING FOR SPACE APPLICATIONS, 4., 2010, Lausanne. **Proceedings...** Lausanne: ESA, 2010. Available from Internet: <http://elib.dlr.de/65913/1/SCHAUS_PAPER.pdf>. 18

SCHENAU, H. van I.; RIJN, L. van; SPAA, J. Test and verification equipment for the attitude and orbit control system of the XMM satellite. In: DATA SYSTEMS IN AEROSPACE, 1998, Athens. **Proceedings...** Athens, 1998. 15, 17, 20

SCHROEDER, W.; LORENSEN, W.; MONTANARO, G.; VOLPE, C. VISAGE: an object-oriented scientific visualization system. In: CONFERENCE ON VISUALIZATION, 1992, Boston, MA. **Proceedings...** Boston: IEEE, 1992. p. 219–226. 32

SCHROEDER, W. J.; MARTIN, K. M.; LORENSEN, W. E. The design and implementation of an object-oriented toolkit for 3D graphics and visualization. In: CONFERENCE ON VISUALIZATION, 7., 1996, Los Alamitos, CA, USA. **Proceedings...** Los Alamitos: IEEE Computer Society Press, 1996. (VIS '96), p. 93–100. ISBN 0-89791-864-9. Available from Internet: <http://dl.acm.org/citation.cfm?id=244979.245018>. 32

SCHUMANN, H.; BERRES, A.; MAIBAUM, O.; RÖHNSCH, A. DLR's virtual satellite approach. In: INTERNATIONAL WORKSHOP ON SIMULATION ON EUROPEAN SPACE PROGRAMMES, 10., 2008, Noordwijk. **Proceedings...** Noordwijk: ESA, 2008. 18

SCODITTI, A.; BLANCH, R.; COUTAZ, J. A novel taxonomy for gestural interaction techniques based on accelerometers. In: INTERNATIONAL CONFERENCE ON INTELLIGENT USER INTERFACES, 16., 2011, New York, NY. **Proceedings...** New York: ACM, 2011. (IUI '11), p. 63–72. ISBN 978-1-4503-0419-1. Available from Internet: <http://doi.acm.org/10.1145/1943403.1943414>. 39

SEBASTIAO, N.; NISIO, N. D. A new standard for simulation model´s portability and its implementation in Simulus. In: INTERNATIONAL WORKSHOP ON SIMULATION ON EUROPEAN SPACE PROGRAMMES, 10., 2008, Noordwijk. **Proceedings...** Noordwijk, 2008. 27

SEBASTIAO, N.; REGGESTAD, V.; SPADA, M.; WILLIAMS, A.; PECCHIOLI, M.; LINDMAN, N.; FRITZEN, P. A reference architecture for spacecraft simulators. In: SPACE OPERATIONS CONFERENCE, 2008, Heidelberg, Germany. **Proceedings...** Heidelberg, 2008. 15, 27

SHAFTO, M.; CONROY, M.; DOYLE, R.; GLAESSGEN, E.; KEMP, C.; LEMOIGNE, J.; WANG, L. **Modeling, simulation, information technology & processing roadmap**. Washington, DC, 2010. Technical Report. 23

SHU, J.; WATSON, L. T.; RAMAKRISHNAN, N.; FREDERICK, K. A.; DESHPANDE, S. Computational steering in the problem solving environment WBCSim. **Engineering Computations**, v. 28, n. 7, p. 29, 2011. ISSN 0264-4401. Available from Internet: <http://www.emeraldinsight.com/journals.htm?issn=0264-4401&volume=28&issue=7&articleid=1949115&show=pdf&PHPSESSID=m87lfuslls3pu9t85u0ha7qdp7>. 47

SKLUZACEK, C.; PLAS, P. van der. OpenIGS 2: A non-intrusive middleware framework for the integration of application and simulation components. In: INTERNATIONAL WORKSHOP ON SIMULATION & EGSE FACILITIES FOR SPACE PROGRAMMES, 11., 2010, Noordwijk. **Proceedings...** Noordwijk: ESA, 2010. p. 8. 9

SONDERMANN, H.; DARBIN, A.; DILLENSCHNEIDER, B.; LAPRADE, Y. Functional verification environment: Current status and breakthrough. In: INTERNATIONAL WORKSHOP ON SIMULATION ON EUROPEAN SPACE PROGRAMMES, 10., 2008, Noordwijk. **Proceedings...** Noordwijk: ESA, 2008. 18

STÖCKLI, R.; VERMOTE, E.; SALEOUS, N.; SIMMON, R.; HERRING, D. **The blue marble next generation: a true color earth dataset including seasonal dynamics from MODIS**. 2005. Available from Internet: <http://eoimages.gsfc.nasa.gov/images/imagerecords/73000/73884/readme.pdf>. 85

STODDEN, D.; GALASSO, G. Space system visualization and analysis using the satellite orbit analysis program (soap). In: AEROSPACE APPLICATIONS CONFERENCE, 1995, Snowmass at Aspen, CO. **Proceedings...** Snowmass at Aspen, CO: IEEE, 1995. p. 369–387 vol.1. 1, 9

STONE, J. E.; KOHLMEYER, A.; VANDIVORT, K. L.; SCHULTEN, K. Immersive molecular visualization and interactive modeling with commodity hardware. **Lecture Notes on Computer Science**, v. 6454, p. 382–393, 2011. 49

STONE, R.; PANFILOV, P.; SHUKSHUNOV, V. Evolution of aerospace simulation: from immersive virtual reality to serious games. In: INTERNATIONAL CONFERENCE ON RECENT ADVANCES IN SPACE TECHNOLOGIES, 5., 2011, Istanbul. **Proceedings...** Istanbul, 2011. p. 655 –662. 1

STUMP, G.; LEGO, S.; YUKISH, M.; SIMPSON, T. W.; DONNDELINGER, J. A. Visual steering commands for trade space exploration: user-guided sampling with example. **Journal of Computing and Information Science in Engineering**, v. 9, n. 4, p. 10, 2009. Available from Internet: <http://www.atsv.psu.edu/webdocs/JCISEjournal.pdf>. 18

SUDHAKAR, P. G.; FAROOQ, A.; PATNAIK, S. Measuring productivity of software development teams. **Serbian Journal of Management**, v. 7, n. 1, p. 65–75, 2012. 54

SYSTEMS, F. **Manufacturing case study**: immersive visualization for virtual prototyipng and presentation applications. 2004. Available from Internet: <http://web.archive.org/web/20050428130931/http://www.fakespacesystems.com/pdfs/EmbraerCStudy.pdf>. Cited 12 Feb. 2012. 41

TANG, J.; GUO, J. 3D visual simulation research on LEO satellite based on PANDA. In: INTERNATIONAL CONFERENCE ON GEOINFORMATICS, 19., 2011, Shanghai. **Proceedings...** Shanghai: IEEE, 2011. p. 1–4. ISSN 2161-024X. 9, 18

TELEA, A. Design of an object oriented computational steering system. In: ECOOP WORKSHOP FOR PHD STUDENTS IN OBJECT-ORIENTED SYSTEMS, 8., 1998, Brussels, Belgium. **Proceedings...** Brussels: Springer Berlin Heidelberg, 1998. p. 12. 33, 38

TELEA, A. C.; WIJK, J. J. **Simulation and visualization in the VISSION object oriented dataflow system**. 1999. 435–442 p. (RANA : reports on applied and numerical analysis, 9933). RANA : reports on applied and numerical analysis, Technical Report. Available from Internet: <http://alexandria.tue.nl/repository/books/532341.pdf>. 33, 38, 45

TI. **Stellaris LM4F120H5QR microcontroller**. Austin, TX, USA: Texas Instruments, 2013. 1191 p. Data sheet. 102

TIMMERMANS, L.; ZWARTBOL, T.; OVING, B.; CASTELEIJN, A.; BROUWER, M. From simulations to operations: developments in test and verification equipment for spacecraft. In: SCHüRMANN, B.; SAWAYA-LACOSTE, H. (Ed.). **Proceedings...** Nice, 2001. 17

TOMINAGA, J.; SILVA, J. D.; FERREIRA, M. A proposal for implementing automation in satellite control planning. In: SPACE OPERATIONS CONFERENCE, 2008, Heidelberg, Germany. **Proceedings...** Heidelberg, 2008. 19

TURNER, A. J. The development and use of open-source spacecraft simulation and control software for education and research. In: INTERNATIONAL CONFERENCE ON SPACE MISSION CHALLENGES FOR INFORMATION TECHNOLOGY, 2., 2006, Washington, DC. **Proceedings...** Washington: IEEE, 2006. 19

VETTER, J. S.; SCHWAN, K. Progress: a toolkit for interactive program steering. In: INTERNATIONAL CONFERENCE ON PARALLEL PROCESSING, 24., 1995, Oconomowoc, WI. **Proceedings...** Oconomowoc: CRC Press, 1995. Available from Internet: <http://hdl.handle.net/1853/6686>. 31

VRIES, R. de; MOELANDS, J. SMP2 developments in EuroSim. In: INTERNATIONAL WORKSHOP ON SIMULATION ON EUROPEAN SPACE PROGRAMMES, 10., 2008, Noordwijk. **Proceedings...** Noordwijk, 2008. 27

VRIES, R. de; MOELANDS, J. M. Collaboration on simulation model platform standardisation in the EuroSim consortium. In: WORKSHOP ON SIMULATION FOR EUROPEAN SPACE PROGRAMMES, 10., 2008, Noordwijk. **Proceedings...** Noordwijk, 2008. 27

VRIES, R. H. de; KEIJZER, J.; LIESHOUT, F. V.; DAM, A. A. ten; MOELANDS, J. M. Enhancements to EuroSim. In: WORKSHOP ON SIMULATION FOR EUROPEAN SPACE PROGRAMMES, SESP'02., 2002, Noordwijk. **Proceedings...** Noordwijk, 2002. 17

WAGNER, C.; FLATKEN, M.; MEINEL, M.; GERNDT, A.; HAGEN, H. FSSteering: A distributed framework for computational steering in a script-based CFD simulation environment. In: HIGH-END VISUALIZATION WORKSHOP, 6., 2010, Obergurgl, Austria. **Proceedings...** Berlin: Lehmanns Media-LOB.de, 2010.

p. 8. ISBN 978-3-86541-361-1. Available from Internet: <http://elib.dlr.de/66376/1/VizWS2010_A1.pdf>. 50

WALSH, A.; WIJNANDS, Q.; LINDMAN, N.; ELLSIEPEN, P.; SEGNERI, D.; EISENMANN, H.; STEINLE, T. The spacecraft simulator reference architecture. In: INTERNATIONAL WORKSHOP ON SIMULATION & EGSE FACILITIES FOR SPACE PROGRAMMES, 11., 2010, Noordwijk. **Proceedings...** Noordwijk: ESA, 2010. p. 7. 27

WASER, J.; FUCHS, R.; RIBICIC, H.; SCHINDLER, B.; BLOESCHL, G.; GROELLER, M. E. World lines. **IEEE Transactions On Visualization And Computer Graphics**, v. 16, n. 6, p. 1458–1467, 2010. 34, 43, 46

WERKMAN, A.; MOSENKIS, R.; PICARD, C. ATV and ISS flight controller training. In: INTERNATIONAL CONFERENCE ON SPACE OPERATIONS, 12., 2012, Stockholm. **Proceedings...** Stockholm, 2012. 19

WHITTY, J. Real time distributed simulations using SIMSAT 4.3. In: INTERNATIONAL WORKSHOP ON SIMULATION & EGSE FACILITIES FOR SPACE PROGRAMMES, 11., 2010, Noordwijk. **Proceedings...** Noordwijk, 2010. p. 6. 27

WIJK, J. J. V.; LIERE, R. V.; MULDER, J. D. Bringing computational steering to the user. In: SEMINAR ON SCIENTIFIC VISUALIZATION, 1997, Dagstuhl. **Proceedings...** Dagstuhl, 1997. p. 304–313. 33, 50

WIJK, J. J. van; SPOELDER, H. J. W.; KNIBBE, W.-J.; SHAHROUDI, K. E. Interactive exploration and modeling of large data sets: a case study with Venus light scattering data. In: CONFERENCE ON VISUALIZATION, 7., 1996, Los Alamitos, CA,. **Proceedings...** Los Alamitos: IEEE Computer Society Press, 1996. (VIS '96), p. 433–516. ISBN 0-89791-864-9. Available from Internet: <http://dl.acm.org/citation.cfm?id=244979.245758>. 48

WIJK, J. van; LIERE, R. van. An environment for computational steering. **Scientific Visualization: Overviews, Methodologies, and Techniques**, IEEE Computer Society Press, Los Alamitos, CA, USA, n. 89–110, p. 1–22, 1997. 31, 33, 38

WILKINS, S.; GARG, S.; MEYYAMMAI, S. **MFC development using Microsoft Visual C++ 6.0**. Redmond, WA: Microsoft, 2000. 605 p. (Microsoft mastering). 36

WILLIAMS, A. P. SIMSAT: An object oriented architecture for real-time satellite simulation. In: INTERNATIONAL SYMPOSIUM ON GROUND DATA SYSTEMS FOR SPACE MISSION OPERATIONS, 2., 1992, Pasadena, CA. **Proceedings...** Pasadena, 1993. p. 711–716. Available from Internet: <http://ntrs.nasa.gov/archive/nasa/casi.ntrs.nasa.gov/19940019467_1994019467.pdf>. 15, 16, 19

WITT, R.; FRITZ, M.; KUWAHARA, T.; BRANDT, A.; LAUREL, C.; RÖSER, H.-P.; EICKHOFF, J. Real-time 3D-visualization in satellite development. In: INTERNATIONAL CONFERENCE ON ASTRODYNAMICS TOOLS AND TECHNIQUES, 4., 2010, Spain. **Proceedings...** Spain, 2010. 9

WU, H.; LI, Z.; HU, J.; TANG, L.; LI, C. Satellite visualization tool based on the arcgis engine and opengl. In: INTERNATIONAL CONFERENCE ON SPACE OPERATIONS, 11., 2012, Stockholm. **Proceedings...** Stockholm, 2012. 9

WU, Q.; ZHU, M.; GU, Y.; RAO, N. System design and algorithmic development for computational steering in distributed environments. **Parallel and Distributed Systems, IEEE Transactions on**, v. 21, n. 4, p. 438–451, Apr. 2010. ISSN 1045-9219. 47

ZANON, O.; MORSCHER, A. The SimTG simulation modeling framework. In: INTERNATIONAL WORKSHOP ON SIMULATION & EGSE FACILITIES FOR SPACE PROGRAMMES, 11., 2010, Noordwijk. **Proceedings...** Noordwijk, 2010. p. 8. 27

ZHANG, W.; YU, Y.; ZHAO, X.; ZHANG, S. Research of framework of SMP2-based maintenance support simulation models. In: INTERNATIONAL CONFERENCE ON RELIABILITY, MAINTAINABILITY AND SAFETY, 9., 2011, Guiyang, China. **Proceedings...** Guiyang, China, 2011. p. 774 – 778. 27

APPENDIX A - STEERABLE SIMULATION DEVELOPMENT PROCESS

The steerable simulation development process proposed in this work is based on the reference model provided by SMP2 standard and reproduced in Figure A.1.

After the mathematical model has been defined, the design of the simulation component starts with a formal description of the model and the generation of a wrapper code that will implement the SMP2 interfaces in C++ language. Since SMP2 adopts concepts from object oriented programming, it is simple to adapt Unified Modeling Language (UML) diagrams to describe components from its Simulation Model Definition Language and then generate e.g. model catalogues. This method is demonstrated by Fritzen et al. (2010) and extended in the current work to represent models and simulation assemblies in the SimDK Editor. The approach developed here consist in defining a set of stereotypes in the Enterprise Architect, a commercial of the shelf tool to perform Computer-Aided Software Engineering (CASE), in which class and object diagrams are used to auto-generate SMP2 artefacts and C++ code. The add-in source code can be downloaded from `http://urlib.net/8JMKD3MGP5W34M/3H56LQH/AppendixA_EA_Addin.tar`.

An example of such representation is given in Figure A.2, in which a *Bapta Controller Model* is described with a class diagram dialect. Using customized stereotypes, parameters can be modelled as class attributes, entry points and operations as

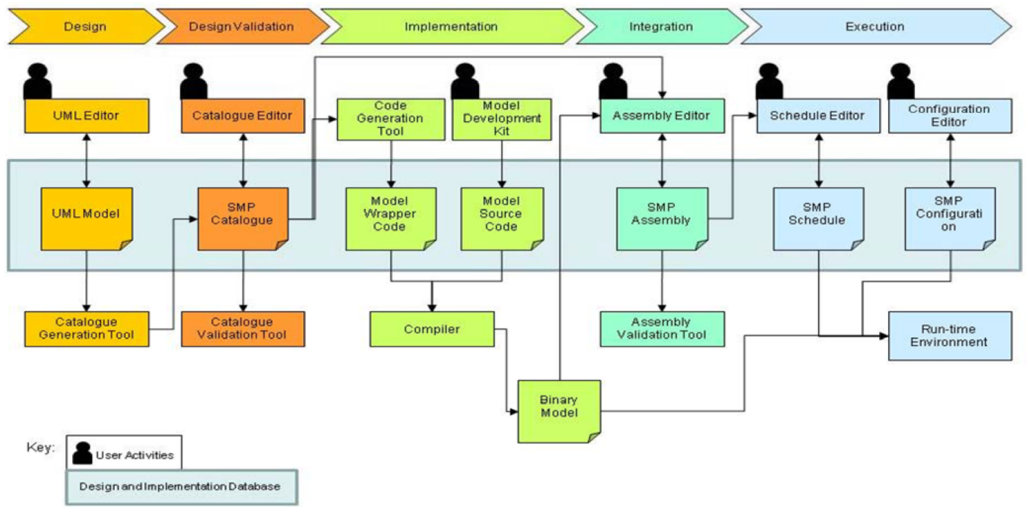

Figure A.1 - SMP2 tool chain overview.
Source: Reproduced from ECSS (2011c)

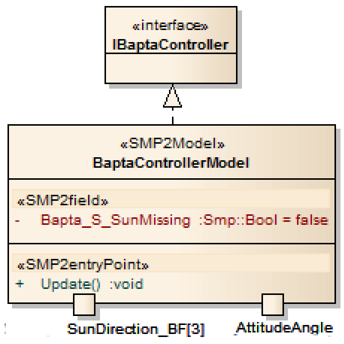

Figure A.2 - Representation of model catalogue using UML class diagrams.

methods, and the input and output parameters as ports. Specialization, aggregation and composition connections can also be used to express model relations.

From this diagram, the C++ source code for wrapping the mathematical model is automatically generated accordingly to the SMP2 standard interfaces. Then, each package can be configured in a model repository for future usage.

The scenario definition consists in selecting the models from the repository that will compose a given simulation. In this step an object diagram from UML is adapted to describe the model instances and to customize the values for their configuration parameters. Further, in this diagram all the connections between model fields are described and later automatically exported to an assembly file.

In a similar strategy adopted for the catalogue, the assembly descrition uses an adapted Object Diagram to describe the run-time instances of simulation models and their connections. The Figure A.3 shows an example of assembling three models using field links. Based on these representations, a plug-in can be used in the editor to automatically generate the XML file containing the assembly artefact and configuration data to a certain simulation scenario.

For each simulation scenario, optional steering widgets and adapter may be created to control the interface between user and simulation parameters.

A.1 The Model Repository

The implementation of this model repository is based on Apache Subversion, a free system for software versioning and revision control. In order to promote reliability of models deployed from the repository, special precautions have to be taken when adding new models to it. In the current approach, a process for quality assurance is

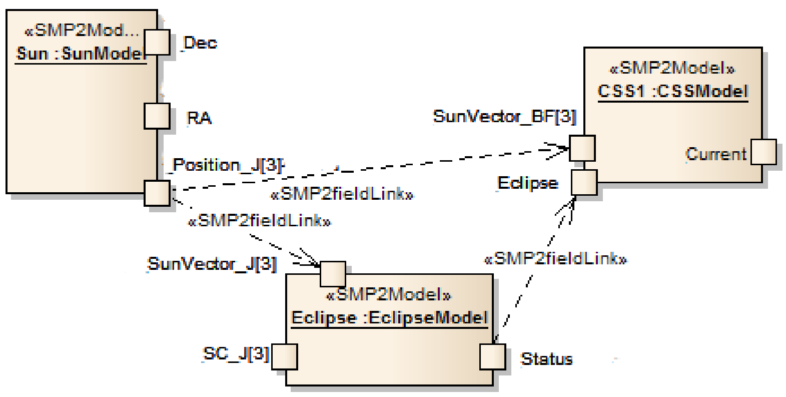

Figure A.3 - Representation of model assembly using UML object diagram.

established and based on the definition of a model bundle.

A certification could also be done based on the completion of the bundle to ensures that the documentation and source code have no discrepancies found and all test cases have been executed for each model. The source code must comply with the coding standard and it is encourage that model adopt the same constant values. Further, a rigorous control can be established to keep track of model versions and known bugs.

A.1.1 Bundle and Manifest file

The model bundle contains all the source code of the model package and additional information for describing the model:

- *Source code*: header, implementation or script files and makefiles needed to build the binary package;
- *Configuration files*: any data used to configure the model in run time;
- *Catalogue*: a XMI file containing a class diagram that describes the model;
- *Manifest*: a formal description of bundle content;
- *Certificate*: a document assuring that the model has been formally verified;
- *Design Documentation*: a set of documents that describes the mathematical modelling of the simulation component, requirements, and design.
- *Test harness*: set of data used to test the model, additional test bench elements for executing the test suite and related documentation.

In addition, each model bundle is accompanied by a MD5 file.

The manifest is a metadata file describing the contents of the bundle, which should clearly present the model, its interfaces, dependences and usage context. In the Table A.1, a complete list of its fields is provided.

Table A.1 - Content of bundle manifest.

Field	**Description**
Identification section	
Identifier	Unique identifier
Name	Name of the model. The name have not to be unique, but all models assembled in a given simulation must be unique.
Purpose	A brief description of the model.
Version	Implementation version of the model.
Author	The author and reference of mathematical model.
Programmer	The responsible for the codification.
Date	Date of implementation.
License	End user agreement, if applicable.
Platform information section	
Language	Programming language and version.
IDE	Name and version of Development Environment used to generate the model.
Wrapper	Type and version of wrapper, e.g. SMP2.
Interface and configuration section	
Inputs	A list of model's inputs, which can be input operation arguments or input parameters. The limits, units and adopted reference frames must be specified for each field.
Outputs	A list of model's outputs, which can be output operation arguments or output parameters. The limits, units and adopted reference frames must be specified for each field.
Paramerters	A list of model's internal parameters. The limits, units and adopted reference frames must be specified for each field.
External Dep.	All configuration data available from external sources, e.g. files or environmental configurations.
Dependencies section	
Libraries	External library usage in compilation time (e.g. matrix operations).
Models	A list of mandatory models and their identifiers that must be present in the simulation.
Providers	A list of optional models and their identifiers that could be attached to the input fields of the current model. Differently from the Models dependencies, an input field can be disconnected on run-time.
Constraints & Limitations section	
Constraints	Operation limits and validity range of model application.
Bugs	Known bugs of the model.

APPENDIX B - A NOVEL DESIGN PATTERN FOR SOLVING ORDINARY DIFFERENTIAL EQUATIONS

In general, numerical methods for solving Ordinary Differential Equations (ODE) consist of two software functions that respectively implement the equations and the integrator. In this work, an object oriented approach is proposed to model these methods in order to reduce the code coupling, by adopting the generic structure presented in the class diagram in the Figure B.1.

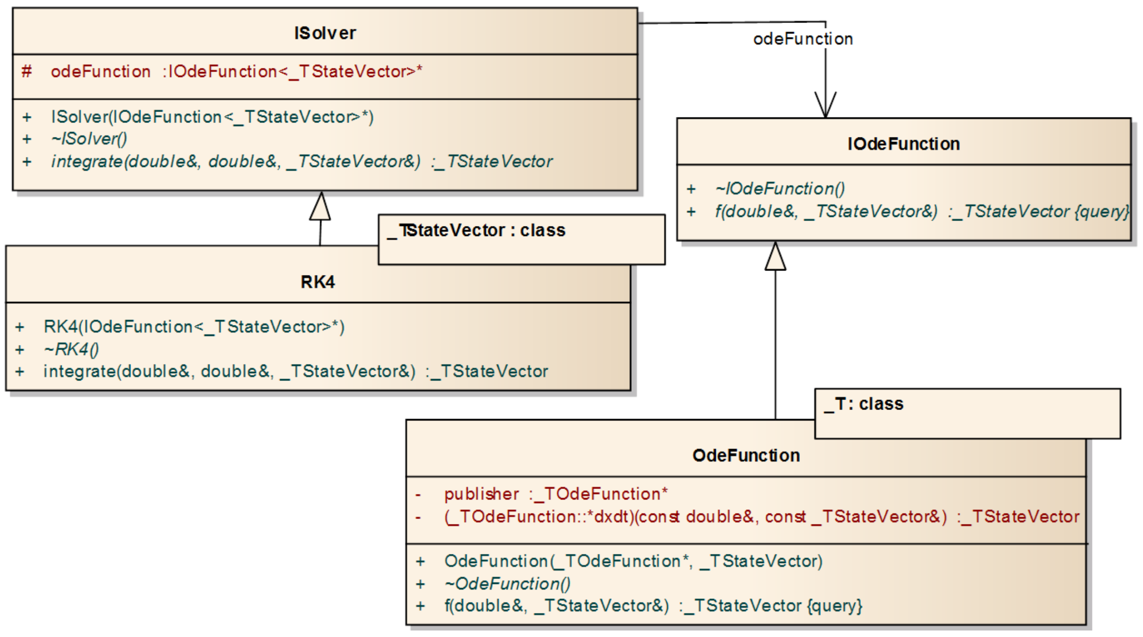
ISolver
# odeFunction :IOdeFunction<_TStateVector>*
+ ISolver(IOdeFunction<_TStateVector>*)
+ ~ISolver()
+ integrate(double&, double&, _TStateVector&) :_TStateVector
odeFunction
IOdeFunction
+ ~IOdeFunction()
+ f(double&, _TStateVector&) :_TStateVector {query}
_TStateVector : class
RK4
+ RK4(IOdeFunction<_TStateVector>*)
+ ~RK4()
+ integrate(double&, double&, _TStateVector&) :_TStateVector
_T: class
OdeFunction
- publisher :_TOdeFunction*
- (_TOdeFunction::*dxdt)(const double&, const _TStateVector&) :_TStateVector
+ OdeFunction(_TOdeFunction*, _TStateVector)
+ ~OdeFunction()
+ f(double&, _TStateVector&) :_TStateVector {query}

Figure B.1 - Class diagram of the proposed `Integrator` design pattern.

The flexible structure comprises in two standard C++ interfaces to describe integrators and ODE function, based on a state vectors template, whose type is defined in compilation time. Moreover, several integration methods may be used by implementing the interface `ISolver` and in the Figure B.1 a *Runge-Kutta* specialization is provided.

On the other hand, the `IOdeFunction` is generalized by a class that holds the reference for a third object that actually will implement the ODE function, whose pointer is passed to the `ODEFunction` object during its construction.

Due to its abstraction level, this scheme can be taken as a reference and used as a design pattern for several types of applications. In the current work, the presented approach is adopted to propagate the spacecraft attitude dynamics, during the demonstrated simulations. For this particular implementation, the state vector definition and the reference to the solver is presented in the class diagram in the Figure B.2.

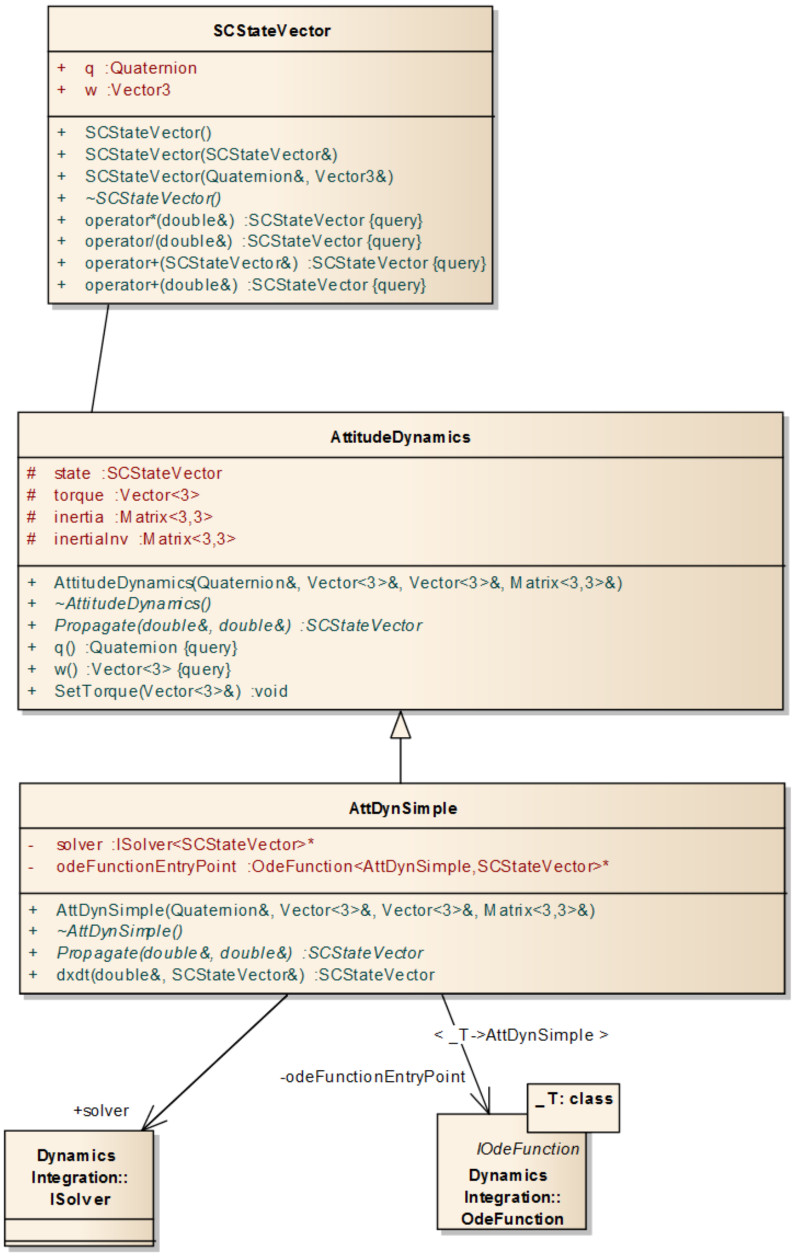
SCStateVector
+ q :Quaternion
+ w :Vector3
+ SCStateVector()
+ SCStateVector(SCStateVector&)
+ SCStateVector(Quaternion&, Vector3&)
+ ~SCStateVector()
+ operator*(double&) :SCStateVector {query}
+ operator/(double&) :SCStateVector {query}
+ operator+(SCStateVector&) :SCStateVector {query}
+ operator+(double&) :SCStateVector {query}
AttitudeDynamics
# state :SCStateVector
# torque :Vector<3>
# inertia :Matrix<3,3>
# inertiaInv :Matrix<3,3>
+ AttitudeDynamics(Quaternion&, Vector<3>&, Vector<3>&, Matrix<3,3>&)
+ ~AttitudeDynamics()
+ Propagate(double&, double&) :SCStateVector
+ q() :Quaternion {query}
+ w() :Vector<3> {query}
+ SetTorque(Vector<3>&) :void
AttDynSimple
- solver :ISolver<SCStateVector>*
- odeFunctionEntryPoint :OdeFunction<AttDynSimple,SCStateVector>*
+ AttDynSimple(Quaternion&, Vector<3>&, Vector<3>&, Matrix<3,3>&)
+ ~AttDynSimple()
+ Propagate(double&, double&) :SCStateVector
+ dxdt(double&, SCStateVector&) :SCStateVector
< _T->AttDynSimple >
-odeFunctionEntryPoint
+solver
Dynamics Integration:: ISolver
_T: class
IOdeFunction
Dynamics Integration:: OdeFunction

Figure B.2 - Class diagram illustrating the use of the `Integrator` design pattern for propagating the spacecraft attitude dynamics.

The specialization of the code during compilation is show in the snipped code below.

An especial entry point for the ODE function is defined by using the `OdeFunction` class, in which the `AttDynSimple` and `SCStateVector` types are defined. During the creation of `OdeFunction` object the references to the current instance (i.e. this) and the `AttDynSimple::dxdt` method are passed in the constructor. After the `OdeFunction` object is referenced in the solver's construction, which type is defined to `RK4`.

```
AttDynSimple(...) {
  OdeFunction<AttDynSimple,SCStateVector>* odeFunctionEntryPoint;
  odeFunctionEntryPoint =
    new OdeFunction<AttDynSimple,SCStateVector>
                (this, &AttDynSimple::dxdt);

  ISolver<SCStateVector>* solver;
  solver = new RK4<SCStateVector>(odeFunctionEntryPoint);
}
```

APPENDIX C - STEERING WIDGETS

This annex briefly describes the developed steering widgets to support the user interventions in the case studies. Several user interaction paradigms have been adopted, in order to demonstrate the flexibility of the steering adapter layer of the simulation facility.

C.1 Orbital Parameters

For changing the orbital parameters, two types of steering widgets have been developed. The first is 3D application that runs in a regular workstation and the second makes uses of multi-touch interfaces provided by a tablet device.

C.1.1 3D User Interface

The interface presented in the Figure C.1 provides a 3D view of the orbit and widget to manipulate the orbit described as Keplerian elements. Typically this interface will be attached to the spacecraft dynamics model and after each update provided by the user, the model will be triggered to refresh its state variables.

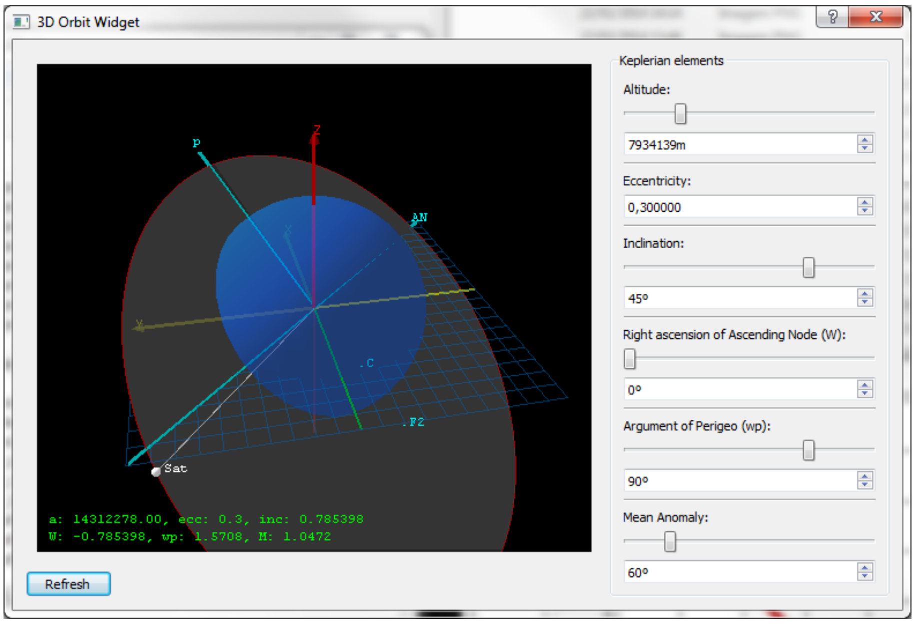

```
a: 14312278.00, ecc: 0.3, inc: 0.785398
W: -0.785398, wp: 1.5708, M: 1.0472
```

Keplerian elements

Altitude: 7934139m

Eccentricity: 0,300000

Inclination: 45º

Right ascension of Ascending Node (W): 0º

Argument of Perigeo (wp): 90º

Mean Anomaly: 60º

Figure C.1 - Steering widget to change orbital elements with a 3D view.

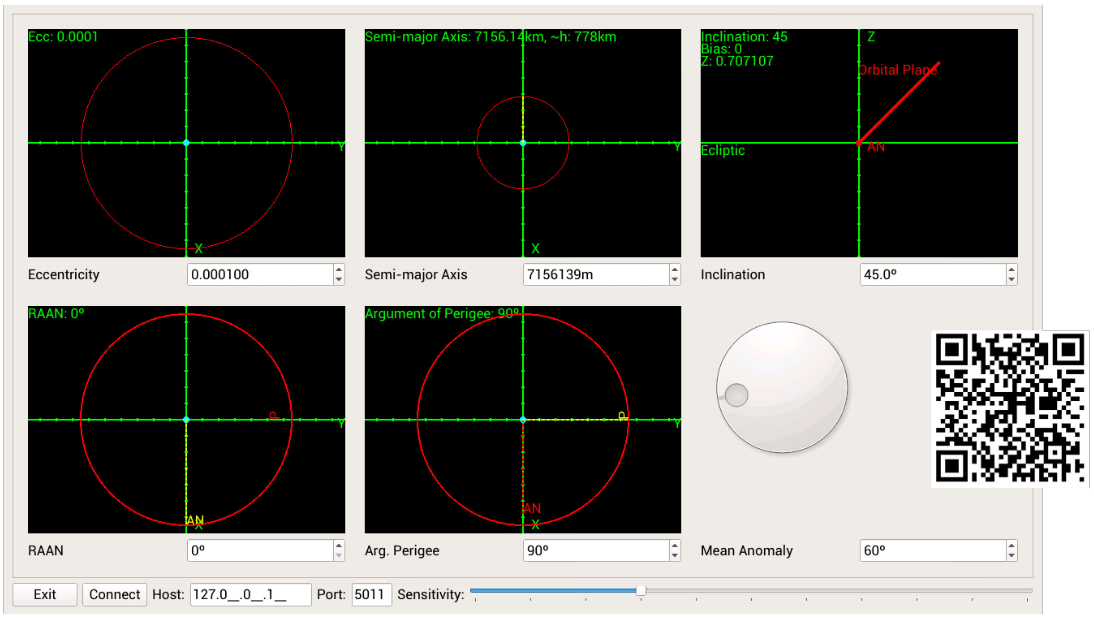

Eccentricity 0.000100
Semi-major Axis 7156139m
Inclination 45.0º
RAAN 0º
Arg. Perigee 90º
Mean Anomaly 60º
Exit Connect Host: 127.0__.0__.1__ Port: 5011 Sensitivity:

Figure C.2 - Steering widget to change orbital elements with gestures and multi-touch interface.

C.1.2 Gestures with multi-touch interaction

Complementary to the 3D Orbit view, the component described in the Figure C.2 support gesture interaction with a multi-touch interface. Each Keplerian element is represented by a dedicated widget[1].

The Figures C.3 and C.4 illustrate a sequence of interaction performed to define the geometry of an orbit. Initially the thumb and index finger are used to pinch in the widget and make the orbit more eccentric. The same type of gesture is applied to enlarge the semi-major parameter, by pinching out the widget. The orbit inclination is steered by using two fingers and swiping up or down on the widget.

In the sequence, from the Figure C.4, the rotation applied with two fingers defines the Right Ascension of the Ascending Node and the Argument of Perigee. Finally, the mean anomaly is set with a regular Qt knob. As the interaction is performed, all the correlated widgets are coherently updated.

[1]A video demonstration of this interface can be accessed in the following link: `http://urlib.net/8JMKD3MGP5W34M/3H56LQH/AppendixC_gestureInteraction.wmv` or using the QR code available in the Figure.

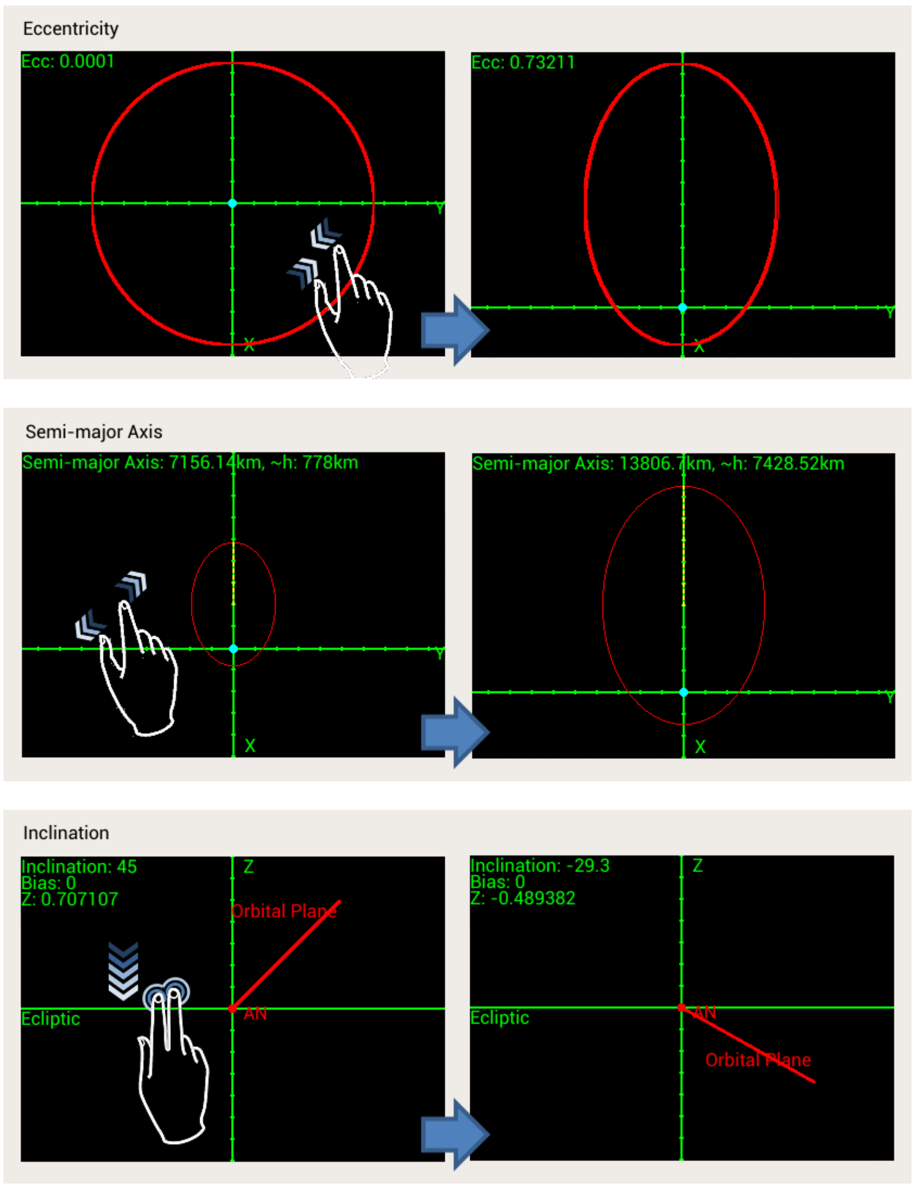

Figure C.3 - Sequence of gesture interactions to define eccentricity, semi-major axis and inclinations values.

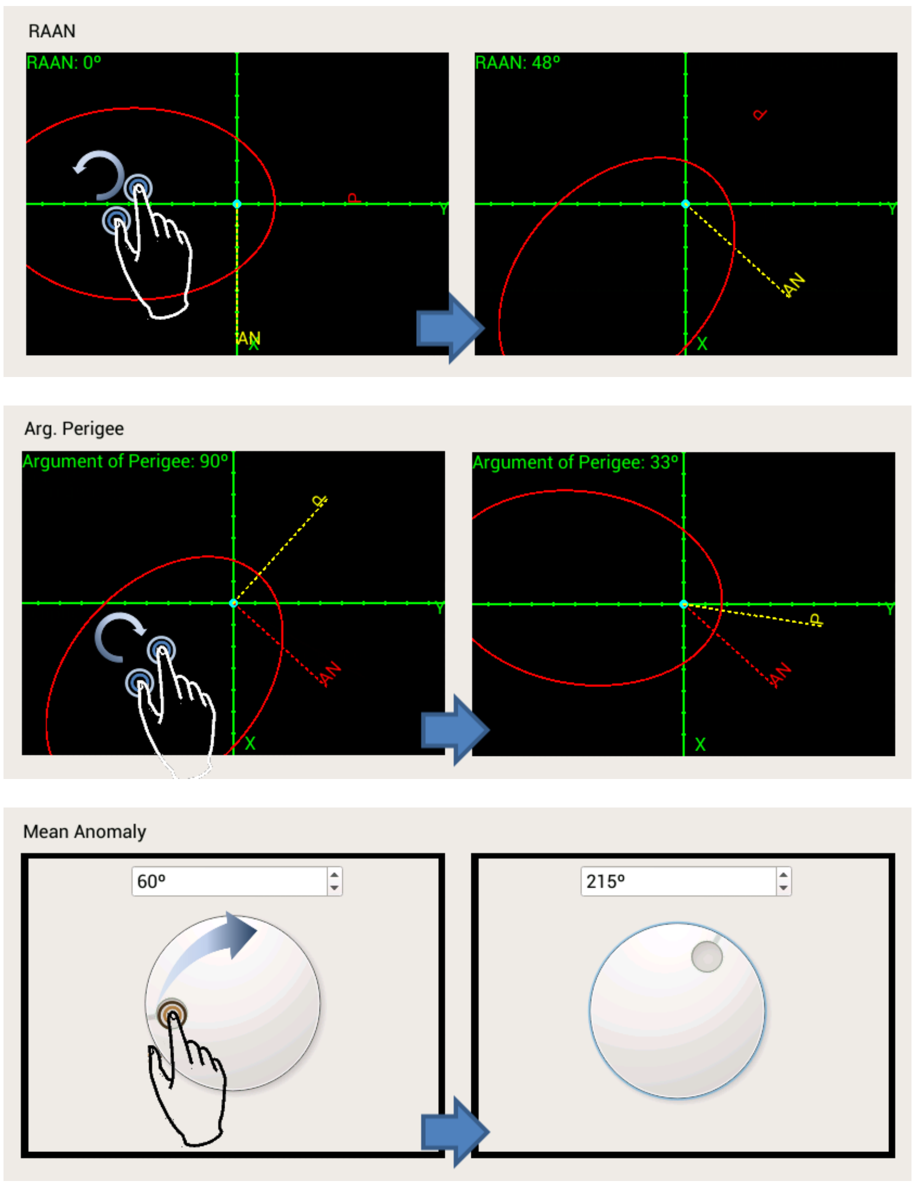

Figure C.4 - Sequence of gesture interactions to define Right Ascension of the Ascending Node, Argument of Perigee and Mean Anomaly values.

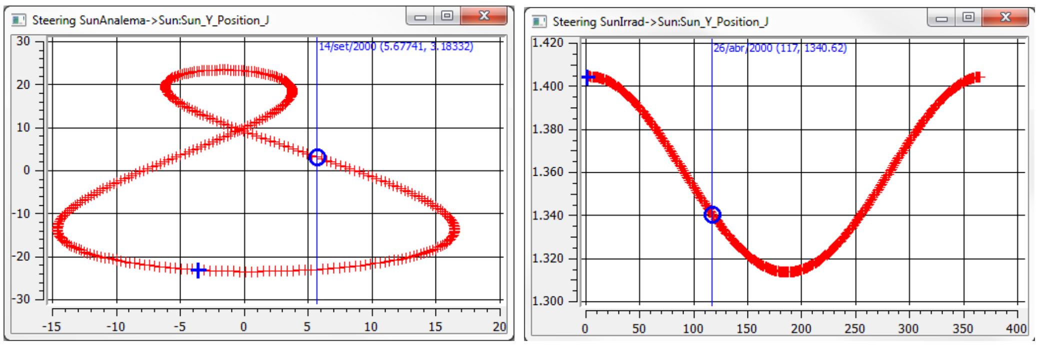

(a) Analema. (b) Irradiance variation along the year.

Figure C.5 - Steering widgets to define Sun's position based on an Analema or expected irradiance.

C.2 Sun Position and Irradiance

The steering widgets presented in Figure C.5 can be connected to the Sun model in order to define its position based on an Analema representation or by choosing a corresponding irradiance level[2].

C.3 Perturbation Torque

This interface presented in Figure C.6 consists in an application embedded in a tablet device, which process the signals from inertial sensors (i.e. accelerometers and gyros), providing a gesture interface for easy and natural injection of perturbations torques in the spacecraft dynamics model.

[2]A video demonstration of this interface can be accessed in the following link: `http://urlib.net/8JMKD3MGP5W34M/3H56LQH/AppendixC_inertialSensors.wmv` or using the QR code available in the Figure.

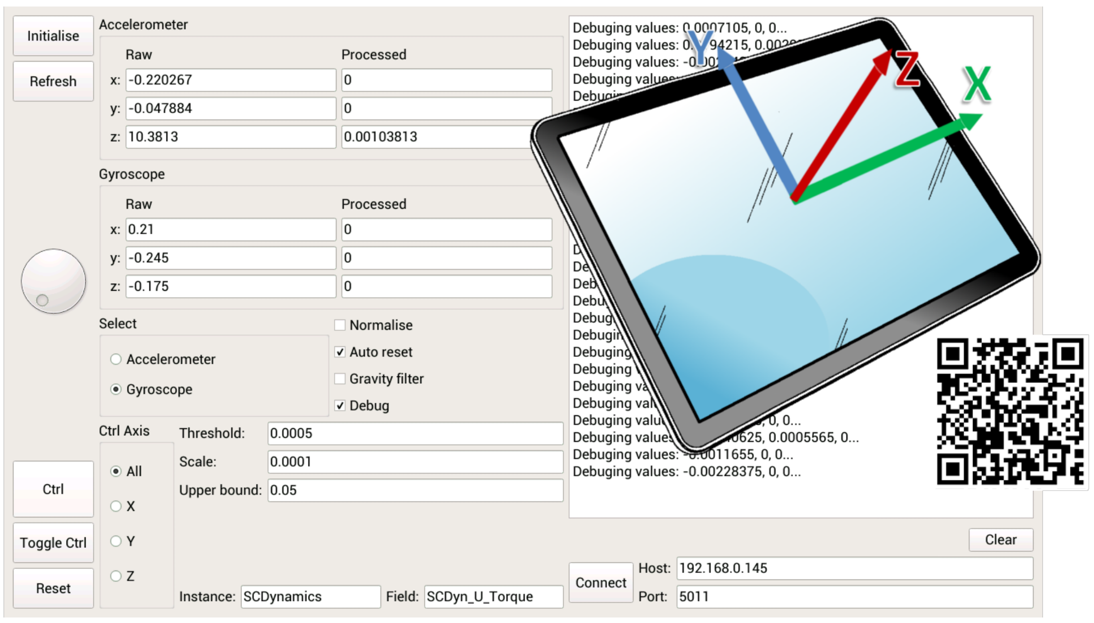

Accelerometer

	Raw	Processed
x:	-0.220267	0
y:	-0.047884	0
z:	10.3813	0.00103813

Gyroscope

	Raw	Processed
x:	0.21	0
y:	-0.245	0
z:	-0.175	0

Select: Accelerometer [✓ Gyroscope]

Normalise; [✓ Auto reset]; Gravity filter; [✓ Debug]

Ctrl Axis: [✓ All] X Y Z

Threshold: 0.0005

Scale: 0.0001

Upper bound: 0.05

Instance: SCDynamics

Field: SCDyn_U_Torque

```
Debuging values: 0.0007105, 0, 0...
Debuging values: 0. 94215, 0.002
Debuging values: -0.00
Debuging values
Debugi
D
De
Deb
Debu
Debug
Debugin
Debuging
Debuging
Debuging va
Debuging val
Debuging valu             , 0, 0...
Debuging values      0625, 0.0005565, 0...
Debuging values: -0.0011655, 0, 0...
Debuging values: -0.00228375, 0, 0...
```

Host: 192.168.0.145

Port: 5011

Figure C.6 - Steering widget interface to inject perturbation torques in the spacecraft dynamics model using inertial sensors.

APPENDIX D - SPACECRAFT SIMULATOR INTEROPERABILITY WITH LEGACY SYSTEM FOR THERMAL SIMULATION

In the simulation scenario presented in the section 6.12, a thermal system is modelled with the commercial tool SINDA/FLUINT, a general purpose network analyser (CULLIMORE et al., 2005). During the simulation, intermediate results can be read from the SINDA/FLUINT to update the satellite simulator with the current temperatures computed for the network's nodes. Similarly, the simulator periodically sets register in the thermal model to changes its environmental conditions or switch heaters.

The overall interoperability scheme is depicted in Figure D.1. The communication between the two simulators is possible thanks to a Component Object Model (COM) interface published by the SINDA/FLUINT Controller, which is used for building customised front-ends for loading, running and controlling scenarios in that tool (e.g. from a Microsoft Excel spreadsheet). Hence a middleware application (here called *Sinda Controller Server*) is built to encapsulate the COM interface and enable the SINDA/FLUINT operation from the spacecraft simulator. In the simulator side, the communication is established by an ad-hoc SMP2 Thermal model that opens a TCP/IP channel with the middleware and commands the SINDA/FLUINT controller.

The Graphical User Interface (GUI) of the middleware, implemented in C#, is presented in the Figure D.2. Using this applicative, the user must perform the initial setup, defining the communication parameters (i.e. server's IP address and port) and loading the SINDA/FLUINT scenario's file. Next the SINDA/FLUINT controller is initialised and the middleware is ready to accept connections from the spacecraft simulator. Further, the GUI also provides information on the SINDA/FLUINT state

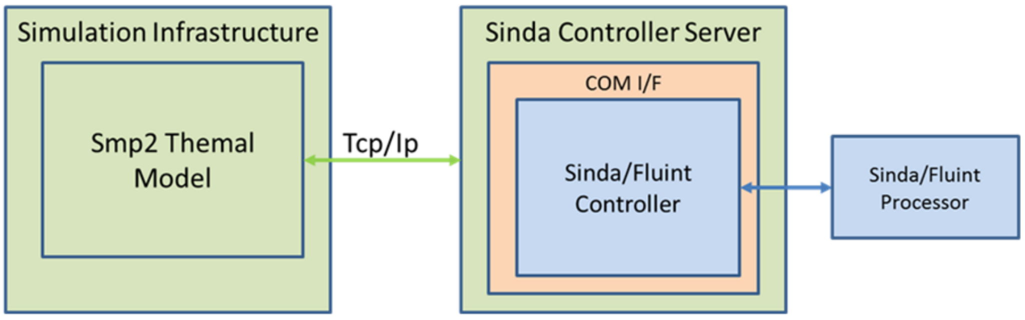

Figure D.1 - Interoperability architecture.

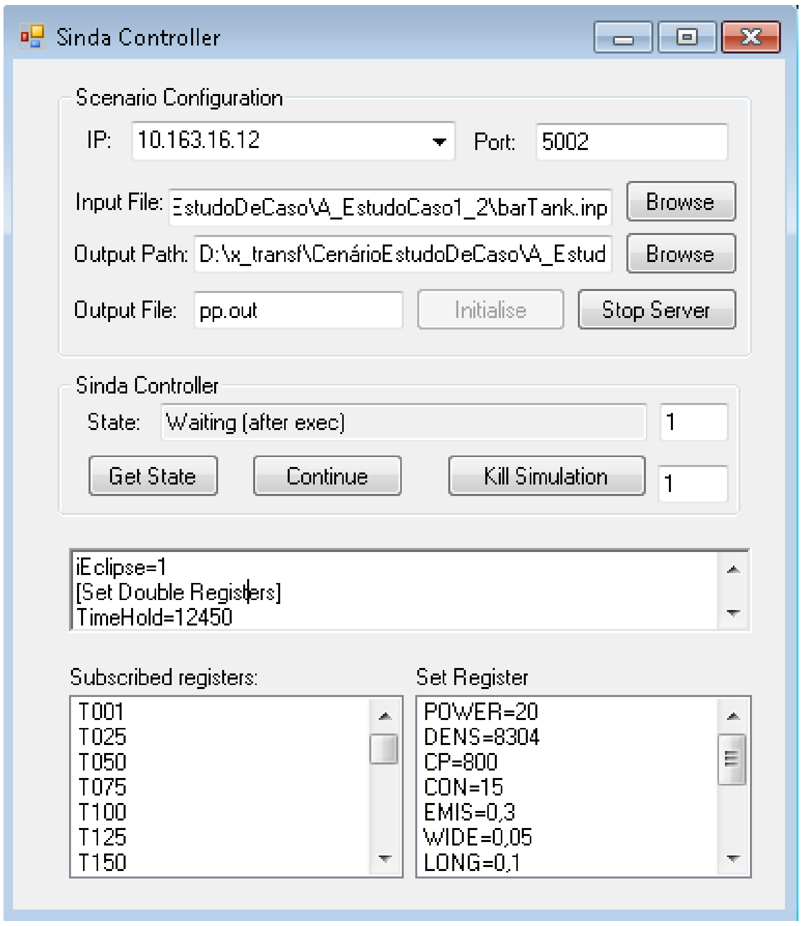

IP: 10.163.16.12
Port: 5002
Input File: EstudoDeCaso\A_EstudoCaso1_2\barTank.inp
Output Path: D:\x_transf\CenárioEstudoDeCaso\A_Estud
Output File: pp.out
State: Waiting (after exec) 1
1

```
iEclipse=1
[Set Double Registers]
TimeHold=12450
```

Subscribed registers:	Set Register
T001	POWER=20
T025	DENS=8304
T050	CP=800
T075	CON=15
T100	EMIS=0,3
T125	WIDE=0,05
T150	LONG=0,1

Figure D.2 - Graphical User Interface of the middleware application.

and a list of registers subscribed and set by the client.

When the spacecraft simulation is started, the SMP2 Thermal model connects to the middle and subscribes to a list of registers, which are variables in the network model that will be monitored by the SMP2 model (e.g. the current temperature in some selected nodes). Following, the SMP2 model commands the SINDA/FLUINT scenario to initialise and the controller replies with acknowledge messages and with the initial values for the subscribed registers. The whole initialisation procedure, which is illustrated by the sequency diagram in the Figure D.3, finishes after the client confirms the SINDA/FLUINT state.

The synchronization between the two simulations, described in Figure D.4, is done on the basis of the SINDA/FLUINT state machine, which basically comprises on the *initializing*, *executing*, *waiting* and *stopped* states. When it enters the executing state, the simulation time evolves as fast as possible until the clock reaches the instant

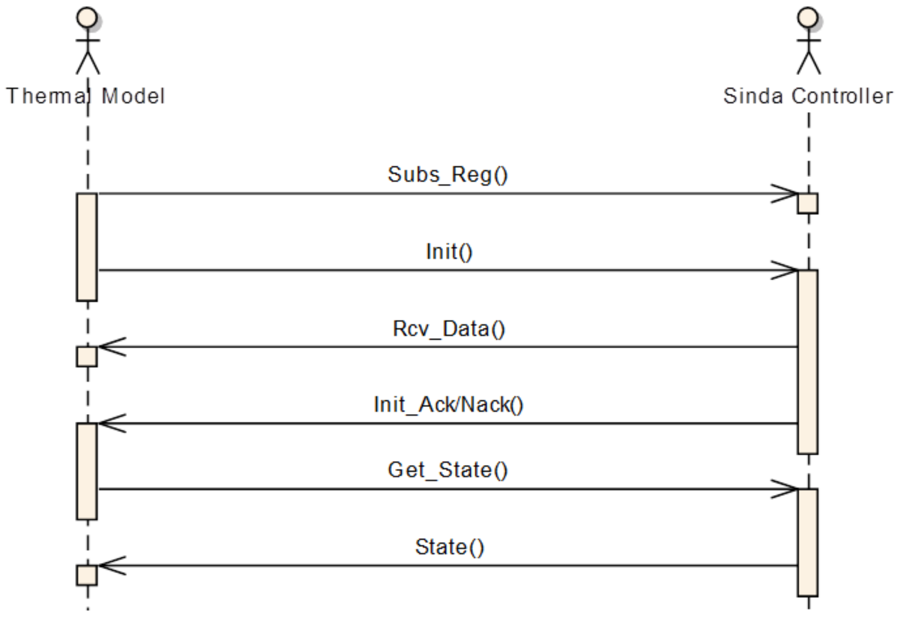

Figure D.3 - Sequence diagram describing the messages exchanged between the SMP2 Thermal Model and the middleware to initialise the simulation.

defined by the *TimeHold* register. Each time the SMP2 model's update entry point is invoked by the infrastructure, the registers are set in the Controller, so the next simulation interval (i.e. *TimeHold*) and control variables (e.g. heater status) are defined in the SINDA/FLUINT. After the simulation time has reached *TimeHold* again, the new values for the subscribed registers are updated in the SMP2 Thermal model, which keeps monitoring the SINDA/FLUINT state to check whether the next simulation cycle can be triggered.

Internally, the SMP2 Thermal model controls the synchronisation with the middleware using a state machine as defined in the Figure D.5. The protocol implemented by the client and server has been specifically defined for this application, based on the COM interface. Failure in the synchronisation may occur if the SINDA/FLUINT takes too long to process and reply its results to the spacecraft simulation. In this case, the SMP2 Thermal model keeps waiting for the server's response before the next simulation step can be executed and it will block temporarily the scheduler. After five seconds, an exception is generated and an error message is logged. This mechanism is represented by the activity diagram in the Figure D.6.

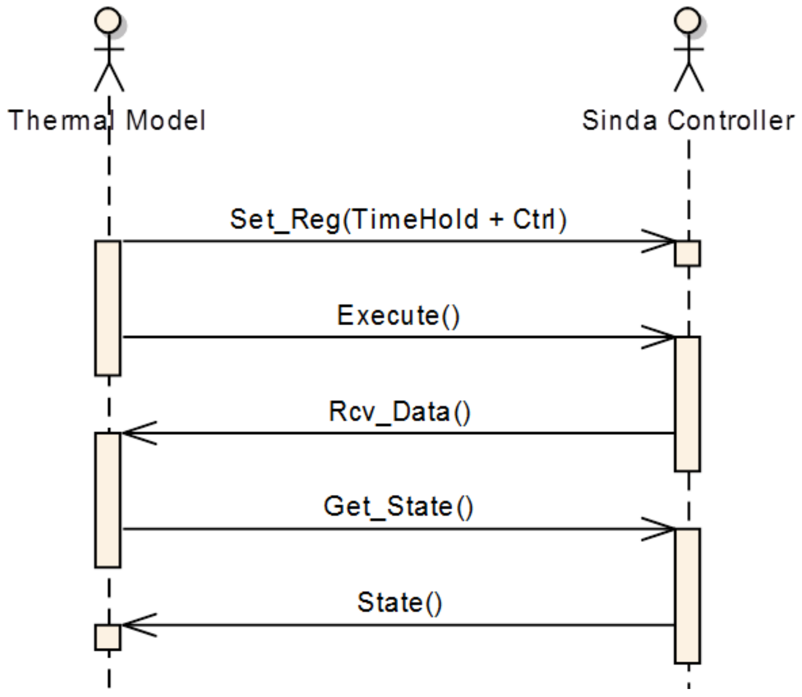

Figure D.4 - Sequence diagram describing the messages exchanged between the SMP2 Thermal Model and the middleware during the simulation execution.

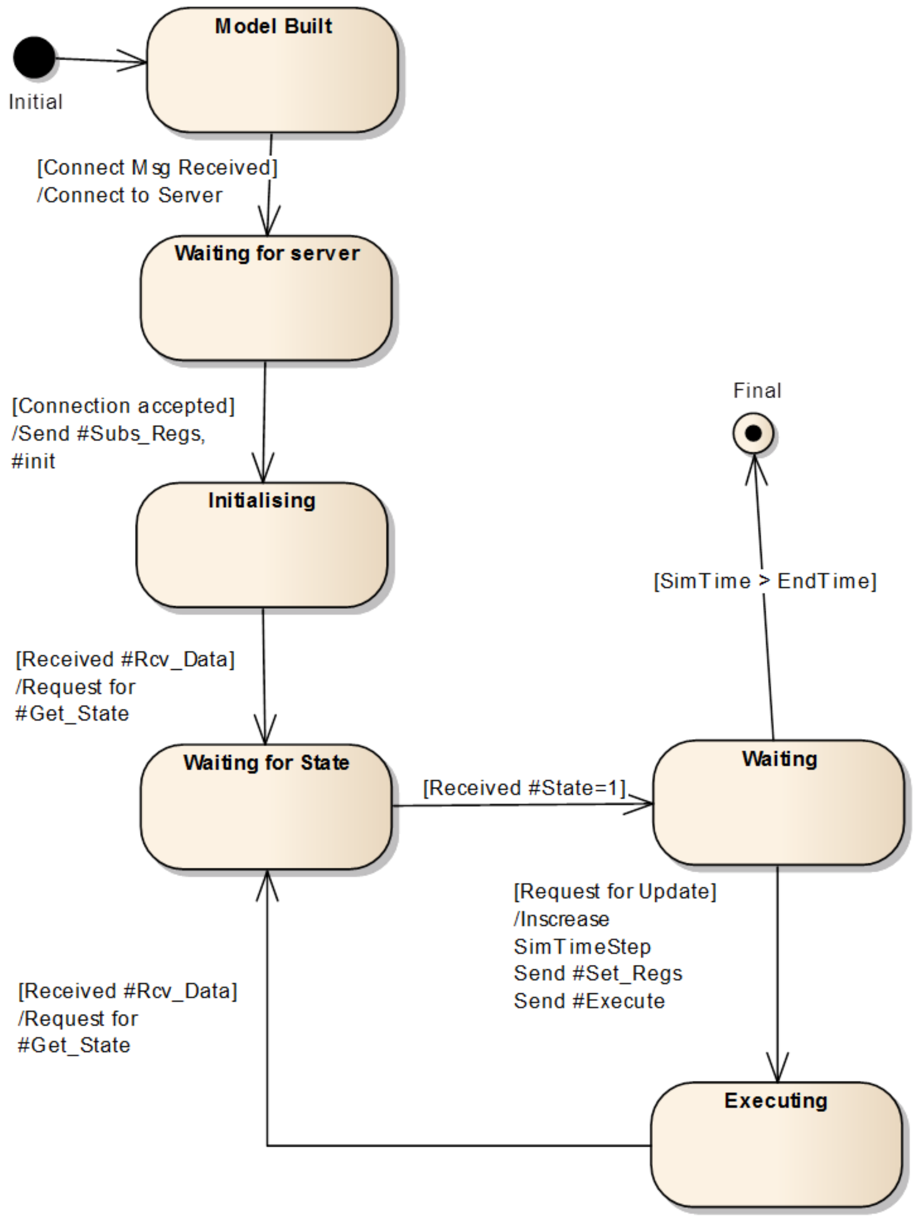

Figure D.5 - State machine diagram implemented by the SMP2 Thermal model to control the synchronisation with the SINDA/FLUINT simulation.

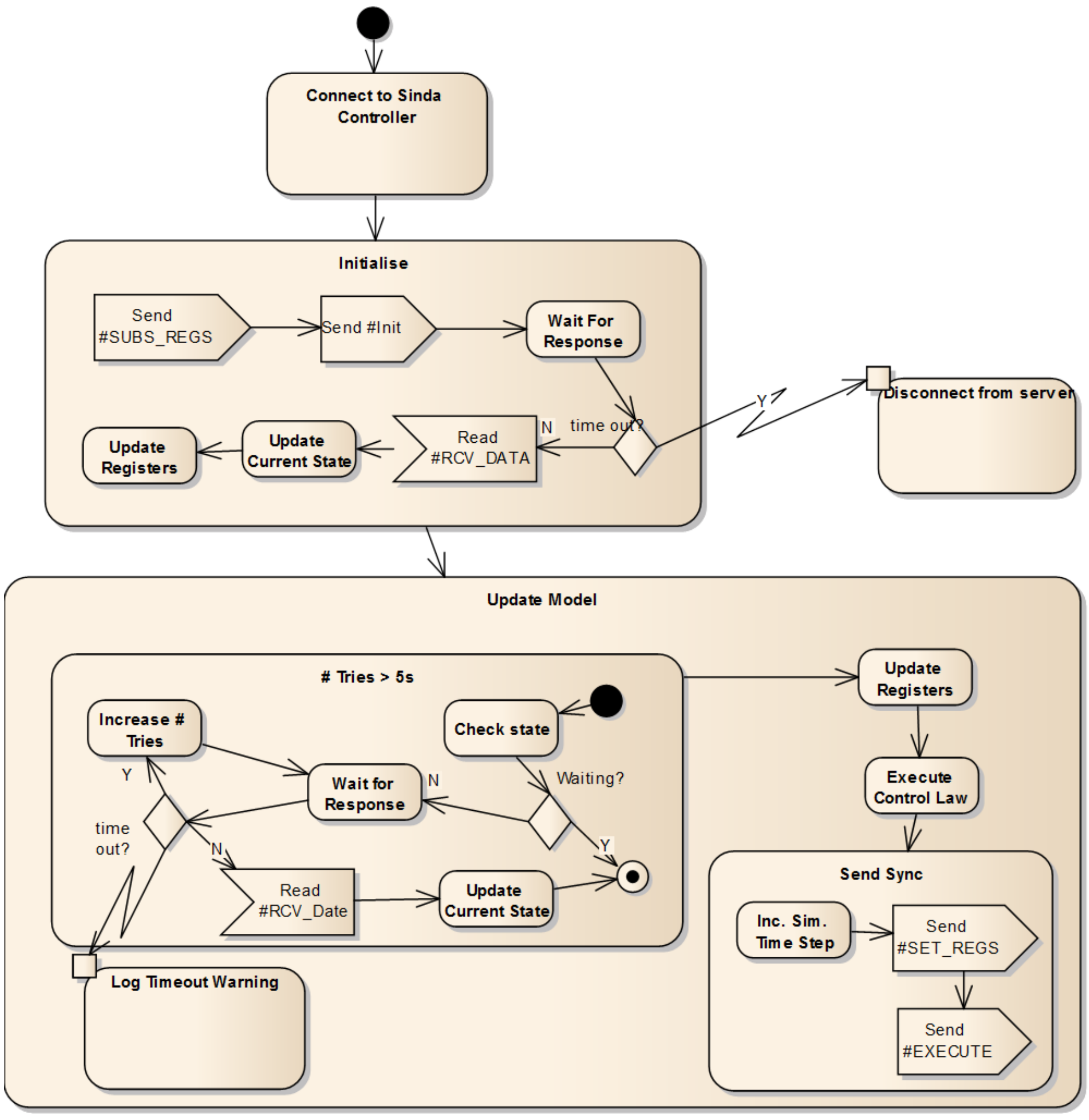

Figure D.6 - Activity diagram describing the communication and synchronisation scheme between the SMP2 Thermal model and the SINDA/FLUINT Controller.

APPENDIX E - USAGE DEMONSTRATION OF THE COMPUTATIONAL STEERING FACILITY

This Appendix is a electronic file containing a video that demonstrates the use of the computational steering facility. In almost 8 minutes, it describes the visualisation system with 3D feedback of the simulation state and gives a few examples on how the parameters can be steered by the user in order to explore the state space and to analyse the behaviour of the system.

The 88.6 MiB-size file uses the Windows Media Video format and it can be accessed in the following link `http://urlib.net/8JMKD3MGP5W34M/3H56LQH/AppendixE_demonstration.wmv` or using the QR code printed in the Figure E.1.

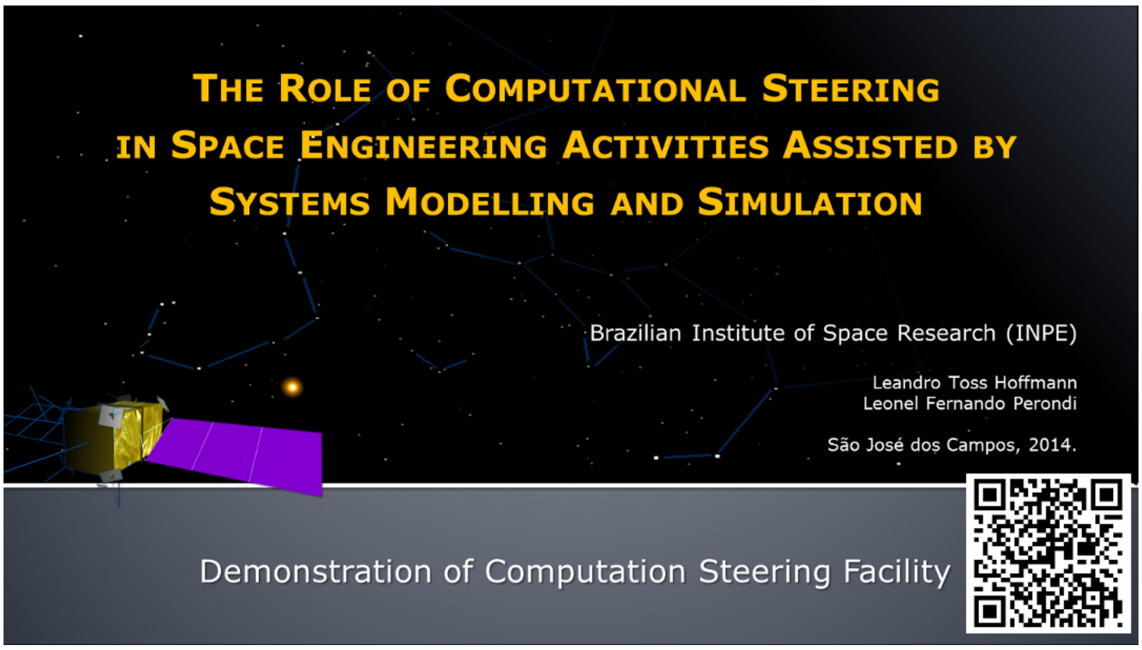

THE ROLE OF COMPUTATIONAL STEERING IN SPACE ENGINEERING ACTIVITIES ASSISTED BY SYSTEMS MODELLING AND SIMULATION

Brazilian Institute of Space Research (INPE)

Leandro Toss Hoffmann
Leonel Fernando Perondi

São José dos Campos, 2014.

Demonstration of Computation Steering Facility

Figure E.1 - Video demonstration of the computational steering facility.